VOLUME II
FLYING QUALITIES PHASE

CHAPTER 14
FLIGHT CONTROL SYSTEMS

DISTRIBUTION STATEMENT A
Approved for public release
Distribution Unlimited

19970117 040

DECEMBER 1988

USAF TEST PILOT SCHOOL
EDWARDS AFB CA

DTIC QUALITY INSPECTED 1

14.1 INTRODUCTION

The study of flight control systems is of central importance in the design and flight test of modern aircraft. Increasingly these aircraft are designed with performance considerations only and sophisticated flight control systems are required to correct a host of handling qualities deficiencies. Today's complex control systems are comprised of various elements, washout filters, prefilters, sensors, electronic compensators and structural filters, in full authority "fly-by-wire" systems.

The purpose of this course is to provide a fundamental understanding of the basic types of aircraft control strategies. Simple mechanical systems are presented including the effect of control system elements, such as actuators, artificial feel systems, and mechanical elements. Stability and control augmentation systems are then discussed, stressing the advantages and disadvantages of each type of feedback commonly used. Electronic compensators are studied as further refinements to the augmented system. Modern analog and digital electronic flight control systems are then analyzed to gain an appreciation for their operation and potential handling qualities deficiencies. In addition, automatic flight control systems are discussed including both autopilots and the more sophisticated integrated systems for automated maneuvering. Aircraft sensors used in most of these flight control systems are also analyzed. Finally, flight control system test techniques are presented.

14.2 HISTORICAL BACKGROUND

The early years of aviation were a dangerous era of trial and error design and test. Prior to 1915 little was known about the theory of flight and aircraft stability. The original Wright flyer was statically unstable and the stability of most of the early aircraft were so marginal that it was only with extreme and cautious alertness that the pilot could keep them in the air. Because of this, the airplane was not then considered a practical device.

During the two years following 1910 Elmer Sperry attempted to change this situation by designing and building a gyro stabilizer to keep the aircraft in level flight. This was the first recorded effort to control an aircraft automatically. Sperry's gyro stabilizer contained the basic elements that were used in all autopilots for the following thirty years. The gyro stabilizer of 1912 used gyros only to establish a substantially horizontal plane in the aircraft and to generate signals to operate servos driving the ailerons and elevator. In 1914, Mr Sperry's son Lawrence won a safety prize of 50,000 francs offered by the Aero Club of France for the most stable airplane. The winning demonstration, which took place in Paris, consisted of a low altitude flight down the Seine in a Curtiss flying boat with the gyro stabilizer installed. As the aircraft approached the judge's stand, the French mechanic climbed out on a wing while Sperry stood up in the cockpit and raised his hands above his head.

During the war years of 1915 to 1920, a great deal was learned about building inherent stability into the airframe. For this reason, the autopilot was no longer needed to provide stability. Over succeeding years, the biplane constructions of wood, fabric and piano wire were rapidly transformed into the basic form of the modern aircraft: a metal-skinned monoplane with a streamlined fuselage, low cantilevered wings and sophisticated flight control surfaces.

World War II brought about a large increase in military design efforts which resulted in airplanes with greatly improved speed and altitude capabilities—a trend that was accelerated through the use of jet propulsion. This was accompanied by a continual increase in control surface hinge moment requirements and a continual decrease in inherent airframe stability.

Early attempts to reduce the control stick forces which resulted from the increased surface hinge moments consisted of such aerodynamic devices as aerodynamic surface balance, servo tabs, spring tabs, etc. As aircraft speed and size continued to increase, however, it was found necessary to provide hydraulic power to aid the pilot in moving the control surfaces. Early versions of hydraulic boost systems aided the pilot by providing a portion of the required hinge moment. However, as the dynamic pressures encountered in flight continued to increase and control surface centers of pressure moved aft due to the effects of transonic and supersonic flow, it was found necessary to increase the portion of the hinge moment supplied by the hydraulic boost system. Consequently most current transonic and supersonic aircraft require that 100 percent of the surface hinge moment be supplied by the hydraulic system. The pilot in such systems merely provides the function of positioning the control surface through the hydraulic system. However, since pilots have been trained to fly by the physical association of control force with airframe responses, the introduction of artificial force producing devices (feel systems) has become necessary.

The reduction in airframe inherent stability that accompanied the improved aircraft performance since World War II stemmed from several sources, such as:

a. Increased speed resulting in wider variation of aerodynamic characteristics.

b. Increased altitude resulting in wider variation of aerodynamic characteristics.

c. Variations of the aerodynamic parameters in the transonic range.

d. Reduced effective aspect ratios and redistribution of aircraft weight components increasing the importance of inertia factors.

e. Smaller wings - higher wing loading.

f. Increase in flexibility of the aircraft structure.

The deterioration in airplane stability which has accompanied the above changes is manifested by an increase in the airframe natural frequencies, a decrease in airframe damping and deterioration of airframe static stability. This trend has continued to the present and there is no indication that future airframe designs will show an improvement. In fact there are many indications that in the future airplanes will increasingly be designed from a performance point of view only, with stability and control provided artificially through highly augmented "fly-by-wire" flight control systems.

The development of artificial means for providing stability and control was paralleled by the development of means for automatic aircraft control. By the late 1920's aircraft performance had improved to the point where the duration of flight and range were so great that pilot fatigue became an element for consideration. The usefulness of the autopilot in providing pilot relief during long hours of flight was first demonstrated publicly by Wiley Post in his solo flight around the world in 1933. The use of the autopilot for this flight attracted a considerable amount of publicity at a time when the commercial airlines were beginning their rapid expansion. It was in this same year that the United States Commerce Department gave the airlines permission to fly passengers under instrument conditions and since 1934 the autopilot has been widely used in both commercial and military aircraft.

Prior to World War II, most of the autopilots were versions of the Sperry gyro stabilizer. Their primary function was to hold the airplane "still" while the human pilot performed other duties. Physically they consisted of air-driven gyros with the gyro gimbals operating air valves.

The first all-electric autopilots were developed in 1941 and one version was used successfully in many of the bombing type aircraft of this era, in combination with the Norden bombsight, to provide automatic control of the airplane during bombing runs. With the exception of the bombsight tie-in, the autopilot was still essentially a pilot relief device, although coordinated turns could be accomplished by means of a single knob. Manual synchronization of the gyro pickoffs was required prior to engagement and the number of adjustments which the human pilot was required to make to insure proper flight control constituted one of the major disadvantages of autopilots of this era.

The first autopilot to provide automatic synchronization of the signal pickoffs was produced in 1943. This same autopilot was also the first to provide a magnetic heading reference. The altitude control function was added in the following year, and automatic landing approach equipment was used successfully in the late 1940's. With the exception of considerable refinement of components, this is the basic pilot relief autopilot used today.

In some current aircraft, the pilot no longer is directly linked to the aircraft aerodynamic control surfaces. The pilot provides inputs to an electronic flight control system which compares the pilot's command to the actual aircraft response. If the two are not in agreement, the flight control system compensates by actuating the aerodynamic control surfaces to provide the commanded response. In aircraft with electronic flight control systems, such as the F-16, the dynamics of the aircraft, and hence the handling qualities provided to the pilot, are no longer merely a function of the stability and control characteristics of the aircraft, but are dictated by the flight control system. These flight control systems provide the pilot with an aircraft which is seemingly stable despite severe aerodynamic instabilities which exist in the unaugmented airframe. We can expect that the use of such "fly-by-wire" flight control systems will increasingly become the standard, as evidenced by the development of this type of flight control system for the Airbus 320 commercial airliner.

The most modern aircraft employ ever more sophisticated flight control designs, incorporating concepts such as fault tolerance, digital computation, integrated flight, fire, and propulsion controls, and data multiplexing. Each of these features offers performance and survivability advantages. For instance, fault tolerant systems capable of reconfiguring aircraft flight control systems to compensate for lost aerodynamic control surfaces have obvious advantages for battle damaged aircraft.

The development of these sophisticated flight control systems presents a challenge to the flight test community which must ensure that new aircraft can safely, efficiently and reliably accomplish their design missions. Flight control systems must be evaluated to determine if they enhance the aircraft to perform its design role effectively without decreasing reliability through unnecessary complexity.

14.3 FLIGHT CONTROL SYSTEM DESIGN

The control system of an airplane, must meet two requirements if the pilot is to have suitable command over his airplane:

a. It must be capable of aerodynamically controlling the aircraft.

b. It must provide the pilot with the proper control force "feel."

Figure 14.1 shows a flow chart of a typical development effort used to design a flight control system to meet these requirements. As can be seen in this diagram, the development of a flight control system is an iterative process, with the results of simulations and flight tests used to make numerous changes to the flight control system before an acceptable system is obtained.

14.3.1 Airframe Design

In the initial stages of design of an aircraft control system, the airframe and its transfer functions may be considered an alterable element. Airframe parameters such as control surface effectiveness and tail size, as

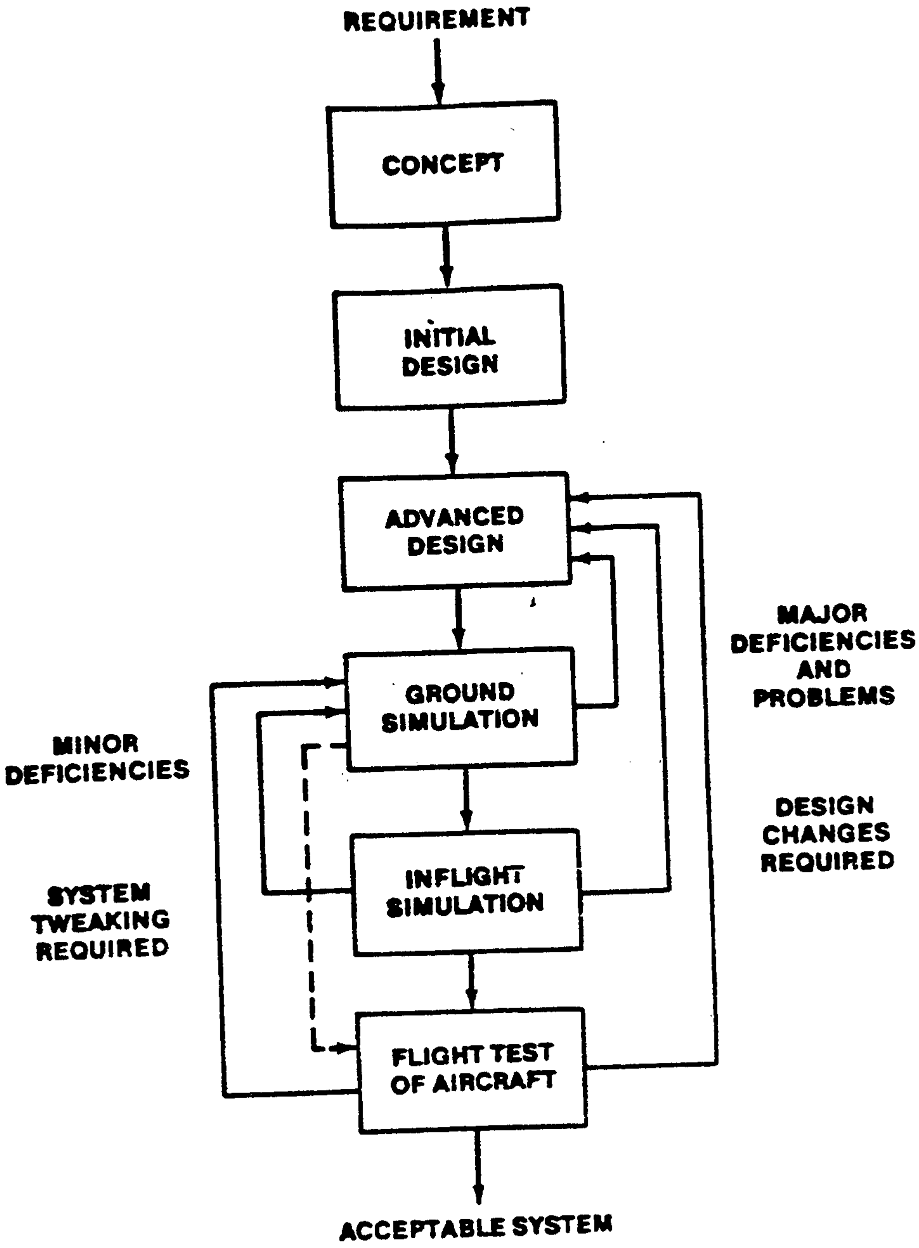
REQUIREMENT
CONCEPT
INITIAL DESIGN
ADVANCED DESIGN
GROUND SIMULATION
INFLIGHT SIMULATION
FLIGHT TEST OF AIRCRAFT
ACCEPTABLE SYSTEM
MINOR DEFICIENCIES
SYSTEM TWEAKING REQUIRED
MAJOR DEFICIENCIES AND PROBLEMS
DESIGN CHANGES REQUIRED

FIGURE 14.1 FLIGHT CONTROL SYSTEM DEVELOPMENT FLOW CHART

well as requirements for split or separate surfaces may be influenced by control system requirements during the preliminary design. Studies for establishing those airframe characteristics which are influenced by the flight control system can be made with computers utilizing the aircraft equations of motion and equations representing portions of the control system, such as a Stability Augmentation System (SAS). Many design parameters affecting the aircraft, however, are fixed by considerations other than control: primarily aircraft performance considerations. In addition, because of production requirements for lead time, the final airframe exterior configuration must be completely established very early relative to other components of the control system. These considerations make it necessary to regard the airframe as an unalterable element relatively early in the development stage, usually during the initial flight control systems design stage as shown in Figure 14.1.

14.3.2 Advanced Design

During advanced design, simulations of the flight control system should be accomplished. The simulation process should begin with a concerted piloted ground simulation phase using sophisticated simulations with high quality visual systems (not necessarily the most visually aesthetic, but having minimal time delays which can overshadow major handling qualities problems). Both operational and test pilots should fly the simulation in as realistic a manner as possible. Major handling qualities deficiencies uncovered during the ground simulation phase should be corrected prior to flight. In-flight simulations should also be used to determine deficiencies before hardware or software for the flight test vehicle are finalized. Flight tests are then used to evaluate the flight control systems and any remaining problems associated with the system design. Once the flight control design has matriculated through all the iterations of design, simulation and flight test, the configuration is judged to be acceptable, although it is unlikely that aircraft flight control system testing on aircraft like the F-16 will end so long as the aircraft is in the inventory. New mission requirements will arise and result in flight control system refinements.

14.3.3 Aircraft Models

Once the aircraft aerodynamic configuration is determined to meet the mission performance specifications, the requirement for a stability and control augmentation system usually arises to correct handling qualities deficiencies. The design of these systems is greatly facilitated when the motions of the airframe are represented by a mathematical model. The equations which represent the mathematical model of the airframe can be derived by equating the aerodynamic forces and moments acting on the airframe to the inertial reactions according to Newton's laws. As shown in Chapter 4, the rigid airframe has six degrees of freedom in space. It was shown that six nonlinear simultaneous differential equations are required to provide a complete representation of rigid airframe motion. Three additional equations are required to describe the airframe orientation with respect to the earth.

For reasons of comfort, safety and mission performance it is desirable that the aircraft fly along a smooth path. It is therefore reasonable to consider departures from a smooth flight path as small perturbations. As shown in Chapter 4, this assumption permits considerable simplification of the airframe equations of motion. As a result of this simplification, the six nonlinear differential equations reduce to two independent sets of three linear simultaneous differential equations, the "aircraft small perturbation equations of motion." The simplification provided by the small perturbation assumption facilitates the manipulation of the airframe mathematical model because the resulting equations are linear and therefore subject to many analytical techniques involving the use of transfer functions. The stability derivatives for these equations can be analytically computed or derived from wind tunnel or flight test data. Appendix A provides the commonly used equations of motion and a brief description of how to obtain the transfer function relating an output dynamic motion parameter to a particular control surface input.

The longitudinal model of the aircraft is shown in Figure 14.2 for an elevator input. The single aerodynamic surface, when deflected, affects several aircraft motion parameters simultaneously. Normally, the aircraft block is simplified, as in Figure 14.2a, showing the elevator input and only the outputs of interest, pitch attitude for instance. The model in Figure 14.2b is always implied.

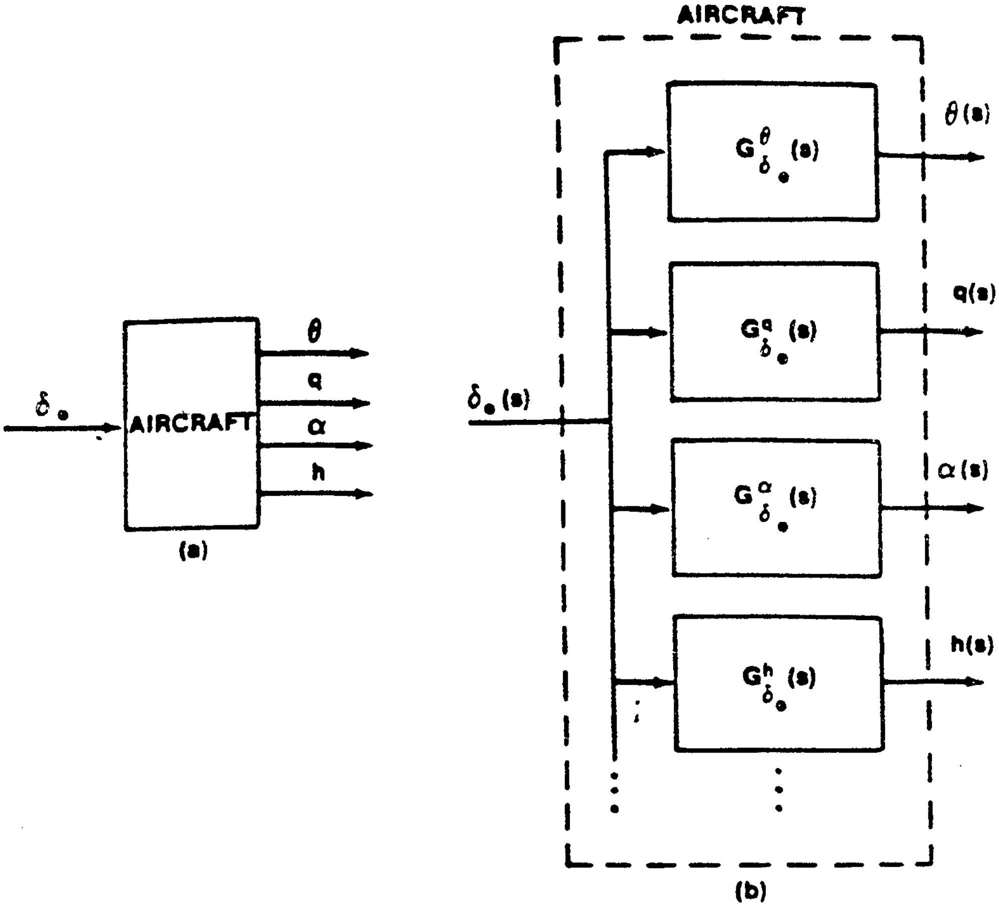

δ_e
AIRCRAFT
θ
q
α
h
(a)
AIRCRAFT
$\delta_e(s)$
$G^{\theta}_{\delta_e}(s)$
$G^{q}_{\delta_e}(s)$
$G^{\alpha}_{\delta_e}(s)$
$G^{h}_{\delta_e}(s)$
$\theta(s)$
q(s)
$\alpha(s)$
h(s)
(b)

14.2 AIRCRAFT LONGITUDINAL AXIS MODEL

The lateral-directional axes model is shown in Figure 14.3. It is complicated by the fact that two controls can simultaneously affect all the aircraft motion parameters. Once again, the aircraft block is usually simplified, as in Figure 14.3, but the more complete diagram of Figure 14.3b is always implied. If two controls are considered in the longitudinal axis, such as flap deflection in addition to the elevator input, then a more complex model, similar to the lateral-directional model, is necessary.

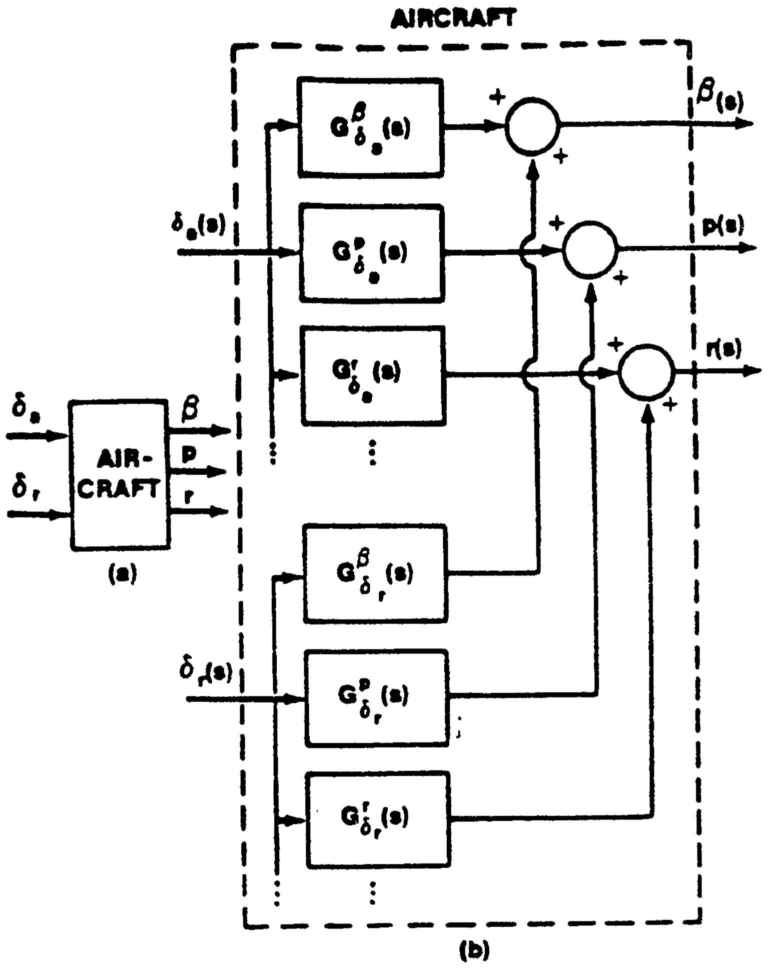
AIRCRAFT
δ_a
δ_r
AIR-CRAFT
β
p
r
(a)
$\delta_a(s)$
$G^{\beta}_{\delta_a}(s)$
$G^{p}_{\delta_a}(s)$
$G^{r}_{\delta_a}(s)$
$\delta_r(s)$
$G^{\beta}_{\delta_r}(s)$
$G^{p}_{\delta_r}(s)$
$G^{r}_{\delta_r}(s)$
+
+
$\beta(s)$
p(s)
r(s)
(b)

FIGURE 14.3 AIRCRAFT LATERAL-DIRECTIONAL AXES MODEL

14.3.4 Control Forces and Deflection

It is of primary importance in flight control system design that the pilot is provided proper control force "feel." The pilot not only gets the "feel" from the forces themselves but from the movement of the cockpit controls. In some flight conditions the cockpit control movement can be considerable. In most cases, however, (particularly at high speed and with aft center of gravity) the cockpit control movement is barely perceptible. For this reason, cockpit control forces are the most important indications of the severity of a maneuver. It follows from this that there should be no reversal of these forces which would require the pilot to reverse his thinking. This line of reasoning leads to the following requirements.

a. A pull force (defined as positive) should always lift the nose and slow the airplane.
b. A push force (defined as negative) should always drop the nose and speed up the airplane.

Control deflections should never reverse either. This requirement can be relaxed considerably (and very often ignored) in those flight conditions where control movement is not very noticeable. If the control movement is negligibly small, a pilot will sense that a pull is required to slow down. The pilot will be unaware that the control may in fact have moved forward a slight amount. In the most modern flight control systems, such as the F-16, there is very little movement of the cockpit controls at all.

14.3.5 Aircraft Sign Conventions

Understanding the sign convention is important prior to starting any analysis, as the phasing (summing junction signs) necessary to obtain proper operation in the feedback control system is dependent on the sign convention used. Using the TPS sign convention, a positive pitch implies the aircraft nose going up and the tail going down (according to the right hand rule with the aircraft Y body axis pointing out the right wing). This implies that a positive elevator deflection indicates the leading edge is deflected down and the trailing edge deflected up. This means that a positive elevator input will produce a positive pitching motion. Using a similar definition, positive rudder produces positive yaw rate.

There are other sign conventions than the one used at the USAF Test Pilot School. Table 14.1 compares the NASA sign convention with the normal TPS Sign convention. The sign convention can be quickly determined by observing the sign of the gain term in the aircraft transfer functions. The sign of the $G^{q}_{\delta_e}$, $G^{p}_{\delta_a}$ and $G^{r}_{\delta_r}$, gain term indicates the direction that the aircraft will initially move when the control surface is deflected in the positive direction (but may not indicate intermediate or final motion directions). A positive sign on $G^{q}_{\delta_e}$ indicates positive elevator trailing edge up in the Test Pilot School sign convention.

TABLE 14.1

SIGN CONVENTION

CONTROL DISPLACEMENT	**TPS**	**NASA**
$+\delta_r$	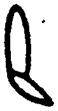 **(TER)**	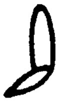 **(TEL)**
$+\delta_e$	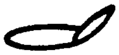 **(TEU)**	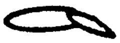 **(TED)**
$+\delta_a$	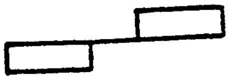	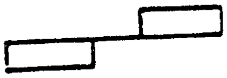

14.4 SIMPLE MECHANICAL AND HYDRAULIC SYSTEMS

There are many ways in which the controls of an aircraft can be arranged. In this section, the basic mechanical and hydraulic components encountered in current aircraft are discussed. The more sophisticated flight control systems presented in later sections build upon these fundamental elements.

Simple mechanical and hydraulic flight control systems use cables, rods, levers, bellcranks, and gears to transmit the pilot control stick or rudder pedal displacement to the aerodynamic control surface—or control actuator (in the case of hydraulically boosted or irreversible control systems). Additional elements, such as springs, dampers, and bobweights may be connected to the mechanical flight control system to improve the handling qualities of the aircraft by providing artificial feel. Very broadly, there are two classes of control systems: reversible and irreversible.

Reversible flight control systems are control systems where movement of the cockpit controls result in movement of the aerodynamic surface controls through a direct mechanical linkage. This linkage may consist of cables, push-rods or any combination thereof. Consequently, movement of the aerodynamic surface controls results in movement of the cockpit controls.

Irreversible flight control systems are control systems where movement of the cockpit controls results in movement of the aerodynamic surface controls either partially or completely with the help of an electro-hydraulic and/or electro-mechanical actuation device. Movement of the aerodynamic surface controls directly with the cockpit controls is usually not even possible. Consequently the system is irreversible.

As may be expected, the effects of reversible and irreversible controls are different. In the reversible flight control system, the control forces are created by the control surface hinge moments and may be interpreted as their reaction to control movements. It is a characteristic of the reversible system that the control surface hinge moment can move the stick (or wheel) as well as the stick (or wheel) force can move the control surface: hence the term reversible. In the irreversible system, there is generally no way for the surface hinge moments to move the stick (or wheel). Therefore, providing the pilot with proper control force feel will require the addition of what is called an artificial feel system.

14.4.1 Simple Mechanical Elements

In its simplest form a mechanical flight control system is made up of levers, bellcranks, rods and cables as shown in the simplified longitudinal flight control system in figure 14.4. Even though this figure suggests that push-rods are used in conventional mechanical controls, the fact is that most often these controls are mechanized by a cable-pulley arrangement. In many airplanes, however, a mixture of the two is employed.

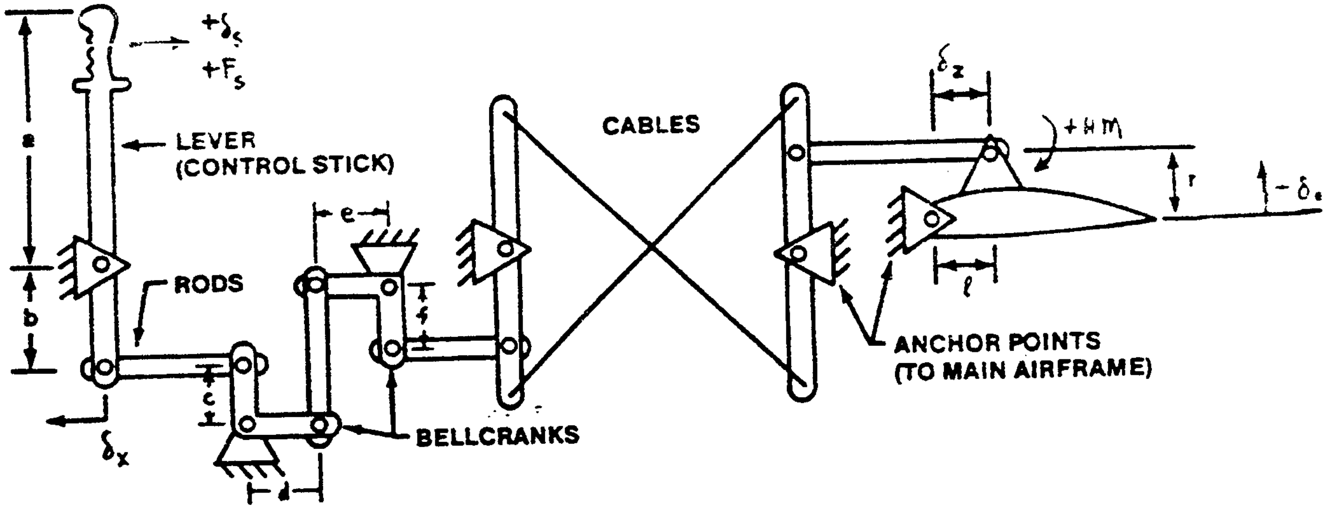

FIGURE 14.4. SIMPLE MECHANICAL FLIGHT CONTROL SYSTEM

These simple mechanical elements act as amplifiers and may be described mathematically and represented in a block diagram relating pilot control deflection to aerodynamic surface deflection. In the longitudinal case this will relate longitudinal stick deflections (δ_s) to elevator deflection (δ_e).

The control stick is a simple lever which relates the movement of the first push rod (δ_x) to the pilot input according to the relationship:

$$\frac{\delta_s}{\delta_x} = -\frac{a}{b} \tag{14.1}$$

rearranging we see that the movement of the control system is reduced and reversed in sign.

$$\delta_x = -\frac{b}{a}\,\delta_s \tag{14.2}$$

Rods and cables are used in the system to transmit the forces over a distance and have a gain of 1.

Bellcranks are used to alter the direction of the applied force. They may have gains different than 1 if the two legs are of different lengths. For this example, the gains of the bellcranks are d/c and f/e. Crossed cables have a net gain of -1. The surface deflection (δ_e) is related to the connecting rod deflection (δ_z) by

$$\sin\delta_e = \frac{\delta_z}{r + \frac{l\tan\delta_e}{2}} \tag{14.3}$$

The anchor point of the elevator is usually positioned at the point where is zero. If we assume this is the case, and make the small angle approximation for the elevator deflection ($\sin\delta_e = \delta_e$) then

$$\delta_e = \frac{\delta_z}{r} \tag{14.4}$$

which can be approximated as

$$\frac{\delta_z}{r} = \delta_e \quad \text{(radians)} \tag{14.5}$$

The block diagram of the system is shown in Figure 14.5.

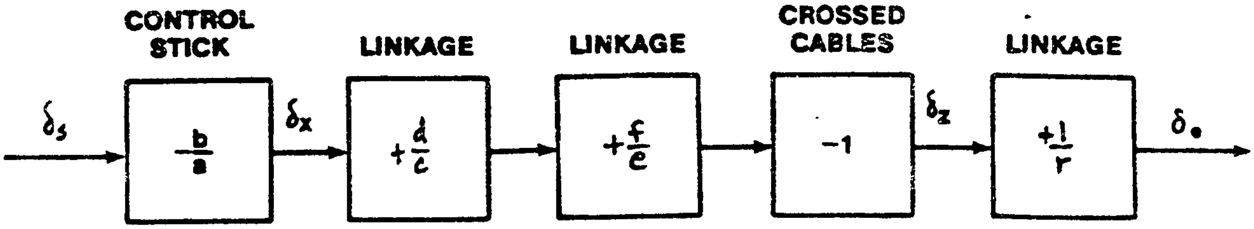
CONTROL STICK
LINKAGE
LINKAGE
CROSSED CABLES
LINKAGE
δ_s
$-\frac{b}{a}$
δ_x
$+\frac{d}{c}$
$+\frac{f}{e}$
-1
δ_z
$+\frac{1}{r}$
δ_e

FIGURE 14.5 BLOCK DIAGRAM OF SIMPLE MECHANICAL FLIGHT CONTROL SYSTEM

From the block diagram we see that the output, δ_e, can be related to the input, δ_s, by multiplying the blocks:

$$\delta_e = \left(\frac{-b}{a}\right)\left(\frac{d}{c}\right)\left(\frac{f}{e}\right)(-1)\left(\frac{1}{r}\right)\delta_s = \left(\frac{b\cdot d\cdot f}{a\cdot c\cdot e\cdot r}\right)\delta_s \tag{14.6}$$

14.4.2 Controlling Hinge Moments in Reversible Control Systems

In a reversible flight control system, the aerodynamic force on the control surface attempts to rotate the surface to the point where aerodynamic forces are neutral on the surface. This causes a torque, called the hinge moment, on the surface. The pilot opposes the hinge moment with stick force. This section will use examples from the longitudinal case. It will be evident that most of what is presented can also apply to roll and rudder controls.

Summing the moments about each of the anchor points for the longitudinal case shown in figure 14.4 we can relate the hinge moment (HM) to the stick force (F_s) as follows (with the term 1/r having the units to convert the moment HM to a force F_s):

$$F_s = \left(\frac{-b}{a}\right)\left(\frac{d}{c}\right)\left(\frac{f}{e}\right)(-1)\left(\frac{1}{r}\right)(HM) = \left(\frac{b \cdot d \cdot f}{a \cdot c \cdot e \cdot r}\right)(HM) \qquad (14.7)$$

Introducing the concept of gearing ratio, G, defined by:

$$G = \left(\frac{-b}{a}\right)\left(\frac{d}{c}\right)\left(\frac{f}{e}\right)(-1)\left(\frac{1}{r}\right) \qquad (14.8)$$

it is seen that

$$F_s = G \quad HM \qquad (14.9)$$

The designer has a certain amount of leeway in selecting G. It should be recognized, however, that the choice of the stick gain, b/a is subject to human limitation (arm movement) as well as cockpit space limitations. The other ratios in equation (14.8) are also subject to geometric and structural limitations. The selection of G affects both speed stability ($\partial F_s/\partial V$) and stick forces during maneuvering flight ($\partial F_s/\partial n$).

As the speed and size of the aircraft increases, the hinge moments that must be overcome with stick force in order to change speed or maneuver may increase to unacceptable levels. If the hinge moment is great enough, adjustments to gearing ratio G are no longer adequate to maintain stick force variation with speed and load factor at acceptable levels. An alternative means of reducing F_s is then necessary. In addition, when the aircraft is stabilized at a new flight condition, the pilot will want to reduce the stick force to zero through some means of trim.

Reversible control systems usually use either trim tabs or variations in horizontal stabilizer incidence in order to trim stick forces. Stick force variation with speed and load factor can be adjusted in two ways: 1) by aerodynamic means, and 2) through power boost.

14.4.2.1 Stick Force Trim

By analogy to other aerodynamic forces and moments the control surface hinge moment can be expressed as

$$HM = q_H S_e c_e C_h \qquad (14.10)$$

where C_h is the elevator hinge moment coefficient. This hinge moment coefficient, for a given control surface hinge line location has been found to depend on the horizontal tail angle of attack (α_H), the elevator deflection (δ_e), Mach and Reynolds number. As was the case with other aerodynamic coefficients, C_h is usually expressed as

$$C_h = C_{h_0} + C_{h_\alpha} \alpha_H + C_{h_{\delta_e}} \delta_e + C_{h_{\delta_t}} \delta_t \qquad (14.11)$$

C_{h_0} is the hinge moment coefficient when the tail is at zero lift. For a symmetric tail, $C_{h_0} = 0$. The hinge moment derivatives $C_{h_\alpha} = \frac{\partial C_h}{\partial \alpha}$, $C_{h_{\delta_e}} = \frac{\partial C_h}{\partial \delta_e}$ and $C_{h_{\delta_t}} = \frac{\partial C_h}{\partial \delta_t}$ are dependent on Mach and Reynolds number. For large values of α_H and δ_e, they are also dependent on α_H and δ_e.

The term δ_t is trim tab deflection. Aircraft with a fixed horizontal stabilizer can achieve stick force trim ($F_s = 0$) with an elevator trim tab. The tab hinge moment is a function of tab deflection relative to the elevator. The pilot is capable of deflecting the tab with a so-called trim-wheel or similar device. By rotating the trim wheel the pilot can set the stick force to zero by introducing enough tab hinge moment to allow the overall hinge moment to vanish.

A useful by-product of the trim function in general is an effective change in that portion of the stick force dependent on speed. The gradient $\partial F_s/\partial V$ is dependent on the trim speed itself and decreases with increasing speed. Consequently the trimability or ability to maintain a prescribed trim speed, while always present, deteriorates in aircraft with reversible flight control systems as trim speed increases.

The trim tab is, therefore, seen to be a very important addition to the conventional mechanical control system by serving two purposes: 1) stick force trim and 2) speed stability.

The trim tab linkage must be arranged to permit tab deflections independent of elevator deflections. Therefore it is necessary to connect the tab follower arm directly to the elevator. Tab deflection is often produced by means of a jackscrew inserted in the follower arm. The cables from the pilot's trim wheel actuate the jackscrew, varying the follower arm length and causing tab deflection. Schematically two possible arrangements were shown in Figure 14.6.

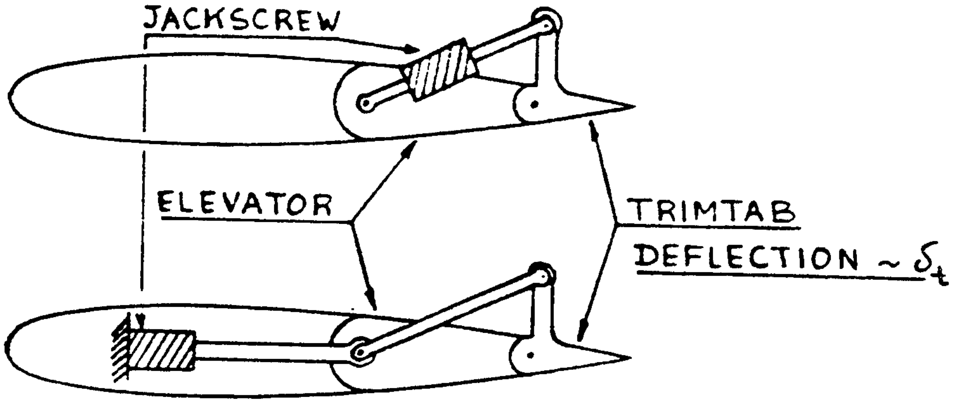

FIGURE 14.6 EXAMPLE OF AN ELEVATOR WITH TWO TYPES OF TRIM TAB CONFIGURATIONS

An alternate method of stick force trim in reversible flight control systems is to change the horizontal tail angle of incidence (i_H). The angle of attack seen at the tail (α) related to the aircraft angle of attack as

$$\alpha_H = \alpha - \varepsilon + i_H \tag{14.12}$$

where = downwash angle.

Substituting this into equation (14.11) and assuming there is no trim tab deflection and $C_h = 0$:

$$C_h = C_{h_\alpha} (\alpha - \varepsilon + i_H) + C_{h_{\delta e}} \delta_e \tag{14.13}$$

From this equation we can see that zero hinge moment HM can be achieved with

$$i_H = \varepsilon - \alpha - \frac{C_{h_{\delta e}}}{C_{h_\alpha}} \delta_e \tag{14.14}$$

Aircraft such as the KC-135 can change the stabilizer setting i_H to make $F_s = 0$ and thereby obtain stick force trim.

14.4.2.2 Aerodynamic Means of Adjusting Stick Force

Stick force variation with speed $(\partial F_s/\partial V)$ and load factor $(\partial F_s/\partial n)$ can be adjusted by aerodynamic means. This is accomplished through adjustments to $C_{h_{\delta_e}}$. Referring to equation 14.11, the hinge moment coefficient C_h can be seen to depend upon $C_{h_{\delta_e}}$ when the elevator is deflected from the trim position $(\delta_e \neq 0)$.

A decrease in $C_{h_{\delta_e}}$ reduces both speed stability and maneuvering force gradients. The opposite is also true. Therefore, the force gradients can be either "stiffened " or "softened" if somehow $C_{h_{\delta_e}}$ can be varied. This is commonly accomplished through the use of balance tabs, blow-down tabs, servo tabs or spring tabs.

14.4.2.2.1 Balance Tabs

A simple way to obtain a variable value of $C_{h_{\delta_e}}$ is a tab with a hinge moment which is proportional to elevator deflection. A tab with these characteristics is called a balance tab. The simplest linkage that achieves the desired tab motion is a follower arm between the tab horn and a horn fixed to the stabilizer structure. Examples are shown in figures 14.7 and 14.8. The ratio of tab and elevator deflections can be selected by proper design of the length of the stabilizer horn. If this length becomes negative the tab deflection reverses. Figures 14.7 and 14.8 illustrate lagging and leading balance tabs, which respectively reduce and increase the magnitude of $C_{h_{\delta_e}}$.

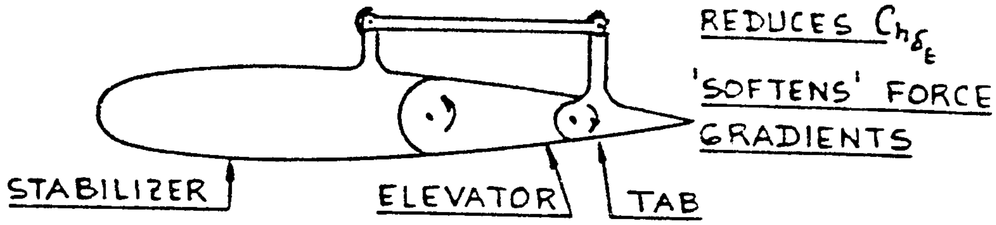

FIGURE 14.7. EXAMPLE OF LAGGING TAB

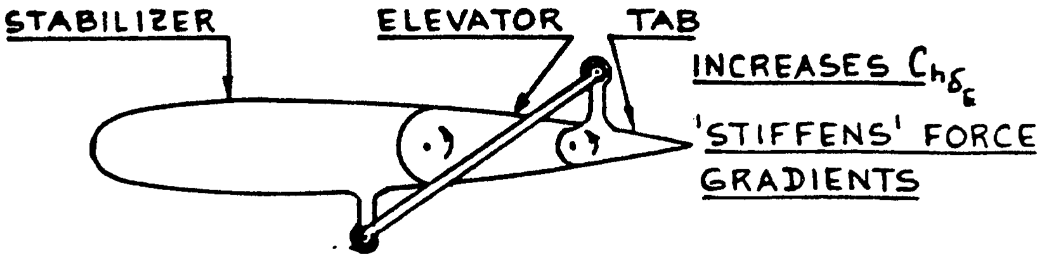
STABILIZER
ELEVATOR
TAB
INCREASES $C_{h_{\delta_E}}$
'STIFFENS' FORCE GRADIENTS

FIGURE 14.8 EXAMPLE OF LEADING TAB

The balance tab can also serve as a trim tab by insertion of a jackscrew in the tab follower arm. An example is shown in Figure 14.9.

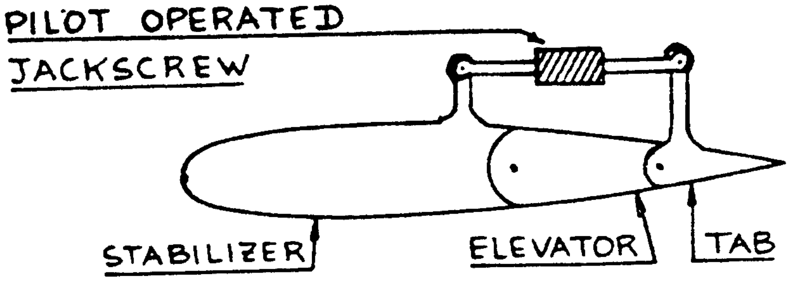
PILOT OPERATED JACKSCREW
STABILIZER
ELEVATOR
TAB

FIGURE 14.9 COMBINATION BALANCE-TRIM TAB

14.4.2.2.2 Blow-Down Tabs

An effective method of adjusting stick force gradient is with a blow-down tab as illustrated in Figure 14.10. The tab linkage consists of a preloaded spring (in tension) fixed to the elevator and pulling on the tab horn such as to produce negative tab deflection. The tab has a hard stop against which it is held by the spring at zero speed. As speed increases the airload deflects the tab away from the stop. Above the speed at which the tab comes off its stop the tab hinge moment about its own hinge line exactly balances the moment derivatives about the tab hinge line and elevator hinge line are proportional, the end result is a constant increment of elevator hinge moment which is felt in the stick as a constant force increment.

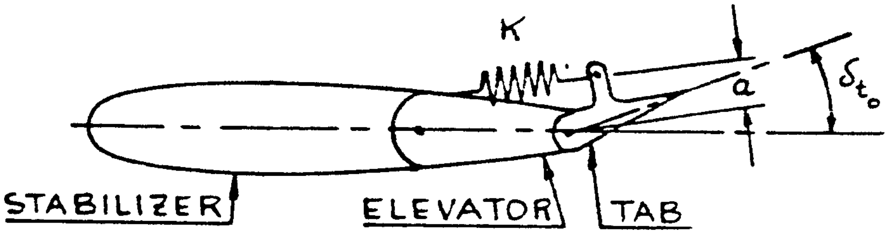
K
a
δ_{t_o}
STABILIZER
ELEVATOR
TAB

FIGURE 14.10 EXAMPLE OF A BLOW-DOWN TAB

The effect of a blow-down tab on the stick force gradient is to add a stick force increment independent of speed. The pilot will interpret this as an increase in stick-free stability $(\partial F_s/\partial V)$.

The reader should remember that the stick force increment produced by the blow-down tab is independent of speed only for speeds above those required to blow the tab away from its stop. If the stick force versus speed (at a constant trim tab setting) is plotted, a sharp discontinuity appears where the blow-down tab leaves its stop. This is illustrated in Figure 14.11. The speed corresponding to the discontinuity can be changed by varying the spring preload.

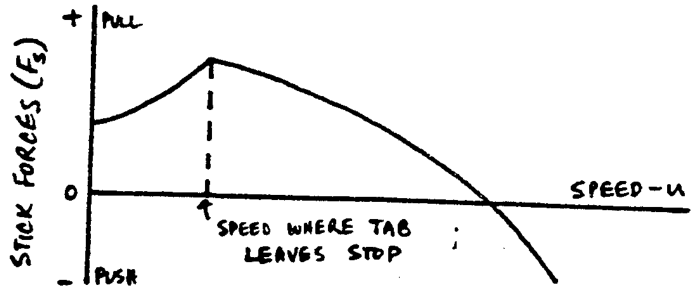

FIGURE 14.11 ILLUSTRATION OF THE EFFECT OF A BLOW-DOWN TAB

It must be remembered that any time a "springy" element is added in the control system, a potential for flutter can arise. A thorough flutter-analysis is then required.

14.4.2.2.3 Servo Tab and Spring Tab

For large aircraft with large flight control surfaces, the pilot can not provide the control forces needed to move the controls. Some form of assistance is required. If it is desired to stay with mechanical controls, servo-tabs may help out. Figure 14.12 illustrates a possible servo-tab arrangement. With this arrangement there exists a direct connection from the stick to the tab. When the tab deflects, the tab moment about the elevator hinge drives the elevator while the pilot needs only to react the tab hinge moment about its own axis. In Figure 14.12, the stick is connected to the free floating link, B-C, via the stick follower arm, A-B. The tab follower arm, B-D, is connected to the tab horn. Stick motion produces a tab deflection relative to a fixed body reference. Except for approximately negligible friction in its bearing, the free-floating link exerts no moment on the elevator. The deflection of the tab drives the elevator to a deflection which is uniquely defined by the condition of zero total hinge moment on the elevator ($C_h = 0$). Schematically, the sequence of a sudden stick displacement is given in Figure 14.12 from an initially trimmed condition.

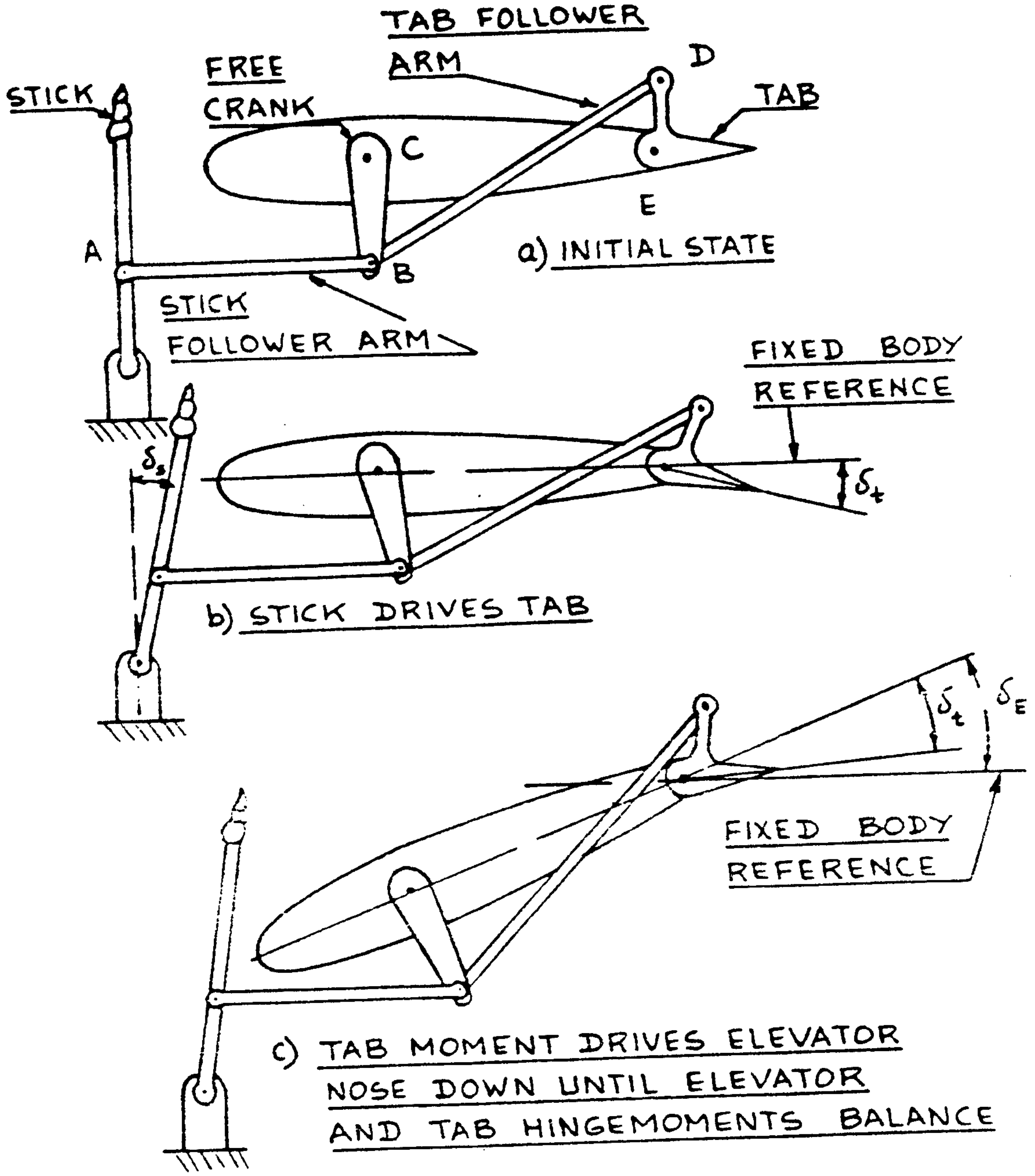
TAB FOLLOWER ARM
FREE CRANK
STICK
D
TAB
C
E
A
B
a) INITIAL STATE
STICK FOLLOWER ARM
FIXED BODY REFERENCE
δ_s
δ_t
b) STICK DRIVES TAB
δ_t
δ_E
FIXED BODY REFERENCE
c) TAB MOMENT DRIVES ELEVATOR NOSE DOWN UNTIL ELEVATOR AND TAB HINGEMOMENTS BALANCE

FIGURE 14.12 EXAMPLE OF A SERVO TAB AND A TYPICAL SEQUENCE OF ITS OPERATION

At low speeds the stick-force required to hold the servo-tab may be small. For that reason a spring tab is often used. A spring tab is obtained by adding a spring between the free link and the elevator as illustrated in figure 14.13. Its function is to provide force feedback to the stick, which is a desirable feature at low speed where the tab hinge moments are low.

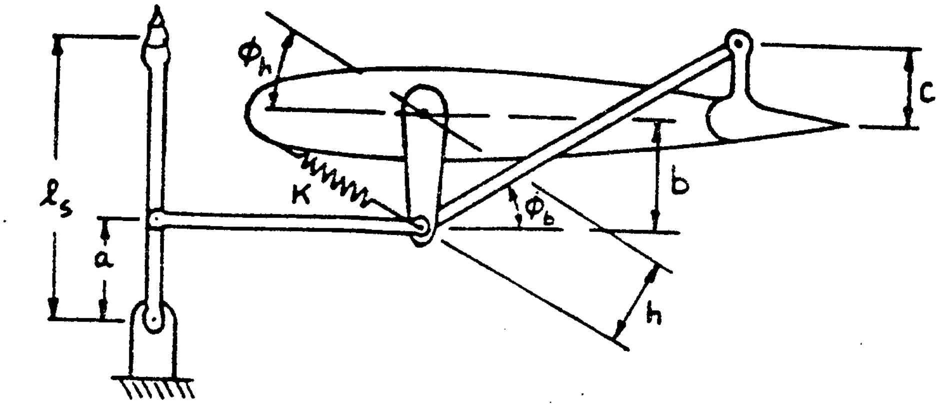

FIGURE 14.13 EXAMPLE OF A SPRING TAB

14.4.2.3 Power Boost

If the control surfaces and control forces become so large that even spring or servo-tabs cannot handle them, a case can be made for control systems with power boost.

There are two methods by which a pilot can be given an assist in moving a control surface:

a) extensible follower arm method

b) extensible bellcrank pivot

Figure 14.14 presents an example of each method. The figure suggests the use of an electromechanical jackscrew. However, any method (hydraulic, pneumatic or mechanical) will achieve the desired objective.

With the very large extension of flight envelopes in military fighter airplanes and the development of large civil jet transport, even power-boost systems are not satisfactory and power is then required for all flight control movement. The flight control systems then becomes an irreversible control which is described in section 14.4.4.

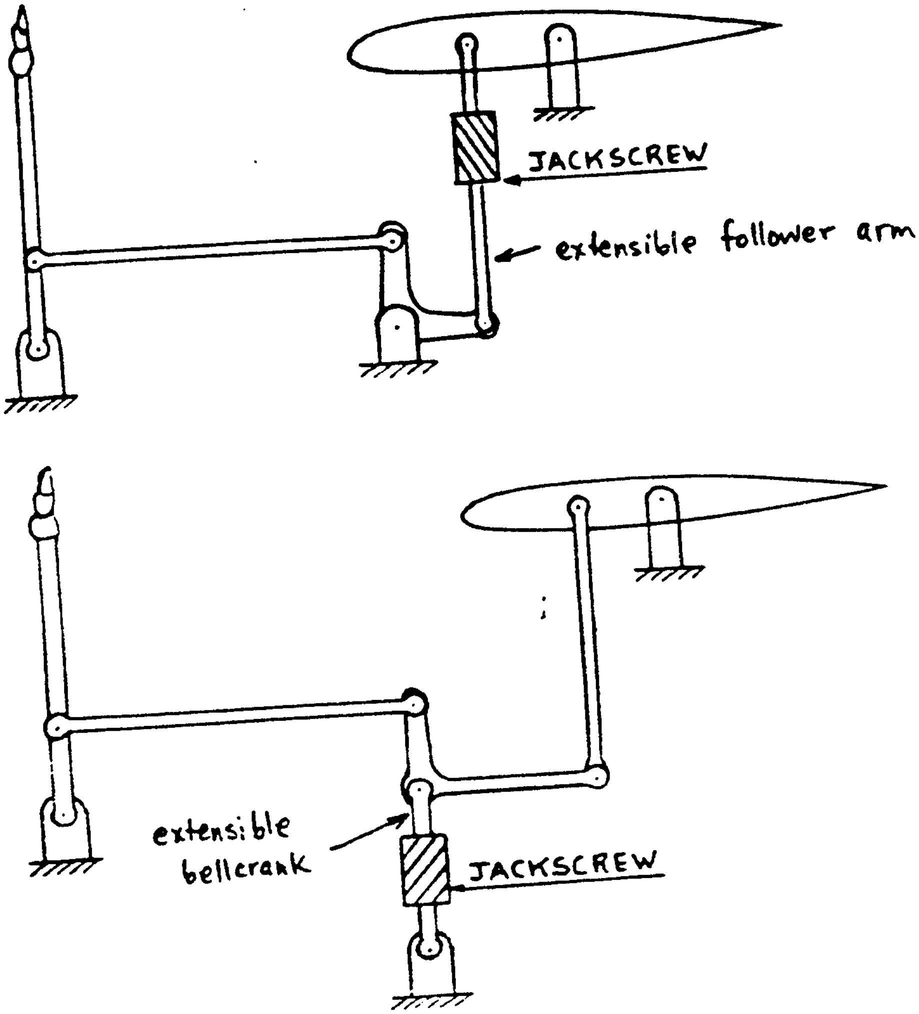
JACKSCREW
extensible follower arm
extensible bellcrank
JACKSCREW

FIGURE 14.14 EXAMPLES OF POWER BOOST

14.4.3 Hydraulic Actuators and Power Boost

Figure 14.15 shows a schematic diagram of a typical hydraulic power actuator commonly used in high performance aircraft to deflect aerodynamic surfaces such as the primary flight controls, flaps, spoilers, and speedbrakes. A servo valve provides hydraulic fluid flow control to a power cylinder that amplifies the applied forces to move the control surface. The servo valve transforms a mechanical displacement to a fluid flow rate. The power cyclinder transforms fluid pressure to a hinge moment to deflect the surface. This type of actuator can be used to move the control surfaces in an irreversible control system (section 14.4.4) or assist in moving the control surfaces in power boost for a reversible control system (section 14.4.2).

The control surface deflection is related to the power cylinder piston position as

$$y = \ell_1 \delta \qquad (\sin \delta \approx \delta) \tag{14.15}$$

for small surface deflections, and the rate of hydraulic fluid flow into the power cylinder is related to the rate of piston movement as

$$A\dot{y} = q \tag{14.16}$$

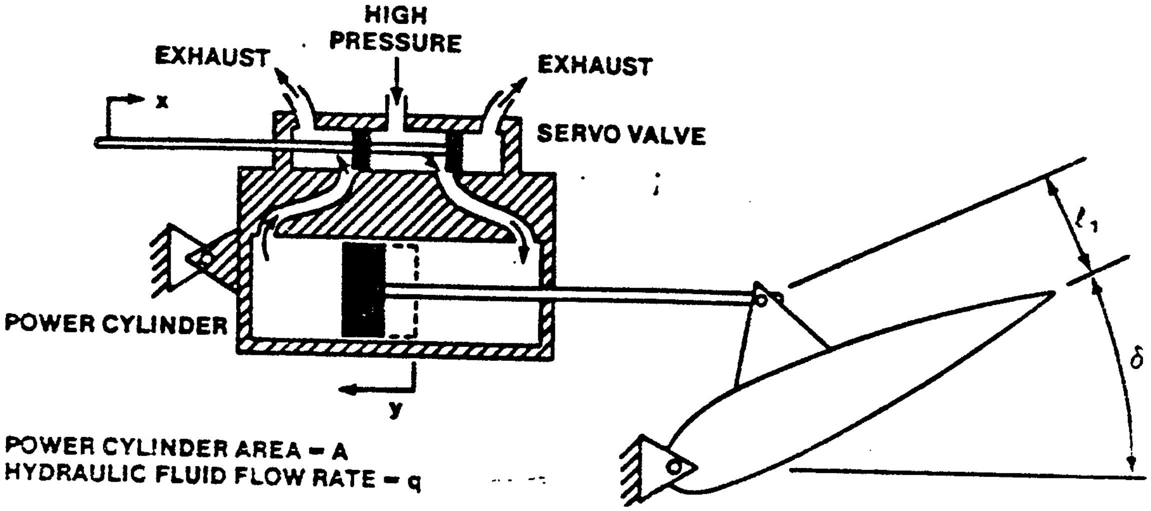
HIGH PRESSURE
EXHAUST
EXHAUST
x
SERVO VALVE
ℓ_1
POWER CYLINDER
δ
y
POWER CYLINDER AREA = A
HYDRAULIC FLUID FLOW RATE = q

FIGURE 14.15 SCHEMATIC DIAGRAM OF A HYDRAULIC ACTUATOR

The fluid rate through the series servo is assumed to be linear and may be expressed as a function of the displacement, x, as

$$q = Cx \tag{14.17}$$

The transfer function between the aerodynamic surface deflection and the input mechanical rod displacement is derived as follows

$$\dot{y} = \ell_1 \dot{\delta} \tag{14.18}$$

$$\frac{q}{A} = \ell_1 \dot{\delta} \tag{14.19}$$

$$\frac{C}{A} x = \ell_1 \dot{\delta} \tag{14.20}$$

$$\frac{\delta(s)}{x(s)} = \frac{C}{A \ell_1 s} = \frac{K}{s} \tag{14.21}$$

This analysis shows that the actuator is an integrator and a constant displacement of the valve results in a constant rate of change in the surface position. This actuator response would be undesirable to a pilot since he would have to apply pulse inputs into the flight control system to obtain a change in elevator position. Feedback of the elevator position to the servo valve is required to change the integral action of the power cylinder so that the pilot input commands an aerodynamic surface position. This feedback can be accomplished mechanically or electrically.

Two implementations are possible—the actuator in parallel or in series with the pilot aerodynamic surface command. The parallel implementation is used in some reversible flight control systems such as the T-33 and A-10 to boost the pilot command signals, thereby reducing the pilot control forces while providing a backup mechanical control system capability. The series approach is used in irreversible flight control systems, such as systems in the T-38 and F-4. Aircraft with high authority control augmentation systems (A-7 and F-15) use a series actuator system which can be controlled mechanically and electrically—mechanically through the backup mechanical flight control system and electrically through the control augmentation system. Fly-by-wire aircraft, such as the F-16, control the hydraulic actuator electrically.

Figure 14.16 presents the aileron control system for the A-10 which is made up of levers, bellcranks, rods, cables, and an electric trim motor as well as a walking beam hydraulic actuator. Figure 14.17 shows a schematic of such an actuator which provides power boost.

The pilot command displacement, x, is applied to the walking beam. Initially, aerodynamic hinge moments effectively fix the mechanical feedback linkage from the aerodynamic surface to the walking beam so that the pilot input causes the servo valve to open. Hydraulic fluid causes the power cylinder to move, deflecting the aerodynamic surface. The mechanical linkage to the walking beam causes the walking beam to rotate about the fixed pilot input linkage, forcing the servo valve to close. This mechanically provides the necessary feedback to change the integral action of the actuator.

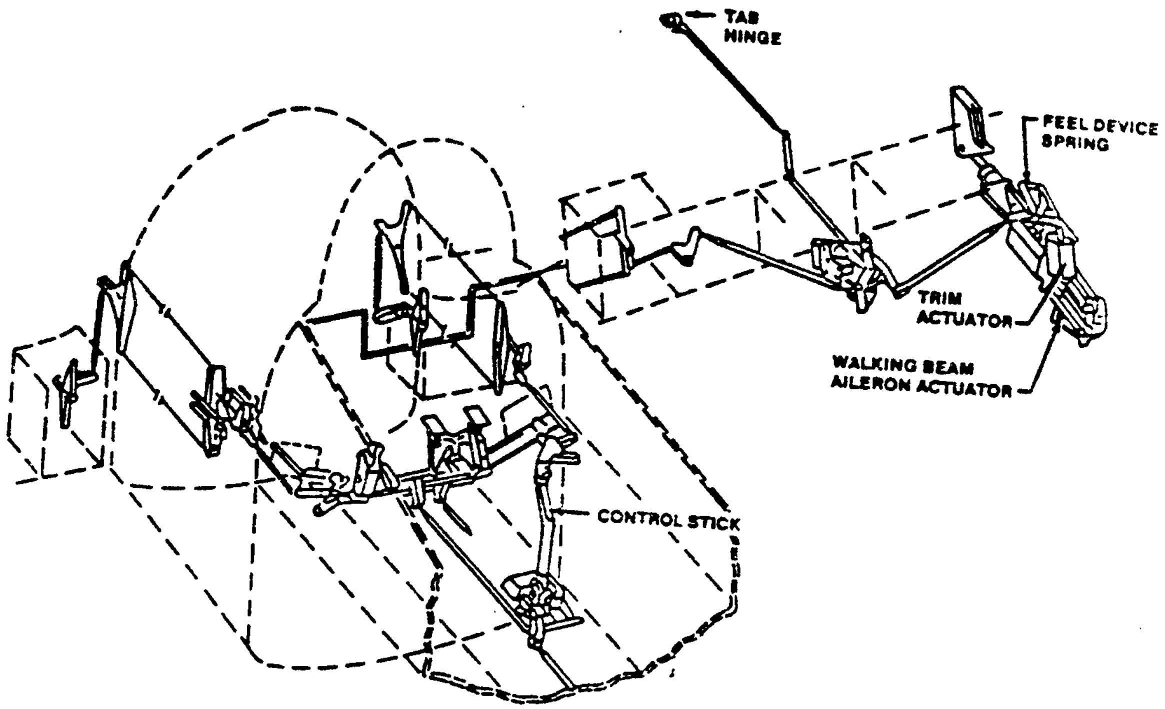
TAB HINGE
FEEL DEVICE SPRING
TRIM ACTUATOR
WALKING BEAM AILERON ACTUATOR
CONTROL STICK

FIGURE 14.16 SCHEMATIC DIAGRAM OF THE A-10 LATERAL CONTROL SYSTEM

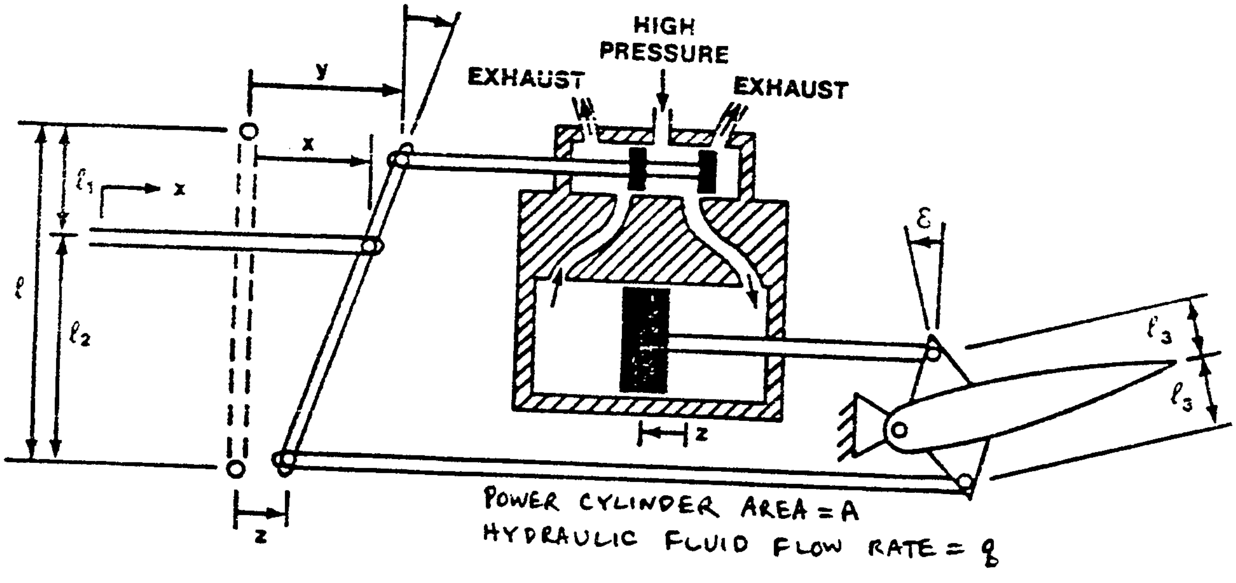
y
x
HIGH PRESSURE
EXHAUST
EXHAUST
ℓ_1
x
ℓ
ℓ_2
ε
ℓ_3
ℓ_3
z
z

POWER CYLINDER AREA = A
HYDRAULIC FLUID FLOW RATE = q

FIGURE 14.17 SCHEMATIC DIAGRAM OF A WALKING BEAM HYDRAULIC BOOST SYSTEM

Mathematically, the aerodynamic surface deflection is related to the piston movement as

$$\varepsilon = \frac{z}{\ell_3} \qquad (\sin\varepsilon \simeq \varepsilon) \tag{14.22}$$

for small surface deflections. The servo valve position is related to the piston position and the pilot input linkage position as

$$y = \frac{\ell}{\ell_2} x - \frac{\ell_1}{\ell_2} z \tag{14.23}$$

The rate of change of the piston position is related to the fluid flow rate (which is related to the servo valve position) as

$$A\dot{z} = q = Cy \tag{14.24}$$

and the rate of change of the surface deflection as:

$$\dot{\varepsilon} = \frac{\dot{z}}{\ell_3} \tag{14.25}$$

Combining the four relations above yields

$$\dot{\varepsilon} = \frac{C}{A\ell_3} y = \frac{C\ell}{A\ell_2\ell_3} x - \frac{C\ell_1}{A\ell_2}\varepsilon \tag{14.26}$$

rearranging,

$$\dot{\varepsilon} + \frac{C\ell_1}{A\ell_2}\varepsilon = \frac{C\ell}{A\ell_2\ell_3} x \tag{14.27}$$

which, using the Laplace transform, provides the transfer function of the actuator

$$\frac{\varepsilon(s)}{x(s)} = \frac{\dfrac{C\ell}{A\ell_2\ell_3}}{s + \dfrac{C\ell_1}{A\ell_2}} = \frac{a}{s+b} \tag{14.28}$$

Figure 14.18 shows a block diagram of the system. The mechanical feedback provides an actuator system which is a pure lag—the integrator action is controlled so that the aerodynamic surface is moved to a distinct position by a step pilot stick input.

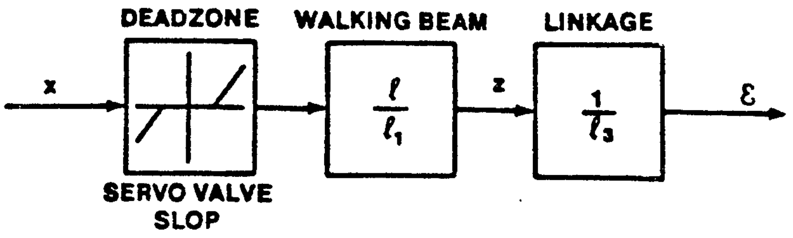

FIGURE 14.18. BLOCK DIAGRAM OF THE WALKING BEAM HYDRAULIC BOOST SYSTEM

An important consideration for any hydraulic actuator is to have as little friction as possible because if its motion is jerky the resultant motion of the elevator will also be jerky and the pilot may complain of control buzz. While it is not possible to eliminate all the friction, there are methods of smoothing the valve motion by springs and dampers inside the valve.

To improve the reliability of the hydraulic control system a rather common practice is to use tandem hydraulic cylinders. Another feature which is frequently used is to split the control surfaces and to use triple or quadruple redundant hydraulic pressure sources. The last feature is used on the Boeing 747.

14.4.4 Irreversible Control Systems

It was seen in section 14.4.2 that a reversible control system can be used on large and fast airplanes. An example is the KC-135. The question can therefore be raised: why change to a considerably more complicated system which also has associated with it a number of reliability problems?

Important reasons for the change to irreversible controls are:

1. In the transonic speed range, aerodynamic coefficients and hinge moments can vary quite erratically making pure mechanical control system design difficult if not impossible.

2. With hydraulically and/or electromechanically powered control surfaces electrical summing of stability augmentation system signals with pilot control signals becomes possible, eliminating annoying feedback to the cockpit controls.

3. For airplanes which must fly at both sub- and supersonic speeds, the irreversible control system can be conveniently designed to provide the pilot with almost constant control and response over the entire flight envelope.

The most common method of designing an irreversible control system is through the use of hydraulic actuators. Figure 14.19 shows a servo actuator used in irreversible flight control systems. The pilot commanded displacement, x_1, causes the servo valve to allow hydraulic fluid flow. The piston, which is anchored to the aircraft at one end, causes the entire actuator housing to move displacing the aerodynamic surface. No direct linkage from the pilot to the surface is present. In the event of a hydraulic system failure, the pilot cannot more the aerodynamic surface through the actuator. The rate of fluid flow into the piston is related to the piston displacement and the pilot command as

$$q = C(x_1 - x_2) \tag{14.29}$$

and the rate of piston displacement is

$$\dot{x}_2 = \frac{q}{A} \tag{14.30}$$

yielding

$$\dot{x}_2 = \frac{C}{A}(x_1 - x_2) \tag{14.31}$$

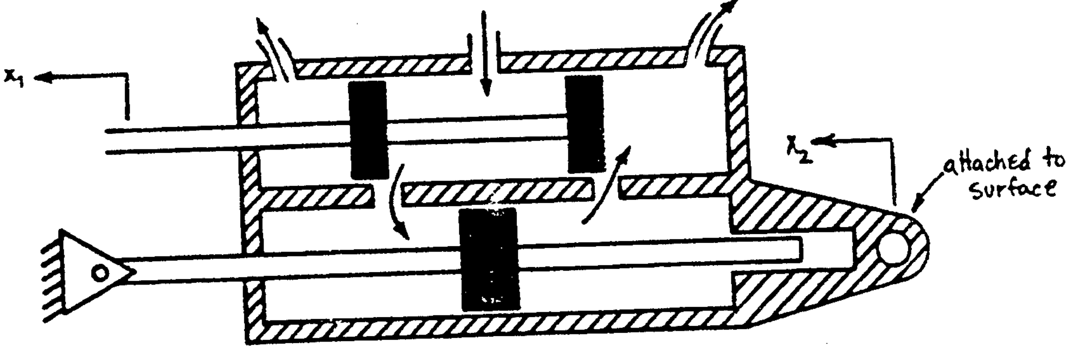

FIGURE 14.19 IRREVERSIBLE CONTROL SYSTEM ACTUATOR SCHEMATIC

The differential equation of the actuator is

$$\frac{A}{C}\dot{X}_2 + X_2 = X_1 \qquad (14.32)$$

resulting in the following transfer function

$$\frac{X_2(s)}{X_1(s)} = \frac{1}{\frac{A}{C}s+1} = \frac{\frac{C}{A}}{s+\frac{C}{A}} = \frac{a}{s+b} \qquad (14.33)$$

Figure 14.20 presents a block diagram of the actuator system. A typical first order actuator model for a fighter aircraft is

$$\frac{\delta(s)}{\delta_c(s)} = \frac{20}{s+20} \qquad (14.34)$$

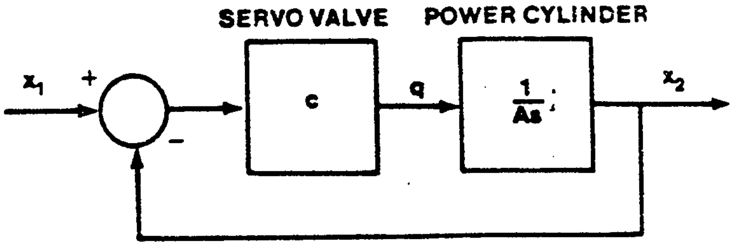

FIGURE 14.20 BLOCK DIAGRAM OF IRREVERSIBLE CONTROL SYSTEM HYDRAULIC ACTUATOR

If the leakage and compressibility effects within the actuator are not neglected, a third order actuator model is appropriate, with the power cylinder modeled as a relatively low frequency (20 radians per second) first order lag and the servo valve modeled as a high frequency second order element. In addition, if a fly-by-wire system is modeled, an additional first order lag occurs as a result of the electrical actuation of the servo valve.

The F-16 actuator is modeled as

$$\frac{(20.2)(144.8)(71.4)^2}{(s + 20.2)(s + 144.8)(s + 52.55 \pm 48.34j)} \qquad (14.35)$$

The effect of the high frequency poles due to the servo valve and the electrical actuator is to add a slight bit of lag to the system so that if time response characteristics are compared, a first order approximation to the

F-16 actuator is

$$\frac{\delta(s)}{\delta_c(s)} = \frac{13}{s + 13} \tag{14.36}$$

The change in dominant root locations during a simplified analysis of the F-16 flight control system is slight if the first approximation is used versus the second.

14.4.5 Artificial Feel Systems

High performance aircraft which use irreversible, hydraulically actuated control surfaces and moveable pilot controllers require artificial feel systems to simulate the control forces due to aerodynamic loads. Pilot controllers with limited movement, such as the F-16 side stick controller, do not require artificial feel systems because they use strain guages to sense pilot stick force. Artificial feel systems include the use of springs, dampers, bobweights and dynamic pressure feedback.

14.4.5.1 Springs and Dampers

A virtually constant stick force may be incorporated into the control system by using a downspring or bungee which tends to pull the top of the stick forward (or aft) as shown in figure 14.21.

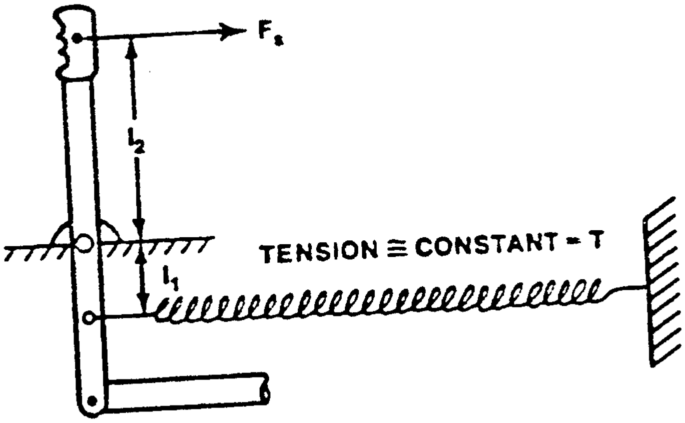

FIGURE 14.21 SPRING

If the spring is a long one, the tension in it will be increased only slightly as the top moves rearward and can be considered to be constant. The effect of adding a spring is to increase or decrease the apparent speed stability of the aircraft ($\partial F_s/\partial V$) but will not affect the stick forces during maneuvering flight ($\partial F_s/\partial n$) because the spring exerts a constant force on the stick no matter what load factor is applied.

A damper provides stick forces which are proportional to the rate of stick deflection and prevent steady oscillations when the pilot releases the stick, improving controller centering characteristics.

14.4.5.2 Bobweights

The addition of a bobweight changes the stick forces during maneuvering flight ($\partial F_s/\partial n$). If a spring is also added to counterbalance the stick force at one g then the original speed stability ($\partial F_s/\partial V$) will be preserved.

14.4.5.2 Dynamic Pressure Feedback

In an irreversible control system stick force F_s can be tailored by making it proportional to dynamic pressure q. This effectively acts as a mechanical gain scheduler.

This can be achieved by a system as shown schematically in figure 14.22. The expandable link in this system can be driven as a function of q via an air-data computer and an electric or hydraulic actuator.

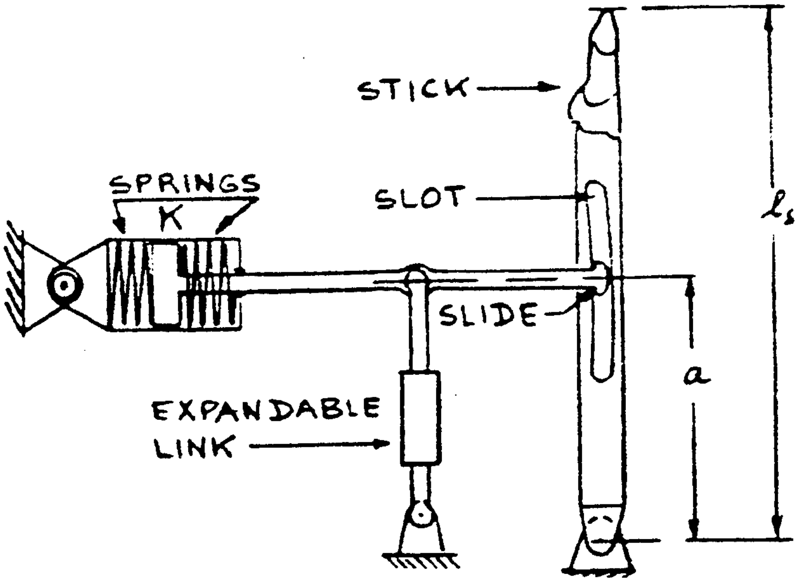

FIGURE 14.22 EXAMPLE OF q-FEEL SYSTEM

Another method for achieving q-feel is to use the so-called q-bellows system which uses ram-air to obtain a reliable source for the q-signal. Its operation is illustrated in figure 14.23.

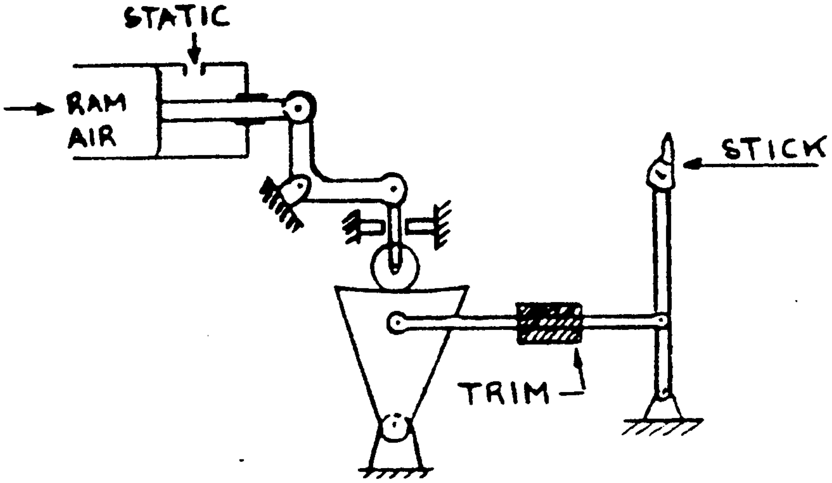

FIGURE 14.23 RAM AIR FEEL SYSTEM

A change in total stick damping is often necessary so that the dampers do not restrict the aircraft maneuverability at flight conditions where a high rate of elevator motion is desirable. This can also be accomplished by dynamic pressure feedback but this time to a viscous damper attached to the stick.

14.4.5.3 Dynamic Effects of Artificial Feel Systems

The addition of springs, dampers, bobweights and dynamic pressure feedback affects the closed loop dynamics of the aircraft in addition to the static stability described in the previous paragraphs. The artificial feel system of the F-4C includes all of these elements which we can use as an example to discuss these effects. The system will first be analyzed without the bobweight and then the bobweight will be added for further analysis.

Figure 14.21 shows the artificial feel system used in the F-4C. The bellows provides a spring gradient which is a function of Mach and altitude, effectively acting as a mechanical gain changer as discussed in section 14.4.5.3. On the ground, the springs exert no forces and the stick is moved to the forward stop by the force exerted by the bobweight. As the airspeed increases, the bellows dynamic pressure increases and the stick moves aft as the force of the spring increases.

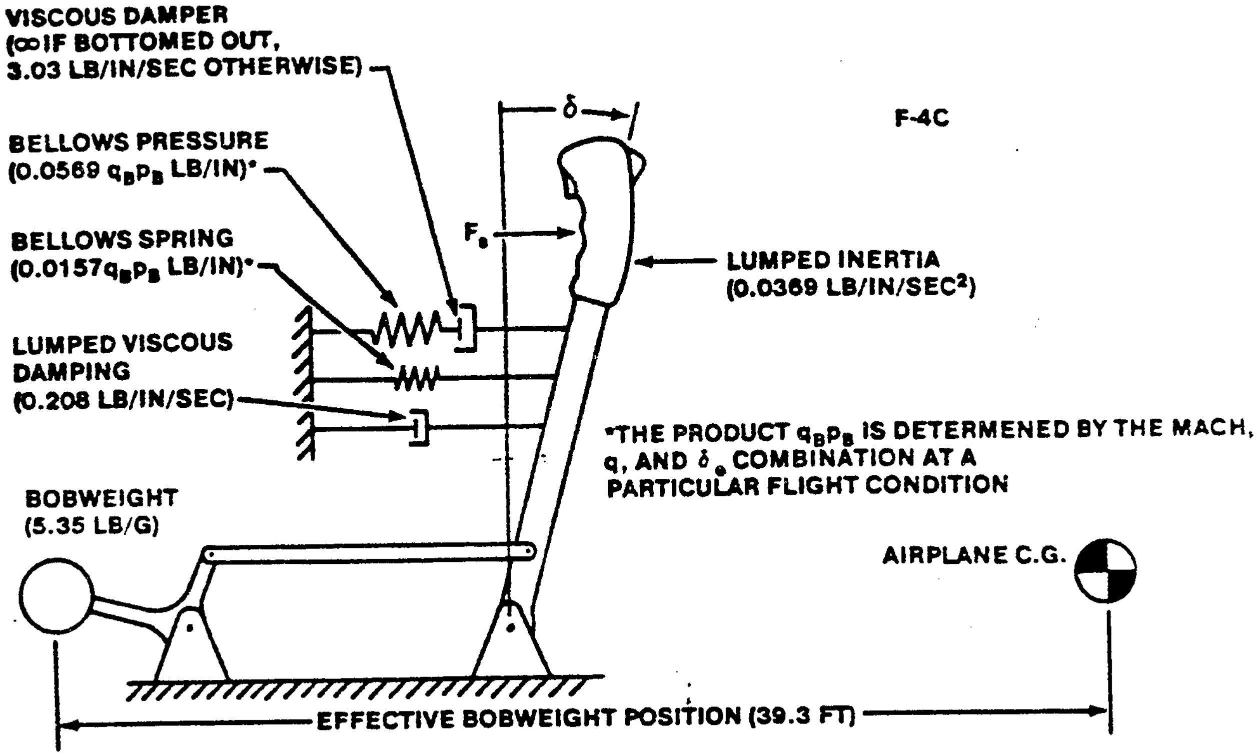
VISCOUS DAMPER
(∞ IF BOTTOMED OUT, 3.03 LB/IN/SEC OTHERWISE)
BELLOWS PRESSURE
(0.0569 $q_B p_B$ LB/IN)*
BELLOWS SPRING
(0.0157 $q_B p_B$ LB/IN)*
LUMPED VISCOUS DAMPING
(0.208 LB/IN/SEC)
BOBWEIGHT
(5.35 LB/G)
δ
F_s
F-4C
LUMPED INERTIA
(0.0369 LB/IN/SEC²)
*THE PRODUCT $q_B p_B$ IS DETERMENED BY THE MACH, q, AND δ_e COMBINATION AT A PARTICULAR FLIGHT CONDITION
AIRPLANE C.G.
EFFECTIVE BOBWEIGHT POSITION (39.3 FT)

FIGURE 14.24 SCHEMATIC DIAGRAM OF THE F-4C FEEL SYSTEM, INCLUDING THE BOBWEIGHT

The damper is a function of the flight condition, being on a physical stop at most flight conditions so that

$$b = \infty$$

and being off the stop at high altitudes and high Mach (above approximately 30,000 ft and 1.0 Mach), where

$$b = 3.03 \text{ lb/in/sec}$$

This system will be analyzed in the following paragraphs in a closed loop system where the pilot is attempting to maintain pitch attitude. The effect upon the longitudinal modes of motion (short period and phugoid) will be presented first with the springs and dampers, and then with the bobweight included.

14.4.5.3.1 F-4C Closed Loop Dynamics with Artificial Feel and No Bobweight

We can approximate the closed loop dynamics of pitch attitude control by assuming a simple pilot model. In this case the pilot will be assumed to be a pure gain controller attempting to precisely control the aircraft's pitch attitude. More complex pilot models are possible, incorporating pilot delays and compensation, but this simple model is adequate to show the effects of the feel system. The pilot induced oscillation (PIO) susceptibility of the aircraft at this flight condition cannot be determined from the following simplified analysis, but an idea of the relative PIO susceptibility due to various feel system characteristics may be obtained by noting the relative pilot gain at which the pilot (pitch attitude control) loop becomes unstable.

We will study the case of the F-4C at 0.8 Mach at sea level without the stability augmentation system operating. In this condition the open-loop transfer function is

$$G^{\theta}_{\delta_e}(s) = \frac{32.2\,(s + .0162)(s + 1.46)}{(s - .0378)(s + .0516)(s + 1.74 \pm 4.08j)} \qquad (14.37)$$

the open loop response due to the short period is second order and well damped. The phugoid mode, however, has degenerated into two real parts, one of which is in the right hand half plane which gives rise to an unstable tuck mode.

The transfer function of the artificial feel system without the bobweight can be determined by summing the moments about the stick pivot point. This yields a feel system transfer function that can be approximated as a second order system. At sea level and 0.8 Mach this yields

$$\frac{x(s)}{F(s)} = \frac{27.1}{s + 2.82 \pm 27.42j} \qquad (14.38)$$

The closed loop system for pitch attitude control when the springs and dampers are included is shown in figure 14.25.

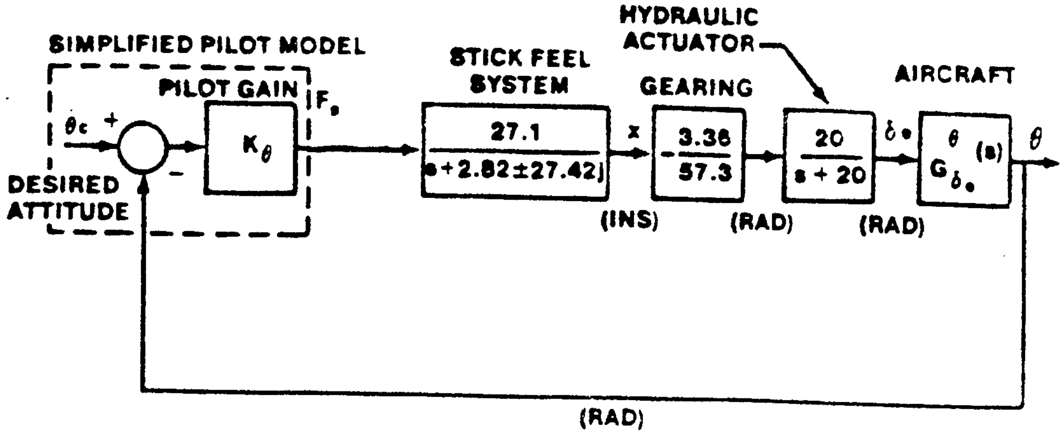
SIMPLIFIED PILOT MODEL
PILOT GAIN
K_θ
F_s
θ_c
+
-
DESIRED ATTITUDE
STICK FEEL SYSTEM
$\frac{27.1}{s+2.82\pm27.42j}$
x
(INS)
GEARING
$-\frac{3.36}{57.3}$
(RAD)
HYDRAULIC ACTUATOR
$\frac{20}{s+20}$
δ_e
(RAD)
AIRCRAFT
$G_{\delta_e}^{\theta}(s)$
θ
(RAD)

FIGURE 14.25 PITCH ATTITUDE CONTROL LOOP FOR F-4C WITH ARTIFICIAL FEEL SYSTEM AND NO BOBWEIGHT

Figure 14.26 shows the effects of this production F-4C feel system with no bobweight. The feel system has light damping and a large natural frequency relative to the basic airframe characteristics. The pilot, by controlling the

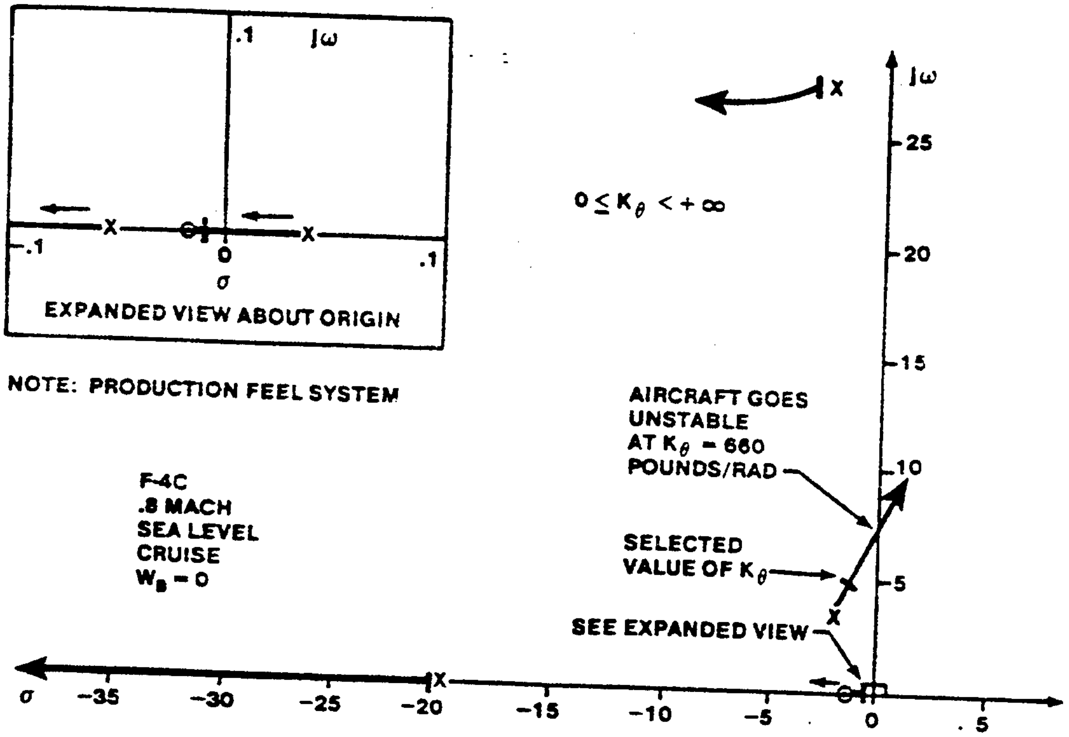

FIGURE 14.26 PITCH ATTITUDE CONTROL ROOT LOCUS FOR F-4C WITH PRODUCTION FEEL SYSTEM NO BOBWEIGHT

aircraft pitch attitude, is easily able to stabilize the tuck mode. The short period roots remain relatively well damped for low to moderate values of gain, but may be driven unstable at high pilot gain.

If the damping on this system were reduced to zero the root locus in figure 14.27 would result. Without the pilot in the loop there would be a residual stick oscillation in open loop response which causes the aircraft to oscillate in pitch at the feel system frequency. The pilot, however, is able to provide the stick damping required to keep the pilot-aircraft combination stable.

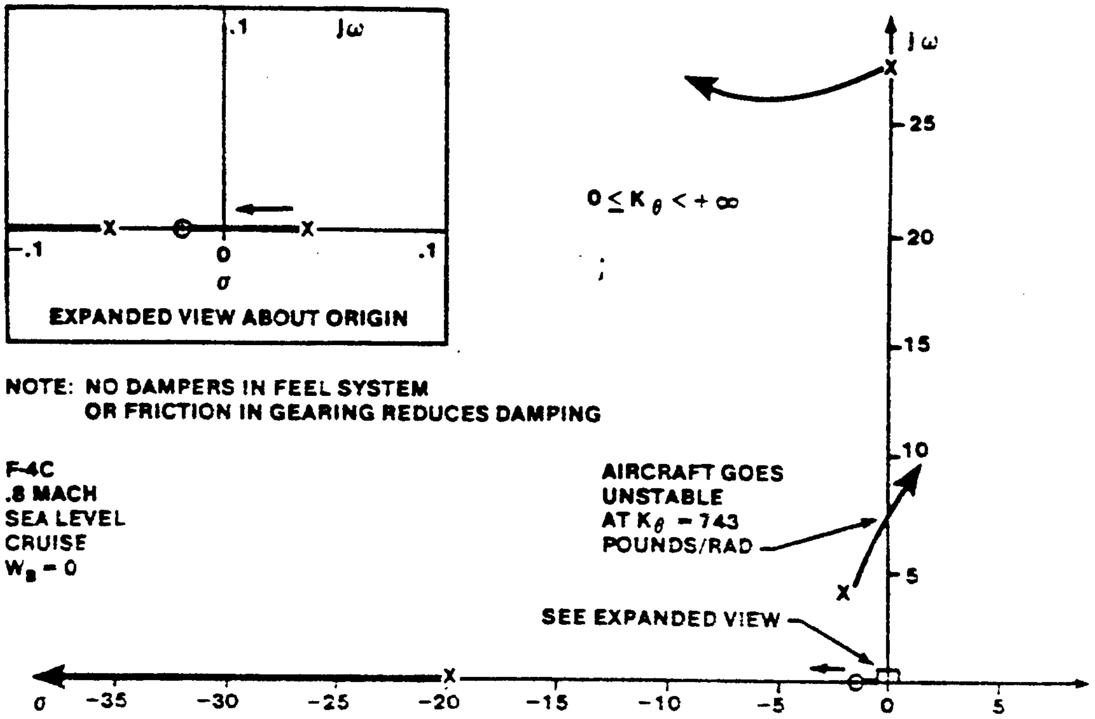

FIGURE 14.27 PITCH ATTITUDE LOOP FOR F-4C WITH SPRINGS ONLY NO FEEL SYSTEM DAMPING OR BOBWEIGHT

Even if slightly negative damping were present in the feel system, the pilot could stabilize the aircraft, although the open loop aircraft would be unstable due to the unstable feel system roots. If the required gain from the pilot to stabilize the feel system were very high (but attainable), the short period roots would migrate to the right and the short period damping would be significantly reduced and poor flying characteristics and increased PIO susceptibility would result due to the high pilot workload and poor pitch attitude control. An example of this could occur in the F-4C with bellows system failure. In this case the feel system roots would be unstable and the pilot would not be able to stabilize them without driving the short period unstable. The pilot would then lose control of the aircraft.

An increase in feel system damping can also increase PIO susceptibility, because the added feel system forces due to the increased damping will reduce the rate at which the pilot can change the elevator position. The short period roots then become unstable at a lower gain.

Figure 14.28 shows the effect of reduced spring forces in the feel system (reduced pilot control forces). The natural frequency of the feel system is much lower, bringing the roots in closer proximity to the basic airframe characteristics. The pilot is still able to control the pitch attitude of the aircraft, but the gain at which the short period roots are driven unstable is reduced considerably, increasing significantly the susceptibility of the aircraft to PIO's.

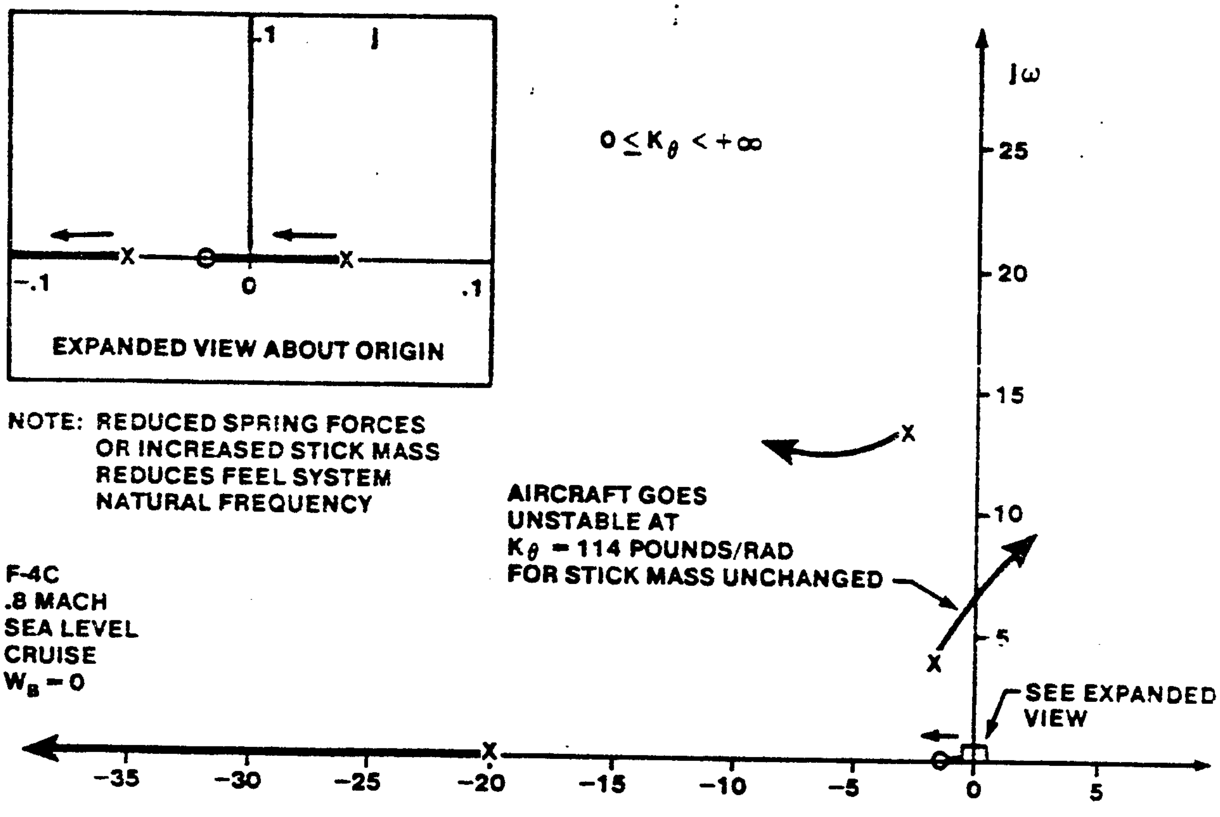

NOTE: REDUCED SPRING FORCES OR INCREASED STICK MASS REDUCES FEEL SYSTEM NATURAL FREQUENCY

AIRCRAFT GOES UNSTABLE AT K_θ = 114 POUNDS/RAD FOR STICK MASS UNCHANGED

F-4C
.8 MACH
SEA LEVEL
CRUISE
$W_B = 0$

FIGURE 14.28 PITCH ATTITUDE LOOP FOR F-4C WITH REDUCED FEEL SYSTEM SPRING FORCES, NO BOBWEIGHT

The worst case would be to have no artificial feel system at all (no damping or spring forces) as shown in figure 14.29. If the pilot controls only pitch attitude, he cannot stabilize the aircraft. The higher the pilot's gain, the more unstable he drives the aircraft.

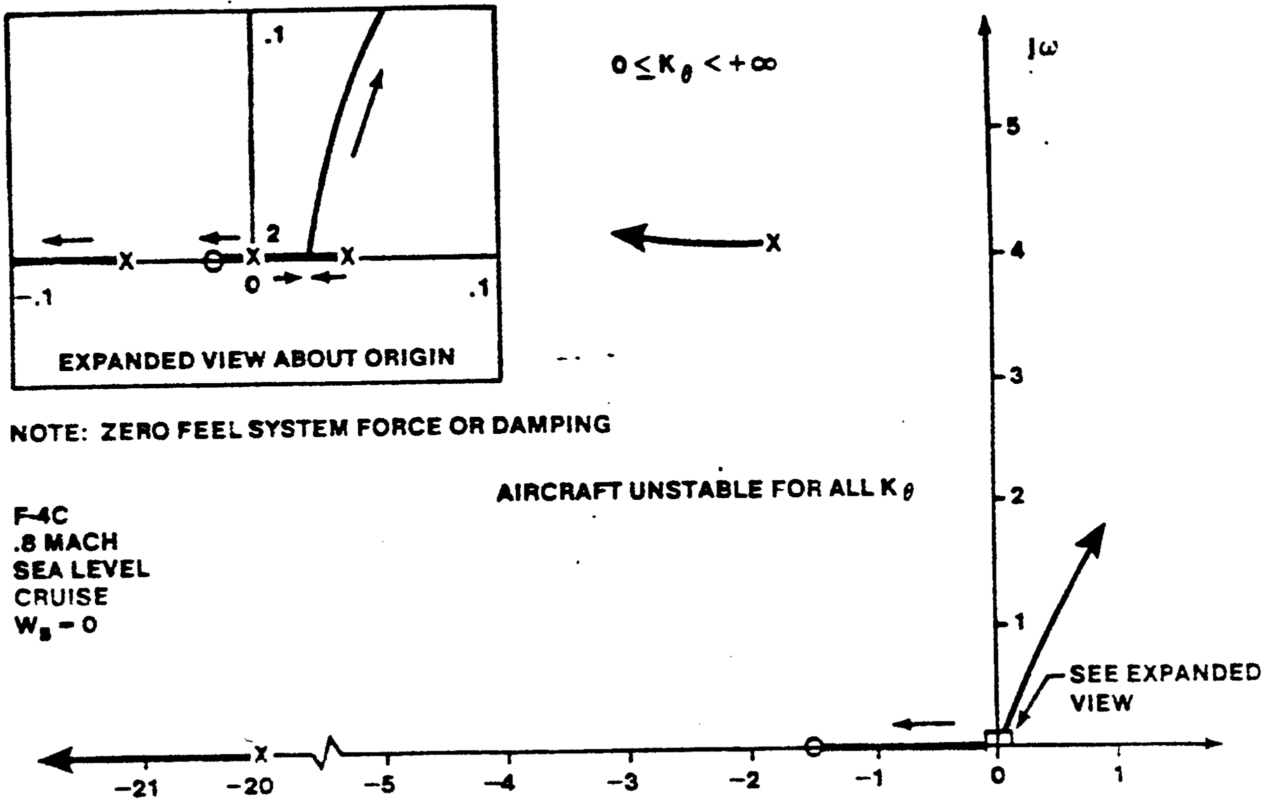

FIGURE 14.29 PITCH ATTITUDE CONTROL LOOP WITH NO STICK DAMPING OR SPRING FORCES, NO BOBWEIGHT

The pilot can stabilize this system if he senses stick position in addition to pitch attitude. This feedback through his neuro-muscular system results in a modified pilot model as shown in figure 14.30. The pilot would, however, have to devote his entire attention to flying the aircraft. This aircraft is highly susceptible to PIO and must be very carefully flown. If the pilot reverts to controlling the aircraft's pitch attitude and does not concentrate on the position of the controller, the aircraft will be driven unstable (this situation might occur during flare and touchdown).

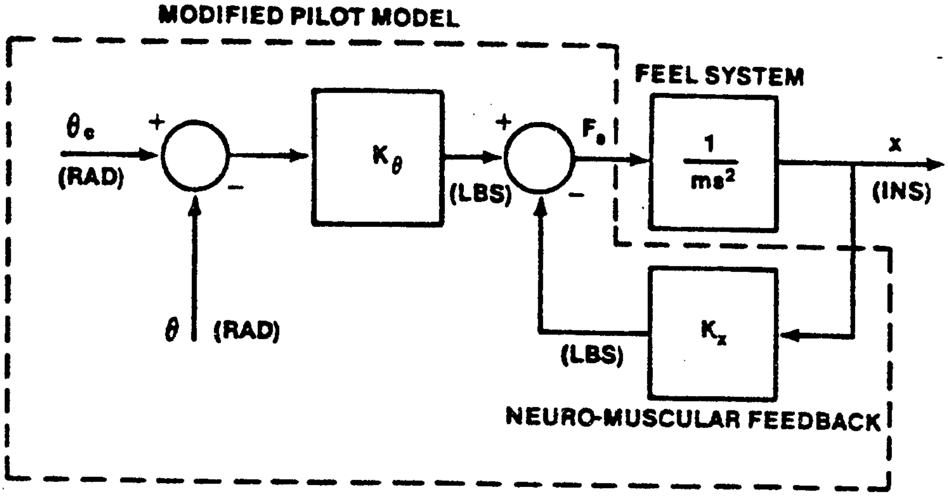

FIGURE 14.30 MODIFIED PILOT MODEL

Our overall conclusion from this simplified analysis is that aircraft with movable controllers in irreversible control systems must have an artificial feel system with springs and damper forces in order to provide proper closed loop dynamics. In selecting the amount of spring forces and damping the following general trends apply:

a. Reduced spring forces greatly increases PIO susceptibility.

b. Reduced damping forces improves PIO resistance, but may cause poor stick centering characteristics and residual, high frequency oscillations.

c. Increased damping forces increases PIO susceptibility.

14.4.5.3.2 F-4C Closed Loop Dynamics with Artificial Feel and Bobweight

Figure 14.31 shows a block diagram of the F-4C feel system including the bobweight effects. A bobweight is effectively an acceleration feedback loop to the pilot applied stick forces. The location of the bobweight relative to the aircraft center of gravity, as well as the size of the bobweight mass, both significantly affect the flying qualities of the aircraft.

The acceleration sensed at the bobweight station is given by

$$a_{z_b} = a_{z_{cg}} - \ell_x \dot{q} \qquad (14.39)$$

where ℓ_x is the distance from the center of gravity of the aircraft to the bobweight (positive forward).

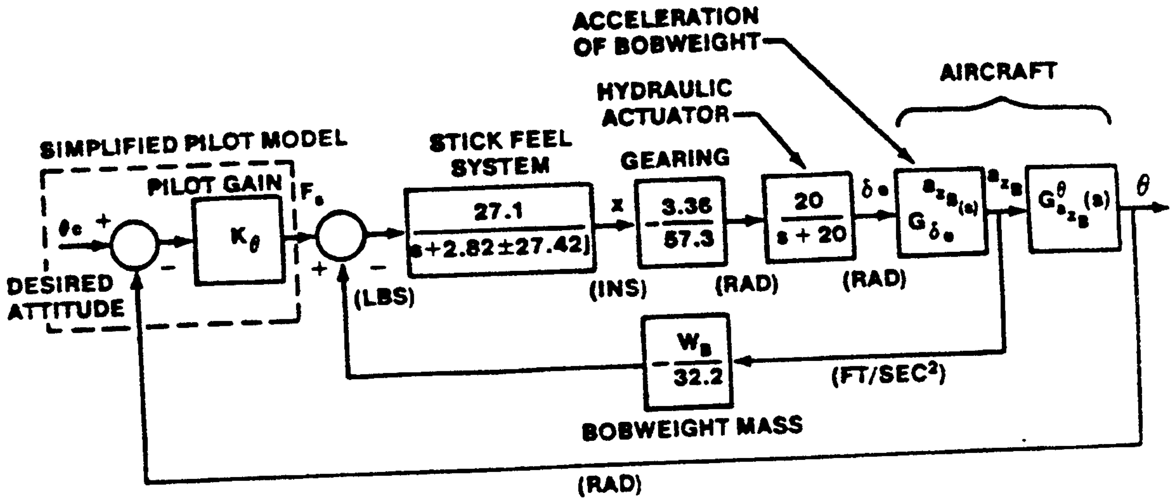
ACCELERATION OF BOBWEIGHT
AIRCRAFT
HYDRAULIC ACTUATOR
SIMPLIFIED PILOT MODEL
STICK FEEL SYSTEM
GEARING
PILOT GAIN
F_s
θ_c
+
−
K_θ
+
−
$\frac{27.1}{(s+2.82\pm27.42j)}$
x
$-\frac{3.36}{57.3}$
$\frac{20}{s+20}$
δ_e
$\frac{a_{z_B}}{G_{\delta_e}}(s)$
a_{z_B}
$G^{\theta}_{a_{z_B}}(s)$
θ
DESIRED ATTITUDE
(LBS)
(INS)
(RAD)
(RAD)
$-\frac{W_B}{32.2}$
(FT/SEC²)
BOBWEIGHT MASS
(RAD)

FIGURE 14.31 BLOCK DIAGRAM OF THE F-4C FEEL SYSTEM WITH A SIMPLIFIED PILOT MODEL INCLUDED AS AN OUTER LOOP CONTROLLER

The dynamic effects of a bobweight are to:

1. Reduce the feel system damping.
2. Increase the feel system natural frequency.
3. Reduce the short period damping.
4. Increase the short period natural frequency.

Reducing bobweight size or moving the bobweight closer to the aircraft center of gravity increases the PIO susceptibility. Of course, the minimum and maximum size of the bobweight and its location are also governed by the stick force gradient requirements ($\partial F_s/\partial n$). The bobweight size and location must, therefore, be chosen to provide the proper stick force gradients and keep the feel system roots in the left hand s-plane. The root locus of the full system is shown in figure 14.32.

A bobweight may cause poor transient feel in high speed aircraft, if not properly designed, due to the lag between normal acceleration response and the pilot input. This may occur if the bobweight is too close to the center of gravity due to the elimination of the pitch acceleration term effects in the bobweight acceleration equation.

There is a possibility of coupling between the bobweight and the aircraft natural frequencies at high speeds, where the aircraft short period frequency is quite high (and may be of nearly the same magnitude as the feel system frequency for a system with light spring forces), which could result in

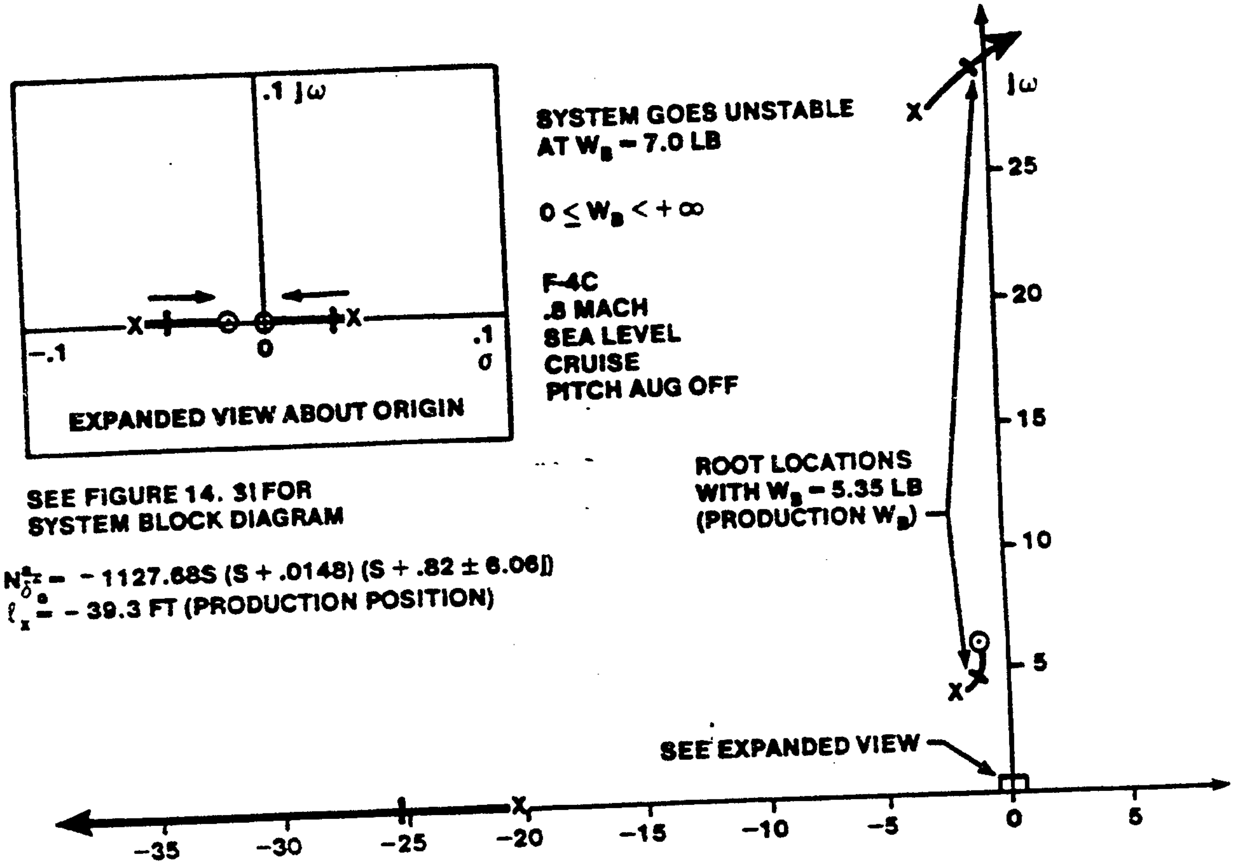

FIGURE 14.32 ROOT LOCUS PLOT OF BOBWEIGHT LOOP FOR THE F-4C WITH FULL STICK FEEL SYSTEM

uncomfortable or dangerous pitch oscillations in gusty conditions.

If the F-4C at Mach 1.1 is analyzed using the feel system dynamics present at 0.8 Mach, then the size of the bobweight must be significantly reduced to preclude the feel system from becoming unstable. The F-4C bellows spring prevents this from occurring normally since the spring forces increase proportionally with dynamic pressure. However, if a leak developed in the bellows, an unstable feel system could result which the pilot would not be able to stabilize without driving the short period roots unstable.

Figure 14.33 to 14.37 show the effect of the size of the bobweight (with and without the feel system dynamics) on the open loop F-4C short period response with the bobweight located at the production position. Figure 14.33 shows the basic aircraft short period response with the feel system and bobweight dynamics neglected. Figure 14.34 shows the same response with the feel system dynamics included. Note the slight deformations in the response

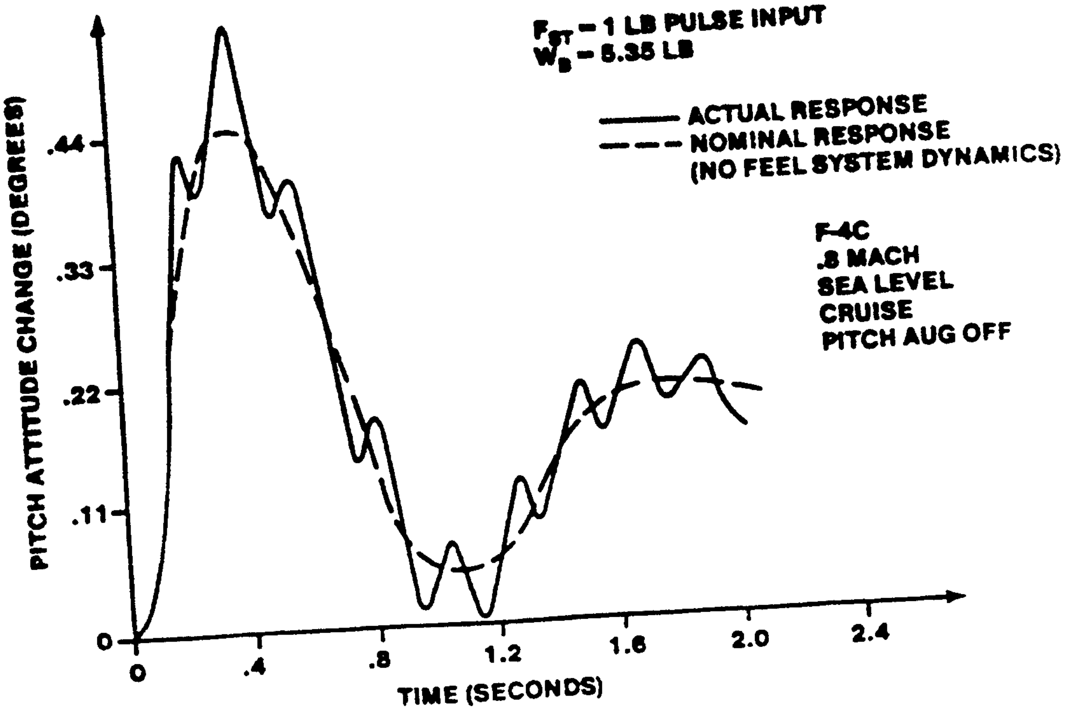

FIGURE 14.33 F-4C BASIC AIRCRAFT RESPONSE WITHOUT BOBWEIGHT OR FEEL SYSTEM

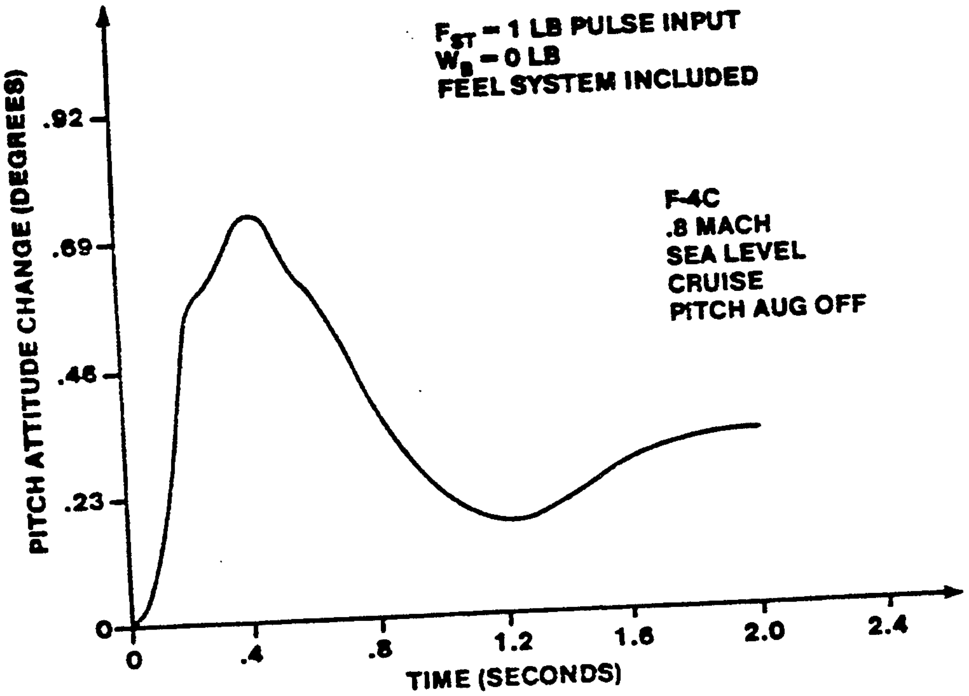

FIGURE 14.34 F-4C RESPONSE WITH FEEL SYSTEM, BOBWEIGHT OMITTED

at the first peak. These are due to the high frequency, lightly damped feel system roots. The damping of the short period is unchanged. Figure 14.35 shows the effect of the bobweight, with the feel system omitted. The short period damping is reduced significantly. Figure 14.36 shows the aircraft response to a pulse stick input with the bobweight and feel system dynamics included. The short period damping is only slightly reduced from the basic aircraft but the feel system dynamics are very evident. Although the feel system is stable, it appears to be very lightly damped. Figure 14.37 shows what happens to the feel system if the bobweight becomes too large. The feel system is driven unstable, appearing as a high frequency divergent motion which is superimposed over the basic aircraft short period response. Much effort was required to achieve a bobweight configuration for the F-4C which provided adequate maneuvering stick force characteristics while avoiding a significant increase in the PIO susceptibility of the aircraft. The pitch damper which is included in the aircraft also helps to reduce the PIO susceptibility of the aircraft.

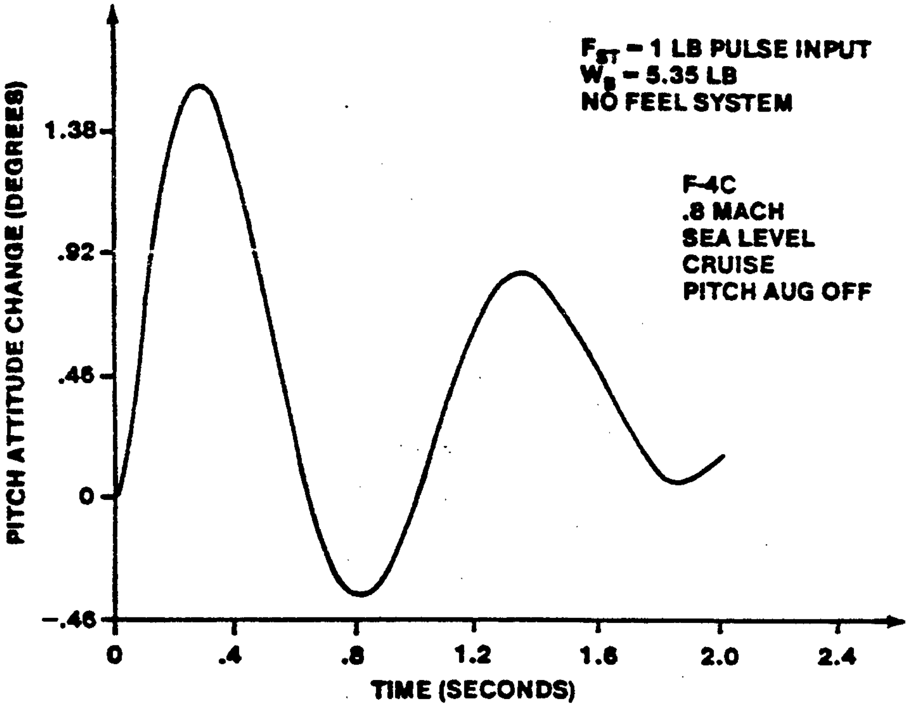

FIGURE 14.35 F-4C RESPONSE WITH BOBWEIGHT, FEEL SYSTEM OMITTED

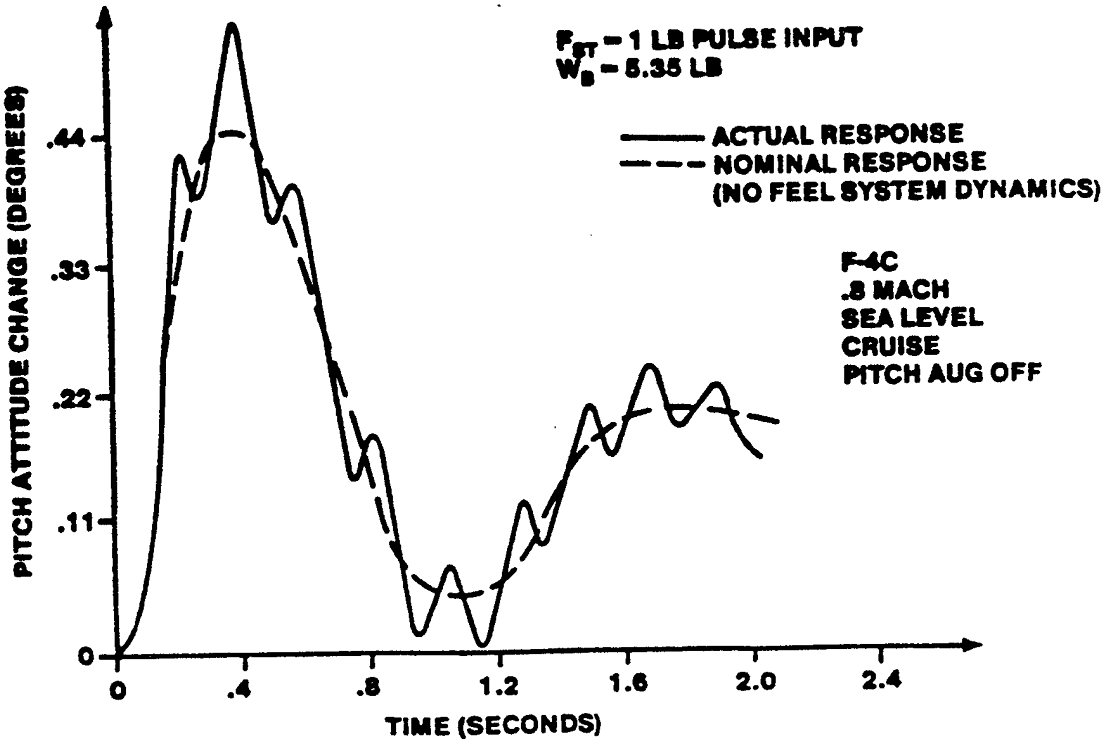

FIGURE 14.36 F-4C RESPONSE WITH PRODUCTION BOBWEIGHT

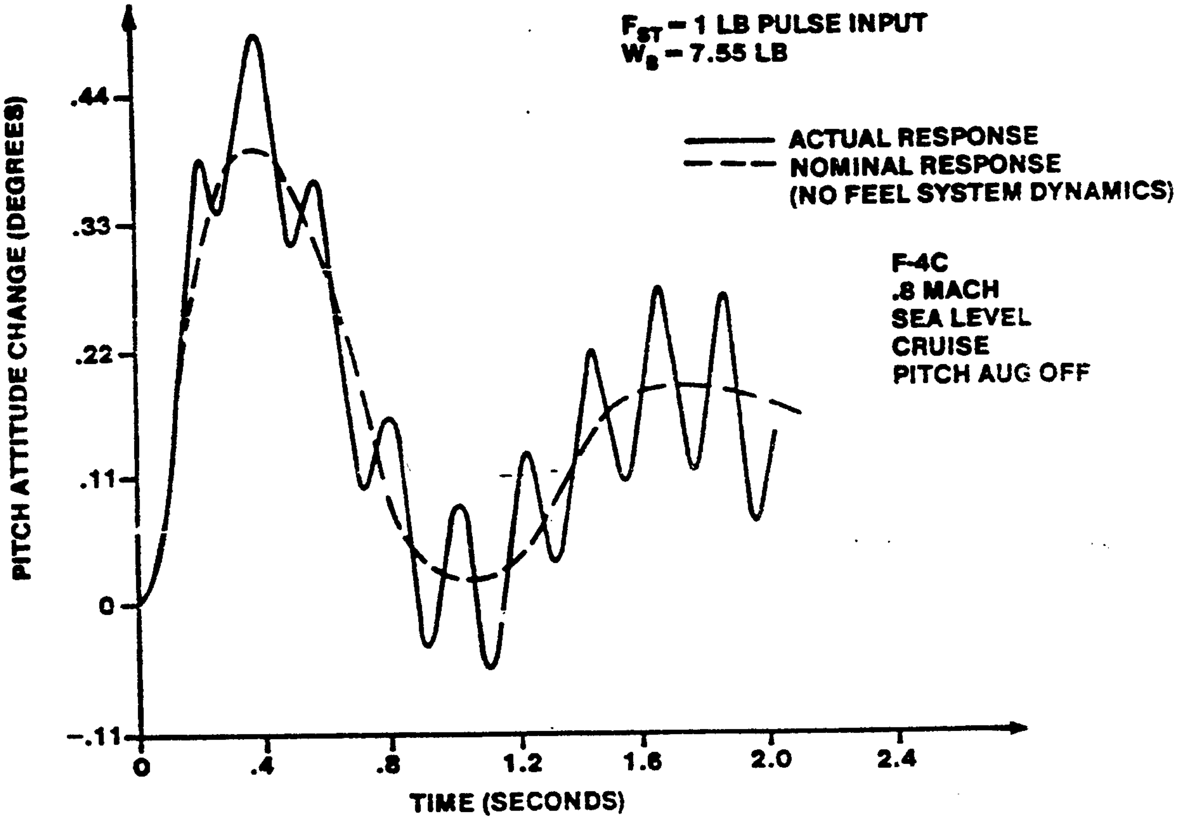

FIGURE 14.37 F-4C RESPONSE WITH BOBWEIGHT TOO LARGE

14.5 AUGMENTATION SYSTEMS

Certain minimum levels of static and dynamic stability are required to make an aircraft acceptable from a flying qualities point of view. It is not always possible, or even desirable, to design an aircraft with these inherent stabilities. From a payload-range or maneuverability point of view, it is better to design with performance consideration only and correct the handling qualities deficiencies with some form of flight control system augmentation.

Control devices for improving aircraft stability have been labelled variously in the past as stabilizers, dampers, auto-pilots, stability augmentors, or stability augmentation systems (SAS). Stability augmentation systems operate almost universally by sensing one or more of the aircraft motions and then moving a control surface to oppose that motion. This is illustrated in figure 14.38. This system is an idealization since control surfaces cannot be moved without actuators, which introduce lag into the system (see section 14.5.1.4 for a discussion of actuator effects).

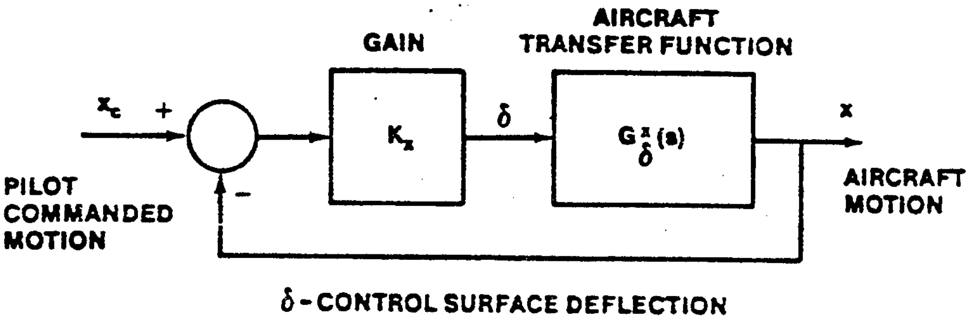

FIGURE 14.38 ELEMENTARY AIRCRAFT FEEDBACK CONTROL SYSTEM

Even with these simplifications, however, the general effects of the feedback system on the aircraft dynamic modes of motion can be determined and are presented in this section.

The purpose of a stability augmentation system is to improve aircraft characteristics for one of more of the characteristic dynamic modes of motion. In order to do this the SAS usually incorporates an electrical damper system in parallel with a conventional flight control system. The damper system obtains aircraft motion information from a sensor and applies an additional input to the control surface to augment pilot input. A SAS usually has less than 10% control authority and is usually non-redundant. Examples of such stability augmentation systems are found on the F-4, T-38 and AV8-B.

More sophisicated flight control system augmentation can be accomplished through a control augmentation system (CAS). The primary difference between a CAS and a SAS is that a CAS adds a command path between the pilot controller and the control surface. Where a SAS only senses aircraft motions (figure 14.39), a CAS takes inputs from the pilot also (figure 14.40). The pilot, therefore, actuates the mechanical and CAS electrical command paths simultaneously. The electrical path typically uses a force sensor on the stick to provide an input to the electrical control system.

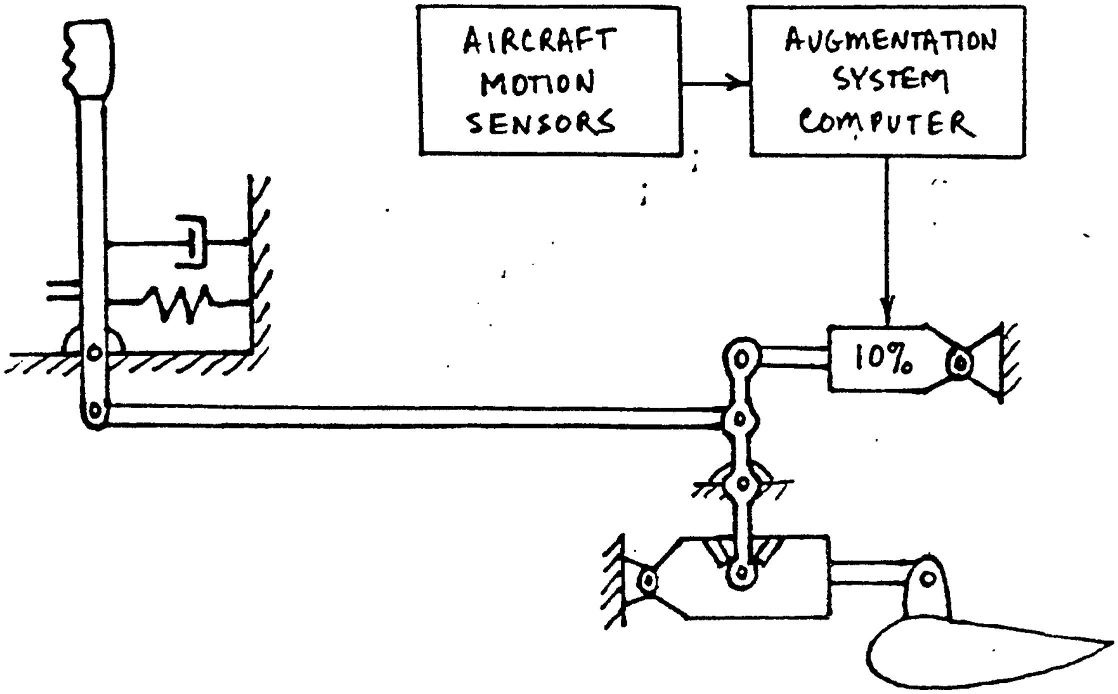

14.39 STABILITY AUGMENTATION SYSTEM

Like a SAS, a CAS is used to improve aircraft characteristics for the characteristic dynamic modes of motion. The CAS is also, however, used to provide improved and more consistent handling qualities. With the CAS engaged, the aircraft response is heavily damped and the control system gains are scheduled to maintain constant aircraft response characteristics throughout the flight envelope. The sensors in the augmentation system

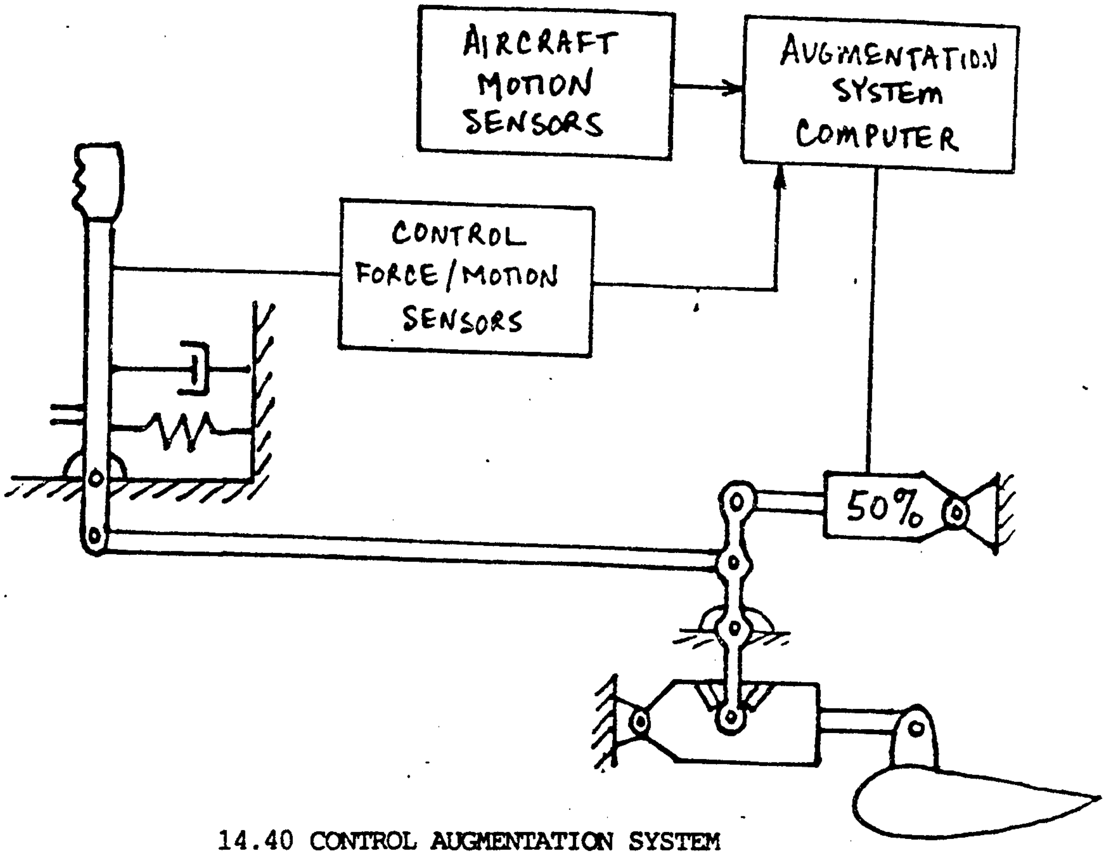

14.40 CONTROL AUGMENTATION SYSTEM

provide feedback signals which are compared to the pilot input (usually a load factor, pitch rate or roll rate signal) to achieve the desired aircraft response. A CAS has large authority (usually greater than 50%) and because of this, must be redundant. Examples of control augmentation systems can be found in the F-15, F-111, F-14 and A-7.

Table 14.2 gives a list of common feedback parameters and actuating signals used for both the longitudinal axis and the lateral-directional axes. These are used in various combinations in stability or control augmentation systems. The effects of some of these combinations are presented in section 14.5.1 which discusses single loop feedback control law effects on the characteristic roots of the aircraft. The effects of multiple loop systems can be deduced from the effects of individual loops. Some of the common multiple loop systems are discussed in section 14.5.2. In section 14.5.3 a general discussion of the common control augmentation system characteristics is presented.

Some of the feedback parameters in Table 14.2 are more appropriate for autopilot operation. A discussion of these feedback strategies is given in section 14.7.

TABLE 14.2

COMMON AIRCRAFT FEEDBACK PARAMETERS AND ACTUATING AERODYNAMIC SURFACES

Feedback Parameter	Actuating Surface
1. Longitudinal Axis	
θ, pitch angle	δ_e, elevator deflection
q, pitch rate	δ_f, flap deflection
u, forward velocity	δ_t, engine throttle deflection
a_x, longitudinal acceleration	δ_{hc}, horizontal canard deflection
a_z, normal acceleration	
h, altitude	
$\dot{h}$, rate of climb	
α, angle of attack (w/U_0)	
2. Lateral-Directional Axes	
ϕ, bank angle	δ_a, aileron deflection
p, roll rate	δ_r, rudder deflection
r, yaw rate	δ_{vc}, vertical canard deflection
β, sideslip angle (v/U_0)	
a_y, lateral acceleration	

Table 14.3 presents a summary of the common feedback strategies that are discussed in detail in section 14.5.1 and are the fundamental parts of stability and control augmentation systems. As shown, each of the strategies has a primary, desired effect, as well as secondary effects.

TABLE 14.3

SUMMARY OF AIRCRAFT FEEDBACK CONTROL LAW EFFECTS ON THE AIRCRAFT CHARACTERISTIC MODES OF MOTION

I. Longitudinal Axis

Primary (Desired) Effect	Feedback Law	Secondary Effects	Augmented Derivative	Section
A. Increase short period damping	$q \to \delta_e$	Short period natural frequency slightly increased	M_q	14.5.1.1.1.1
	$\dot{\alpha} \to \delta_e$		M_{α}	14.5.1.1.1.2
B. Increase short period natural frequency	$\alpha \to \delta_e$		M_{α}	14.5.1.1.2
	$n_z \to \delta_e$			14.3.3.1
C. Stabilize phugoid	$\theta \to \delta_e$	Short period somewhat degraded		14.5.1.1.3.1
	$u \to \delta_e$	Short period somewhat degraded	M_u	14.5.1.1.3.2
D. Stabilize aft c.g. aircraft	$\alpha \to \delta_e$		M_{α}	14.5.1.1.4.1
	$\theta \to \delta_e$	Stabilize phugoid		14.5.1.1.4.2
	$q \to \delta_e$			14.5.1.1.4.3

II. Lateral-Directional Axes

Primary (Desired) Effect	Feedback Law	Secondary Effects	Augmented Derivative	Section
A. Increase Dutch roll damping	$r \to \delta_r$	Spiral stabilized somewhat	N_r	14.5.1.2.1
	$\beta \to \delta_r$			14.5.1.2.6
B. Decrease roll mode time constant	$p \to \delta_a$	Spiral stabilized, Dutch roll excitation by ailerons suppressed	L_p	14.5.1.2.2
C. Stabilize spiral mode	$\phi \to \delta_a$	Roll mode time constant slightly increased		14.7.3
	$r \to \delta_a$	Roll mode time constant decreased somewhat, may destabilize Dutch roll		14.5.1.2.3
	$\beta \to \delta_a$	Dutch roll destabilized, roll mode time constant decreased somewhat		14.5.1.2.3

TABLE 14.3
(continued)

Primary (Desired) Effect	Feedback Law	Secondary Effects	Augmented Derivative	Section
D. Provide rudder coordination	$\beta \rightarrow \delta_r$	Destabilize spiral, Dutch roll frequency increased	N_β	14.5.1.2.4.1
	$n_y \rightarrow \delta_r$	Destabilize spiral, Dutch roll frequency increased		14.5.1.2.4.2
E. Reduce adverse yaw	$\delta_a \rightarrow \delta_r$ (ARI)			14.5.1.2.5
F. Alter roll axis for aggressive maneuvering	$\beta \rightarrow \delta_r$	Dutch roll damping increased		14.5.1.2.6

14.5.1 Single Loop Stability Augmentation Systems

The following discussion of single loop augmentation systems is divided into a discussion of the longitudinal axis and the lateral-dircetional axes. In the case of the longitudinal axis, the discussion will first concentrate on the analysis of aircraft with conventional static stability (c.g. forward of the aerodynamic center) and will then proceed to an analysis of unstable aircraft (c.g. aft of the aerodynamic center). The lateral directional axes presentation will include discussions of aileron-rudder interconnects, systems for rudder coordination and systems to improve handling qualities for gun aiming. A brief discussion of augmenter effects of reversible control systems and the effects of actuators will also be given.

14.5.1.1 Longitudinal Axis Single Loop SAS

The purpose of the longitudinal flight control system is to provide acceptable short period dynamics to accomplish high gain tasks, such as gunnery, in-flight refueling, formation, and landing, and to provide adequate speed and maneuverability stability cues to the pilot. Slight phugoid instability can be tolerated for piloted flight (although not for autopilot operation as discussed in section 14.7).

The unaugmented aircraft longitudinal characteristics in figure 14.41 are typical of pitch attitude control for a reasonably well behaved aircraft in cruising flight at moderate altitudes. The Bode plot illustrates these

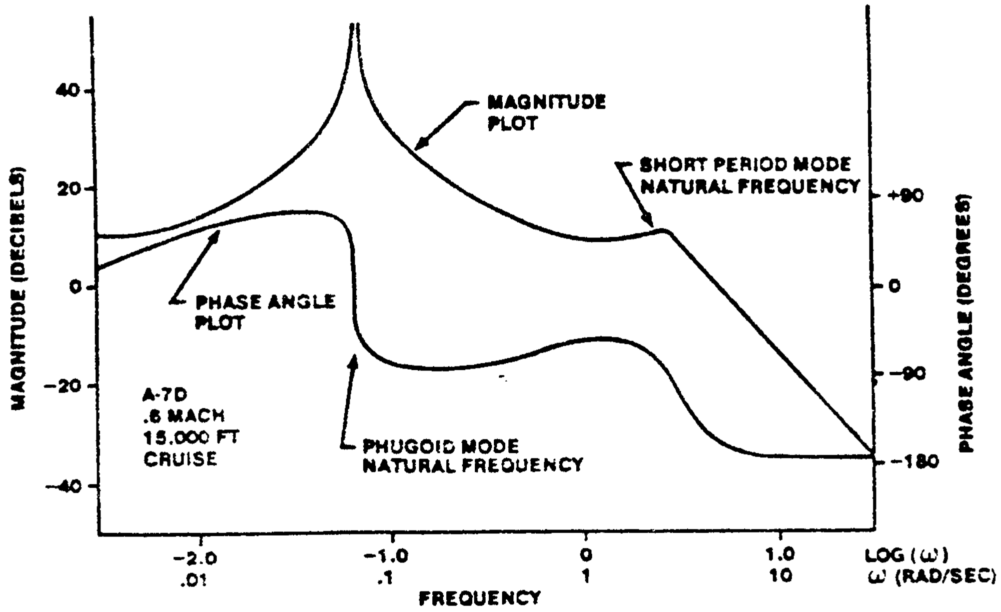

FIGURE 14.41 BODE PLOT OF PITCH ATTITUDE LOOP FOR AN AIRCRAFT WITH GOOD DYNAMICS

characteristics, which include a wide separation between the short period and phugoid breakpoints, in both amplitude ratio and frequency, and the relatively heavy damping of the short period.

If the aircraft pitch attitude control is not similar to that shown, a SAS is often used to modify the aircraft characteristics.

14.5.1.1.1 Increasing Short Period Damping

Aircraft with poor short period damping (flying wings, aircraft at high altitude, low speed or high Mach, or aircraft with aft c.g.'s) require pitch damping augmentation to improve their short period handling qualities. The most common method of augmenting short period damping is to feed back pitch rate to the elevator although, angle attack rate is another method.

14.5.1.1.1.1 Pitch Rate Feedback to Increase Short Period Damping - As an introduction, the method of "equivalent stability derivatives" will be used to achieve certain levels of handling qualities. The stability derivative M_q has a very powerful effect on the short period damping ratio ζ_{sp}. An increase in pitch damping can be obtained by a pitch damper which senses aircraft pitch rate q and then moves the elevator in a manner proportional to q, but such as to oppose q. Assuming that a "perfect" pitch damper can be built, the incremental pitching moment obtained by such a device can be written as:

$$\Delta M = M_{\delta_e} K_q q \tag{14.40}$$

where K_q is the pitch damper gain, or elevator per unit pitch rate. The corresponding increase in M_q is therefore

$$\Delta M_q = M_{\delta_e} K_q \tag{14.41}$$

As a result of this "perfect" pitch damper, the aircraft now has a new value of M_q equal to

$$M_{q_{DESIRED}} = M_{q_{AUG}} = M_{q_{BASIC}} + K_q M_{\delta_e} \tag{14.42}$$

where $M_{q_{AUG}}$ is called an equivalent stability derivative.

The amount of required pitch damper gain can now be calculated from

$$K_q = \frac{M_{q_{DESIRED}} - M_{q_{BASIC}}}{M_{\delta_e}} \tag{14.43}$$

A word of caution is required. The pitch damper, while artificially augmenting M_q, will also unavoidably augment the derivative L_q. It will be necessary to use both augmented derivatives of M_q and L_q in the characteristic equation to establish the overall effect of the pitch damper on longitudinal dynamic stability. As it turns out, however, the effect of the change in L_q caused by the pitch damper is usually minor.

The feedback of pitch rate to the elevator is also commonly called a pitch rate command system since the pilot stick input is compared directly to the aircraft pitch rate. Such a system using a pure gain controller is shown in figure 14.42.

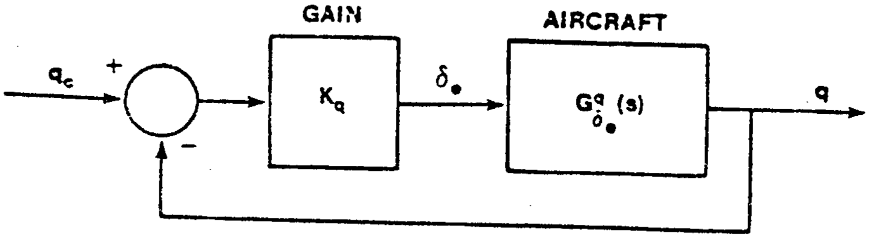

FIGURE 14.42 PITCH RATE COMMAND SYSTEM

Figure 14.43 presents a root locus plot of the pitch rate command system implemented on a well behaved aircraft. At low gain, the aircraft short period roots move rapidly towards the real axis, dramatically increasing the short period damping while changing the short period natural frequency only slightly. At a relatively low gain, the two short period roots become real

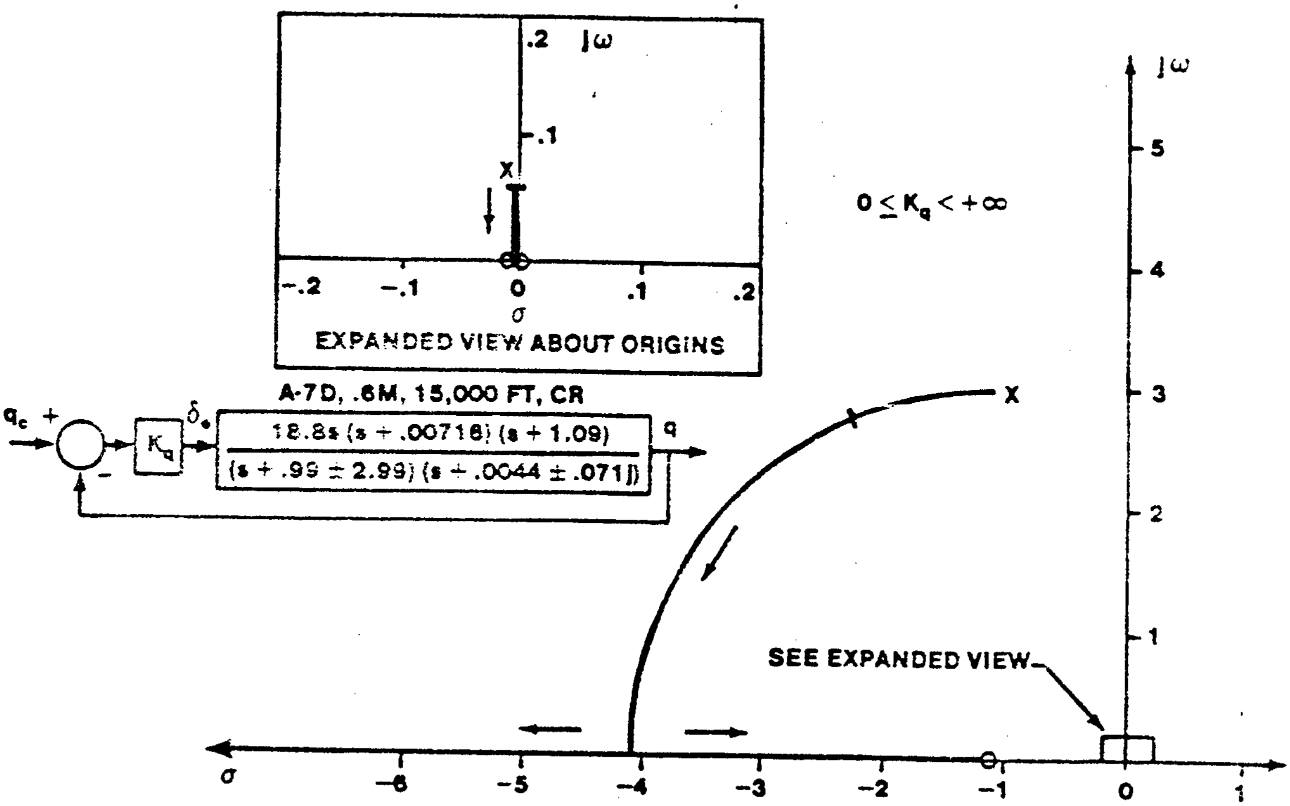

FIGURE 14.43 ROOT LOCUS PLOT OF PITCH RATE LOOP FOR AN AIRCRAFT WITH GOOD DYNAMICS

(overdamped). The phugoid roots move toward two zeros near the origin, but for the same values of gain that dramatically affected the short period, the phugoid mode damping is hardly changed and the natural frequency decreases only slightly. It is apparent from this analysis that the feedback of pitch rate to the elevator has little effect on the phugoid mode unless high gain is used. High gain, however, increases the short period response time causing a sluggish (slow) response to pilot inputs. This sluggishness is caused by the real axis root which approaches the zero near s = -1.

If the aircraft speed increases to the transonic region so that the tuck mode appears, the pitch rate feedback remains effective in damping the short period mode at low gain, as shown in figure 14.44. The tuck mode root, however, remains unstable despite the augmentation system, showing that pitch rate feedback is ineffective in completely stabilizing the aircraft. The unstable tuck mode is usually not objectionable to the pilot as long as the time to double amplitude is large, where

$$T_2 = -\frac{\ln 2}{\sigma} \qquad (14.43)$$

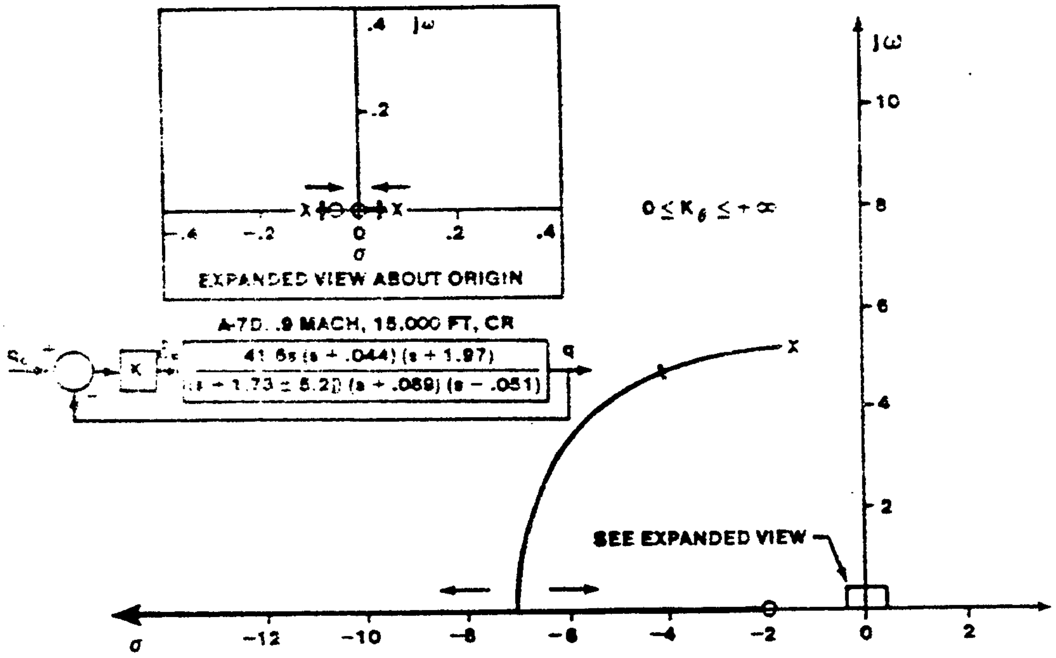

FIGURE 14.44 PITCH RATE ROOT LOCUS OF AIRCRAFT WITH TUCK MODE

14.5.1.1.1.2 Angle of Attack Rate Feedback to Increase Short Period Damping - The feedback of the rate of change of angle of attack augments the $M_{\dot{\alpha}}$ stability derivative, which increases the short period damping, as seen from the short period approximate transfer function, since

$$2\zeta_{sp}\omega_{n_{sp}} = -(Z_w + M_q + M_{\dot{\alpha}}) \tag{14.44}$$

The use of angle of attack rate feedback is similar in its effects on the aircraft characteristic roots as the pitch rate feedback system. The difficulty in using this feedback strategy involves problems in accurately sensing the angle of attack rate.

14.5.1.1.2 Increasing Short Period Natural Frequency

An increase in short period natural frequency may be desired if the aircraft pitch response is too sluggish. An increase in the frequency will cause the aircraft to repond more rapidly to pilot inputs. The usual method of accomplishing this is to feed back angle of attack to the elevator. This can also be done by feeding back normal acceleration (n_z) to the elevator, but this is more common in control augmentation systems that are designed for a load factor command system (see section 14.5.3.1 for a discussion of load factor command).

From the short period approximate transfer function, the effect of increasing the magnitude of $M\alpha$ is to increase the natural frequancy of the short period, since

$$\omega_{n_{sp}} = \sqrt{-(Z_w M_q + M_\alpha)} \tag{14.45}$$

By feeding back angle of attack to the elevator the magnitude of the M_α stability derivative is effectively increased (becomes more negative for improved static stability). The equivalent stability derivative would be

$$M_{\alpha_{AUG}} = M_{\alpha_{BASIC}} + K_\alpha M_{\delta_e} \tag{14.46}$$

The effect of angle of attack feedback on the longitudinal dynamics of an aircraft with generally acceptable characteristics is presented in figure 14.45. The short period roots move rapidly with a gain increase. At extrememly high gain, the short period roots become real, one going to the

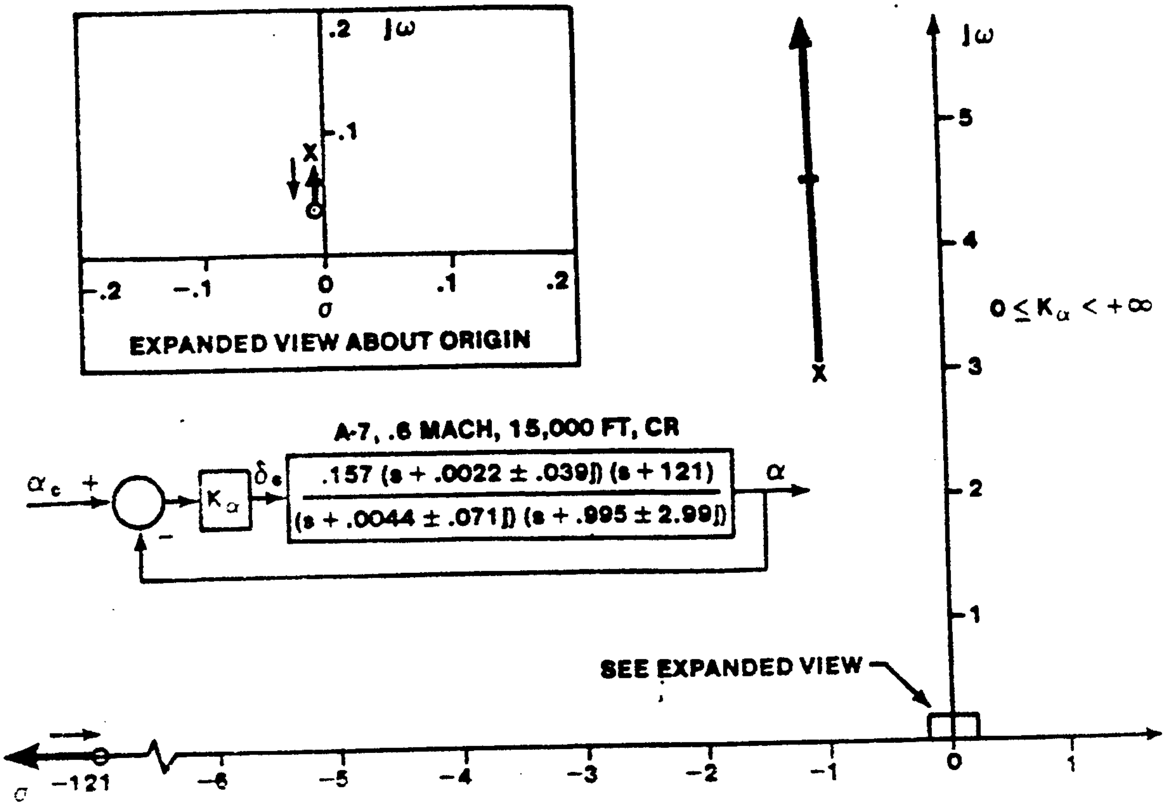

FIGURE 14.45 ROOT LOCUS PLOT OF ANGLE OF ATTACK LOOP FOR AN AIRCRAFT WITH GOOD DYNAMICS

high frequency zero on the real axis and the other tending to negative infinity. Very high gain can ideally provide heavy short period damping. This is difficult to achieve in practice due to servo (actuator) and sensor lag effects that drive the short period roots into the right half s-plane. Also, high gains tend to drive the power servo to its limits for all but the smallest inputs or disturbances. Besides, high short period natural frequencies are undesirable to the pilot since the aircraft tends to respond too abruptly.

The proximity of the complex zeros to the phugoid roots implies that angle of attack feedback causes very little change in the phugoid mode. The phugoid of the angle of attack feedback augmented aircraft is suppressed to a greater extent than for the unaugmented aircraft, but the phugoid characteristics are otherwise not appreciably altered.

14.5.1.1.3 Stabilizing the Phugoid Mode

The phugoid mode is characterized by changes in pitch attitude (θ) and forward velocity (u) which take place at approximately constant angle of attack. The feedback of θ or u to the elevator are effective means of improving the characteristics of the phugoid mode. As discussed below, the feedback of θ is common in autopilot operations, while the feedback of u is not common at all in military aircraft.

14.5.1.1.3.1 Pitch Attitude Feedback to Improve the Phugoid - Pitch attitude feedback is commonly used in autopilots (see section 14.7.1) but can also be used for piloted operations. Figure 14.46 shows a block diagram of a pitch attitude feedback control system with a pure gain controller. This system is also known as a pitch attitude command system because the negative feedback compares the pilot input to the actual response and commands the appropriate elevator deflection. If the aircraft pitch attitude response is less than that commanded, an increased deflection of the elevator is required.

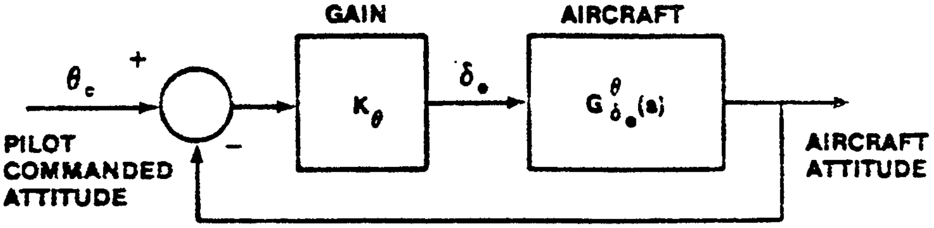

FIGURE 14.46 PITCH ATTITUDE COMMAND SYSTEM

Figure 14.47 presents the root locus of the pitch attitude command system. At moderate gain, the phugoid roots are driven close to the zeros, while the short period roots move to a higher natural frequency and a slightly lower damping ratio. This degradation of the short period damping is not necessarily undesirable unless the unaugmented aircraft short period damping is marginal. The important point to remember is that pitch attitude feedback increases the phugoid damping, effectively suppressing the phugoid dynamics — in this case at the expense of the short period. The total system damping is unchanged by the pitch attitude feedback loop since none of the aerodynamic stability derivatives that contribute to dynamic damping, such as X_u, Z_α, M_α, or M_q are augmented by the feedback, a requirement if overall system damping is to be increased.

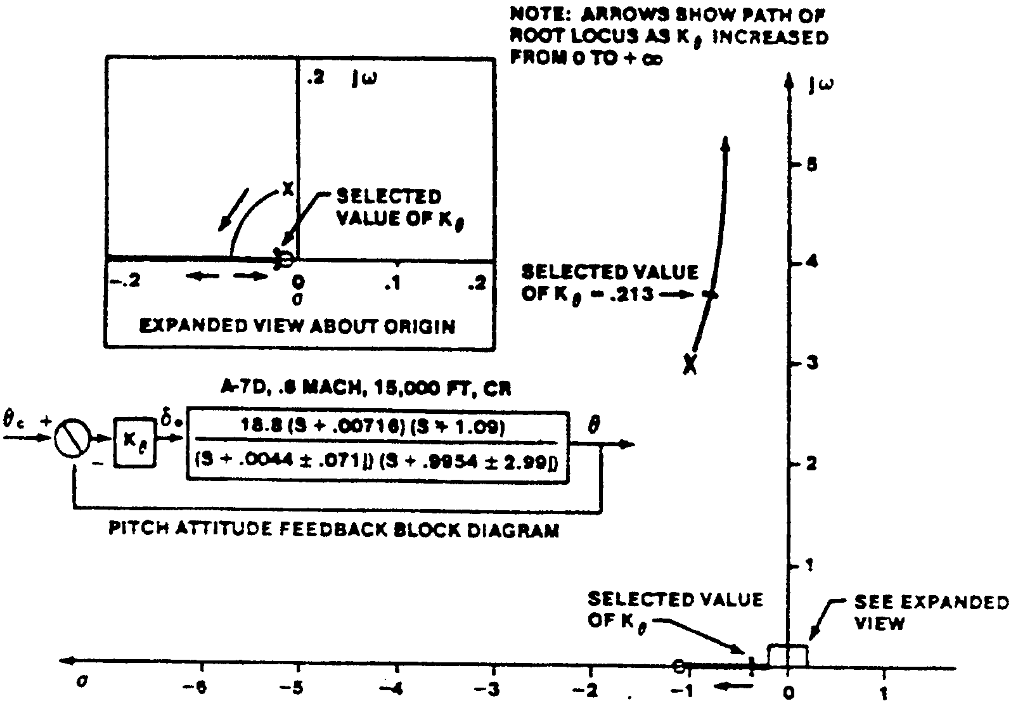

FIGURE 14.47 PITCH ATTITUDE ROOT LOCUS FOR AIRCRAFT WITH GOOD DYNAMICS

Interceptor aircraft, during high altitude supersonic flight, often have similar characteristics to the situation described above except that the damping of the unaugmented aircraft short period is very low. The feedback of the pitch attitude degrades the damping ratio of the short period rapidly as the gain increases. The suppression of the phugoid in this case extacts too high a price by excessively destabilizing the short period mode.

Figure 14.48 presents an aircraft at high subsonic speed that exhibits a longitudinal divergence (instability) commonly known as "tuck." Instead of the normal phugoid oscillation, the mode is characterized by two real roots, one stable and one unstable. This mode usually exhibits a slow increase in speed and nose down attitude. This is the result of a sufficiently negative rate of change of pitching moment due to Mach (proportional to M_u), which is caused when the aerodynamic center shifts from the one-quarter chord characteristic of subsonic flight towards the one-half mean aerodynamic chord characteristic of supersonic flight. The root locus of the pitch attitude

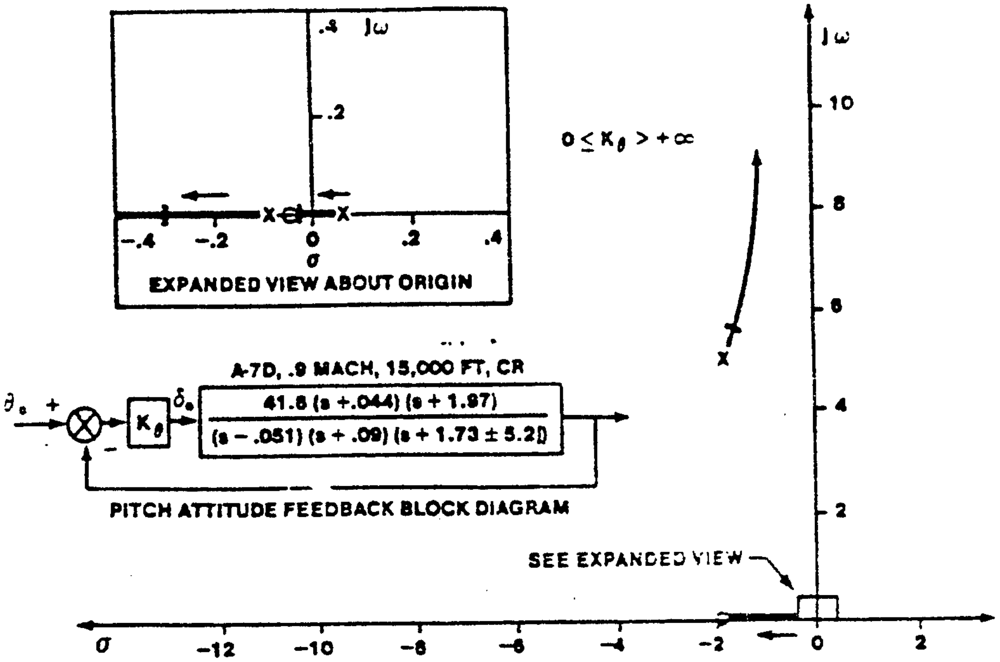

FIGURE 14.48 PITCH ATTITUDE ROOT LOCUS FOR AN AIRCRAFT WITH GOOD DYNAMICS

feedback loop shows that at a moderate gain, the tuck mode moves from the right half s-plane to the left half s-plane so that the closed loop aircraft system becomes stable.

In these pitch attitude feedback augmentation schemes, the open loop gain does not become infinite at low frequencies since a pole at the origin does not exist (type 0 system). The closed loop frequency response, therefore, has an amplitude ratio slightly less than one at low frequencies, as illustrated in figure 14.49 for an aircraft with well behaved unaugmented characteristics and a selected value of system gain. The higher the gain, the lower the steady state error. But an infinite (or very large) gain cannot be used since the short period damping would approach zero. Several ways to eliminate the steady state error in the pitch command system will be discussed in paragraph 14.7.1.

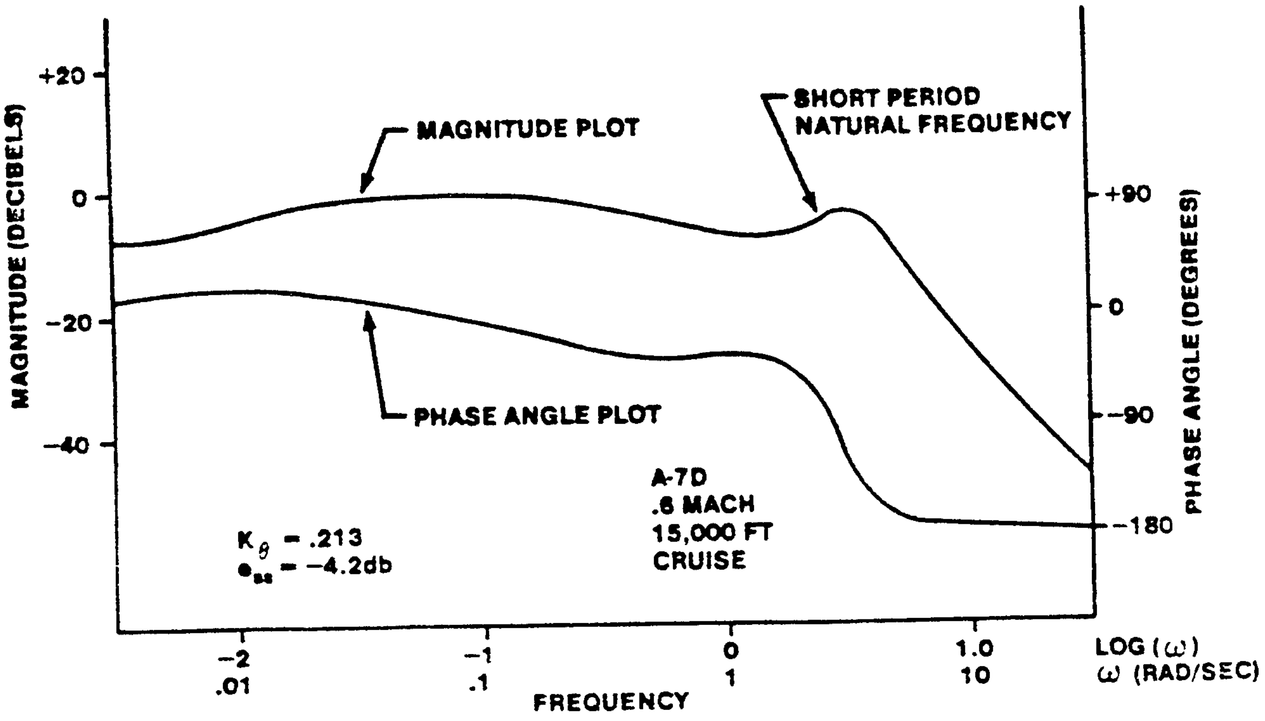

FIGURE 14.49 BODE PLOT OF CLOSED LOOP PITCH ATTITUDE CONTROL SYSTEM FOR AN AIRCRAFT WITH GOOD DYNAMICS

14.5.1.1.3.2 Forward Velocity Feedback to Improve the Phugoid - The feedback of forward velocity to the elevator has a powerful effect on the phugoid mode, as shown in figure 14.50. The augmented phugoid roots move rapidly to a higher natural frequency and the phugoid damping is greatly increased. Comparatively large phugoid damping ratios can be achieved before the short period is altered significantly. The effect of velocity feedback is to augment the M_u stability derivative, which increases both the phugoid natural frequency and damping.

In many situations, the complex zero in the $G^u_{\delta_e}(s)$ transfer function are replaced by a pair of zeros on the real axis. In this situation, the phugoid damping due to velocity feedback is more pronounced that that of the example used in figure 14.50.

The same beneficial effect on the phugoid also occurs if a tuck mode is present. A relatively low forward loop gain will stabilize the tuck mode root while not significantly affecting the short period.

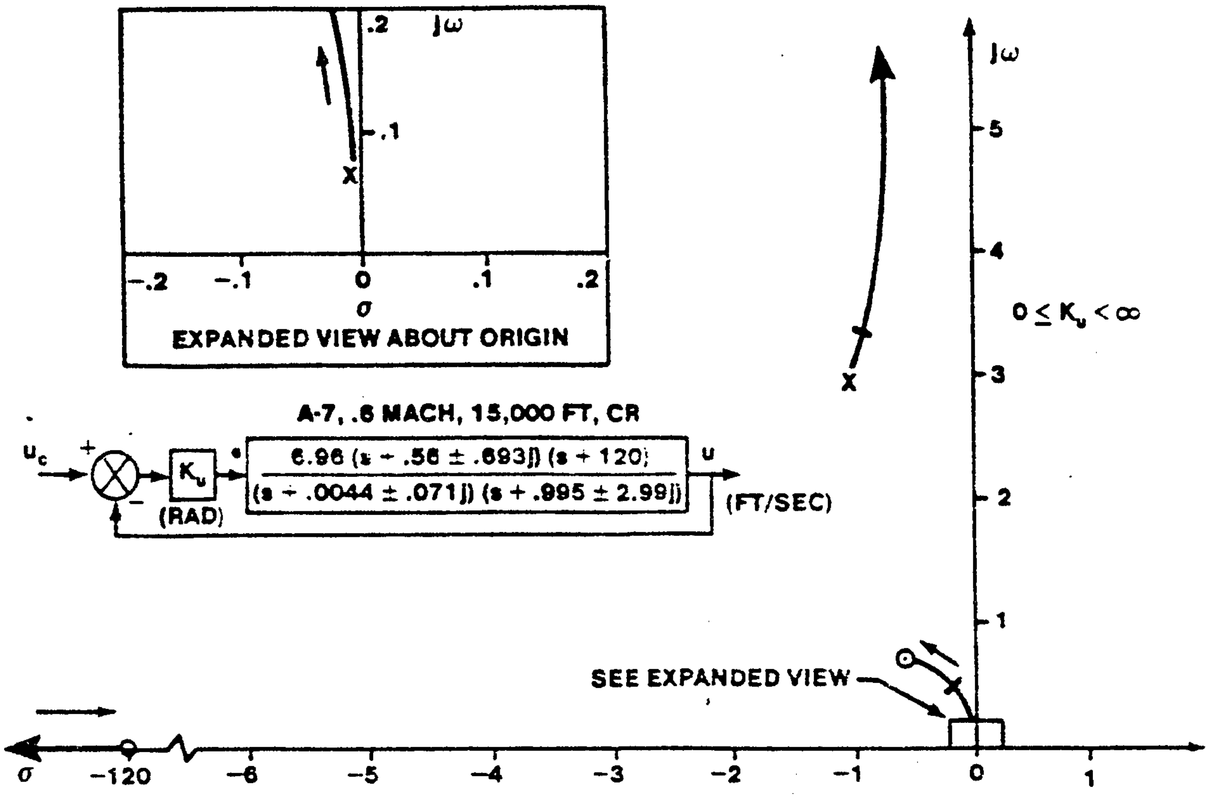

FIGURE 14.50 FORWARD VELOCITY ROOT LOCUS FOR AN AIRCRAFT WITH GOOD DYNAMICS

Although the augmented phugoid damping ratio improved by the feedback of forward velocity error alone, the damping is improved further if forward acceleration is also fed back. This creates a new stability derivative, $M_{\dot{u}}$ which augments the $2\zeta_p\omega_{n_p}$ term in the approximate transfer function.

The effect of using pitch attitude to augment the phugoid mode is to regulate airspeed by applying a pitching moment whenever the speed changes. This can be disconcerting to the pilot if the pitching moment is too great, especially in turbulence. Because of this, the use of the elevator to control airspeed and in turn the phugoid is not common in military aircraft.

14.5.1.1.4 Stabilizing Aft c.g. Aircraft

The most modern fighter aircraft are designed with relaxed static stability. This term is used to describe the situation where the static margin is zero or slightly negative. This increases a fighter aircraft's maneuvarability and payload-range performance. We can expect in the near future for large aircraft to also be designed with relaxed static stability in order to achieve improved payload-range performance. The most common method of providing artificial stability to these aircraft is through angle of attack (α) feedback to the elevator. Pitch attitude (θ), and pitch rate (q) can also be used to stabilize an aft c.g. aircraft.

14.5.1.1.4.1 Angle of Attack Feedback on Aft C.G. Aircraft - Figure 14.51 shows the root locus of an angle of attack command system for an aircraft which is statically unstable, longitudinally, where the center of gravity (c.g.) is aft of the aerodynamic center, so that $M_\alpha > 0$.

A relatively low gain causes the unstable root to move into the left half s-plane. The two oscillatory roots move rapidly to the real axis, one moving

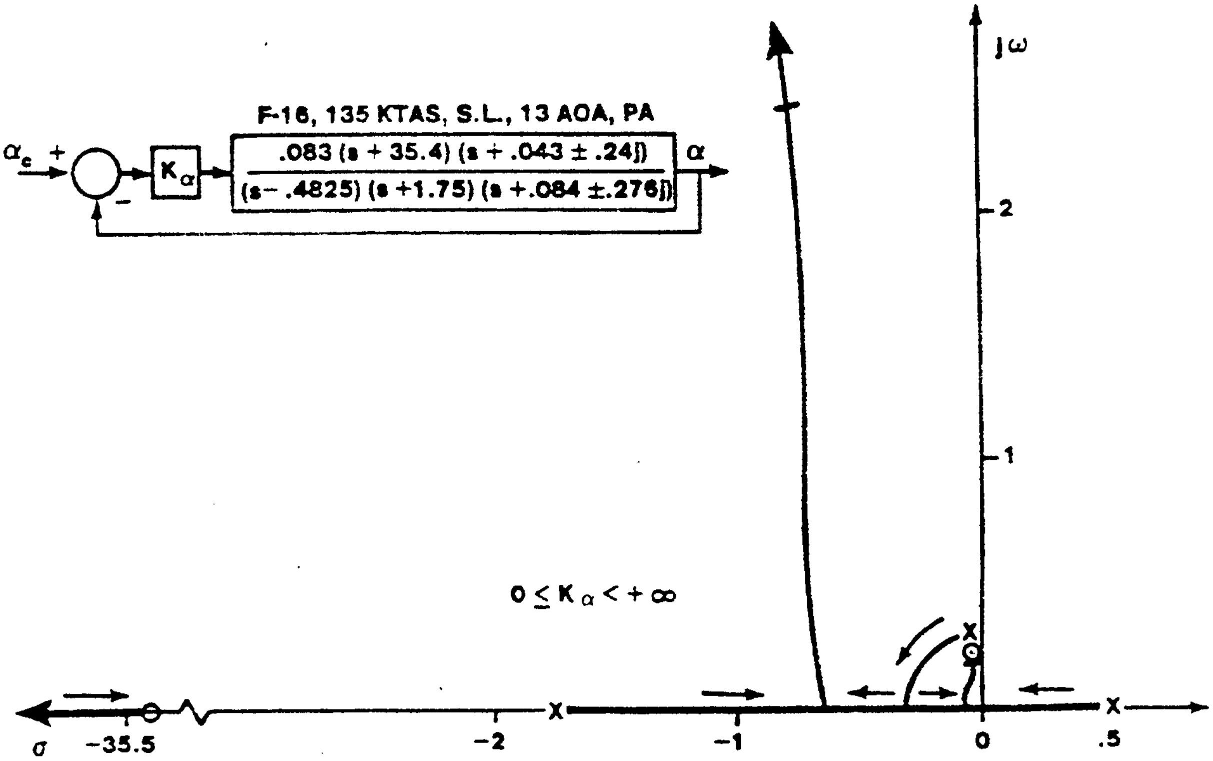
F-16, 135 KTAS, S.L., 13 AOA, PA
α_c
+
−
K_α
$\frac{.083(s+35.4)(s+.043\pm.24j)}{(s-.4825)(s+1.75)(s+.084\pm.276j)}$
α
$j\omega$
2
1
$0 \leq K_\alpha < +\infty$
σ
−35.5
−2
−1
0
.5

FIGURE 14.51 ANGLE OF ATTACK ROOT LOCUS FOR LONGITUDINALLY STATICALLY UNSTABLE AIRCRAFT

towards the origin and the other towards the stable real axis root. At a low gain, two of the roots become a phugoid mode pair while the other two form the short period roots. As the gain increases, the phugoid frequency increases and the damping decreases. At very high gain, the phugoid is suppressed by the pair of zeros near the origin. The short peroid frequency increases and the damping decreases with increasing gain. The effects of angle of attack feedback for the statically unstable aircraft are identical to that for the aircraft with reasonably good dynamics as the gain becomes very large. The aircraft possesses static stability once the characteristic roots move into the left half s-plane.

14.5.1.1.4.2 Pitch Attitude Feedback on Aft C.G. Aircraft - Figure 14.52 shows the effect of pitch attitude feedback on the F-16, an aircraft which uses an aft c.g. to decrease trim drag during cruise and improve maneuverability.

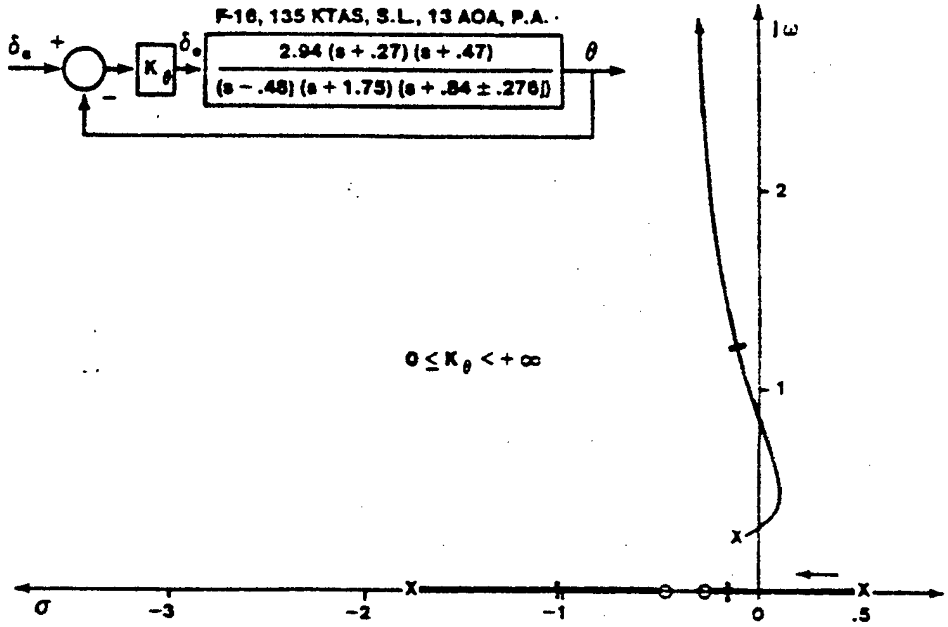
F-16, 135 KTAS, S.L., 13 AOA, P.A.
δ_e
+
−
K_θ
δ_e
$\dfrac{2.94\,(s+.27)\,(s+.47)}{(s-.48)\,(s+1.75)\,(s+.84\pm.276j)}$
θ
$j\omega$
2
1
$0 \le K_\theta < +\infty$
σ
−3
−2
−1
0
.5

FIGURE 14.52 PITCH ATTITUDE ROOT LOCUS FOR LONGITUDINALLY STATICALLY UNSTABLE AIRCRAFT

Figure 14.53 shows the effect of pitch attitude feedback on the AV-8A Harrier vertical takeoff and landing (VTOL) fighter during transition from wingborne (conventional) flight to jetborne (VTOL) flight. The unstable

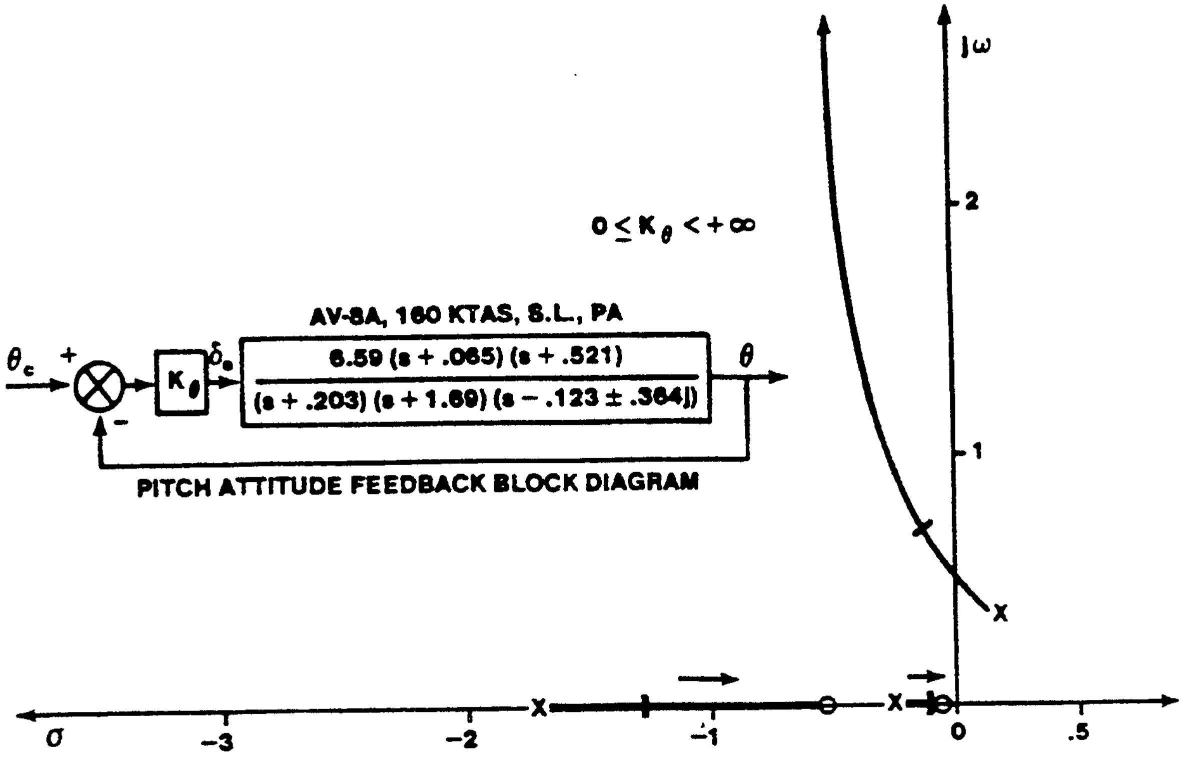
jω
2
1
$0 \le K_\theta < +\infty$
AV-8A, 160 KTAS, S.L., PA
θ_c
+
−
K_θ
δ_e
$\frac{6.59(s+.065)(s+.521)}{(s+.203)(s+1.69)(s-.123\pm.364j)}$
θ
PITCH ATTITUDE FEEDBACK BLOCK DIAGRAM
σ
−3
−2
−1
0
.5

FIGURE 14.53 PITCH ATTITUDE ROOT LOCUS FOR AIRCRAFT WITH UNSTABLE OSCILLATORY MODE

oscillatory pair are stabilized at a low value of gain and the damping of the short period is initially increased. The behavior of the short period mode of the augmented aircraft then behaves in a manner similar to conventional aircraft in that the damping is reduced and the natural frequency increased as tha gain becomes larger. The two roots on the real axis remain stable for all values of gain.

14.5.1.1.4.3 Pitch Rate Feedback on Aft C.G Aircraft - Figure 14.54 presents the effects of a pitch rate command system on an aircraft with an unstable oscillatory mode. For some minimum gain the unstable oscillatory roots move into the left half s-plane. The damping ratio increases and the natural frequancy decreases rapidly with increasing gain. The oscillatory mode is effectively suppressed at a reasonably low gain.

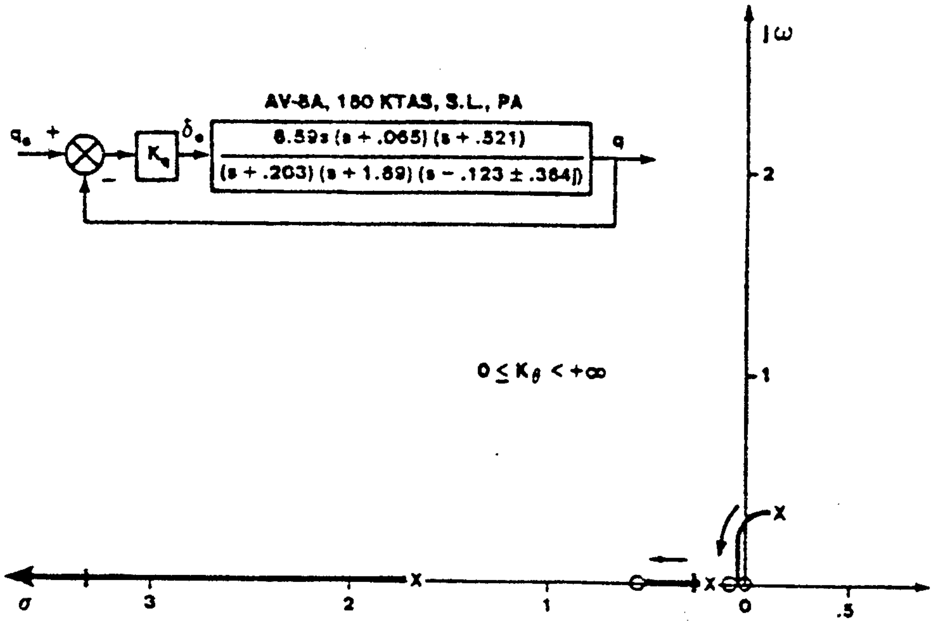
AV-8A, 180 KTAS, S.L., PA
q_c
+
−
K_q
δ_e
$\frac{6.59s(s+.065)(s+.521)}{(s+.203)(s+1.89)(s-.123\pm.364j)}$
q
jω
2
1
$0 \le K_\theta < +\infty$
σ
3
2
1
0
.5

FIGURE 14.54 PITCH RATE ROOT LOCUS FOR AN AIRCRAFT WITH AN UNSTABLE OSCILLATORY MODE

14.5.1.2 Lateral-Directional Axes Single Loop SAS

The primary purpose of the lateral-directional stability augmentation system is to provide acceptable Dutch roll characteristics while retaining a sufficiently fast roll response for the aircraft. The spiral mode stability is often sacrificed in augmentation systems, since the pilot can easily control a slight tendency for the aircraft to increase its bank angle during a turn. Poor Dutch roll characteristics are usually quite annoying, especially if the aircraft is disturbed by turbulence or if the pilot is trying to perform tight tracking tasks such as formation flying, air-to-air or air-to-ground tracking, or approach and landing. Lateral-directional stability augmentation systems are also used to decrease the roll mode time constant, increase spiral stability, provide rudder coordination in turns, reduce adverse yaw or alter the aircraft roll axis for gun aiming.

14.5.1.2.1 Increasing Dutch Roll Damping

One of the several modes of the aircraft motion which have been affected by the deterioration in stability of the basic aircraft is the Dutch roll oscillation. Although the Dutch roll damping frequently is still positive, it is often so low that continuous oscillations occur in flight due to frequent excitation by gusts and control inputs. Continuous Dutch roll is not only uncomfortable to both the pilot and crew, but can also be an impediment to the accomplishment of the mission. For example, tactical military aircraft aircraft must be capable of flying a smooth path for gunnery or rocket firing, bombing, or photography. It is therefore necessary that any erratic airframe motion than cannot be controlled by the pilot be controlled by some other method.

The usual method of augmenting Dutch roll damping is to feed back yaw rate (r) to the rudder. Sideslip angle rate ($\dot{\beta}$) can also be used but it is difficult to accurately sense sideslip angle rate. This type of feedback is used extensively, however, in fighter aircraft in order to improve handling qualities during aggressive maneuvering, such as for gun aiming. This is discussed in section 14.5.1.2.6.

A SAS that feeds back yaw rate to the rudder in order to increase Dutch roll damping is usually called a yaw damper. A yaw damper senses yaw rate and moves the rudder in a manner proportional to and opposite to the yaw rate. This augments the stability derivative N_r. An equivalent value of N_r may be found for a "perfect" yaw damper from

$$N_{r_{AUG}} = N_{r_{BASIC}} + K_r N_{\delta_R} \tag{14.47}$$

It should be kept in mind that the yaw damper, while operating through the rudder, will also augment L_r. The new equivalent value of L_r is found from

$$L_{r_{AUG}} = L_{r_{BASIC}} + K_r L_{\delta_R} \tag{14.48}$$

The spiral mode and roll mode are both affected by L_r and the effect of the yaw damper on these modes should not be generalized.

The common mechanization of a yaw damper is shown in figure 14.55. The washout circuit acts as a highpass filter which does not allow the steady state (low frequency) yaw rate signals present in a steady turn to deflect the rudder from neutral. This ensures that the yaw damper provides a feedback signal only during transient motions. If the yaw rate signal did not go to zero in a steady turn then, for a positive yaw rate, a positive rudder deflection would result. This would yield an uncoordinated turn

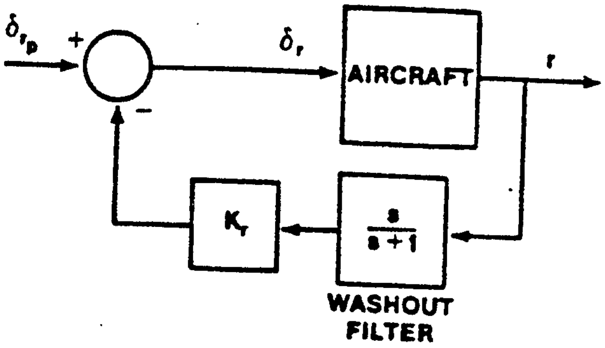

FIGURE 14.55 TYPICAL YAW DAMPER SYSTEM

maneuver which would require a larger than normal rudder input by the pilot to obtain coordination. The transient signals (high frequency) present when the Dutch roll mode is excited are passed with unity gain by the washout circuit and used to deflect the rudder to oppose the motion.

Figure 14.56 present a root locus of a yaw rate command system. The spiral mode is stabilized for low values of K_r and the Dutch roll damping

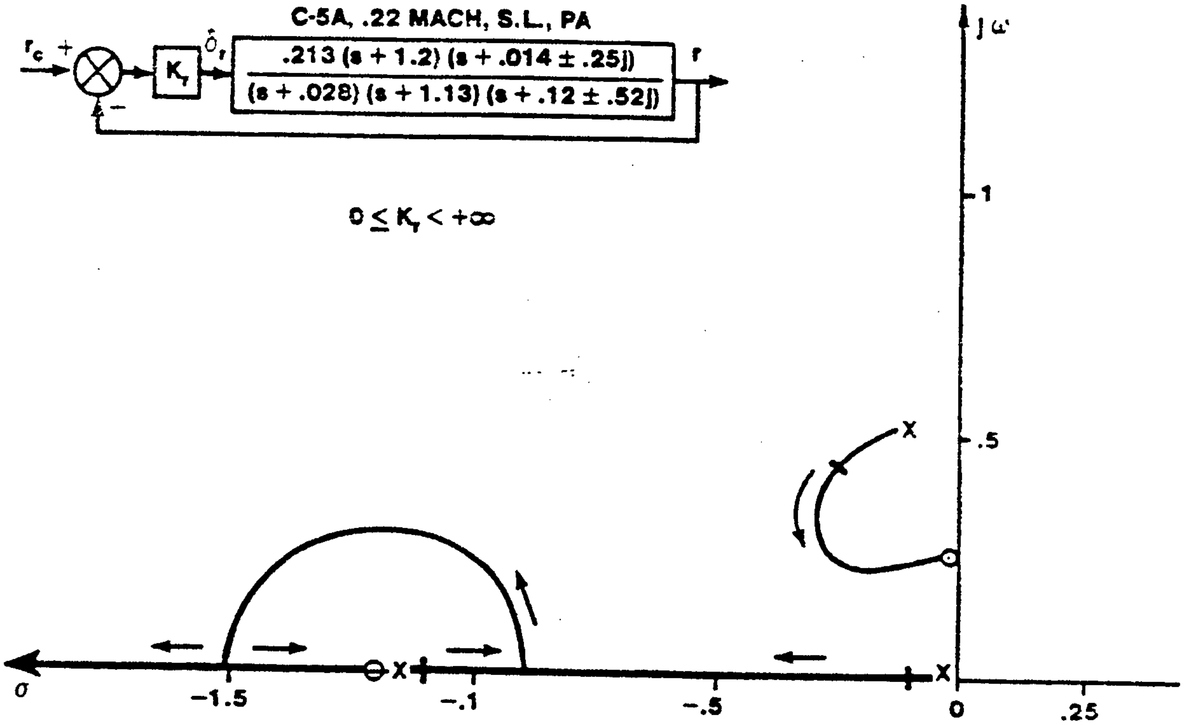

FIGURE 14.56 ROOT LOCUS OF YAW RATE FEEDBACK TO THE RUDDER

increases rapidly as the gain increases. The roll mode time constant is not significantly affected for moderate values of gain but may decrease or increase slightly depending on the exact location of the real axis zero.

14.5.1.2.2 Decreasing Roll Mode Time Constant

When an aircraft's roll mode time constant is too high a roll damping SAS is generally used to augment the L_p stability derivative. An increase in L_p will decrease the roll mode time constant

$$t_R = \frac{-1}{L_p} \tag{14.49}$$

One disadvantage of a roll damper is that it subtracts from the maximum steady state roll rate which the aircraft is capable of reaching

$$P_{ss} = \frac{-L_{\delta_a} \delta_a}{L_p} \tag{14.50}$$

An equivalent value of L_p may be found for a "perfect" roll damper from

$$L_{p_{AUG}} = L_{p_{BASIC}} + K_p L_{\delta_a} \tag{14.51}$$

Sometimes an increase in roll damping is also found to improve Dutch roll damping. This occurs when ailerons are a source of Dutch roll excitation. Under these conditions, the effect of the damper would also be to reduce the Dutch roll ϕ/β ratio.

Larger aircraft often employ roll dampers. Modern fighters with full authority control augmentation systems use roll rate command systems for lateral control. Figure 14.57 shows the effect of a roll rate command system on the C-5A in the power approach configuration. The Dutch roll mode is effectively suppressed for relatively low values of gain. The roll mode time constant decreases slightly (maximum roll acceleration increases). The spiral mode is destabilized and, for high gain, may become unstable, although spiral dynamics which can easily be controlled by the pilot are retained.

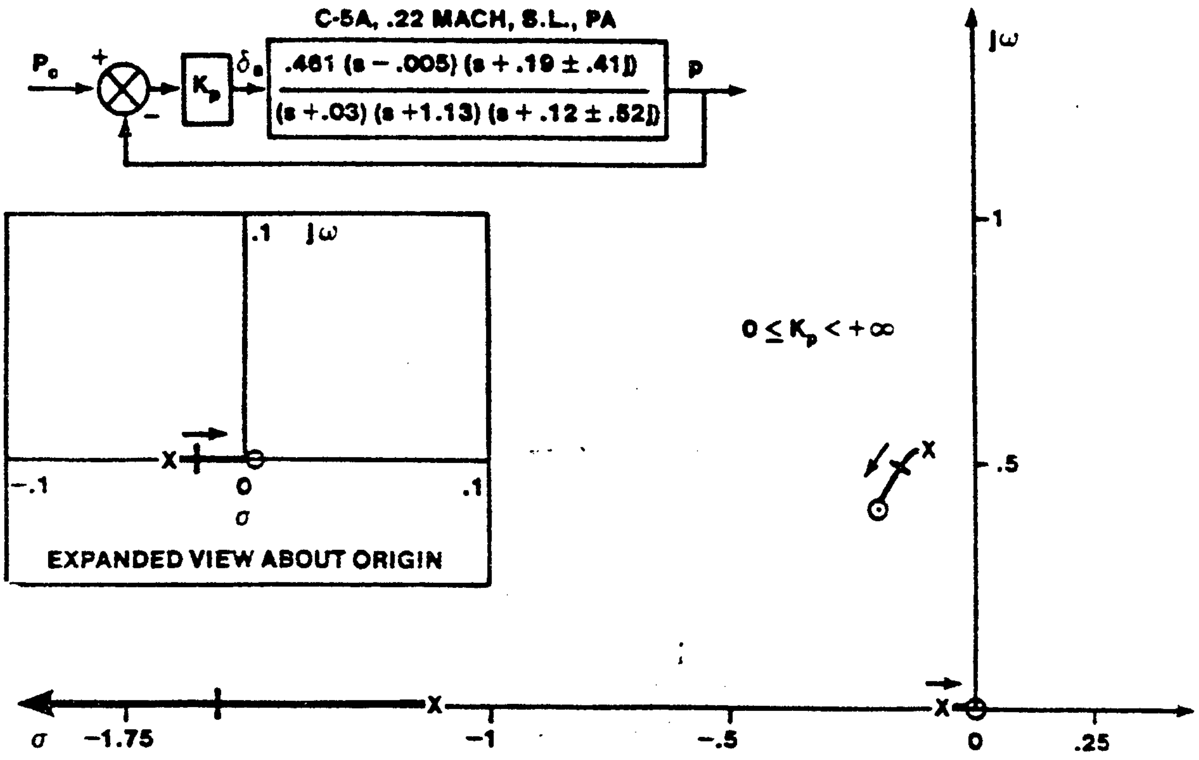

FIGURE 14.57 ROOT LOCUS OF ROLL RATE FEEDBACK TO THE AILERONS

14.5.1.2.3 Stabilizing the Spiral Mode

The spiral mode time constant is usually very high and, even if the spiral mode is unstable, it is usually easily controlled by the pilot. For autopilot operation, however, the spiral mode must be stabilized. This is usually done by the feedback of bank angle (and often roll rate also) to the ailerons. Autopilot operation is discussed in section 14.7.3.

The use of sideslip angle as a feedback to the ailerons alters the L_β and N_β stability derivatives and is seldom used (not used in any modern military aircraft). Sideslip angle feedback to the ailerons can provide some good features, such as spiral mode stabilization (increased effective dihedral), but is usually accompanied by decreased Dutch roll damping or Dutch roll destabilization which outweigh the advantages, as shown in figure 14.58.

The feedback of yaw rate to the ailerons can be an effective means of stabilizing the spiral mode by augmenting the L_r derivative. If the basic aircraft possesses sufficient proverse yaw due to ailerons, the Dutch roll mode damping may also be improved, as shown in figure 14.59. For the more

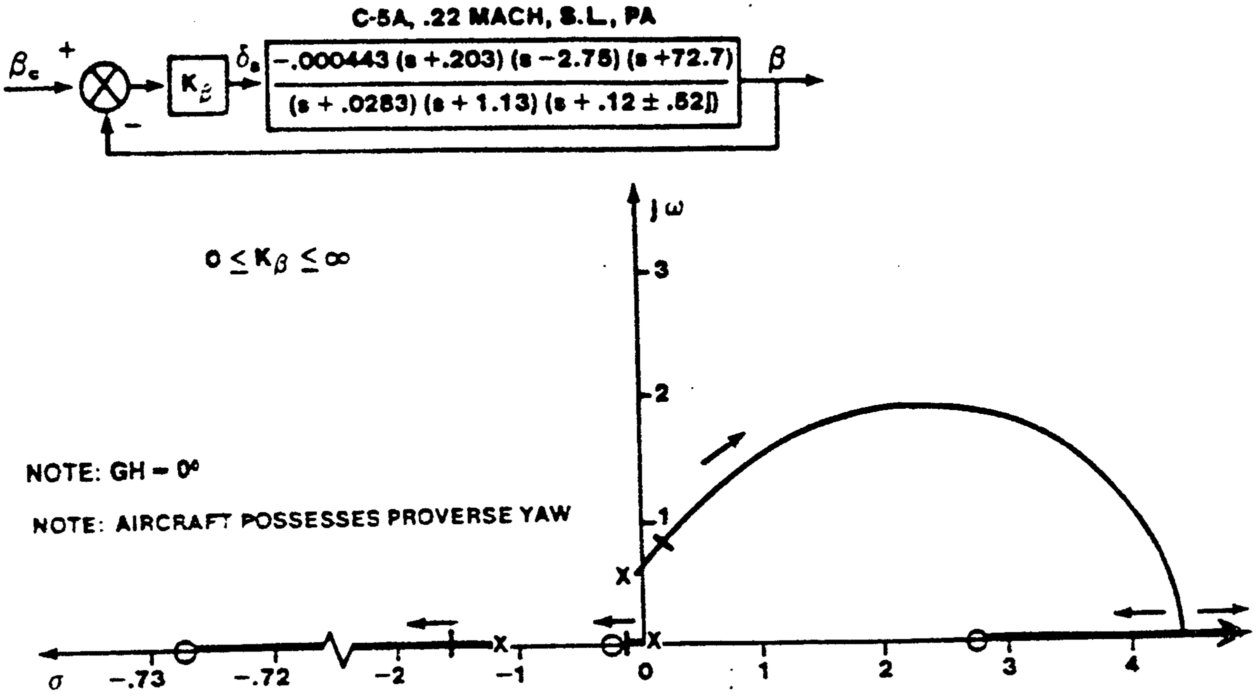
C-5A, .22 MACH, S.L., PA
β_c
+
−
K_β
δ_a
$\frac{-.000443 (s+.203)(s-2.78)(s+72.7)}{(s+.0283)(s+1.13)(s+.12\pm.52j)}$
β
$j\omega$
$0 \le K_\beta \le \infty$
NOTE: GH = 0°
NOTE: AIRCRAFT POSSESSES PROVERSE YAW
σ
−.73
−.72
−2
−1
0
1
2
3
4
1
2
3

FIGURE 14.58 ROOT LOCUS OF SIDESLIP ANGLE FEEDBACK TO THE AILERONS

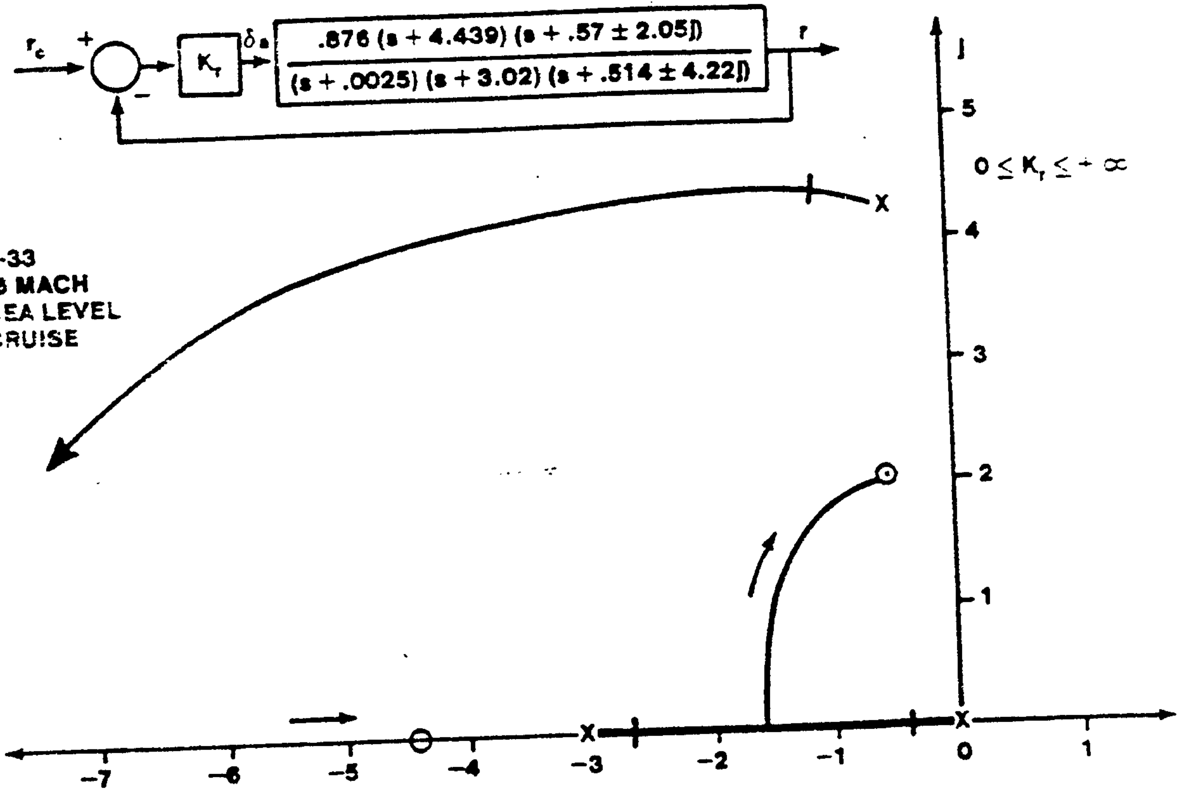
r_c
+
−
K_r
δ_a
$\frac{.876 (s+4.439)(s+.57\pm2.05j)}{(s+.0025)(s+3.02)(s+.514\pm4.22j)}$
r
j
$0 \le K_r \le +\infty$
T-33
.6 MACH
SEA LEVEL
CRUISE
5
4
3
2
1
−7
−6
−5
−4
−3
−2
−1
0
1

FIGURE 14.59 ROOT LOCUS OF YAW RATE FEEDBACK TO THE AILERONS

common case of adverse yaw (or slightly proverse yaw) due to the aileron, as shown in figure 14.60, the yaw rate feedback gain cannot be increased too much without making the Dutch roll mode go unstable.

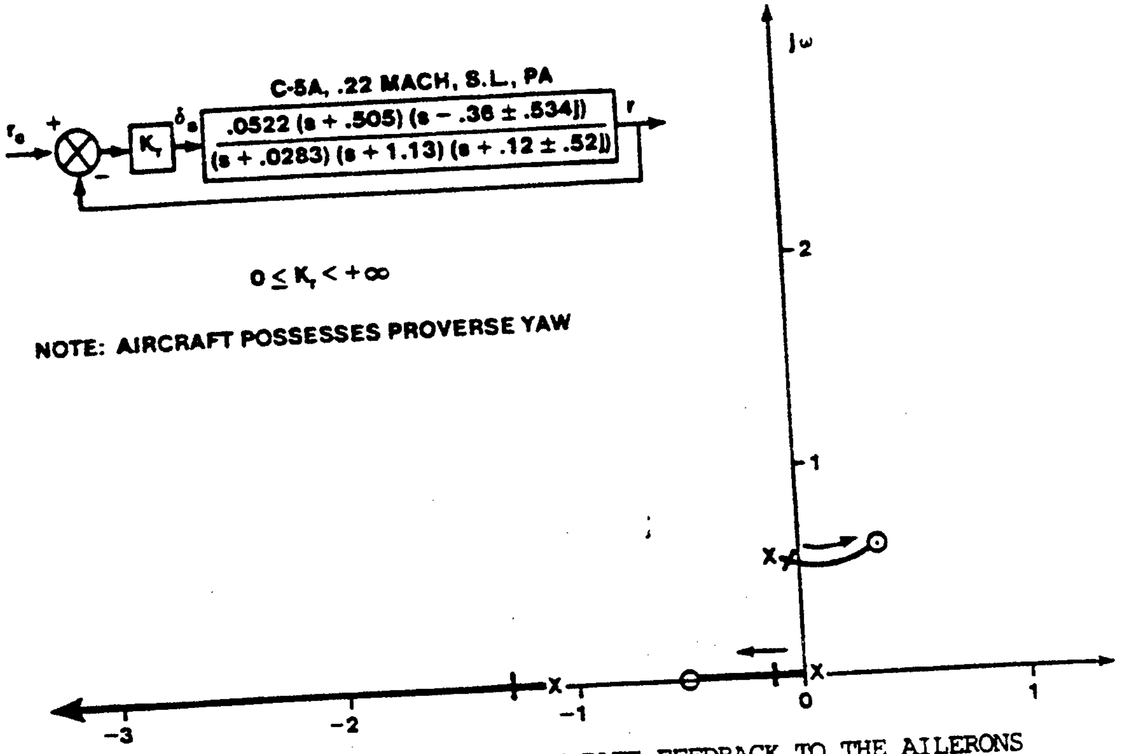

C-5A, .22 MACH, S.L., PA
r_c
+
−
K_r
δ_a
$\frac{.0522(s+.505)(s-.36\pm.534j)}{(s+.0283)(s+1.13)(s+.12\pm.52j)}$
r
$0 \le K_r < +\infty$
NOTE: AIRCRAFT POSSESSES PROVERSE YAW
jω
2
1
−3
−2
−1
0
1

FIGURE 14.60 ROOT LOCUS OF YAW RATE FEEDBACK TO THE AILERONS

14.5.1.2.4 Providing Rudder Coordination in Turns

Turn coordination can be effectively achieved by feedback of either sideslip angle or lateral acceleration to the rudder. Both methods also increase Dutch roll natural frequency and destabilize the spiral mode.

14.5.1.2.4.1 Sideslip Angle Feedback for Turn Coordination - The feedback of sideslip angle to the rudder effectively augments the weathercock stability of the aircraft — the N_β stability derivative. It is a useful way to provide aircraft coordination if properly implemented. Figure 14.61 shows the effect of sideslip angle feedback. The roll mode root location is not significantly altered. The spiral mode is destabilized but the time to double amplitude is long and is easily controlled by the pilot. The Dutch roll damping ratio is not changed until high values of gain are used, but the natural frequency increases rapidly for low gain. To increase the Dutch roll damping, yaw rate or sideslip angle rate feedback may be added as an additional feedback loop.

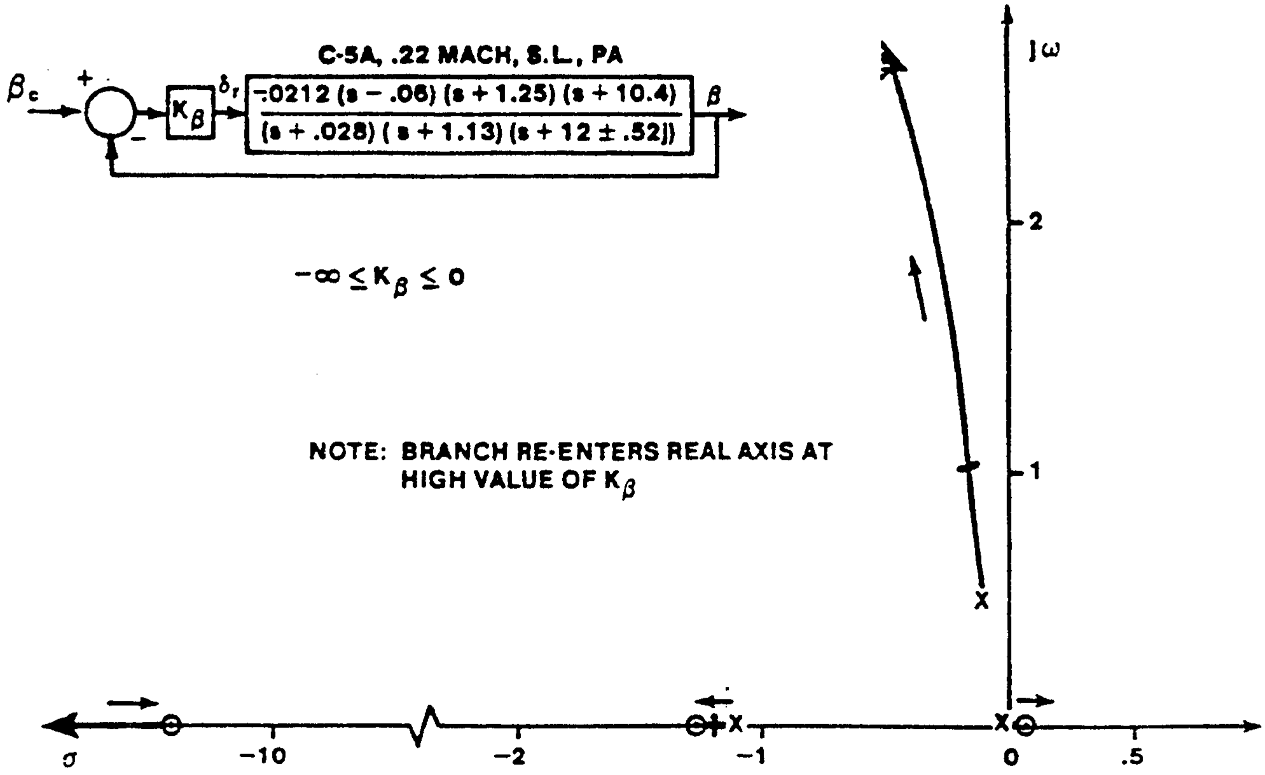

FIGURE 14.61 ROOT LOCUS OF SIDESLIP ANGLE FEEDBACK TO THE RUDDER

The main disadvantage of the sideslip angle system is the practical one of instrumenting high quality sideslip sensors.

14.5.1.2.4.2 Lateral Acceleration Feedback for Turn Coordination - The difficulty in sensing sideslip angle can be overcome by using a properly located lateral accelerometer, where lateral acceleration can be expressed as (center of gravity)

$$a_y = U_0 (\beta + r) - g \phi \cos \theta_0 \quad \text{(stability axis)} \qquad (14.52)$$

The accelerometer should be located close to

$$\ell_x = \frac{-Y_{\delta_r}}{N_{\delta_r}} \qquad (14.53)$$

so that the initial part of the lateral acceleration response to a step rudder input is proportional to the sideslip angle response due to a rudder deflection. This location corresponds to the instantaneous center of rotation about the Z body axis. The lateral acceleration feedback thus acts to provide aircraft coordination, and is used for this purpose in the A-7. Figure 14.62 shows the effect of lateral acceleration feedback with the accelerometer at the center of gravity.

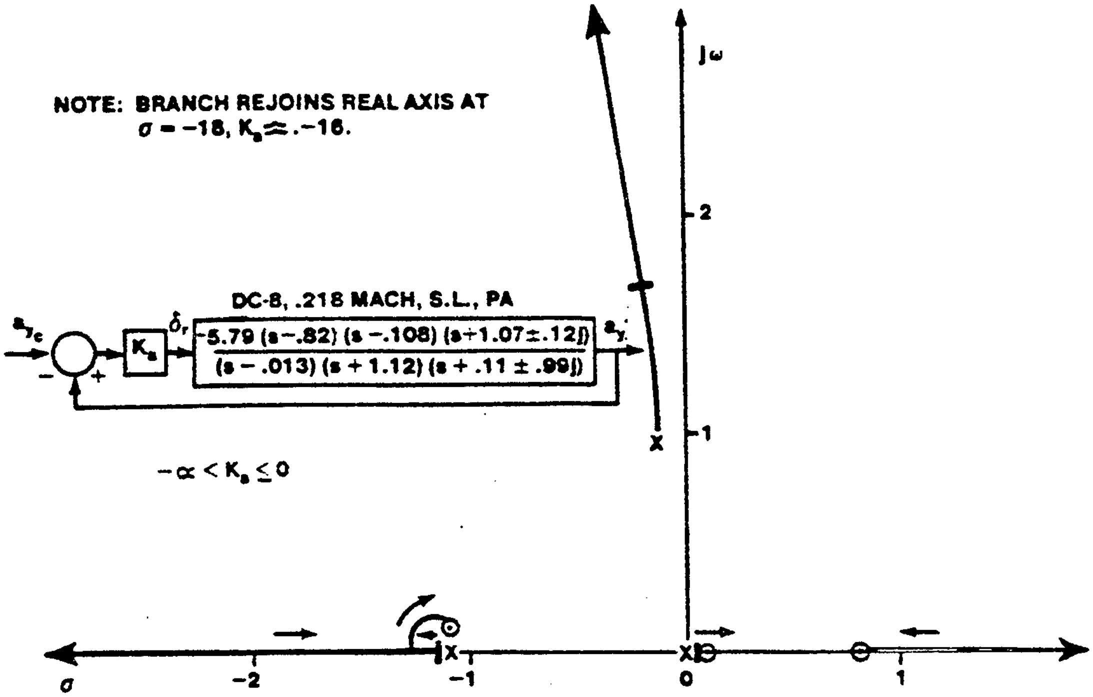

FIGURE 14.62 ROOT LOCUS OF LATERAL ACCELERATION FEEDBACK TO RUDDER

14.5.1.2.5 Reducing Adverse Yaw

Aileron-rudder interconnects are often used in flight control systems to counteract the adverse yaw induced by deflecting the ailerons. The aileron-rudder interconnect, if properly designed, acts to minimize sideslip excursions during rolling maneuvers, but is occasionally designed to provide proverse yaw if roll rate can be increased. Figure 14.63 shows an aileron-rudder interconnect system for an aircraft with no augmentation systems engaged. The equation for the aircraft response is

$$\beta = G^{\beta}_{a}\,\delta_a + G^{\beta}_{r}\,\delta_r \qquad (14.54)$$

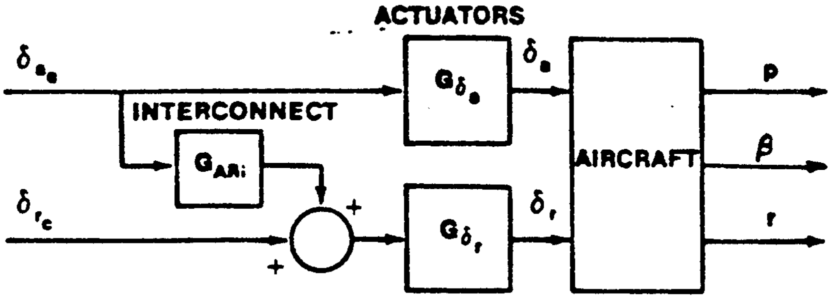

FIGURE 14.63 AIRCRAFT WITH AILERON-RUDDER INTERCONNECT

Since no feedback is provided to either control surface, the characteristic roots of the unaugmented aircraft cannot be effected. If the interconnect provides perfect coordination then $\beta = 0$ and the ratio of rudder to aileron becomes

$$\frac{\delta_r}{\delta_a} = -\frac{G^{\beta}_{\delta_a}}{G^{\beta}_{\delta_r}} = -\frac{N^{\beta}_{\delta_a}}{N^{\beta}_{\delta_r}} = G_{ARI} \qquad (14.55)$$

The above expression yields the ideal aileron-rudder interconnect transfer function and is valid if the aileron and rudder actuators have the same dynamics. If the dynamics differ, then the aileron-rudder interconnect transfer function must account for the different actuator dynamics for perfect coordination, and becomes

$$G_{ARI} = -\frac{K_{\delta_a} D_{\delta_r} N^{\beta}_{\delta_a}}{K_{\delta_r} D_{\delta_a} N^{\beta}_{\delta_r}} \qquad (14.56)$$

Often the aileron-rudder interconnect is mechanized to provide slightly proverse yaw during roll. The roll rate due to an aileron input will then be increased, since the rudder is also deflected. The response of the aircraft due to rudder inputs alone are unaffected by the aileron-rudder interconnect since the Dutch roll, spiral and roll mode roots are not affected.

14.5.1.2.6 Altering Roll Axis for Aggressive Maneuvering

The use of computed sideslip angle rate feedback (commonly called a beta-dot system) to the rudder has been used in fighter aircraft, such as the A-10, F-16, and A-7D Digitac aircraft. The advantage of beta-dot feedback is that the aircraft can be made to roll about a depressed roll axis, usually slightly below the gun line, which can improve the aircraft handling qualities during aggressive maneuvers such as air-to-surface weapon delivery. Proper rudder coordination must also, however, be applied by the augmentation system to keep the sideslip angle near zero (see section 14.5.2.5).

The sideslip angle rate is difficult to measure accurately but can be computed from other easily measured quantities as

$$\dot{\beta} = -r + \alpha p + \frac{g}{U_0} \sin \phi \cos \theta + \frac{a_{y_{cg}}}{U_0} \qquad (14.57)$$

Often, if the gun line is designed to nearly coincide with the velocity vector of the aircraft, it is desirable to have the aircraft roll about an axis which is slightly depressed below the gun line (velocity vector) to eliminate any pendulum effect in the fixed gunsight by providing initial pipper motion in the direction of the target as a roll toward the target is initiated. The estimate for sideslip angle rate is then modified as

$$\dot{\beta} = -r + (\alpha + \alpha_B)\, p + \frac{g}{V_A} \sin \phi \cos \theta \qquad (14.58)$$

where α_B is a bias added to depress the roll axis below the relative velocity vector of the aircraft.

Often, the full equation is not used to estimate the sideslip angle rate. The system in the A-10 eliminates the pitch angle input into the equation, setting $\cos \theta = 1$. When performing a loop or other vertical maneuver, the beta-dot system deflects the rudder fully whenever the aircraft nose passes through the vertical, that is, whenever $\theta = \pm 90^\circ$, since the bank angle is undefined in this situation. The full authority rudder input then causes a yaw transient. This shows that implementations which do not use the full equation must be carefully studied to determine the impact of the simplification on the aircraft flying qualities.

Figure 14.64 presents a root locus plot of a sideslip angle rate feedback system. The Dutch roll mode damping is increased rapidly with increasing gain. The spiral and roll modes are hardly affected except for moderately large gain.

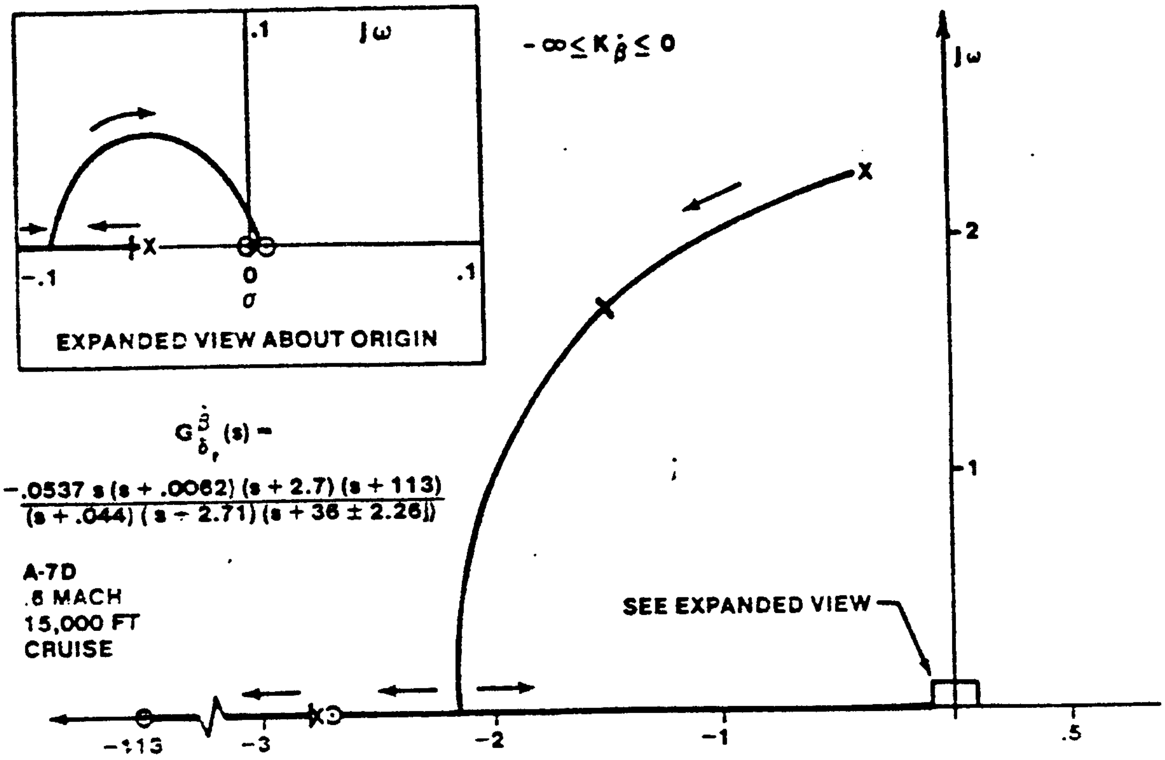

FIGURE 14.64 ROOT LOCUS OF SIDELIP ANGLE RATE FEEDBACK TO RUDDER

14.5.1.3 Augmentors in Reversible Control Systems

In a boosted or reversible control system the pilot may sense damper movement of the controls because of the direct link of the control to the aerodynamic surface (as shown in figure 14.56a). The pilot often senses an increase in control forces caused by the damper attempting to oppose transient aircraft motions, such as when using yaw damper systems during a wing-low crosswind landing (KC-135 or A-37). For most applications, these are undesirable and annoying effects. A dual servo arrangement, as shown in figure 14.65b, could be used to prevent augmentation movement of the cockpit controls.

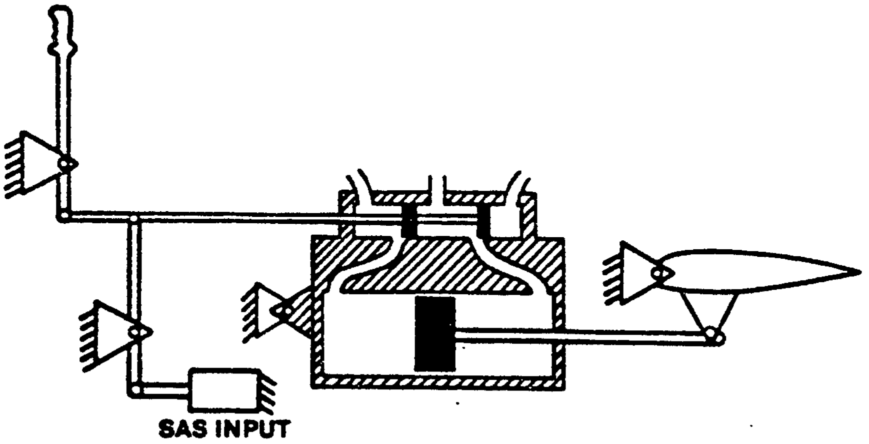

a. SURFACE MOVEMENT REFLECTED IN PILOT CONTROLLER

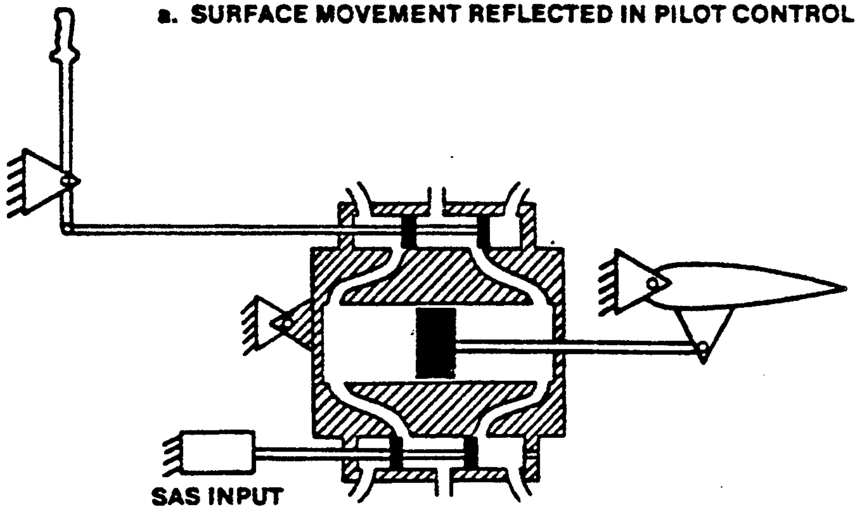

b. SURFACE MOVEMENT NOT REFLECTED IN PILOT CONTROLLER

FIGURE 14.65 AUGMENTATION SYSTEM ACTUATOR INPUT IMPLEMENTATIONS

14.5.1.4 Actuator Effects

The general effect of an actuator is to introduce lag into the flight control system. Figure 14.66 shows the effect of typical hydraulic actuator dynamics on the characteristics of a pitch attitude control system. Notice that the short period dynamics of the aircraft become unstable at relatively low system gain. This is due to the added lag caused by the actuator forces as can be seen by comparing figure 14.66 to figure 14.47 which shows the same aircraft conditions without actuator characteristics included (short period roots are not driven unstable). This reveals that for a given controller gain the short period damping is reduced by the actuator lag.

Figure 14.67 shows that a slower actuator has the effect of further

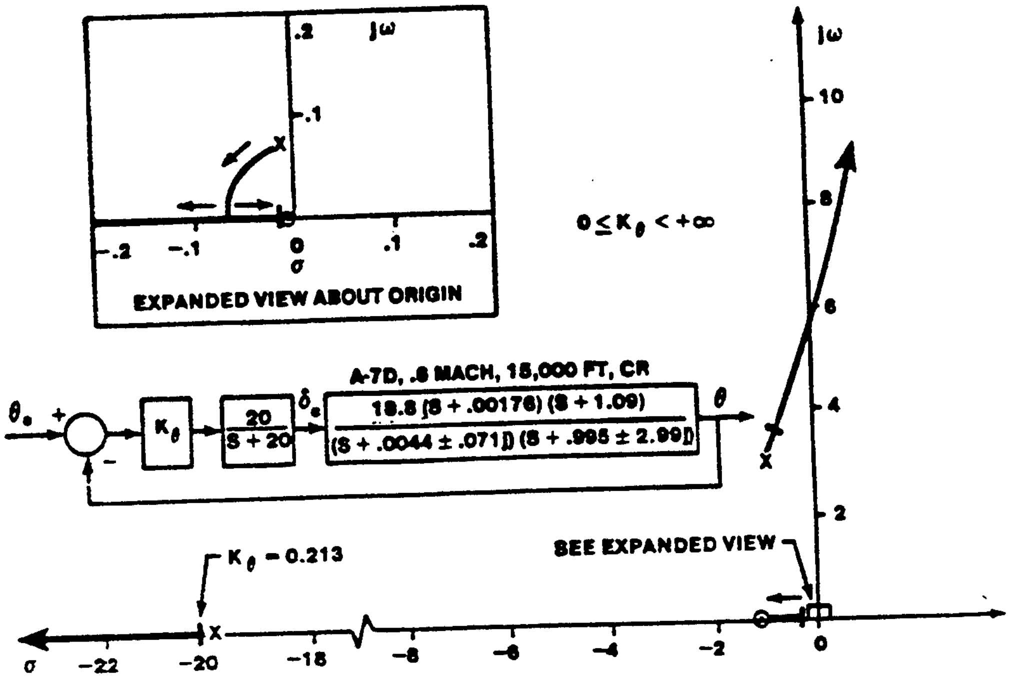

.2
jω
.1
-.2
-.1
0
.1
.2
σ
EXPANDED VIEW ABOUT ORIGIN
0 ≤ K_θ < +∞
jω
10
8
6
4
2
A-7D, .6 MACH, 15,000 FT, CR
θ_c
+
−
K_θ
20
S + 20
δ_e
18.8 (S + .00176) (S + 1.09)
(S + .0044 ± .071j) (S + .995 ± 2.99j)
θ
K_θ = 0.213
SEE EXPANDED VIEW
σ
-22
-20
-18
-8
-6
-4
-2
0

FIGURE 14.66 ROOT LOCUS OF PITCH ATTITUDE LOOP INCLUDING TYPICAL ACTUATOR CHARACTERISTICS

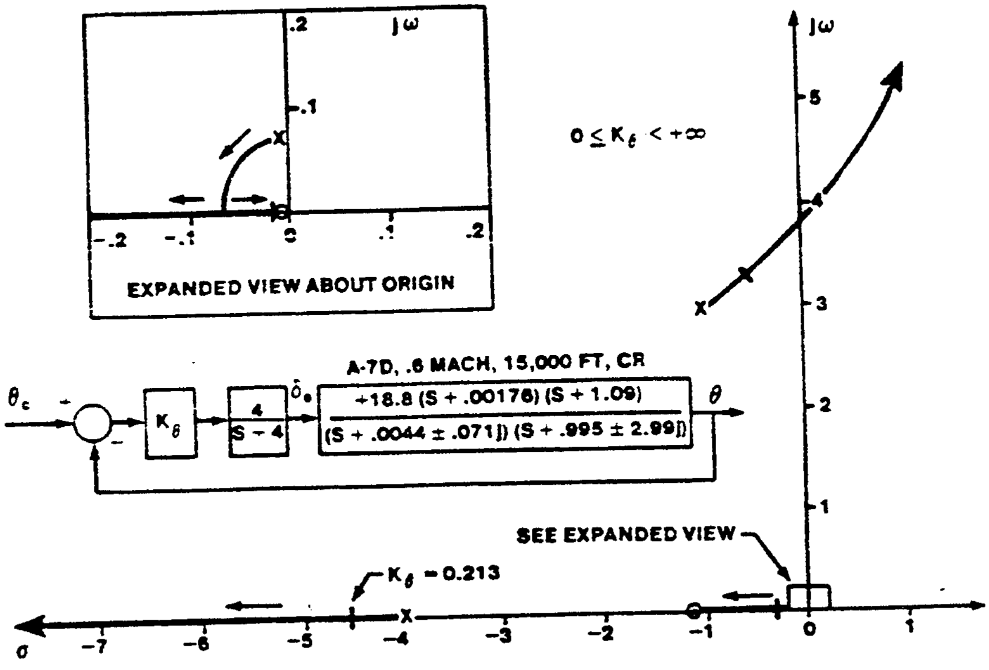

.2
jω
.1
-.2
-.1
0
.1
.2
EXPANDED VIEW ABOUT ORIGIN
0 ≤ K_θ < +∞
jω
5
4
3
2
1
A-7D, .6 MACH, 15,000 FT, CR
θ_c
+
−
K_θ
4
S + 4
δ_e
+18.8 (S + .00176) (S + 1.09)
(S + .0044 ± .071j) (S + .995 ± 2.99j)
θ
SEE EXPANDED VIEW
K_θ = 0.213
σ
-7
-6
-5
-4
-3
-2
-1
0
1

FIGURE 14.67 ROOT LOCUS OF PITCH ATTITUDE LOOP INCLUDING SLOW ACTUATOR CHARACTERISTICS

destabilizing the aircraft. Slow actuators are typically used in transport or bomber aircraft. Figure 14.68 shows the time response for the system of figure 14.66 at a selected controller gain. The additional lag introduced by the actuator is apparent.

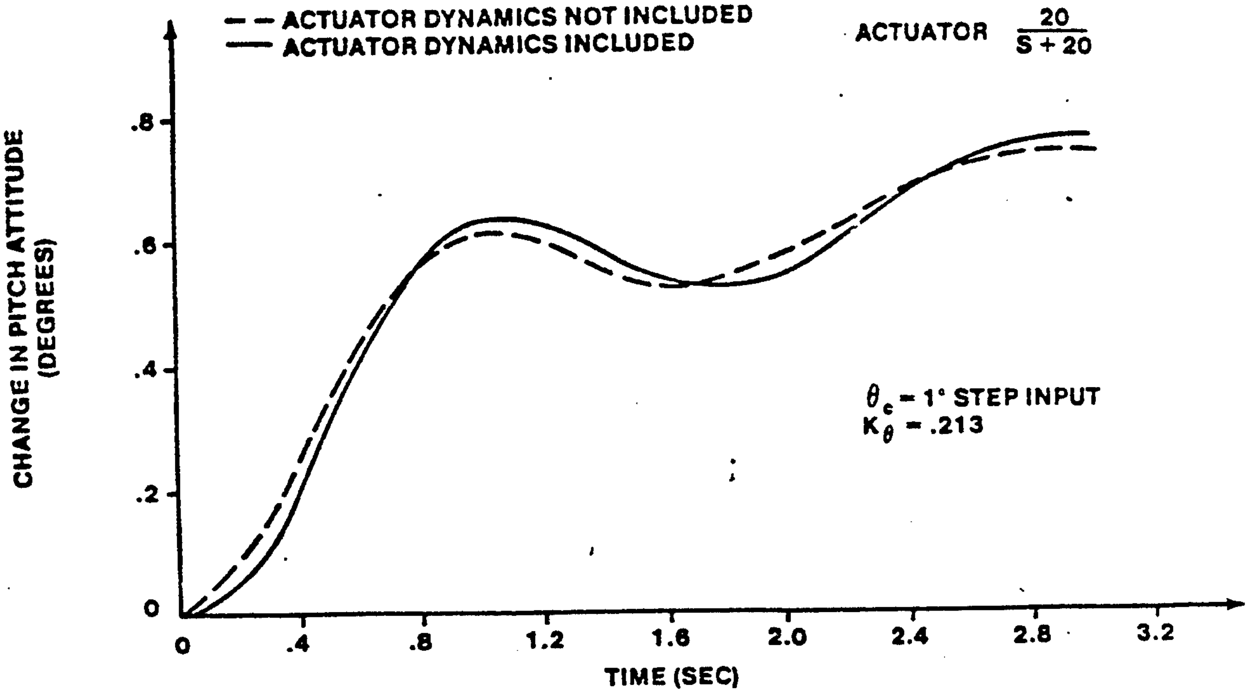

FIGURE 14.68 A-7D PITCH ATTITUDE REPONSE COMPARISON SHOWING THE EFFECT OF ACTUATOR DYNAMICS

14.5.2 Multiple Loop Stability Augmentation Systems

Single parameter feedback strategies are common in less sophisticated flight control systems, where stability augmentation is the primary consideration. In single loop systems, if the desired flying qualities for the aircraft cannot be obtained as a result of the feedback strategy alone, then additional compensation (lead or lag filters) must be added to the flight control system (see section 14.6). These additional compensator poles and zeros increase the order of the combined aircraft and flight control system, often causing an unanticipated degredation in flying qualities. Also, additional compensation is added to the flight control system to deal with difficulties such as structural resonance (flight control system excitation of the aircraft structure), sensor noise, or excessive steady state error.

The flying qualities of modern fighter aircraft are instead most frequently augmented through the feedback of two or more motion parameters to a single (or multiple) aerodynamic control surface. What is unique about the multiloop feedback approach is that the characteristics of the aircraft can be significantly altered to improve the flying qualities without introducing the additional poles and zeros of the compensators and filters. The best flight control systems will generally be the simplest — those that add a bare minimum of additional compensators and filters — relying instead on simple multiloop control strategies by taking advantage of the manner in which each feedback parameter influences the characteristic motions of the aircraft.

The characteristics of a multiloop SAS generally combine the characteristics of the individual single loop systems. In the following sections this will be shown for the most common longitudinal (α and q, α and $\dot{\alpha}$, n_z and q) and lateral-directional (β and r, β and $\dot{\beta}$) strategies. Other multiple loop combinations are used for autopilot operations which are discussed in section 14.7.

14.5.2.1 Angle of Attack and Pitch Rate Feedback

The primary effect of angle of attack feedback to the elevator is to increase the short period natural frequency. The primary effect of pitch rate feedback to the elevator is to increase short period damping. These effects can be combined by feeding back both α and q to the elevator. The characteristics of such a system is shown in figure 14.69. Notice that phugoid suppression does not occur in this situation since neither angle of attack nor pitch rate feedback are effective for this purpose.

14.5.2.2 Angle of Attack and Angle of Attack Rate Feedback

Angle of attack rate can be used for the inner loop instead of pitch rate to achieve similar effects on the damping of the short period roots as those achieved in the last section. Figure 14.70 presents the composite root locus for an angle of attack rate and angle of attack system. The difficulty with this system is in sensing the rate of change of angle of attack. It is almost always inadvisable to attempt to differentiate the signal of a sensor since noise and phase lag are introduced into the control system. One approach is to compute the angle of attack from the equations of motion, using easily measured parameters, as

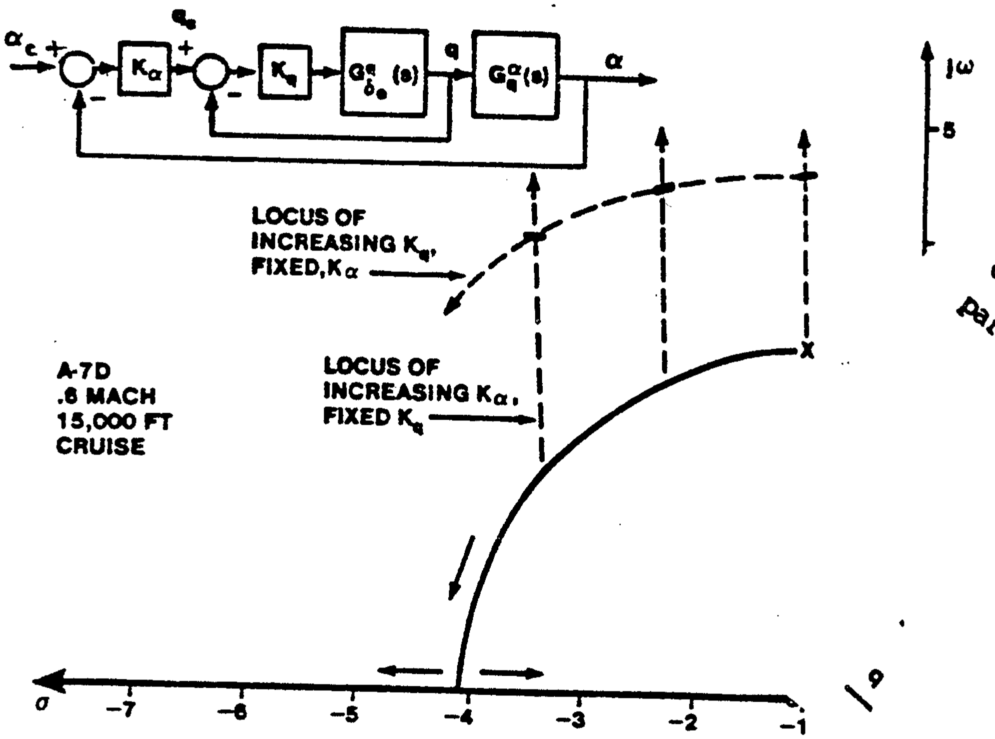
α_c
+
−
K_α
q_c
+
−
K_q
$G^q_{\delta_e}(s)$
q
$G^\alpha_q(s)$
α
jω
5
LOCUS OF
INCREASING K_q,
FIXED, K_α
A-7D
.6 MACH
15,000 FT
CRUISE
LOCUS OF
INCREASING K_α,
FIXED K_q
X
σ
−7
−6
−5
−4
−3
−2
−1

FIGURE 14.69 ROOT LOCUS OF PITCH RATE AND ANGLE OF ATTACK FEEDBACK

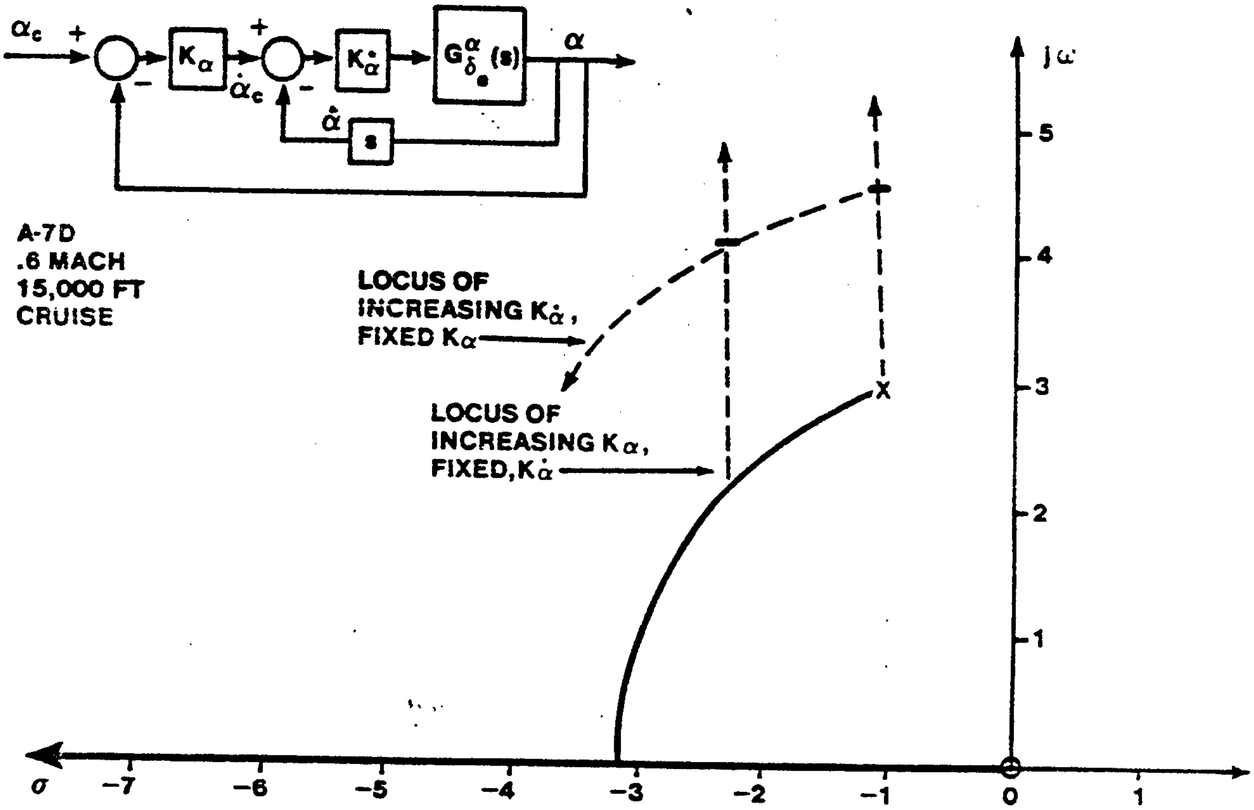
α_c
+
−
K_α
$\dot{\alpha}_c$
+
−
$K_{\dot{\alpha}}$
$G^\alpha_{\delta_e}(s)$
α
$\dot{\alpha}$
s
jω
5
4
3
2
1
A-7D
.6 MACH
15,000 FT
CRUISE
LOCUS OF
INCREASING $K_{\dot{\alpha}}$,
FIXED K_α
LOCUS OF
INCREASING K_α,
FIXED, $K_{\dot{\alpha}}$
X
σ
−7
−6
−5
−4
−3
−2
−1
0
1

FIGURE 14.70 ROOT LOCUS OF ANGLE OF ATTACK RATE AND ANGLE OF ATTACK FEEDBACK

$$\dot{\alpha} = \frac{1}{gU_0}(-n_z + \cos\theta\cos\phi) + \frac{q}{g} \qquad (14.59)$$

The nonlinear block diagram of figure 14.71 can be used to compute the angle of attack rate. Angle of attack rate is not currently used as a feedback parameter except in some variable stability aircraft applications.

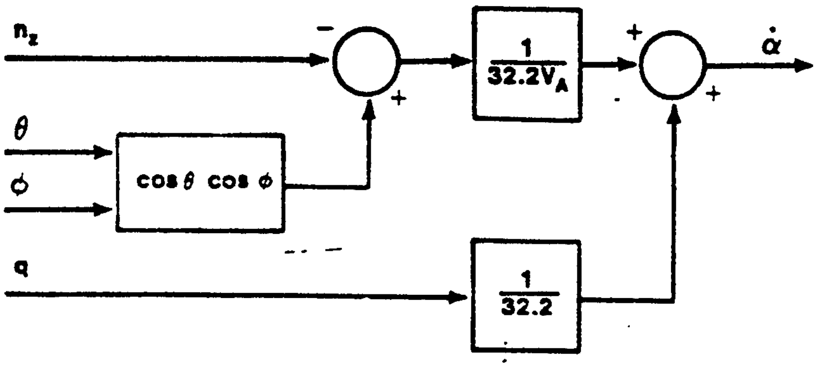

FIGURE 14.71 ANGLE OF ATTACK RATE COMPUTATION

14.5.2.3 Normal Acceleration and Pitch Rate Feedback

If normal acceleration is fed back as an outer loop instead of angle of attack (with q as the inner loop), the effect on the short period and phugoid roots is similar to the α and q system shown in section 14.5.2.1. An advantage of normal acceleration feedback is to help linearize the stick force gradient of the aircraft (used in the A-7D for this purpose).

14.5.2.4 Sideslip Angle and Yaw Rate Feedback

The feedback of yaw rate to the rudder effectively augments Dutch roll damping which greatly improves handling qualities during aggressive maneuvering as discussed in section 14.5.1.2.1. Yaw rate feedback, by itself, cannot eliminate a residual sideslip angle during air-to-surface weapon delivery. Since this residual sideslip angle greatly affects weapon delivery accuracy, coordination is required. The pilot frequently has difficulty providing this coordination during minimum tracking time attacks (curvilinear approach). Sideslip angle (or lateral acceleration) feedback may be used to provide the desired coordination during strafing or bombing. Figure 14.72 presents a composite root locus plot of a yaw rate and sideslip angle multiloop feedback system. The yaw rate feedback, for low to moderate gains,

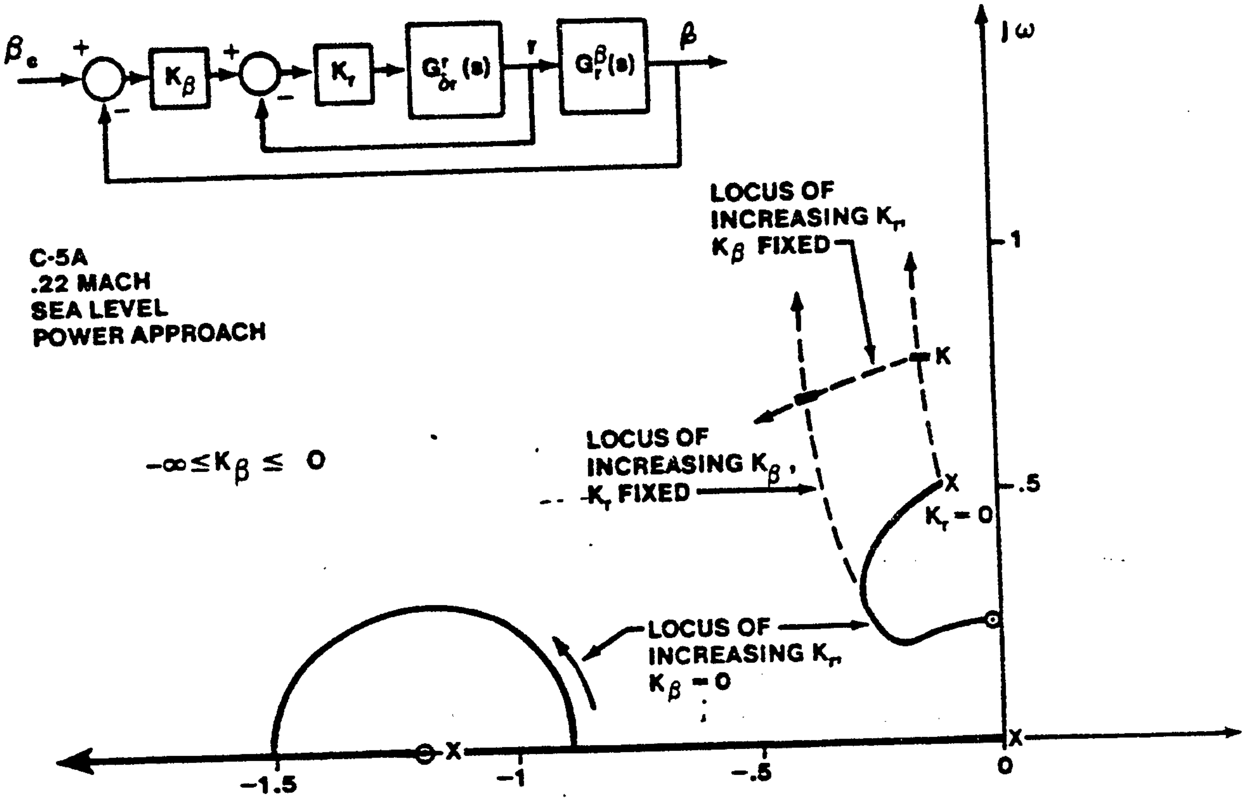
β_c
+
K_β
+
−
−
K_r
$G^r_{\delta_r}(s)$
r
$G^\beta_r(s)$
β
jω
LOCUS OF INCREASING K_r, K_β FIXED
K
1
C-5A
.22 MACH
SEA LEVEL
POWER APPROACH
$-\infty \leq K_\beta \leq 0$
LOCUS OF INCREASING K_β, K_r FIXED
X
.5
$K_r = 0$
LOCUS OF INCREASING K_r, $K_\beta = 0$
X
X
−1.5
−1
−.5
0

FIGURE 14.72 ROOT LOCUS OF YAW RATE AND SIDESLIP ANGLE FEEDBACK

significantly increases the Dutch roll damping while not altering the natural frequency. The Dutch roll roots can be moved sufficiently far into the left half s-plane to provide heavy damping while the sideslip angle feedback can improve the weathercock stability (turn coordination) of the aircraft.

14.5.2.5 Sideslip Angle and Sideslip Angle Rate Feedback

As shown in section 14.5.1.2.6 the feedback of sideslip angle rate is an effective means of altering the aircraft roll axis to provide better handling qualities during aggressive maneuvering. As with yaw rate feedback, lateral coordination ($\beta = 0$) is required for accurate weapons delivery. Sideslip angle (or lateral acceleration) feedback is an effective means of coordination and provides similar results to that shown in the previous section.

14.5.3 Control Augmentation Systems

Control augmentation systems (CAS) improve upon the basic stability augmentation systems by adding a command path between the pilot controller and the augmentation system. The pilot then influences directly the output of the augmentor. With this capability the aircraft handling qualities can be modified in more fundamental ways and the handling qualities can be made more consistent throughout the flight envelope.

In the longitudinal axis the CAS is usually designed to provide the pilot a load factor or pitch rate command system. In the lateral-directional axes the roll control system is usually modified to provide roll rate command while the Dutch roll and spiral modes are usually supressed.

In order to provide consistent operation throughout the flight envelope, the gains in the CAS are often scheduled as a function of dynamic pressure, Mach, or other parameters.

A CAS operates in parallel with the mechanical flight control system. An analysis of a CAS must, therefore, be careful to consider the effects of having parallel mechanical and electrical paths.

1.5.3.1 Load Factor Command System

A load factor command system can be accomplished by feeding back normal acceleration (n_z) to the elevator. The pilot then commands normal acceleration through the pilot controller. Load factor command systems (often called g command systems) are usually designed to have neutral speed stability ($\delta F_s/\delta V = 0$) which requires the elimination of the steady state error through the use of an integrator in the forward path of the system. This is discussed in section 14.6.3.1.

It is seldom possible, or even desirable, to measure the normal acceleration at the center of gravity (c.g.). An accelerometer located at the c.g. is impractical because the c.g. position shifts as fuel is burned, or payload is changed (weapons are released). In addition, when the accelerometer is located ahead of the c.g. the system is more stable.

The acceleration at the center of gravity is

$$a_{z_{cg}} = U_0 (\dot{\alpha} - q) + g(\sin \theta_0)\, \theta \qquad (14.60)$$

where the last term is normally negligible due to the small angle assumption for a 1 g trim condition. If the accelermoeter is located some distance away from the center of gravity (acceleration measured in the plane of symmetry) the normal acceleration measured is

$$a_z = a_{z_{cg}} - \ell_x \dot{q} s \qquad (14.61)$$

Figure 14.73 presents the block diagram and root locus plot of a load factor command system with the accelerometer located at the aircraft center of gravity. The short period roots move rapidly with only a small increase in gain. Initially, the short period damping decreases somewhat as the natural frequency increases. At a relatively high gain, the two oscillatory short period roots meet and become real. At very high gains, one of the real roots is driven to the right half s-plane, causing the system to become unstable. The effect is essentially the same as that of the angle of attack situation for low system gains, since

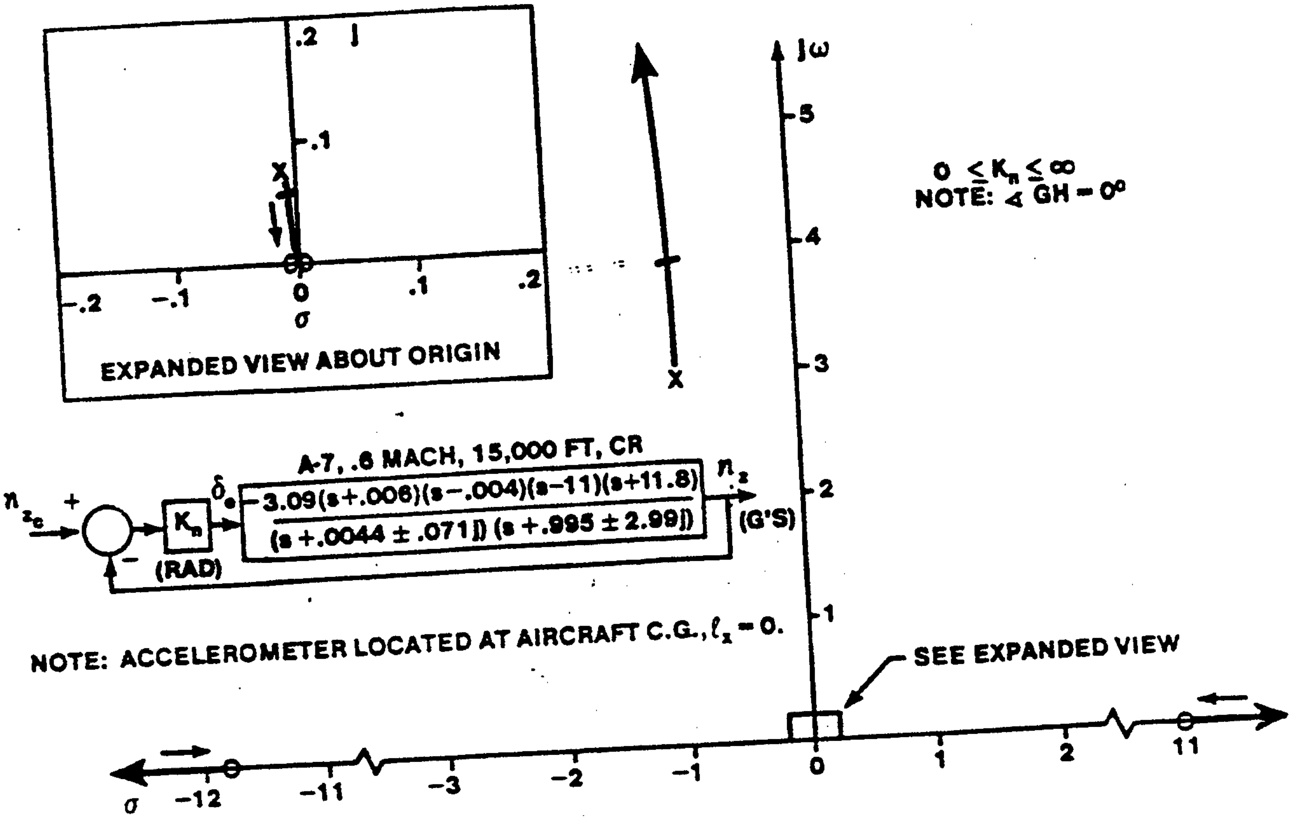

.2
.1
-.2
-.1
0
.1
.2
σ
EXPANDED VIEW ABOUT ORIGIN
jω
5
4
3
2
1
$0 \le K_n \le \infty$
NOTE: $\angle GH = 0°$
A-7, .6 MACH, 15,000 FT, CR
n_{z_c}
+
−
K_n
(RAD)
δ_e
$\frac{-3.09(s+.006)(s-.004)(s-11)(s+11.8)}{(s+.0044 \pm .071j)(s+.995 \pm 2.99j)}$
n_z
(G'S)
NOTE: ACCELEROMETER LOCATED AT AIRCRAFT C.G., $\ell_x = 0$.
SEE EXPANDED VIEW
σ
−12
−11
−3
−2
−1
0
1
2
11

FIGURE 14.73 ROOT LOCUS OF LOAD FACTOR COMMAND SYSTEM FOR AIRCRAFT WITH GOOD DYNAMICS

$$n_z = \frac{L}{W} = \frac{\rho V_A^2 \, S \, C_{L_\alpha} \, \alpha}{2W} \qquad (14.62)$$

where the density altitude, aircraft speed, wing area, weight, and lift curve slope are all essentially constant in the short term, making the load factor proportional to the angle of attack.

The phugoid natural frequency is reduced somewhat as the gain increases and the damping of the phugoid is not affected significantly until the gain becomes high. At very high gain, one of the phugoid roots will become an unstable real root.

An elevator actuator, a necessary part of any practical system, causes additional lag, which forces the short period roots to migrate into the right half s-plane as a complex pair at low gain.

Figure 14.74 shows a root locus of a g-command system with the accelerometer located ahead of the center of gravity. When an actuator is added to this system, the short period roots are not driven into the right half s-plane as in the case of the accelerometer located at the c.g.

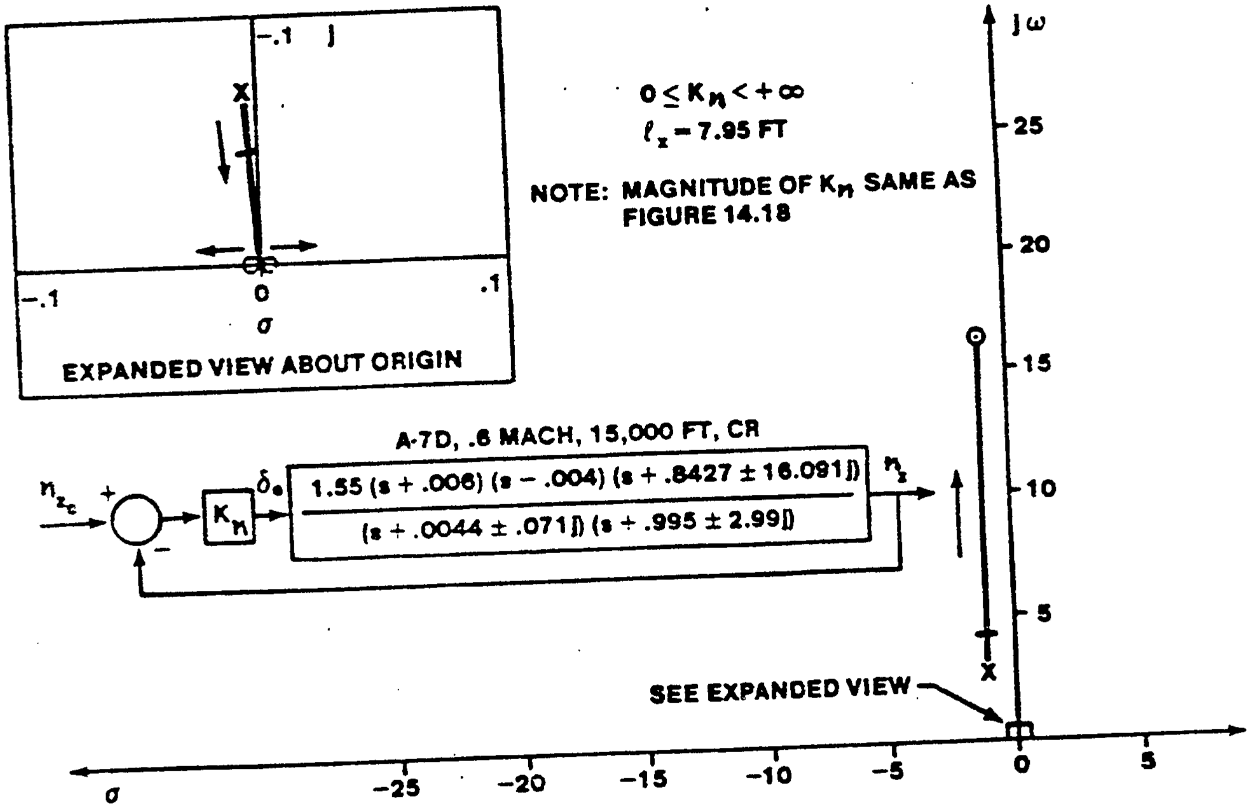

-.1 j
X
-.1
0
.1
σ
EXPANDED VIEW ABOUT ORIGIN
$0 \leq K_n < +\infty$
$\ell_x = 7.95$ FT
NOTE: MAGNITUDE OF K_n SAME AS FIGURE 14.18
jω
25
20
15
10
5
A-7D, .6 MACH, 15,000 FT, CR
n_{z_c}
+
−
K_n
δ_e
$\frac{1.55(s+.006)(s-.004)(s+.8427 \pm 16.091j)}{(s+.0044 \pm .071j)(s+.995 \pm 2.99j)}$
n_z
X
SEE EXPANDED VIEW
σ
−25
−20
−15
−10
−5
0
5

FIGURE 14.74 ROOT LOCUS OF G COMMAND SYSTEM WITH ACCELEROMETER AHEAD OF CENTER OF GRAVITY

The F-15 achieves a load factor command system by a mechanical accelerometer (bobweight) arrangement as shown in figure 14.75. This system senses an error between the commanded load factor (a function of stick position) and the actual load factor (as sensed by the bobweight). If the bobweight is displaced from the neutral position the pitch trim compensator (a motor) activates the stabilator to correct the commanded load factor. A block diagram of the system is shown in figure 14.76. The spring and damper attached to the bobweight mechanism are omitted since they are a part of the mechanical accelerometer, the dynamics of which are negligible.

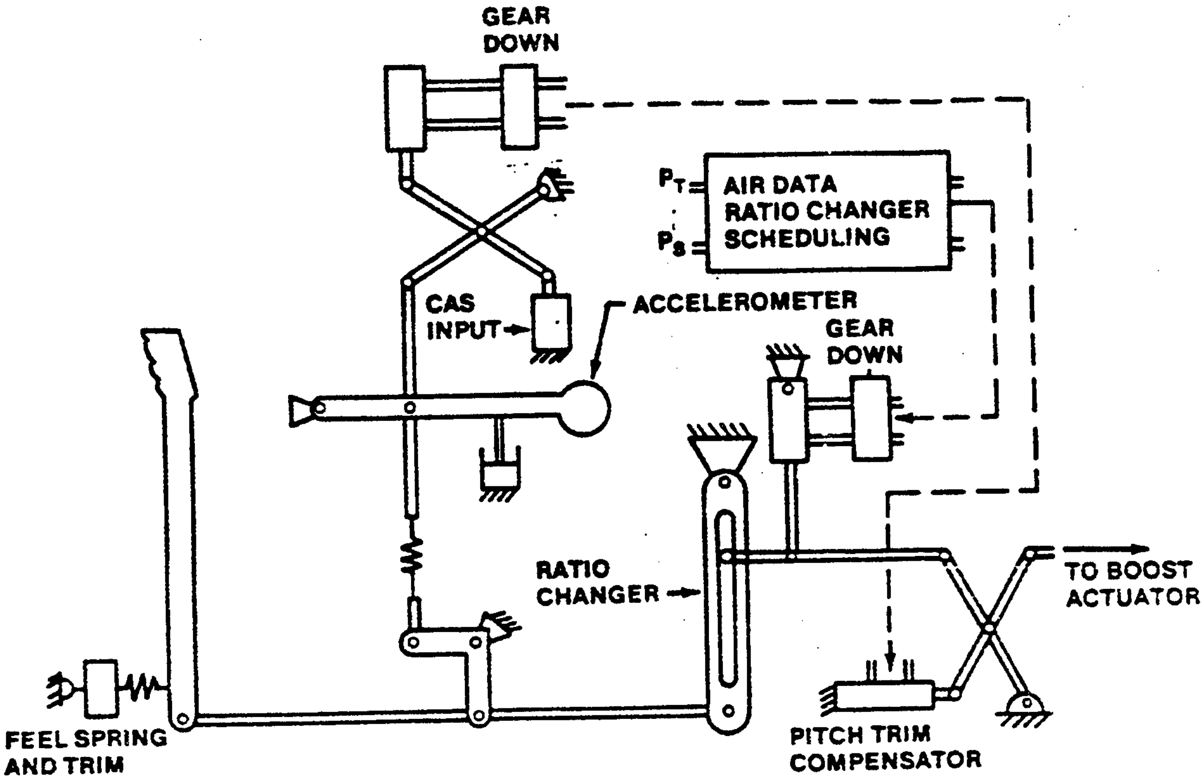
GEAR DOWN
P_T
P_S
AIR DATA RATIO CHANGER SCHEDULING
CAS INPUT
ACCELEROMETER
GEAR DOWN
RATIO CHANGER
TO BOOST ACTUATOR
FEEL SPRING AND TRIM
PITCH TRIM COMPENSATOR

FIGURE 14.75 SCHEMATIC OF F-15 LONGITUDINAL MECHANICAL CONTROL SYSTEM

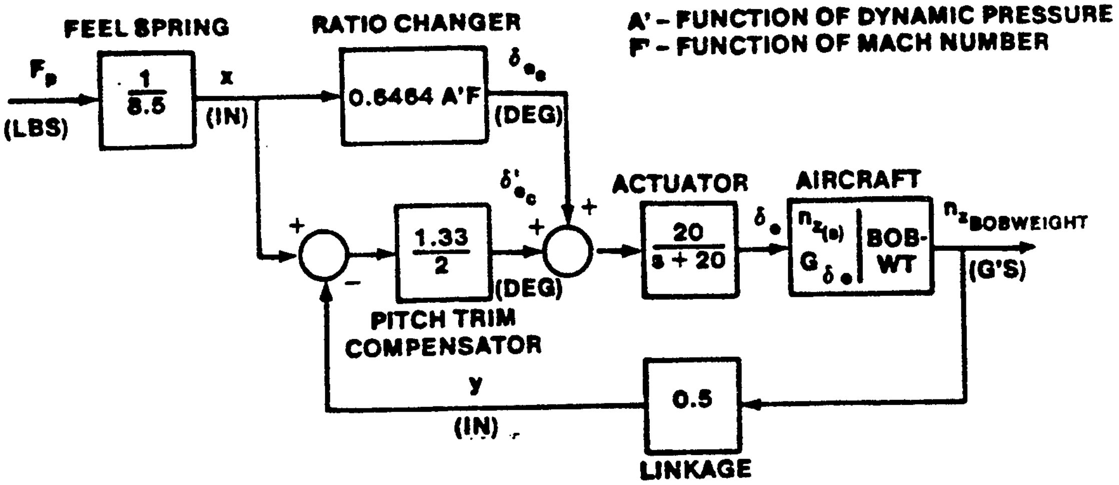
FEEL SPRING
RATIO CHANGER
A' - FUNCTION OF DYNAMIC PRESSURE
F' - FUNCTION OF MACH NUMBER
F_s
(LBS)
$\frac{1}{8.5}$
x
(IN)
0.6464 A'F
δ_{e_e}
(DEG)
δ'_{e_c}
ACTUATOR
AIRCRAFT
+
+
+
−
$\frac{1.33}{2}$
(DEG)
$\frac{20}{s+20}$
δ_e
$n_{z(s)}$
G_{δ_e}
BOB-WT
$n_{z_{BOBWEIGHT}}$
(G'S)
PITCH TRIM COMPENSATOR
y
(IN)
0.5
LINKAGE

FIGURE 14.76 BLOCK DIAGRAM OF F-15 LONGITUDINAL MECHANICAL CONTROL SYSTEM

14.5.3.2 Pitch Rate Command System

The characteristics of a pitch rate command system were discussed in section 14.5.1.1.1.1. This section showed that the effect of pitch rate feedback to the elevator was to increase short period damping while having little effect on the phugoid mode. If the aircraft has a transonic tuck mode then further compensation will be required as discussed in section 14.6.

14.5.3.3 Roll Rate Command System

The characteristics of a roll rate command system were discussed in section 14.5.1.2.2.

14.5.3.4 Gain Scheduling

It is frequently necessary to change the control system gains as a function of the flight condition for aircraft with large flight envelopes. The purpose of gain scheduling is to retain nearly constant handling qualities within a large region of the flight envelope. Gains are usually scheduled as a function of dynamic pressure or Mach, although other parameters may be used such as airspeed or altitude. The scheduling of gains may be accomplished electrically or mechanically.

In the F-15 pitch axis (figure 14.75) the control stick deflection is sent directly to the hydraulic actuator through the ratio changer, a mechanical device that adjusts the stabilator gearing as a function of dynamic pressure and Mach to keep the aircraft pitch response constant for a given stick deflection throughout the flight envelope. The air data system provides inputs to a device that adjusts the output rod position in the ratio changer slot, thus varying the gain of the ratio changer transfer function.

14.5.3.5 Parallel Electrical and Mechanical Paths

The analysis of control augmentation systems is complicated by the two command paths (mechanical and electrical). An analysis of a CAS cannot ignore the effects of the mechanical system when examining the augmented aircraft response.

Figure 14.77 presents a block diagram of the F-15 longitudinal flight control system including the CAS interconnect servo. Since the steady state stick force gradients of the mechanical and electrical systems are different (4.25 pounds per g for the mechanical system and 3.75 pounds per g for the electrical system), the load factor feedback cannot satisfy both steady state conditions simultaneously. The inability of the load factor feedback to satisfy the two systems is alleviated via the CAS interconnect servo, which allows the pitch CAS gradient to be met by providing a bias signal to the mechanical path. This feature also causes a transfer of any steady state CAS series servo offset to the mechanical system so as to keep the series servo position near center, providing full CAS authority under most conditions and preventing large transients upon CAS disengagement.

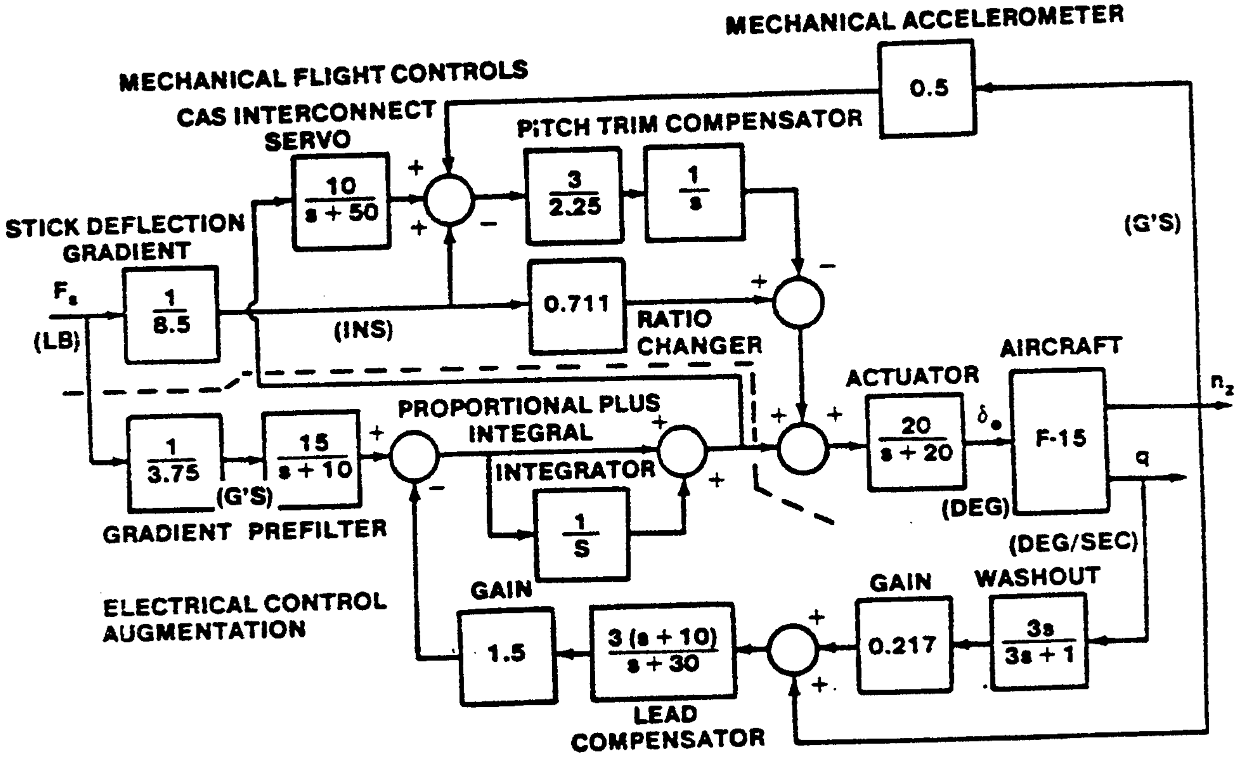
MECHANICAL ACCELEROMETER
0.5
MECHANICAL FLIGHT CONTROLS
CAS INTERCONNECT SERVO
$\frac{10}{s+50}$
PITCH TRIM COMPENSATOR
$\frac{3}{2.25}$
$\frac{1}{s}$
(G'S)
STICK DEFLECTION GRADIENT
F_s
(LB)
$\frac{1}{8.5}$
(INS)
0.711
RATIO CHANGER
ACTUATOR
$\frac{20}{s+20}$
δ_e
AIRCRAFT
F-15
n_z
q
(DEG)
(DEG/SEC)
PROPORTIONAL PLUS INTEGRAL
INTEGRATOR
$\frac{1}{s}$
$\frac{1}{3.75}$
(G'S)
$\frac{15}{s+10}$
GRADIENT PREFILTER
ELECTRICAL CONTROL AUGMENTATION
GAIN
1.5
$\frac{3(s+10)}{s+30}$
LEAD COMPENSATOR
GAIN
0.217
WASHOUT
$\frac{3s}{3s+1}$
+
−

FIGURE 14.77 COMPLETE F-15 LONGITUDINAL CONTROL SYSTEM

Figure 14.78 compares the aircraft response with the CAS disengaged, with the CAS engaged and the effects of the mechanical system omitted, and of the augmented aircraft including the effects of both the CAS and the mechanical system. Notice that the mechanical system helps to make the augmented aircraft reponse more abrupt and to increase the initial load factor obtained for a given applied stick force. Without considering the effects of the mechanical system with the CAS engaged, one might wrongly conclude that the aircraft response is sluggish. Notice also that while the augmented aircraft steady state stick force gradient of 3.75 pounds per g, a closer approximation to the force gradient during practical maneuvering would be near 4.5 pounds per g, since the pilot would apply whatever additional force is necessary to attain the desired load factor as quickly as possible.

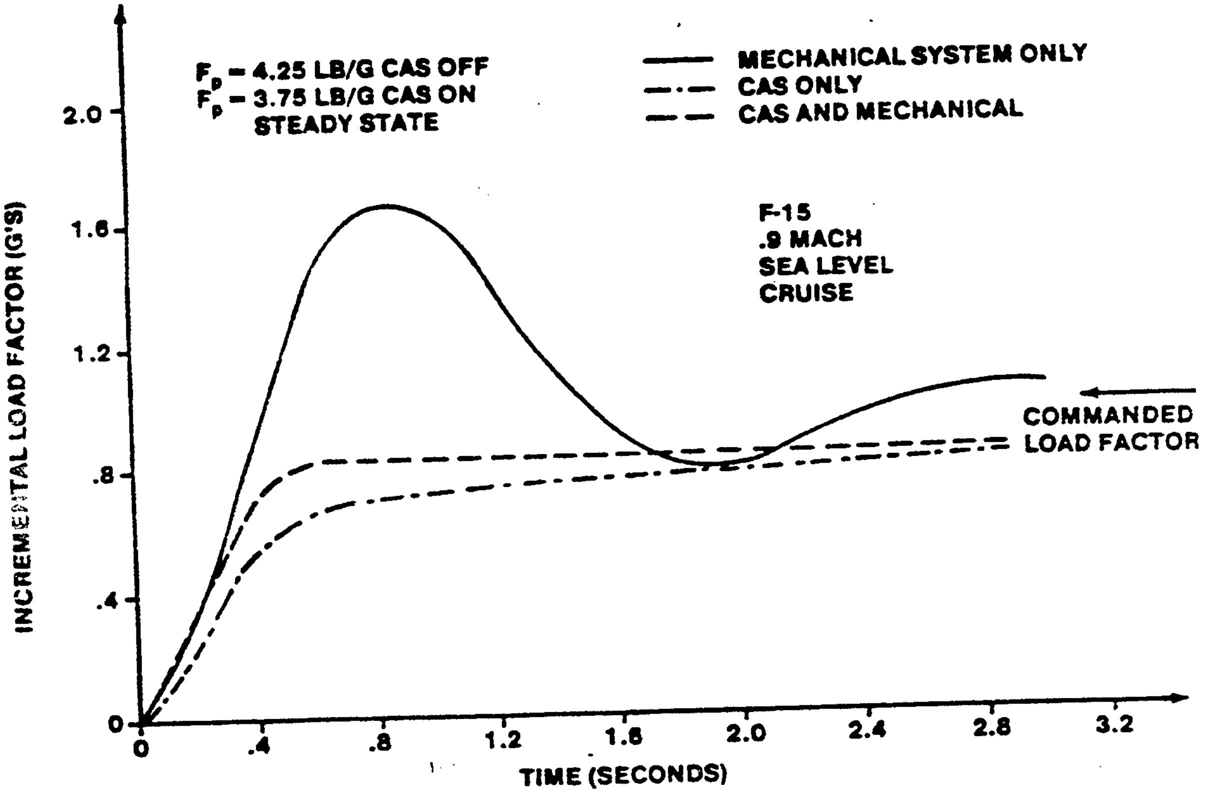

FIGURE 14.78 COMPARISON OF F-15 TIME RESPONSE CHARACTERISTICS

14.6 COMPENSATION DEVICES

The previous section presented the basic single and multiple loop augmentation schemes. Most of the systems analyzed used simple gain controllers. There are times when these simple gain controllers do not give satisfactory aircraft dynamics. It is also often not possible or practical to increase the number of feedback loops in order to remain with a simple system using gain controllers only. In these cases devices are often added to the control system to improve the aircraft time reponse characteristics.

The process of introducing additional equipment into a system to reshape its time response is called compensation. The compensation devices may consist of electrical networks or mechanical equipment containing levers, springs, dashpots, etc. When analyzing a flight control system these devices are often a source of confusion because of the many terms used to describe the devices: high pass filter, low pass filter, notch filter, washout filter, integrator, passive compensator, lead compensator, lag compensator, lag-lead compensator, etc. The effects of the devices also depend upon where in the system the device is placed, which results in terms such as prefilters, cascade compensation, feedback compensation, series compensation, parallel compensation, etc.

In order to reduce confusion we will simplify the discussion by placing these devices into four basic categories which can be placed in one of three locations. The four basic types are derived from the frequency domain and they are: 1) high pass filters, 2) low pass filters, 3) high-low pass filters and, 4) bandpass filters. Table 4.4 gives the types of compensators found in each category. Each of these is described in more detail in the following sections. The possible location of the devices is shown in figure 14.79.

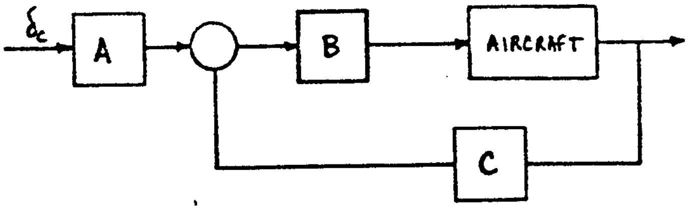

A. Prefilter (command path compensation)
B. Cascade Compensation (series compensation)
C. Feedback Compensation (parallel compensation)

FIGURE 14.79 LOCATION OF COMPENSATION DEVICES

TABLE 14.4
COMPENSATION DEVICES

Category	Type	Transfer Function	
1) High pass filter	A. Differentiator	A. Ks	
	B. Derivative plus proportional controller	B. $1 + Ks$	
	C. Lead compensator	C. $K \frac{(s + a)}{(s + b)}$	$a < b$
	D. Washout filter	D. $K \frac{s}{(s + b)}$	
2) Low pass filter	A. Integrator	A. $\frac{K}{s}$	
	B. Integral plus proportional controller	B. $K \frac{(s + a)}{s}$	
	C. Lag compensator	C. $K \frac{(s + a)}{(s + b)}$	$a > b$
	D. Noise filter	D. $\frac{K}{(s + b)}$	
3) High-Low pass filter	A. Lead-Lag compensator	A. $K \frac{(s + a)(s + c)}{(s + b)(s + d)}$	$a > b$ $c < d$ $a < c$
	B. Notch filter	B. $K \frac{(s^2 + 2\zeta_N \omega_N + \omega_N^2)}{(s^2 + 2\zeta_D \omega_D + \omega_D^2)}$	
4) Bandpass filter	Bandpass filter	A. $K \frac{(s + a)(s + c)}{(s + b)(s + d)}$	$a < b$ $c > d$ $b < d$

When located in the pilot command path (A) a compensation device is known as a prefilter. If it is in cascade with the forward transfer function (B) it is known as cascade compensation, while it is known as feedback compensation if it is located in the feedback path (C). The use of each type of compensation device, in each location, will be discussed following the description of the device categories.

14.6.1 Compensation Device Types

It is easiest to see the general characteristics of compensation devices in the frequency domain. In this domain the device is seen to attenuate or amplify signals to various degrees depending upon frequency. Because of this, these devices have become known as filters — passing signals with certain frequencies and filtering out signals with other frequencies. When analyzed in the s-plane (root locus) these devices are more commonly referred to as integrators, differentiators, washout filters, or lead, lag, or lag-lead compensators. In the remaining discussion the frequency domain terms will usually be used (type of filter) but a device may be further described by other terms in order to more specifically describe its characteristics.

14.6.1.1 High Pass Filters

The general characteristics of high pass filters are that they tend to attenuate signals at low frequencies and amplify signals at high frequencies. When a high pass filter is used, the system response is quickened as shown by the root locus which is shifted to the left. This is reflected in the time domain by an increase in the undamped natural frequency. This also results in an increase in the overall system stability.

An ideal high pass filter is one which differentiates the signal and has a transfer function of the form

$$G_c(s) = Ks \qquad (14.63)$$

This high pass filter is termed an ideal differentiator and would have a Bode plot as shown in figure 14.80.

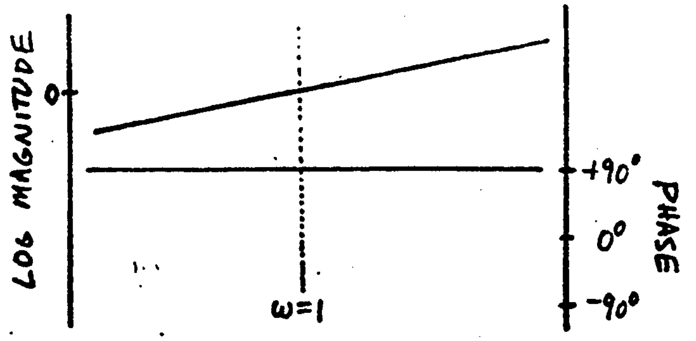

FIGURE 14.80 BODE PLOT OF IDEAL DIFFERENTIATOR

Ideal differentiation greatly attenuates the low frequency signals because the system only responds to the rate of change of the signal. This is usually not desirable and pure differentiators are not normally used.

A more desirable arrangement would be to have the output of the filter proportional to both the magnitude and the derivative of the signal as shown in the block diagram of figure 14.81.

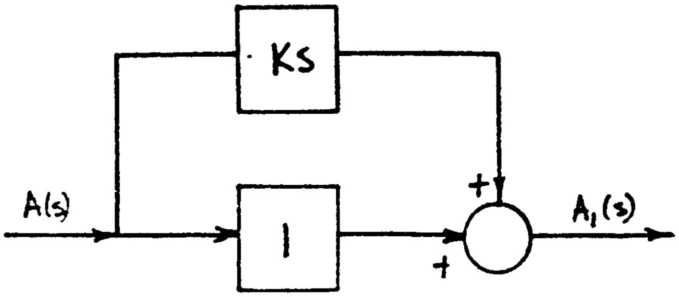

FIGURE 14.81 IDEAL DERIVATIVE PLUS PROPORTIONAL CONTROL

The transfer function of this controller would be

$$G_c(s) = 1 + Ks = K(s + \frac{1}{K}) \quad (14.64)$$

The Bode plot for this high pass filter is shown in figure 14.82, which shows that the low frequency signals are not attenuated to the same extent as with a pure differentiator.

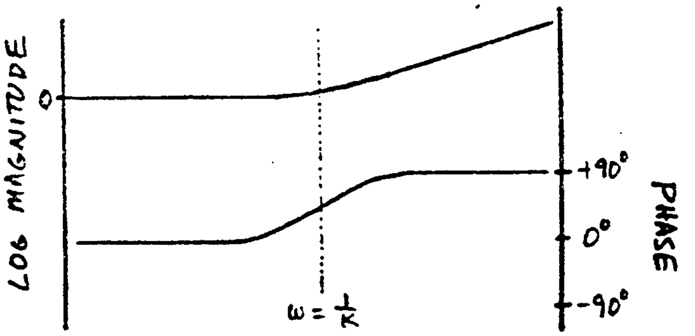

FIGURE 14.82 BODE PLOT OF IDEAL DERIVATIVE PLUS PROPORTIONAL CONTROL

Physically, the effect of this high pass filter is to introduce anticipation into the system. The system not only reacts to the magnitude of the signal but also to its probable value in the future. The net result is to speed up the response of the system.

Ideal derivative plus proportional control is, however, not normally used because an ideal differentiator is difficult to construct and requires much equipment that must be critically adjusted. In addition, the derivative action amplifies any spurious signal or noise that may be present in the actuating signal.

The most common type of high pass filter is the lead compensator. The transfer function is

$$G_c(s) = K \frac{(s + a)}{(s + b)} \qquad a < b \qquad (14.65)$$

The Bode plot for this high pass filter is shown in figure 14.83, which shows that the very high frequency signals are not amplified to as great an extent as with ideal derivative plus proportional control.

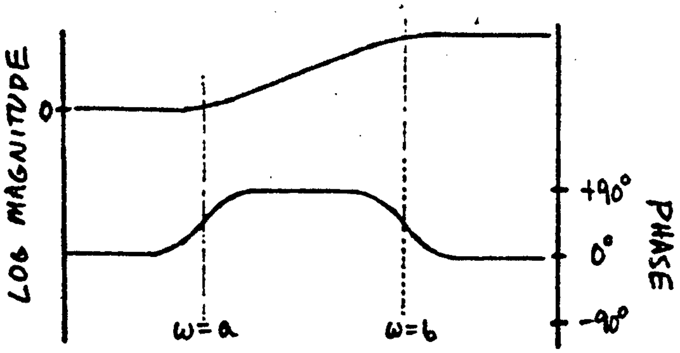

FIGURE 14.83 BODE PLOT OF LEAD COMPENSATOR

If b is very much greater than a (the practical limit is approximately b = 10a) then the lead compensator approximates a derivative plus proportional controller. This is often seen when a lead compensator is used in cascade. Less of a difference between the pole and zero is often found in prefilters.

A final type of high pass filter can be achieved by placing the zero of the filter at the origin. This is commonly called a washout filter and has a transfer function of the form

$$G_c(s) = K \frac{s}{(s + b)} \tag{14.66}$$

This is a high pass filter that passes signals above b radians per second while attenuating lower frequancy signals. The steady state signal passing through this filter is zero. Signals will be passed only during the transient portion of the aircraft response and the steady state signal will be attenuated. The Bode plot of a washout filter is shown in figure 14.84.

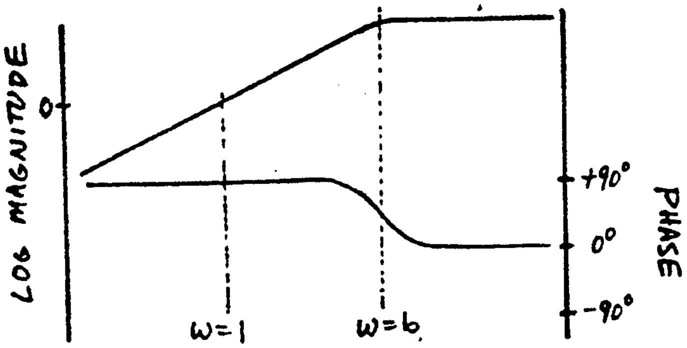

FIGURE 14.84 BODE PLOT OF WASHOUT FILTER

14.6.1.2 Low Pass Filters

The general characteristics of low pass filters are that they tend to amplify signals at low frequencies and attenuate signals at high frequencies. This results in a reduction of steady state error but also results in a more sluggish system response (decreased undamped natural frequency). It can also be used to eliminate unwanted noise in the system. The root locus is shifted to the right which results in a reduction of overall stability.

An ideal low pass filter is one which integrates the signal and has a transfer function of the form

$$G_c(s) = \frac{K}{s} \tag{14.67}$$

This low pass filter is termed an ideal integrator and has the Bode plot as shown in figure 14.85.

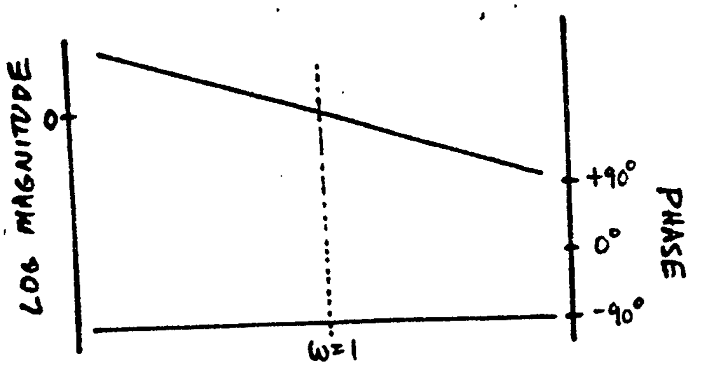

FIGURE 14.85 BODE PLOT OF IDEAL INTEGRATOR

The use of pure integral control has the disadvantage of excessive lag and poor convergence characteristics. This can be seen by noting that if this was part of a piloted command system, the pilot would not have a direct path to the control surface and he would have to wait for integration to occur prior to seeing the aircraft respond.

A more common arrangement is to use both the integrated signal and a proportional signal. The low pass filter would then be called an integral plus proportional controller which would have the block diagram shown in figure 14.86.

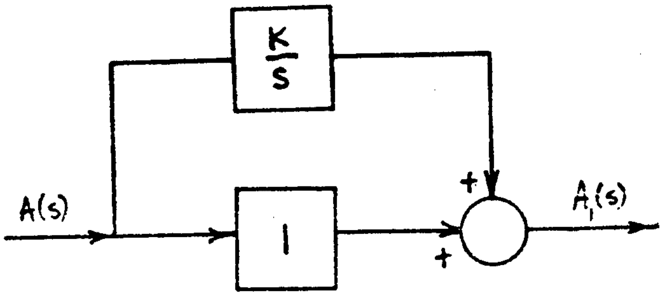

FIGURE 14.86 IDEAL INTEGRAL PLUS PROPORTIONAL CONTROL

The transfer function of the low pass filter would be

$$G_c(s) = K\frac{(s + a)}{s} \tag{16.68}$$

The Bode plot would be as shown in figure 14.87.

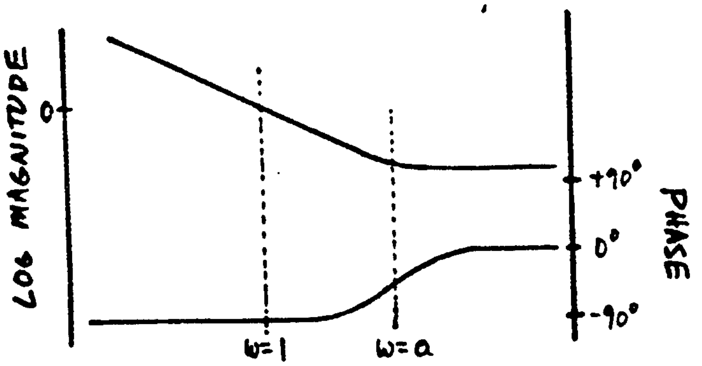

FIGURE 14.87 BODE PLOT OF IDEAL PLUS PROPORTIONAL CONTROL

This low pass filter increases the system type and, depending on system type and input, may eliminate a steady state error. The pole moves the root locus to the right, thereby slowing the time reponse. The zero must be near the origin in order to minimize the increase in response time of the complete system.

The main limitation of the use of ideal integral plus proportional control is the equipment required to obtain the integral signal. This generally requires an amplifier in a positive feedback system. Mechanically the integral signal can be obtained by an integrating gyroscope, which is used in aircraft where improved performance justifies the cost.

Frequently a passive electrical network can be used to approximate proportional plus integral control. This low pass filter is known as a lag compensator and has the transfer function

$$G_c(s) = K\,\frac{(s + a)}{(s + b)} \qquad a > b \tag{14.69}$$

The Bode plot of a lag compensator is shown in figure 14.88. The location of the pole and zero can be made close to those of an ideal integral plus proportional low pass filter. If the pole and zero are close together most of the original root locus remains unchanged while the operating gain of the system is greatly increased, which greatly reduces steady state error.

A final type of low pass filter can be achieved by placing a pole without a zero near the origin. This type of low pass filter is commonly used to eliminate noise and is, therefore, usually referred to as a noise filter. It

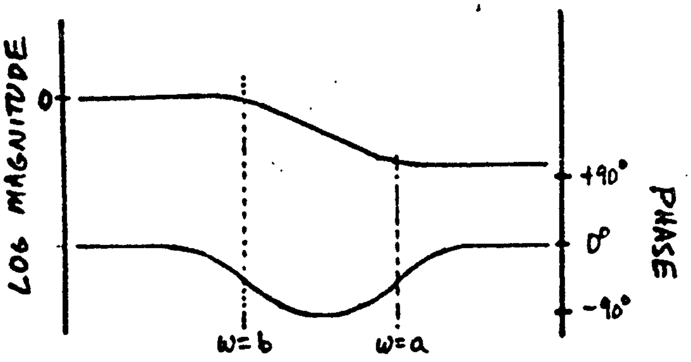

FIGURE 14.88 BODE PLOT OF LAG COMPENSATOR

has the transfer function

$$G_c(s) = \frac{K}{(s + b)} \qquad (14.70)$$

and the Bode plot shown in figure 14.89.

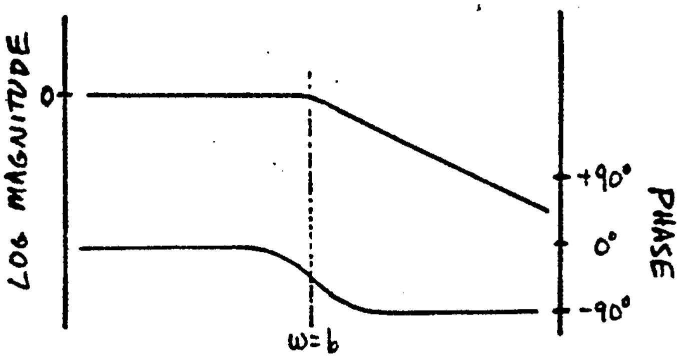

FIGURE 14.89 BODE PLOT OF NOISE FILTER

14.6.1.3 High-Low Pass Filters

By using both a high pass and a low pass filter the advantages of both can be realized simultaneously; that is, a large increase in gain (reduced steady state error) and a large increase in undamped natural frequency (quicker response) can be obtained. Instead of using two seperate networks, is it possible to use one network which is usually called a lag-lead compensator. The transfer function of this compensator is

$$G_c(s) = K\frac{(s + a)(s + c)}{(s + b)(s + d)} \tag{14.71}$$

where a > b, a < c, and c < d.

The fraction $(s + a)/(s + b)$ represents the low pass filter (lag compensation) and the fraction $(s + c)/(s + d)$ represents the high pass filter (lead compensator). The Bode plot of this filter is shown in figure 14.90.

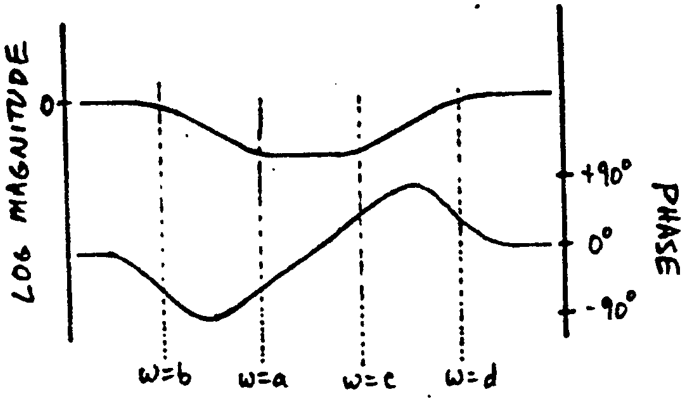

FIGURE 14.90 BODE PLOT OF LAG-LEAD COMPENSATOR

Sometimes it is desired to concentrate the attenuation of a high-low pass filter at a specific frequency, called the tuned frequency. This is accomplished with a notch filter which has a transfer function of the form

$$G_c(s) = \frac{K\,(s^2 + 2\zeta_N\omega_N s + \omega_N^2)}{(s^2 + 2\zeta_D\omega_D s + \omega_D^2)} \tag{14.72}$$

Figure 14.91 shows a Bode plot of a typical notch filter. The notch depth and relative width are primarily a function of the ratio ζ_N/ζ_D. As this ratio becomes smaller, the depth of the notch increases while its width in terms of frequency decreases. Conversely, an increase in the ratio produces the opposite effect -- less depth and wider notch. The tuned frequency is governed by the frequencies ω_N and ω_D. If the notch filter is symmetric, then the tuned frequency is $\omega_N = \omega_D$. If the notch filter is asymmetric, then $\omega_N \neq \omega_D$ and the tuned frequency is determined by ω_N if $\zeta_N < \zeta_D$.

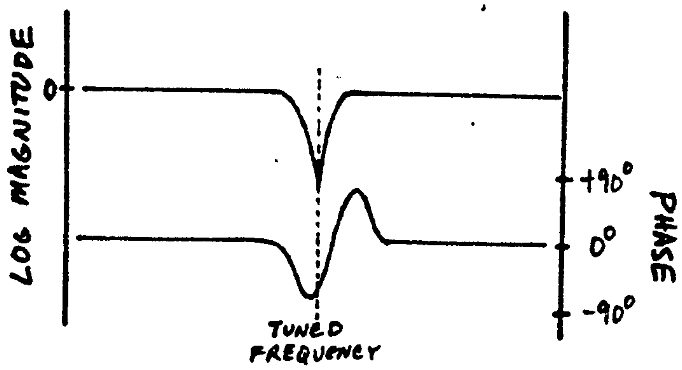

FIGURE 14.91 BODE PLOT OF NOTCH FILTER

14.6.1.4 Bandpass Filters

High and low pass filters can be combined to attenuate both low and high frequency signals and pass the middle range of frequencies. This compensator has the transfer function

$$G_c(s) = K\frac{(s+a)(s+c)}{(s+b)(s+d)} \tag{14.73}$$

where a < b, b < d, c > d. This gives the Bode plot in figure 14.92.

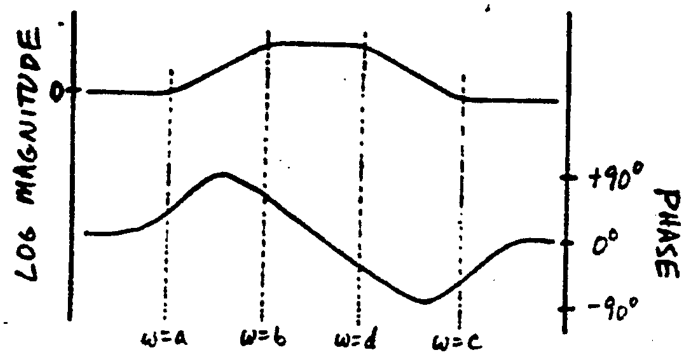

FIGURE 14.92 BODE PLOT OF BANDPASS FILTER

14.6.2 Prefilters

Electronic compensation devices are often added to the pilot command path of a flight control system to shape the response. When compensation devices are used in this location they are usually termed prefilters. Figure 14.93 shows an example of a prefilter used in a pitch rate command system.

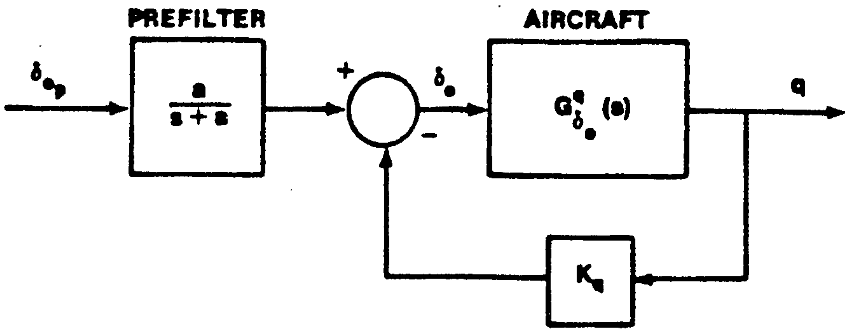

FIGURE 14.93 PREFILTER IMPLEMENTATION

A prefilter can be either a high pass filter, to provide a quickening of the initial aircraft response for a sluggish aircraft, or a low pass filter, to reduce the abruptness of the response of an overly sensitive aircraft. Figure 14.94 shows the effect of a high pass prefilter on the pitch rate response of an aircraft. Notice that the basic aircraft response is sluggish and heavily damped. With the high pass prefilter on the pilot input, the response is much more abrupt. Figure 14.95 shows the effect of a low pass prefilter on the pitch rate response of an aircraft with a pitch damper

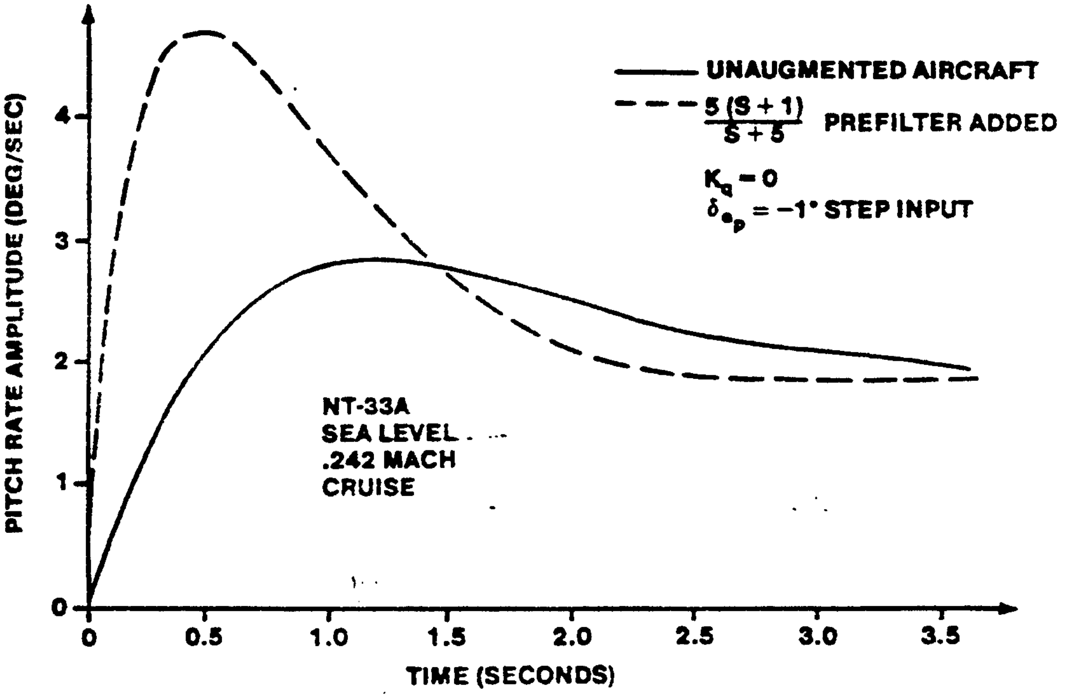

FIGURE 14.94 HIGH PASS PREFILTER EFFECTS ON AIRCRAFT PITCH RATE RESPONSE

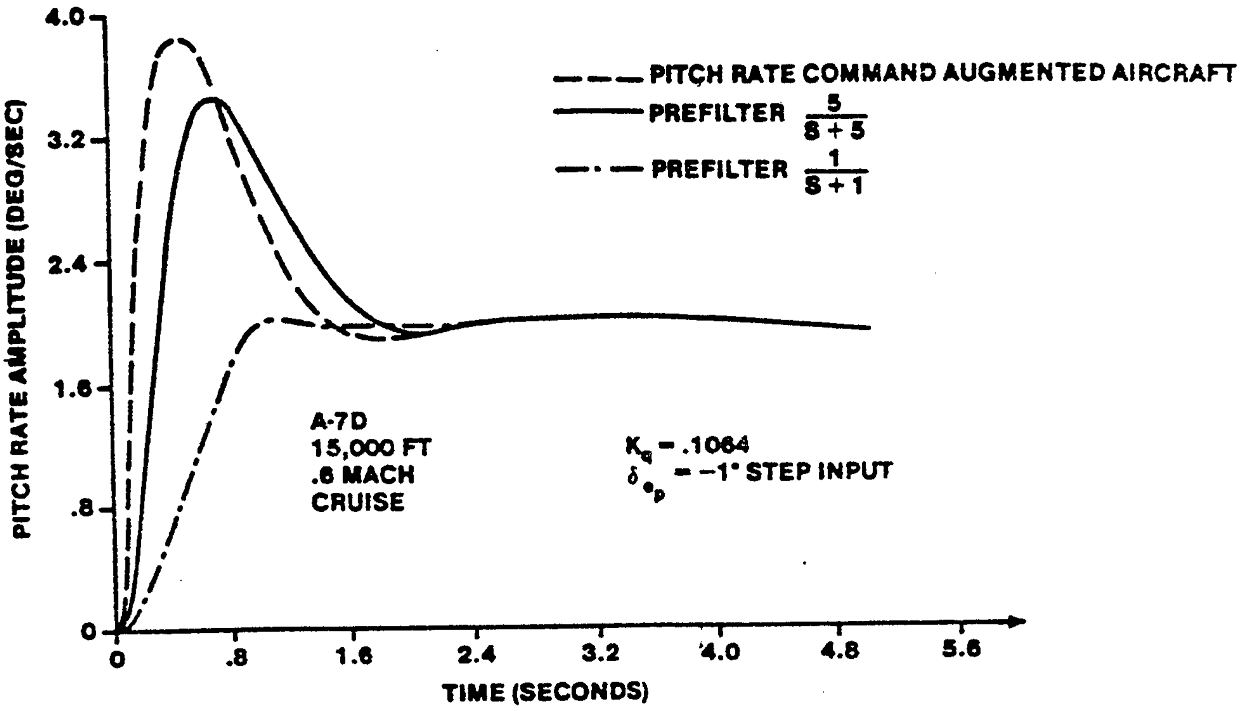

FIGURE 14.95 LOW PASS PREFILTER EFFECTS ON AIRCRAFT PITCH RATE RESPONSE

augmentation system. Notice that the larger the time constant of the prefilter, the more the aircraft response resembles the first order response of the prefilter.

14.6.3 Cascade Compensation

The use of high pass, low pass and high-low pass filters are often used for cascade compensation. High pass filters are used to quicken the aircraft response, by increasing the undamped natural frequencies, and to increase stability. Low pass filters are used to slow the response of the system or to decrease steady state error. High-low pass filters are used to accomplish both.

It should be noted that steady state errors in feedback flight control systems are sometimes useful and sometimes undesirable. For example, if speed stability is desired, a small steady state error is necessary in the longitudinal axis of the control system. Since the aircraft will not precisely hold a commanded attitude or airspeed by itself, the pilot must provide a control input, either through the stick or trim system, to maintain the desired flight condition. The amount of additional control input or trim required is dependent on the aircraft characteristics and may be altered in several ways.

The use of cascade compensation is discussed in the following sections for longitudinal load factor, pitch attitude, and pitch rate command systems. Cascade compensation in the lateral-directional axes is similar, such as in the elimination of sideslip (lateral acceleration) but are not specifically covered in this text.

14.6.3.1 Cascade Compensation in Load Factor Command Systems

Cascade compensation is often used in load factor command systems in order to achieve neutral speed stability. Neutral speed stability is a desirable feature in fighter aircraft because of the reduction in trim requirements during aggressive maneuvering such as air-to-surface weapon delivery. For these aircraft, however, speed stability has been found to be desirable for power approach and aircraft which normally have neutral speed stability, such as the F-15 and F-16, are designed to acquire speed stability when the landing gear is extended.

Perfect neutral speed stability is not attainable except with an altitude hold system. Aircraft with near neutral speed stability can be realized with a g command system. If nearly neutral speed stability is desired for piloted flight, an integrator (low pass filter) is required in the forward path (cascade) of a load factor command control system. Two implementations are possible — the addition of a pure integrator or the use of an integral plus proportional scheme. If speed stability is desirable, but a lower stick force gradient is required, then a lag filter may be added which reduces the steady state error but does not completely eliminate it.

The use of a pure integrator in cascade of a load factor command system provides apparent neutral speed stability, but is seldom used. The control strategy suffers because the pilot has no direct command path to the elevator. The pilot's inputs are applied to the integrator and the pilot must wait for the integration to occur before the aircraft responds. A large amount of lag is added to the system which can drive the short period roots unstable at a low system gain, as shown in figure 14.96. The phugoid roots move rapidly to the real axis, creating an unsuppressed real root which can adversely affect the time response of the aircraft, as shown in figure 14.98. Notice the significant effective time delay which initially occurs. Also, the integrator

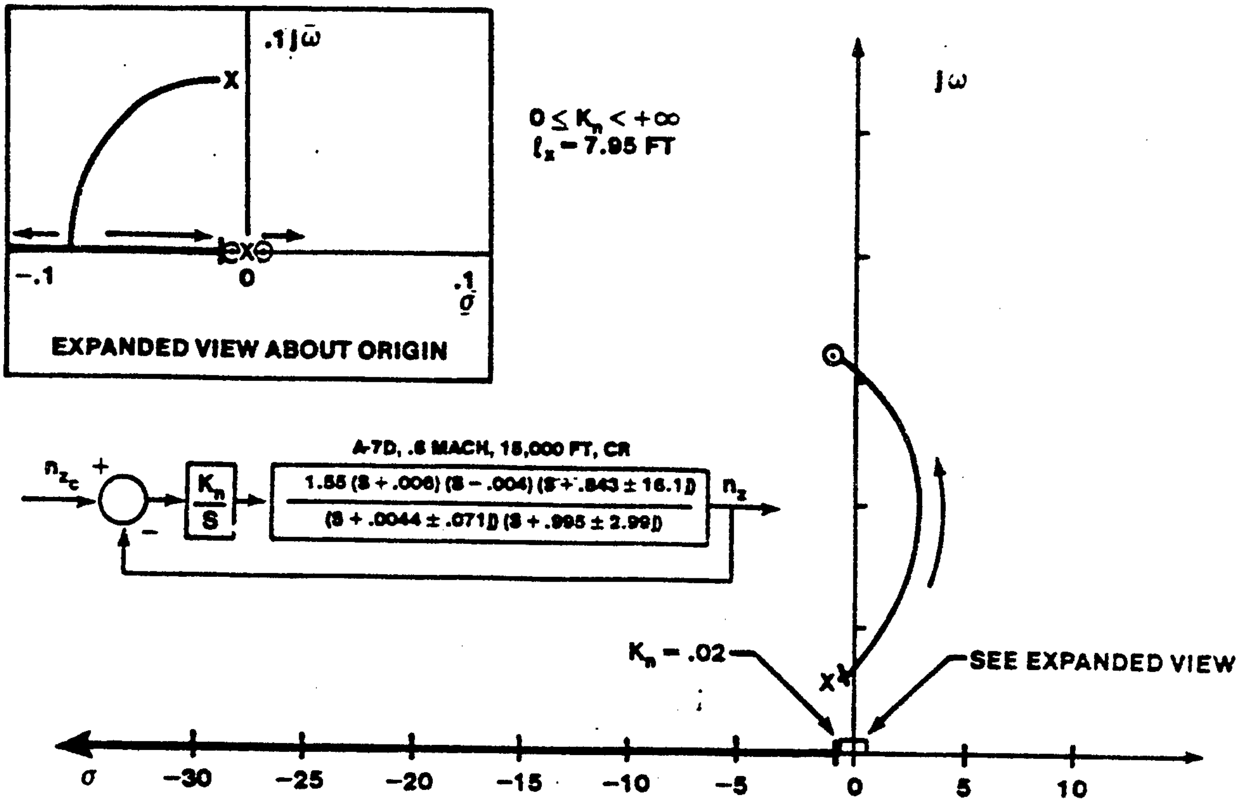
.1 jω
X
−.1
0
.1
σ
EXPANDED VIEW ABOUT ORIGIN
jω
0 ≤ K_n < +∞
ℓ_x = 7.95 FT
A-7D, .6 MACH, 15,000 FT, CR
n_{z_c}
+
−
$\frac{K_n}{S}$
$\frac{1.55 (S + .006) (S - .004) (S + .843 \pm 16.1j)}{(S + .0044 \pm .071j) (S + .995 \pm 2.99j)}$
n_z
K_n = .02
X
SEE EXPANDED VIEW
σ
−30
−25
−20
−15
−10
−5
0
5
10

FIGURE 14.96 ROOT LOCUS OF G COMMAND SYSTEM WITH INTEGRAL CONTROLLER

causes an unstable root near the origin which will eventually cause the aircraft to diverge (compare figure 14.95 with figure 14.74). If the time constant of the unstable root is long, however, neutral speed stability will be realized for all practical purposes.

An integral plus proportional control implementaion can be used to achieve near neutral speed stability while avoiding the main disadvantages of the pure integral control implementation. Figure 14.97 shows the root locus for a g command system with an integral plus proportional controller. The zero added by the proportional path prevents the excessive lag present in the system with the pure integral controller so that the short period roots are not driven unstable at any system gain.

Figure 14.98 compares the responses of two g command systems, one with a pure integral controller, and one with an integral plus proportional controller. The effective time delay is reduced and system convergence improved with the integral plus proportional controller.

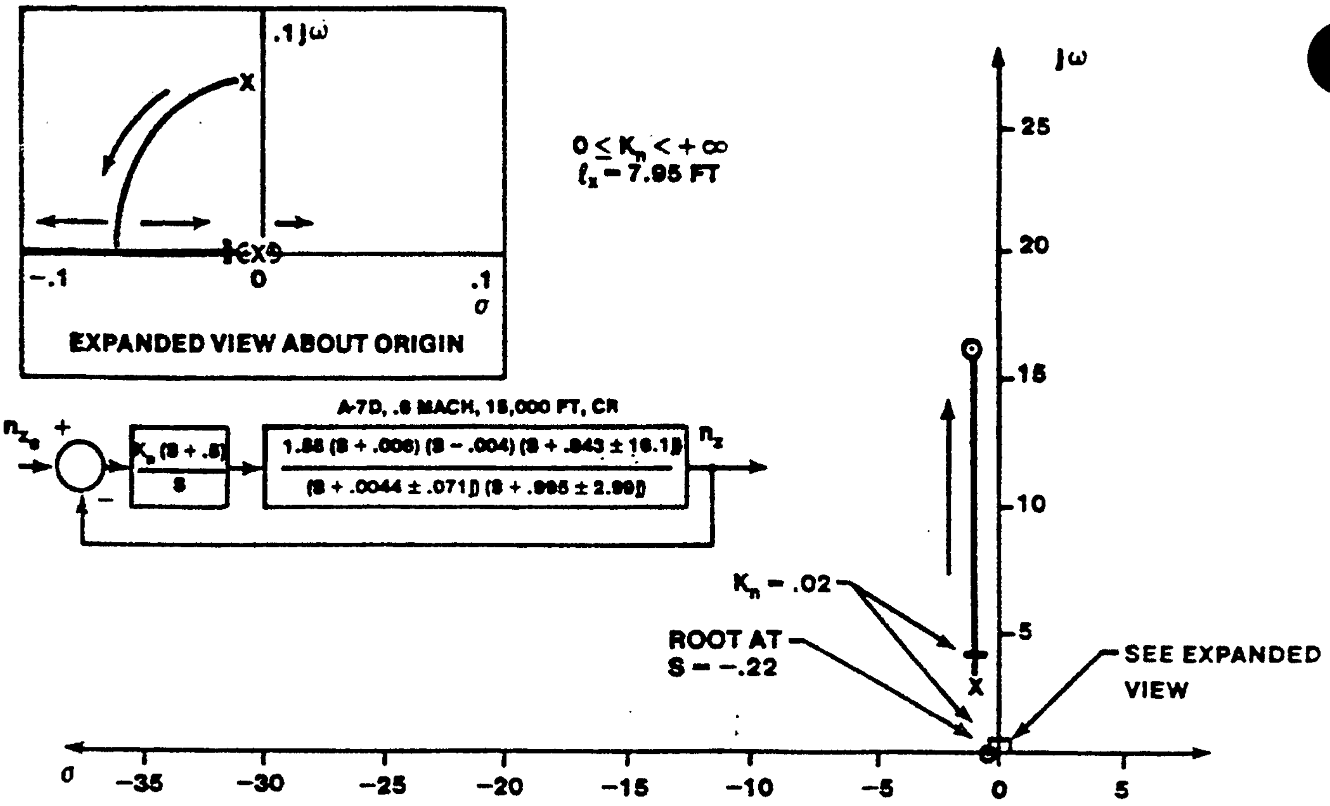

.1 jω
X
−.1
0
.1
σ
EXPANDED VIEW ABOUT ORIGIN
0 ≤ K_n < +∞
ℓ_x = 7.95 FT
jω
25
20
15
10
5
A-7D, .6 MACH, 15,000 FT, CR
n_zc
+
−
K_n (S + .5) / S
1.86 (S + .006) (S − .004) (S + .843 ± 16.1j) / (S + .0044 ± .071j) (S + .985 ± 2.99j)
n_z
K_n = .02
ROOT AT S = −.22
X
SEE EXPANDED VIEW
σ
−35
−30
−25
−20
−15
−10
−5
0
5

FIGURE 14.97 ROOT LOCUS OF G COMMAND AND INTEGRAL PLUS PROPORTIONAL CONTROLLER

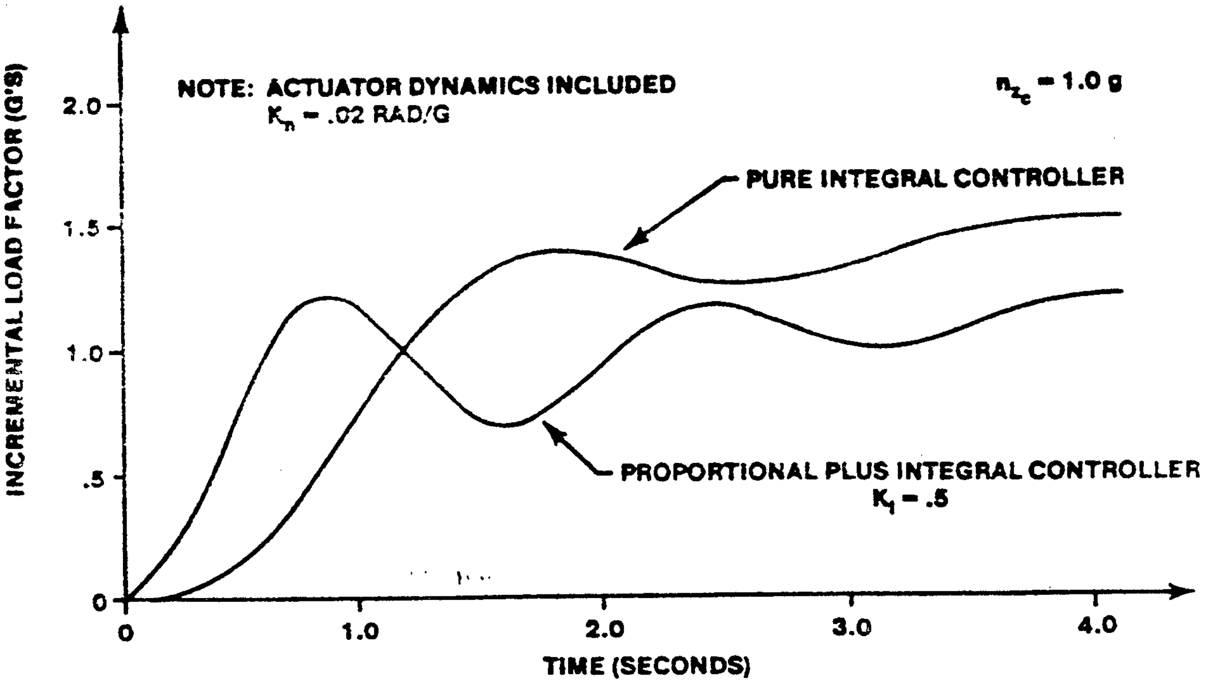

FIGURE 14.98 COMPARISON OF TIME RESPONSE FOR TWO G COMMAND SYSTEMS

14.6.3.2 Cascade Compensation in Pitch Attitude Command Systems

Cascade compensation is often used in pitch attitude command systems in order to reduce steady state error (low pass filters) or quicken aircraft response (high pass filters) as discussed in the following sections.

14.6.3.2.1 Low Pass Filters in Pitch Attitude Command Systems

If reduced steady state error in pitch attitude is desired for a pitch attitude command system this can be accomplished by using a low pass filter in cascade. As with a g command system, if a pure integrator is placed in cascade, a zero steady state error for a step input will result, since

$$e_{ss} = \lim_{s \to 0} \frac{1}{1 + \frac{K_\theta}{s} G^{\theta}_{\delta_e}(s)} = \frac{1}{1 + \infty} = 0 \tag{14.74}$$

Figure 14.99 shows the effect of an integrator added in cascade with a simple pitch attitude command system (compare this root locus to figure 14.47). The phugoid roots may move rapidly as the gain increases to a very high frequency (greater than 1.5 radians per second) while the short period roots very quickly become unstable. At low to moderate gain, two pairs of complex roots, those starting as the phugoid pair and those starting as the short period, can both occur in the frequencies normally associated with the short period. The aircraft motion can no longer be described by a simple second order response and the requirements of MIL-F-8785C will be difficult to use. Figure 14.102 shows the time reponse of the aircraft pitch attitude with the pure integral controller. The excessive overshoot and poor convergence to the final aircraft pitch attitude is due to the lag introduced by the integrator. Notice the large initial time delay before the aircraft starts to respond to the pilot input. Better convergence can be achieved with higher integrator gains, but instability problems generally preclude the use of high gains.

If an integral plus proportional low pass filter is used instead of a pure integral filter the steady state error for pitch attitude command will still be zero since

$$e_{ss} = \lim_{s \to 0} \frac{1}{1 + K_\theta \frac{(s + K)}{s} G^{\theta}_{\delta_e}(s)} = \frac{1}{1 + \infty} = 0 \tag{14.75}$$

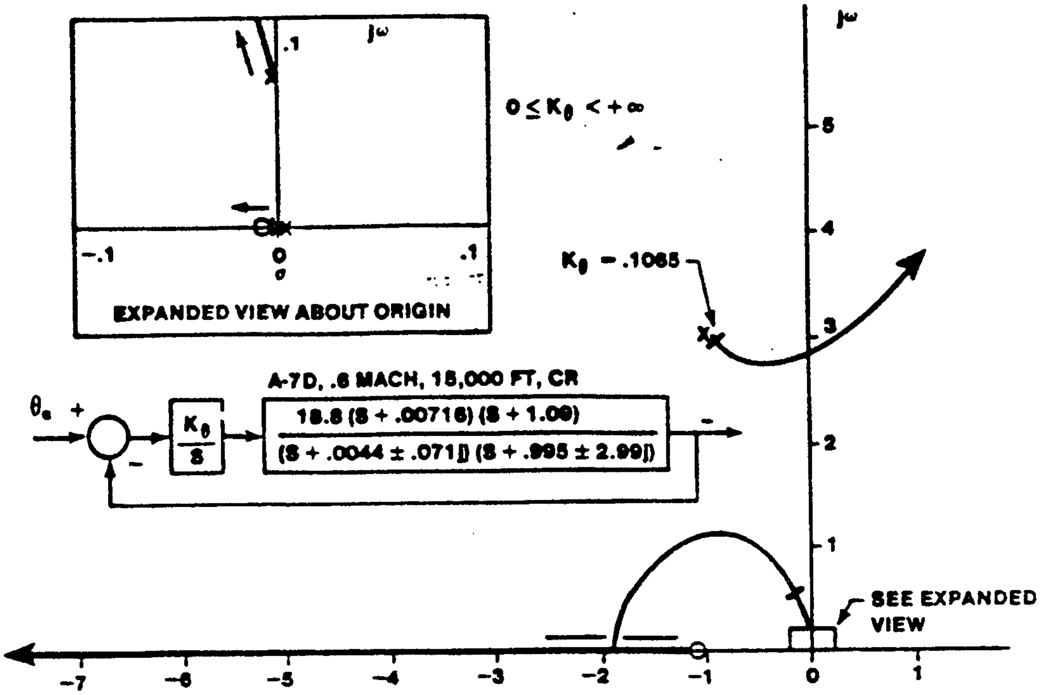

jω
.1
0 ≤ K_θ < +∞
5
4
3
2
1
−.1
0
σ
.1
EXPANDED VIEW ABOUT ORIGIN
K_θ = .1065
A-7D, .6 MACH, 15,000 FT, CR
θ_c
+
−
K_θ / S
18.8 (S + .00716) (S + 1.09)
(S + .0044 ± .071j) (S + .995 ± 2.99j)
SEE EXPANDED VIEW
−7
−6
−5
−4
−3
−2
−1
0
1

FIGURE 14.99 ROOT LOCUS OF PITCH ATTITUDE LOOP WITH CASCADE INTEGRATOR

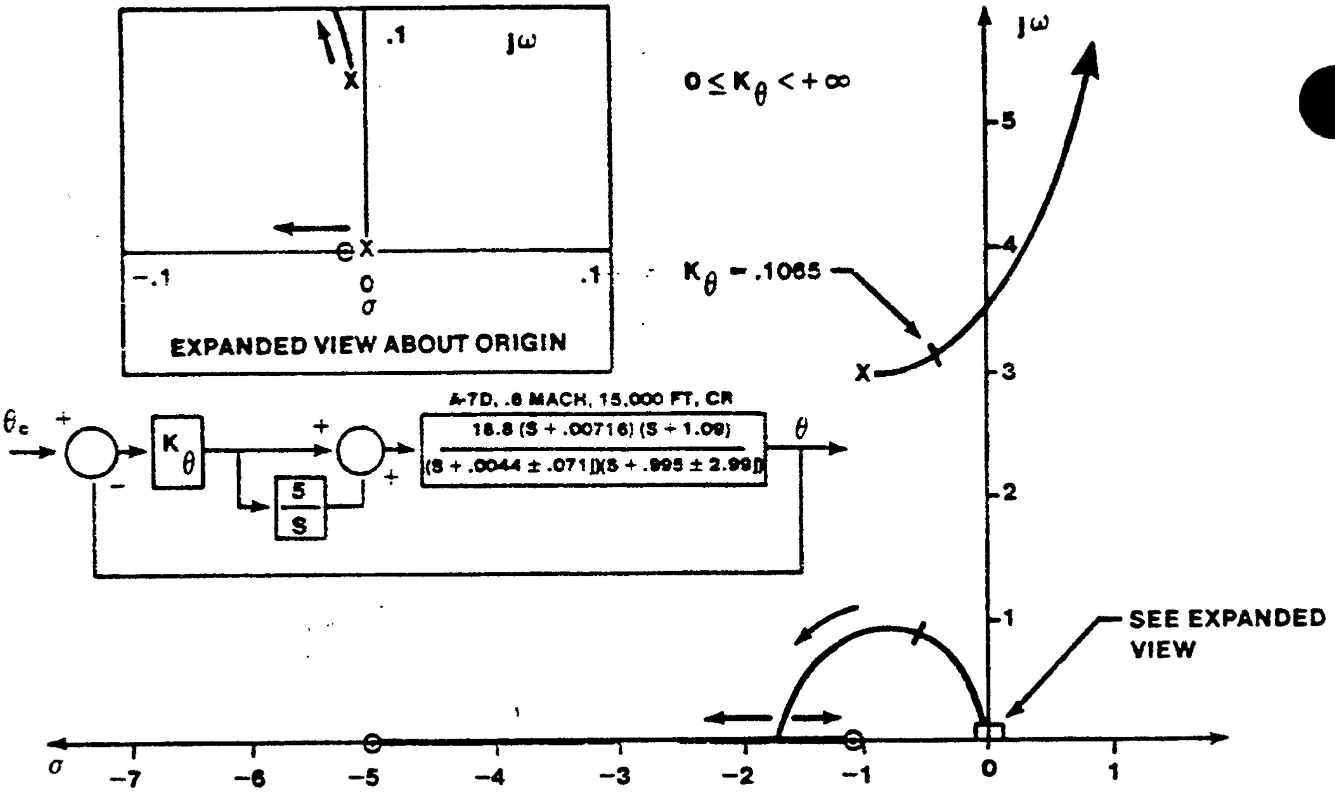

.1
jω
0 ≤ K_θ < +∞
5
4
3
2
1
−.1
0
σ
.1
EXPANDED VIEW ABOUT ORIGIN
K_θ = .1065
A-7D, .6 MACH, 15,000 FT, CR
θ_c
+
−
K_θ
+
+
5 / S
18.8 (S + .00716) (S + 1.09)
(S + .0044 ± .071j)(S + .995 ± 2.99j)
θ
SEE EXPANDED VIEW
σ
−7
−6
−5
−4
−3
−2
−1
0
1

FIGURE 14.100 PITCH ATTITUDE LOOP WITH PROPORTIONAL PLUS INTEGRAL CONTROL, HIGH INTEGRATOR GAIN

Figure 14.100 shows the effect of a cascade integral plus proportional low pass filter in a pitch attitude command system. The effect of integral plus proportional control on the augmentated aircraft characteristics is nearly a direct function of the integrator gain, K. For high values of K the effect is similar to that of a pure integrator in cascade (compare figure 14.100 to figure 14.99). The added zero due to the proportional plus integral controller causes the augmented aircraft roots to move further on the root locus for a specified gain than in the case of the pure integral controller, depending on the integrator gain K. For low values of K, the effect more closely approximates that of the lag filter (discussed in the next section) except that the step input steady state error is zero. The effect of low integrator gain is shown in figure 14.101.

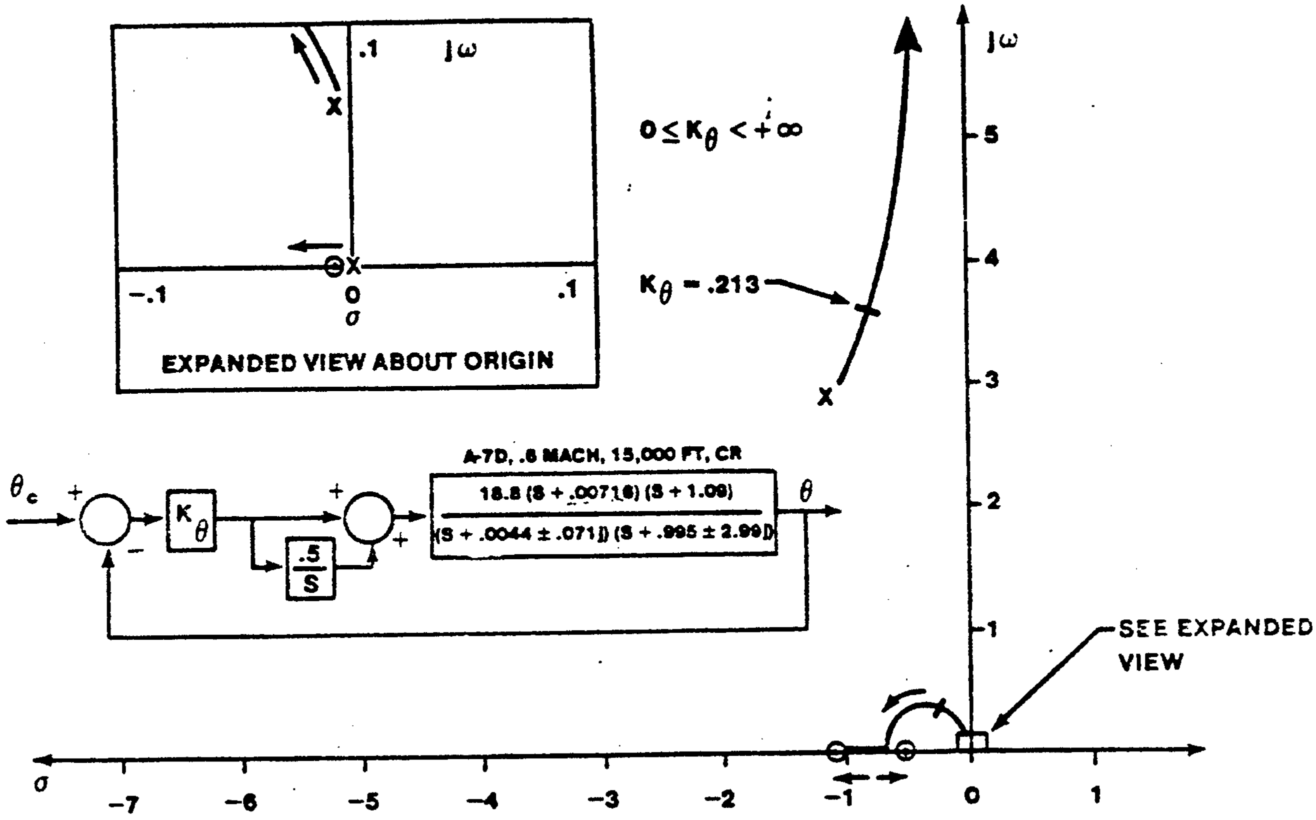
.1
jω
X
−.1
0
σ
.1
EXPANDED VIEW ABOUT ORIGIN
$0 \leq K_\theta < +\infty$
$K_\theta = .213$
X
jω
5
4
3
2
1
SEE EXPANDED VIEW
A-7D, .6 MACH, 15,000 FT, CR
θ_c
+
−
K_θ
+
+
$\frac{.5}{S}$
$\frac{18.8\,(S + .00716)\,(S + 1.09)}{(S + .0044 \pm .071j)\,(S + .995 \pm 2.99j)}$
θ
σ
−7
−6
−5
−4
−3
−2
−1
0
1

FIGURE 14.101 ROOT LOCUS OF PITCH ATTITUDE LOOP WITH INTEGRAL PLUS PROPORTIONAL CONTROL, LOW INTEGRATOR GAIN

The main advantage of integral plus proportional control over the pure integrator approach is, again, that the pilot is provided a direct path to the elevator and does not have to wait for an integration to occur prior to seeing the aircraft respond. The zero helps to quicken the response over the pure integrator scheme at low values of K. Higher values of K contribute to an effective time delay due to the increased lag caused by the integrator. Higher integrator gains, however, are generally possible using an integral plus proportional scheme than when using a pure integral controller, shortening the convergence time of the system to the commanded status.

Figure 14.102 shows the time response characteristics of a pitch attitude command system with an integral plus proportional controller in cascade. Both responses are higher order and the requirements of MIL-F-8785 are difficult to apply. The higher integrator gain causes a faster rise time and more rapidly approaches the final value. Also note the difference in the initial response (below 0.2 seconds). The zero at s = -K does not aid the initial reponse of the system with the high integrator gain, resulting in an effective time delay of nearly 0.2 seconds (versus 0.1 seconds for the lower integrator gain).

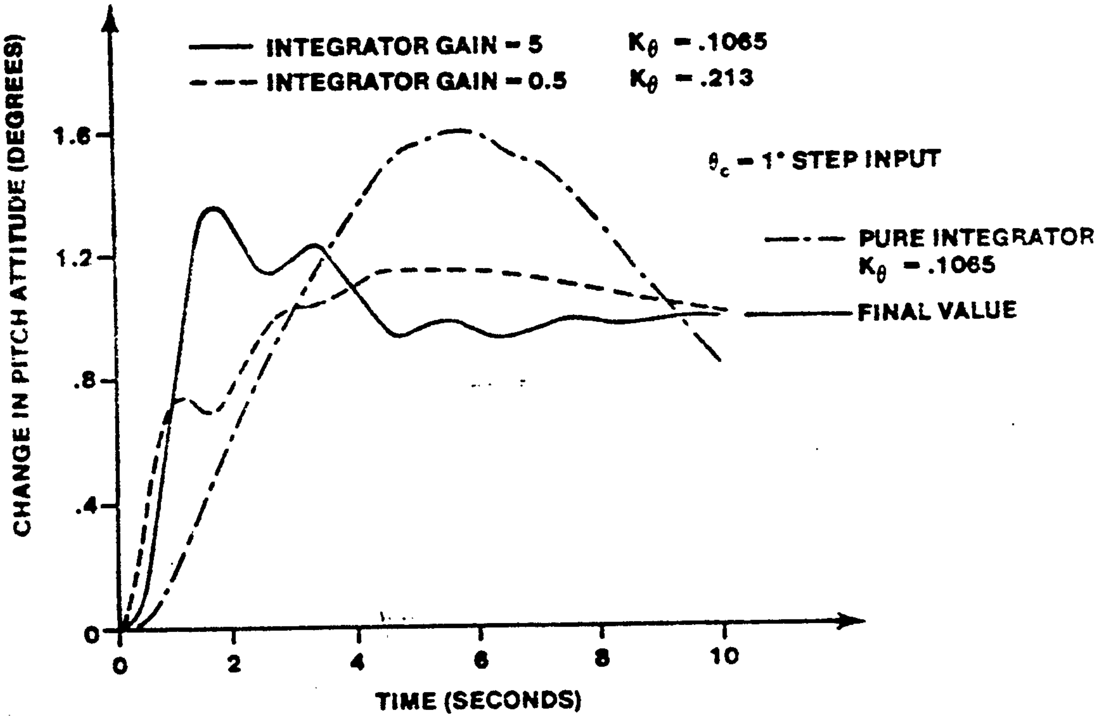

FIGURE 14.102 A-7D PITCH ATTITUDE RESPONSE WITH LOW PASS FILTERS

This effective time delay characteristic of highly augmented analog systems (no actual time delay occurs in analog systems, only in digital systems) has been correlated with a severe degredation in handling qualities when excessive.

Figure 14.103 shows the output signals associated with the proportional part of the network, the integrator, and the complete controller. Notice that the integrator rapidly assumes the majority of the error signal while the proportional path must act to reduce the total network output. The integrator actually causes the overshoot of the final pitch attitude value (commanded attitude) to occur.

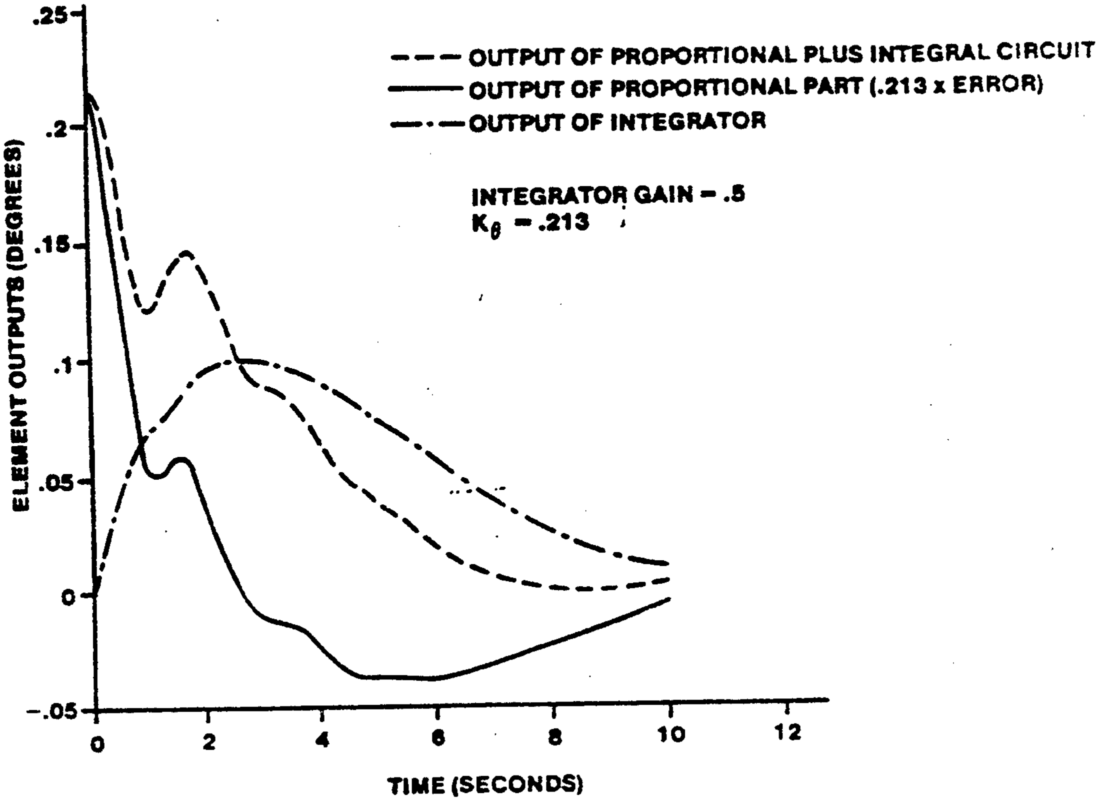

FIGURE 14.103 OUTPUTS OF INTEGRAL PLUS PROPORTIONAL CIRCUIT

A lag compensator can be used to approximate the action of the integrator at low frequencies. The ratio of the distance of the pole away from the origin compared to the zero is usually not greater than 10, due to practical design considerations, so that the zero is not more than 10 times further from the origin than the pole.

The lag filter reduces the steady state error for a step input by a significant amount. For a system without the lag filter (figure 14.47)

$$e_{ss} = \lim_{s\to 0} \frac{1}{1 + K_\theta G^{\theta}_{\delta_e}(s)} = \frac{1}{1 + 2.92\,K_\theta} = 0.62 \quad (K_\theta = 0.213) \tag{14.76}$$

With the lag filter added

$$e_{ss} = \lim_{s\to 0} \frac{1}{1 + \frac{K_\theta(s + 0.1)}{(s + 0.01)} G^{\theta}_{\delta_e}(s)} = \frac{1}{1 + 29.2\,K_\theta} = 0.139 \tag{14.77}$$

A 78% reduction in the steady state error occurs. Larger percentage reductions can occur for higher gain, since high gain contributes to lower errors. In this system, however, high gain also causes low short period damping which would be unacceptable. A residual steady state error for step

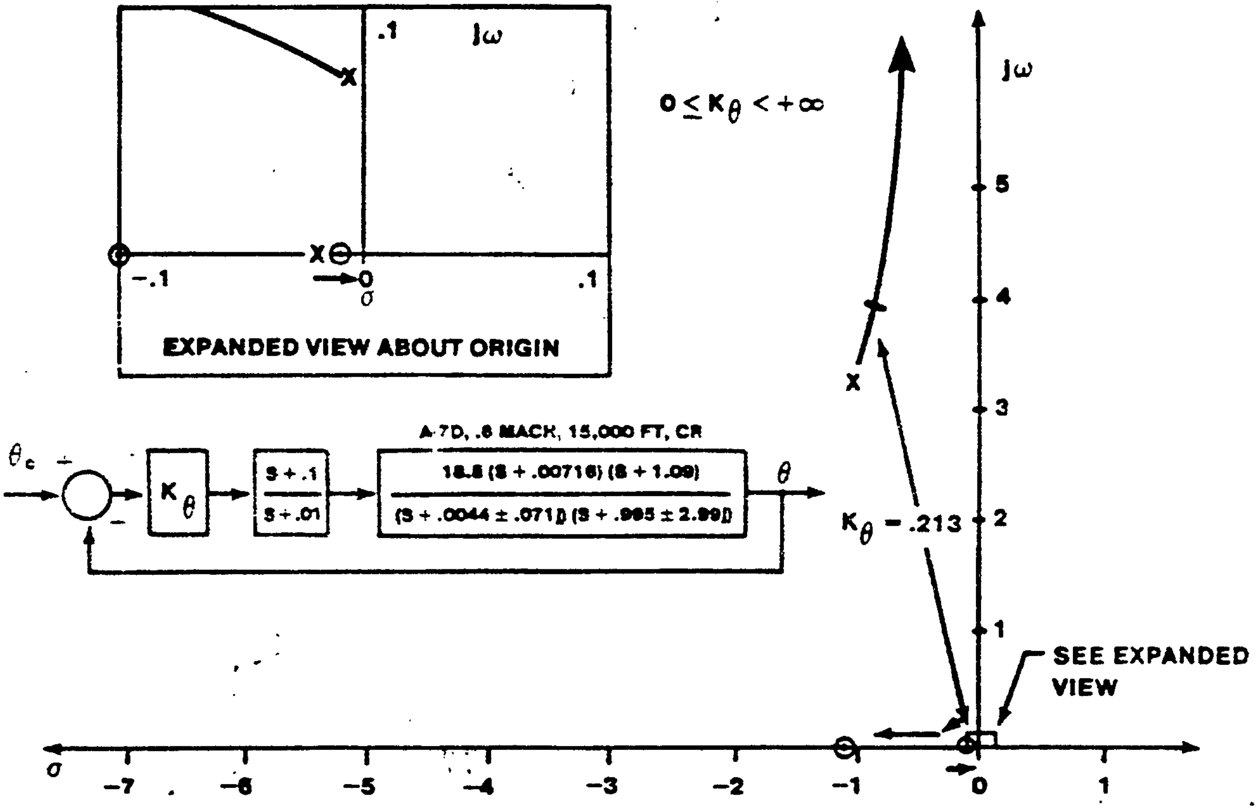
.1
jω
X
X
.1
−.1
0
σ
.1
EXPANDED VIEW ABOUT ORIGIN
0 ≤ K_θ < +∞
jω
5
4
3
X
2
1
K_θ = .213
SEE EXPANDED VIEW
A-7D, .6 MACH, 15,000 FT, CR
θ_c
+
−
K_θ
S + .1
S + .01
18.8 (S + .00716) (S + 1.09)
(S + .0044 ± .071j) (S + .965 ± 2.99j)
θ
σ
−7
−6
−5
−4
−3
−2
−1
0
1

FIGURE 14.104 ROOT LOCUS OF PITCH ATTITUDE LOOP WITH LAG FILTER

inputs exists since an integrator is not present. The lag filter is usually placed in the low frequency region so as not to affect the short period response of the aircraft while changing the phugoid response significantly. Referring to figure 14.104, it is apparent that the phugoid natural frequency and damping are increased significantly while the short period response is not significantly altered from the system of figure 14.47. Figure 14.105 shows the time response of the aircraft pitch attitude illustrating the effects of the lag filter.

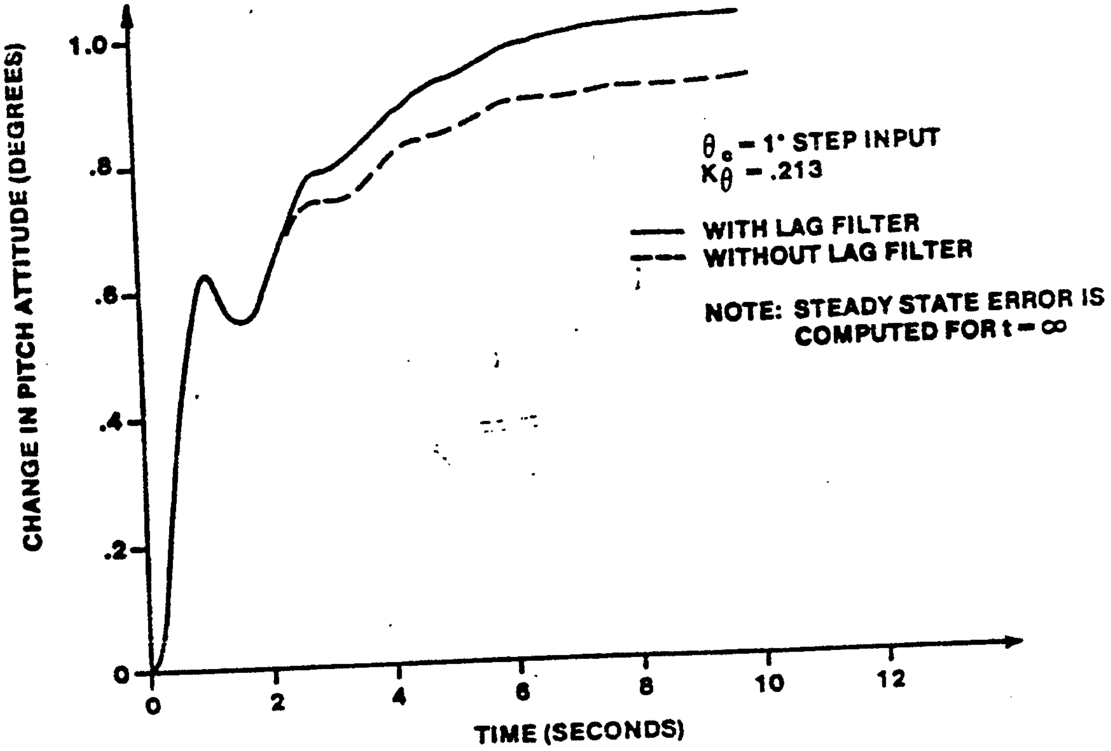

NOTE: STEADY STATE ERROR IS COMPUTED FOR t → ∞

FIGURE 14.105 A-7D PITCH ATTITUDE REPONSE WITH LAG FILTER

The A-7D digitac aircraft used a lag filter in the pitch axis to reduce the speed stability of the aircraft relative to the normal A-7D, thereby reducing the pilot stick forces necessary to maintain a constant dive angle during dive bombing, where a speed increase from 300 knots at roll-in to 450 knots at release is typical.

In summary, the steady state error is most effectively reduced to zero for a step input (pitch attitude command system) through the use of integral plus proportional control. The actual effect depends heavily upon the integrator gain. An alternative is to use a lag low pass filter which reduces but does not eliminate the steady state error.

16.6.3.2.2 High Pass Filters in Pitch Attitude Command Systems

The best way to quicken the response of the pitch attitude command system (improve damping ratio) is to feed back pitch rate to the elevator (see sections 14.5.1.1.1.1 and 14.5.1.1.4.3). Another approach is to add lead compensation in cascade (or in the feedback path).

Figures 14.106 and 14.107 present the effects of a lead compensator (with two different values of K) on a pitch attitude command system. The lead compensator can significantly alter the closed loop response. The lead compensator is generally centered near the short period frequency so as to increase the phase angle in that region, thereby improving the system short period damping ratio. The more lead provided (greater relative distance between the pole and zero), the more damping is improved. Practical limitations in components generally restrict the ratio of the pole to the zero to 10 or less in analog systems. If the control loop gain is too high the

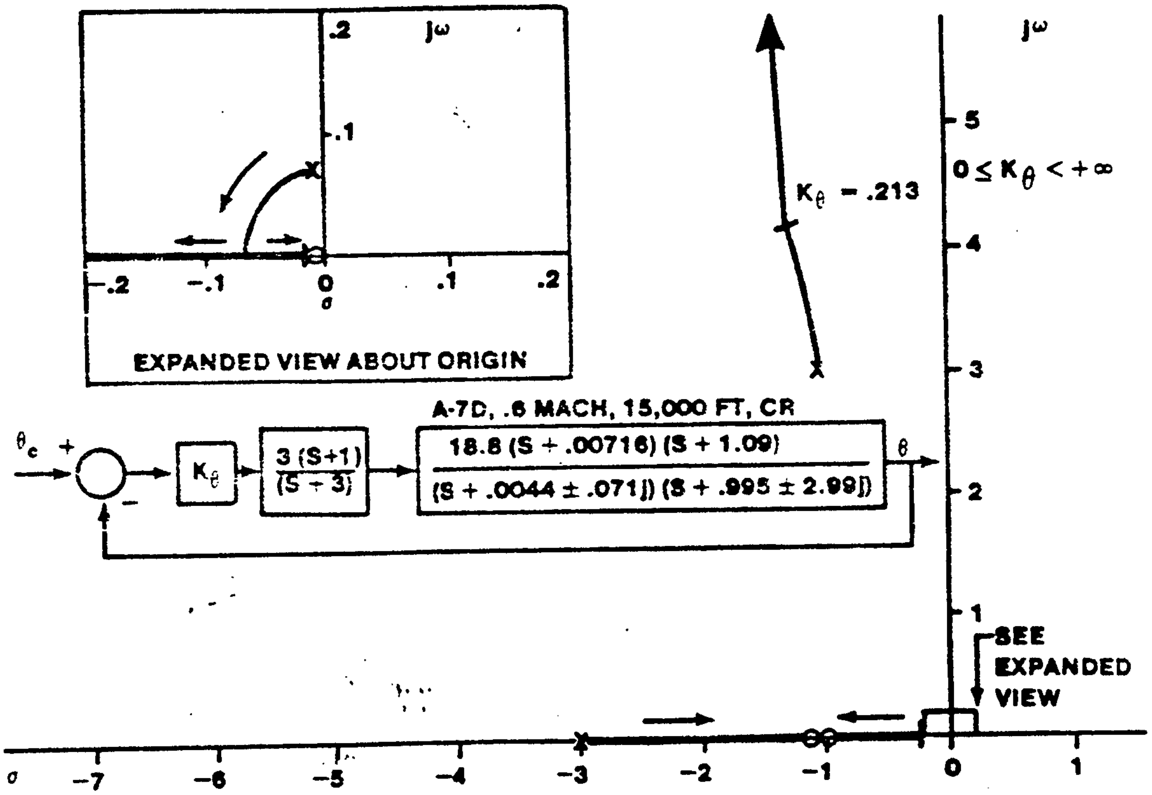
.2
jω
.1
-.2
-.1
0
σ
.1
.2
EXPANDED VIEW ABOUT ORIGIN
$K_\theta = .213$
jω
5
$0 \le K_\theta < +\infty$
4
3
A-7D, .6 MACH, 15,000 FT, CR
θ_c
+
−
K_θ
$\frac{3(S+1)}{(S+3)}$
$\frac{18.8(S+.00716)(S+1.09)}{(S+.0044 \pm .071j)(S+.995 \pm 2.99j)}$
θ
2
1
SEE EXPANDED VIEW
σ
-7
-6
-5
-4
-3
-2
-1
0
1

FIGURE 14.106 ROOT LOCUS OF PITCH ATTITUDE LOOP WITH LEAD COMPENSATOR

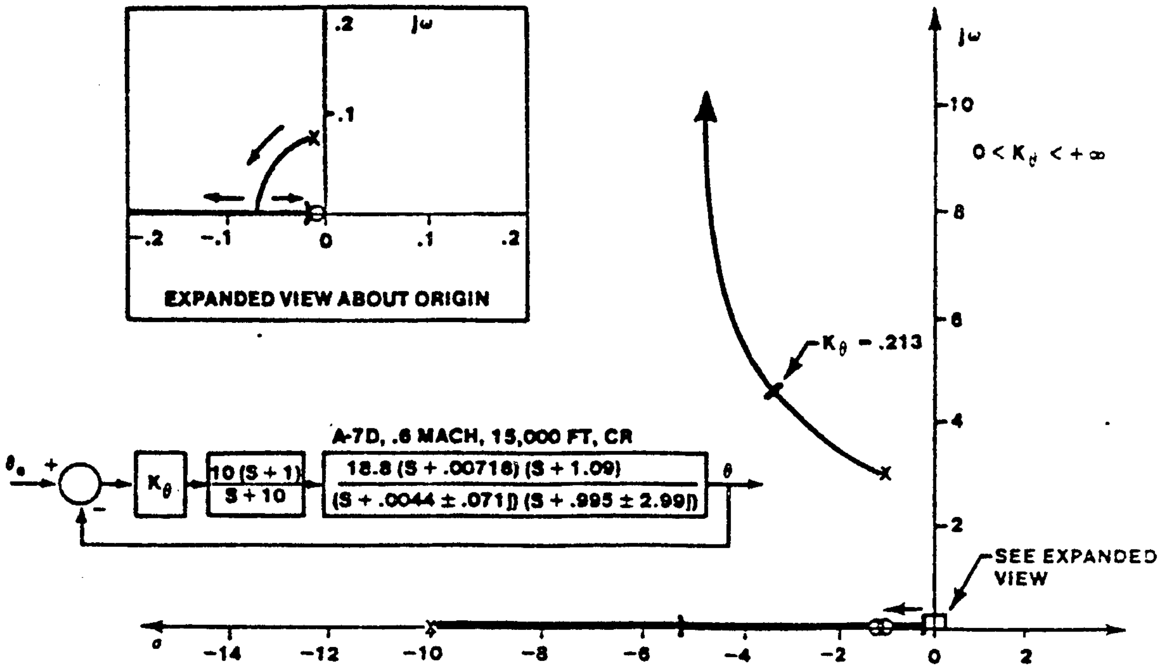

FIGURE 14.107 ROOT LOCUS OF PITCH ATTITUDE LOOP WITH LEAD COMPENSATOR

damping ratio will decrease and the natural frequency will increase in the pitch attitude systems presented.

14.6.3.3 Cascade Compensation in Pitch Rate Command Systems

If an integrator is used in a pitch rate command system on an aircraft with conventional stability, then a steady state error occurs in the pitch rate but not in the pitch attitude. This will result in two effects. The pitch rate command system root locus will be identical to the uncompensated pitch attitude root locus, where the short period natural frequency increases and the damping ratio decreases while the phugoid characteristics are suppressed. This is not what would be expected from a pitch rate feedback system (which increases short period damping primarily). Also, the integrator suppresses the large initial pitch rate overshoot which normally occurs in conventional aircraft. Excessive suppression of this characteristic is detrimental to acceptable handling qualities.

If an integral plus proportional low pass filter is added in cascade on a pitch rate command system, the pitch rate overshoot characteristic of conventional aircraft is suppressed somewhat, but not as severely as in the pure integrator case. For low values of integrator gain, the overshoot suppression is small. For high values the overshoot suppression is substantial and approaches the poor flying qualities of the pure integrator scheme.

Pitch rate command systems are unsuccessful in stabilizing an unstable aircraft whose instability is due either to the tuck mode in the transonic regime or to a longitudinal static instability (figure 14.44). This inability to stabilize the aircraft is due to the presence of the zero at the origin in the pitch rate transfer function. The use of an integrator in cascade to cancel the zero at the origin is a solution, but one with hidden difficulties for piloted flight (this solution may be quite successful for autopilot operation). With pure integral control, a decrease in the short period damping and an increase in the short period natural frequency occurs, the roots of the augmented aircraft migrating in a manner similar to a pitch attitude feedback system (see section 14.5.1.1.3.1). A relatively high gain is required to stabilize the aircraft. Figure 14.108 shows the time response of the pitch rate command system with a pure integral controller. A large

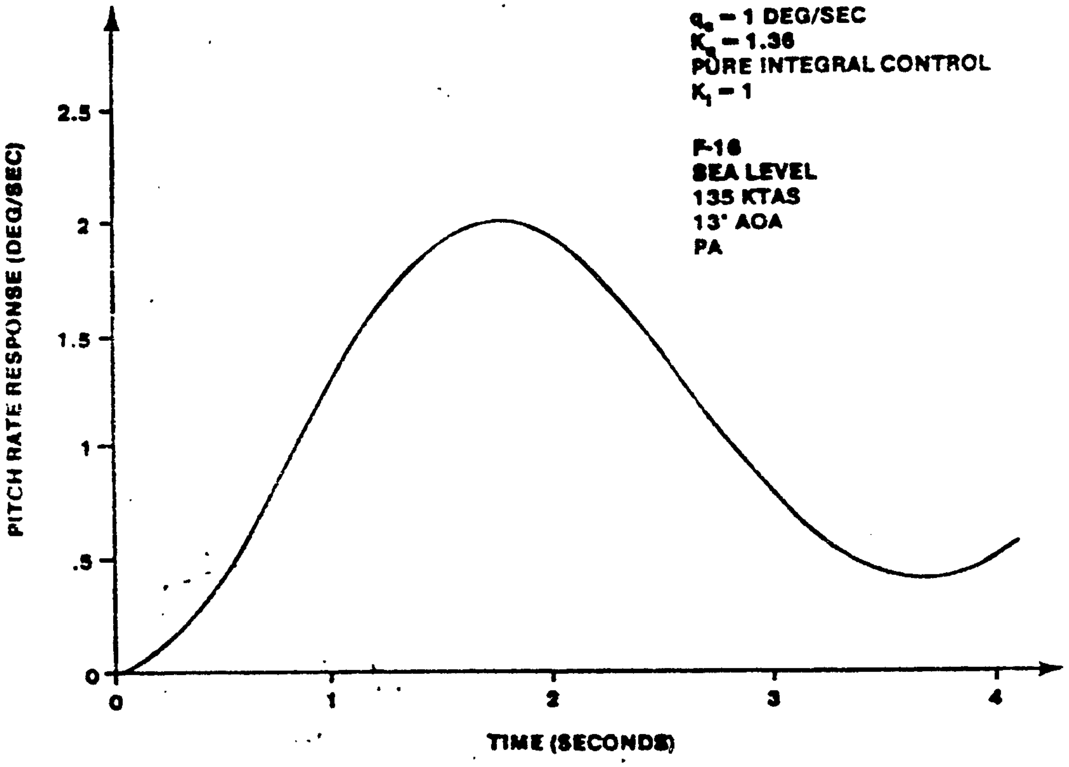

FIGURE 14.108 UNSTABLE AIRCRAFT PITCH RATE RESPONSE, PURE INTEGRAL CONTROL

effective time delay is apparent and poor handling qualities could be expected due to the low response damping. Further compensation would be required to obtain acceptable characteristics.

The use of an integral plus proportional controller may overcome the difficulties encountered when using the pure integral controller. Figures 14.109 and 14.110 illustrate the effects of two integral plus proportional controllers on the root locus of the pitch rate command system. The higher the integrator gain, the more closely the situation with the pure integral controller is approached. Figure 14.111 compares the time response of the two systems. The system with the lower integrator gain suppresses the pitch rate overshoot characteristic of the aircraft and may yield poor handling qualities as a result. The system with the higher integrator gain provides a response characteristic which is closer to what is obtained with conventional aircraft and generally preferred by pilots.

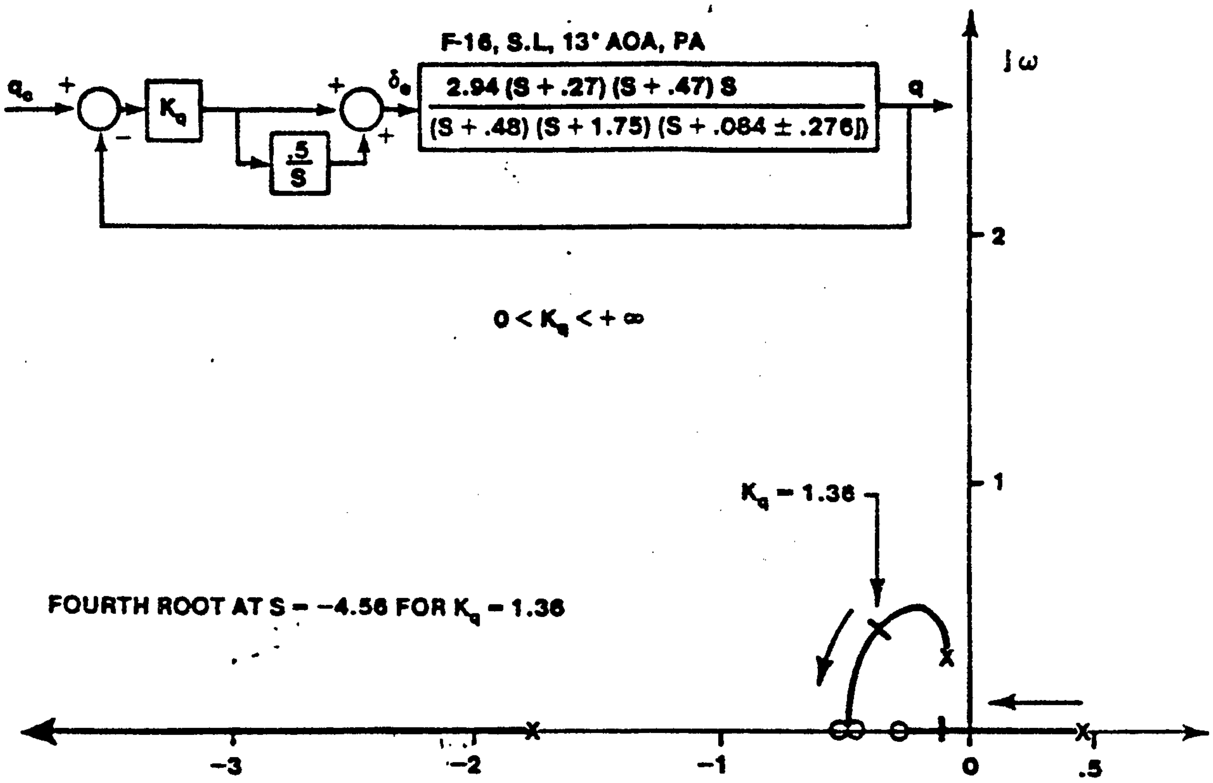
F-16, S.L, 13° AOA, PA
q_c
+
−
K_q
$\frac{.5}{S}$
+
+
δ_e
$\frac{2.94\,(S+.27)\,(S+.47)\,S}{(S+.48)\,(S+1.75)\,(S+.084\pm.276j)}$
q
jω
2
1
$0 < K_q < +\infty$
$K_q = 1.36$
FOURTH ROOT AT S = −4.56 FOR $K_q = 1.36$
−3
−2
−1
0
.5

FIGURE 14.109 UNSTABLE AIRCRAFT PITCH RATE LOOP, INTEGRAL PLUS PROPORTIONAL CONTROL

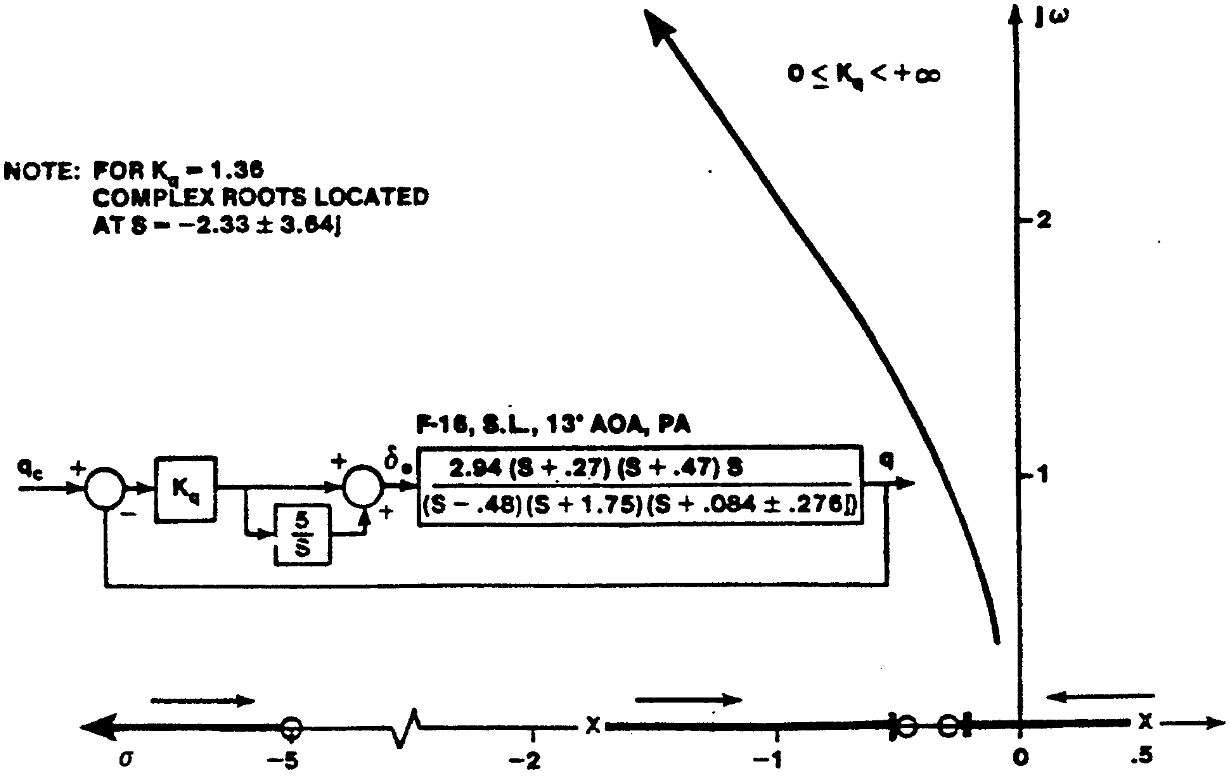
NOTE: FOR $K_q = 1.36$
COMPLEX ROOTS LOCATED
AT $S = -2.33 \pm 3.64j$
$0 \leq K_q < +\infty$
$j\omega$
2
1
F-16, S.L., 13° AOA, PA
q_c
+
−
K_q
$\frac{5}{S}$
+
+
δ_e
$\frac{2.94(S+.27)(S+.47)S}{(S-.48)(S+1.75)(S+.084 \pm .276j)}$
q
σ
−5
−2
−1
0
.5

FIGURE 14.110 UNSTABLE AIRCRAFT PITCH RATE LOOP, INTEGRAL PLUS PROPORTIONAL CONTROL

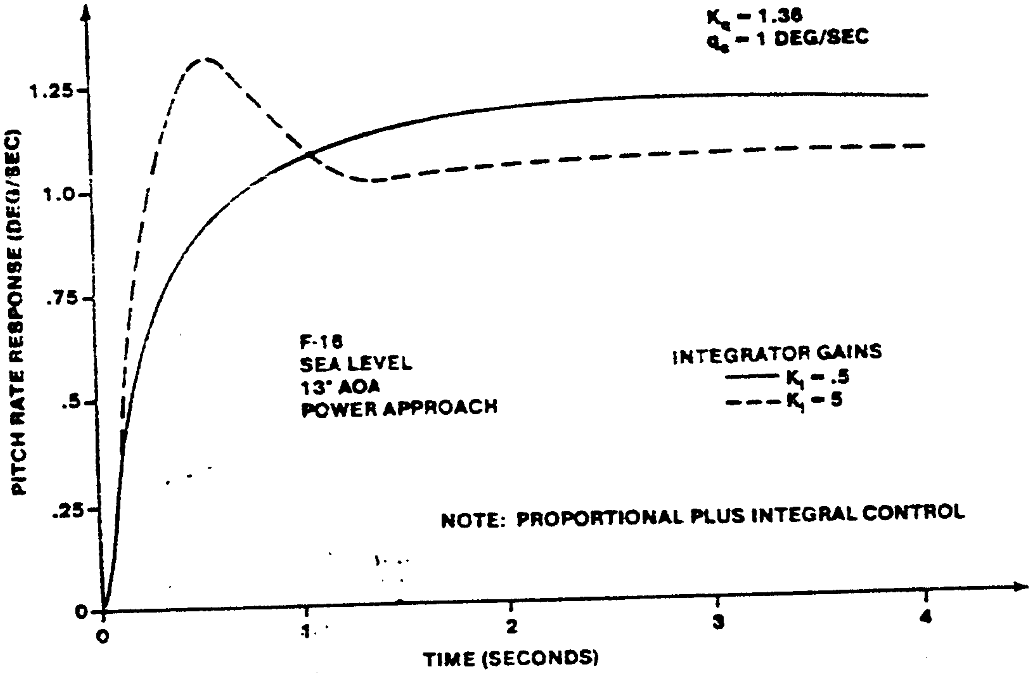

FIGURE 14.111 UNSTABLE AIRCRAFT PITCH RATE LOOP, INTEGRAL CONTROL COMPARISON

Engineers have postulated that the optimal location of the zero which arises from the integral plus proportional controller is such that it cancels the stable real root in the aircraft characteristic equation. Figures 14.112, 14.113, and 14.114 show the effect of varying the integrator gain about the stable real pole. Figure 14.115 compares the time responses of the three systems for a specified gain. It is apparent that the location of the zero relative to the pole does not significantly alter the aircraft response characteristics as long as the zero is relatively close to the pole. The higher the integrator gain, however, the lower the response rise time. The overshoot tendency of the pitch rate response is slight. Notice that if the system gain is reduced at a fixed integrator gain, the overshoot magnitude is increased somewhat but the response is also sluggish (lower effective short period frequency).

Using integral plus proportional control with relatively high integrator gain is preferred and cancellation of the stable real root may not be the optimal solution. The higher the integrator gain, the higher the frequency of the short period and the lower the short period damping for a fixed controller gain. The addition of lead compensation may be required to obtain the desired characteristics. Ground and inflight simulations are required to assess the impact of the integrator gain on aircraft handling qualities.

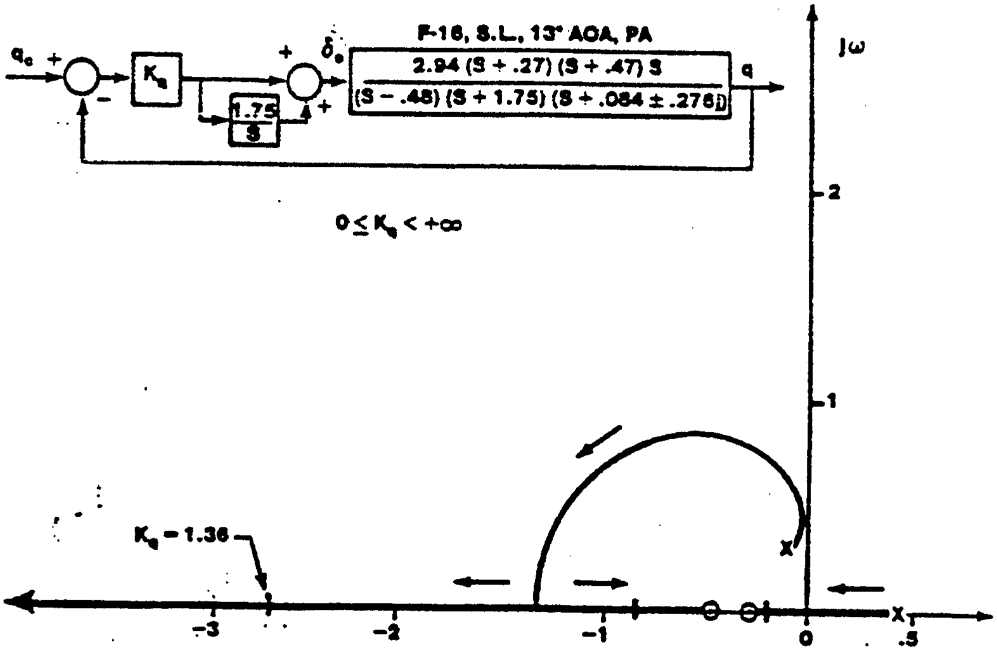

FIGURE 14.112 UNSTABLE AIRCRAFT LOOP INTEGRAL PLUS PROPORTIONAL CONTROL

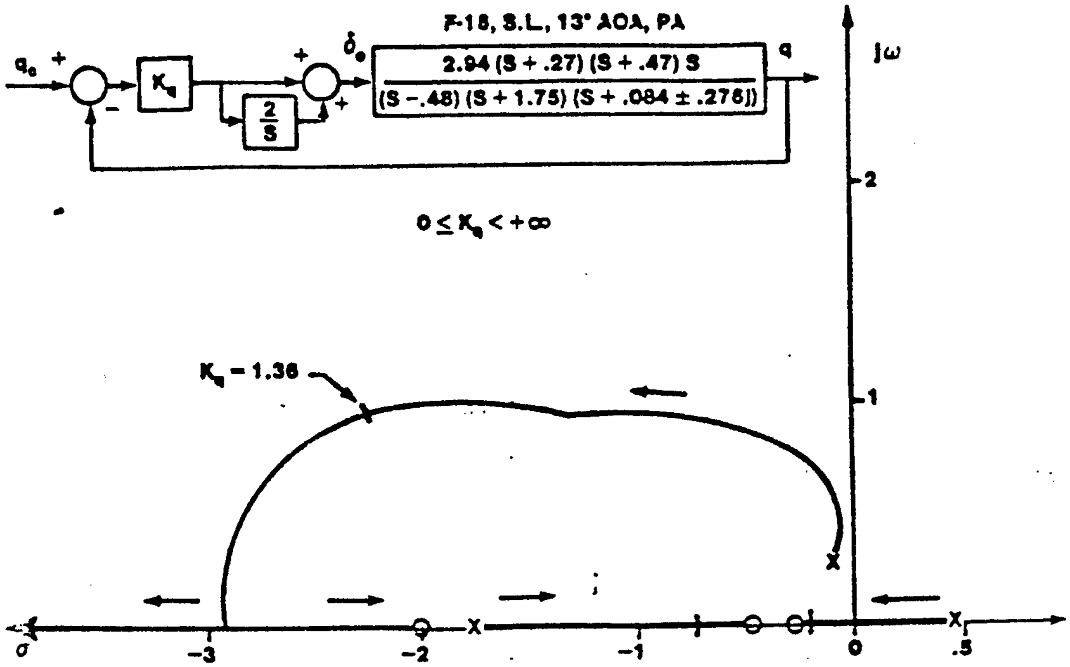
F-18, S.L., 13° AOA, PA
q_c
+
−
K_q
+
+
2/S
δ_e
2.94 (S + .27) (S + .47) S
(S − .48) (S + 1.75) (S + .084 ± .276j)
q
jω
2
1
0 ≤ K_q < +∞
K_q = 1.36
σ
−3
−2
−1
0
.5

FIGURE 14.113 UNSTABLE AIRCRAFT PITCH RATE LOOP, INTEGRAL PLUS PROPORTIONAL CONTROL

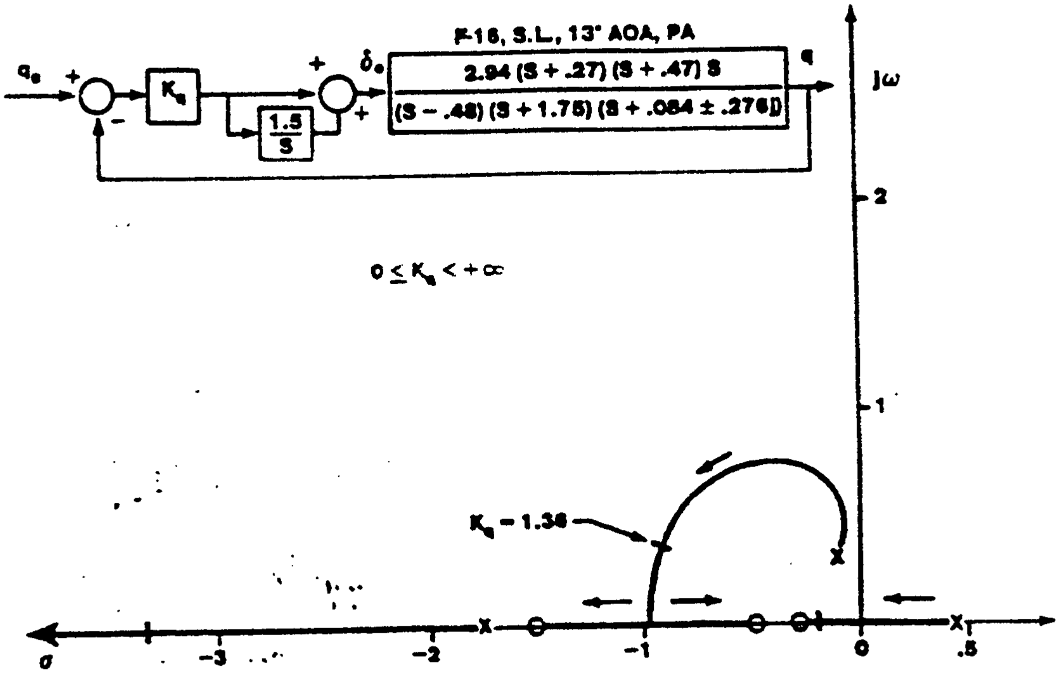
F-18, S.L., 13° AOA, PA
q_c
+
−
K_q
+
+
1.5/S
δ_e
2.94 (S + .27) (S + .47) S
(S − .48) (S + 1.75) (S + .084 ± .276j)
q
jω
2
1
0 ≤ K_q < +∞
K_q = 1.36
σ
−3
−2
−1
0
.5

FIGURE 14.114 UNSTABLE AIRCRAFT PITCH RATE LOOP, INTEGRAL PLUS PROPORTIONAL CONTROL

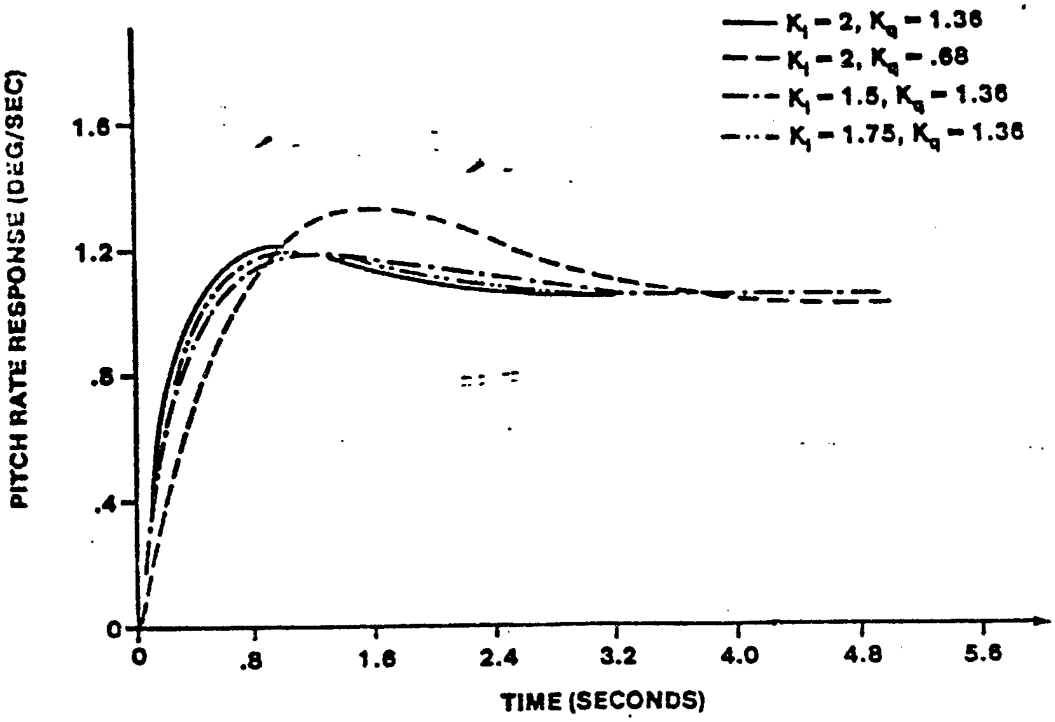

FIGURE 14.115 COMPARISON OF TIME REPONSE FOR UNSTABLE AIRCRAFT, PITCH RATE COMMAND, INTEGRAL PLUS PROPORTIONAL CONTROL

14.6.4 Feedback Compensation

Devices which are used in cascade to reduce steady state error (low pass filters), are not normally used in the feedback path. For example, if a lag filter is used in the feedback path, the aircraft steady state error will be unity.

In the lateral-directional axes, the use of an integrator in the feedback path of a lateral acceleration feedback system will maintain the sideslip angle at zero, a desirable feature in the elimination of unwanted lateral acceleration. The use of integrators in autopilots is common and is usually required to achieve the desired precision.

Low pass filters are used in the feedback path to eliminate unwanted noise while high pass filters can be used to quicken the aircraft response (similar to high pass filters in cascade or as a prefilter), or attenuate lower frequency signals.

14.6.4.1 Low Pass Filters in the Feedback Path

Low pass filters are frequently necessary in feedback paths to eliminate unwanted signal noise due to atmospheric turbulence, sensor dynamics, structural effects or electrical noise. Figure 14.116 presents the effect of the noise filter on the root locus of the angle of attack system discussed in paragraph 14.5.1.1.2 (compare to figure 14.45). The noise filter does not appreciably alter the effect the control system has on the aircraft phugoid characteristics. The short period mode, however, is significantly altered. At a relatively low gain, the damping of the short period is rapidly reduced and, at a lower gain, becomes negative. Figure 14.117 shows the time response of the angle of attack of the aircraft and the shift in the feedback signal caused by the low pass filter. This phase shift causes the instability for higher gains since the error signal which drives the elevator does not represent the order of the closed loop system, which effectively increases the initial lag in the aircraft response. A third effect is to attenuate high frequency angle of attack signals.

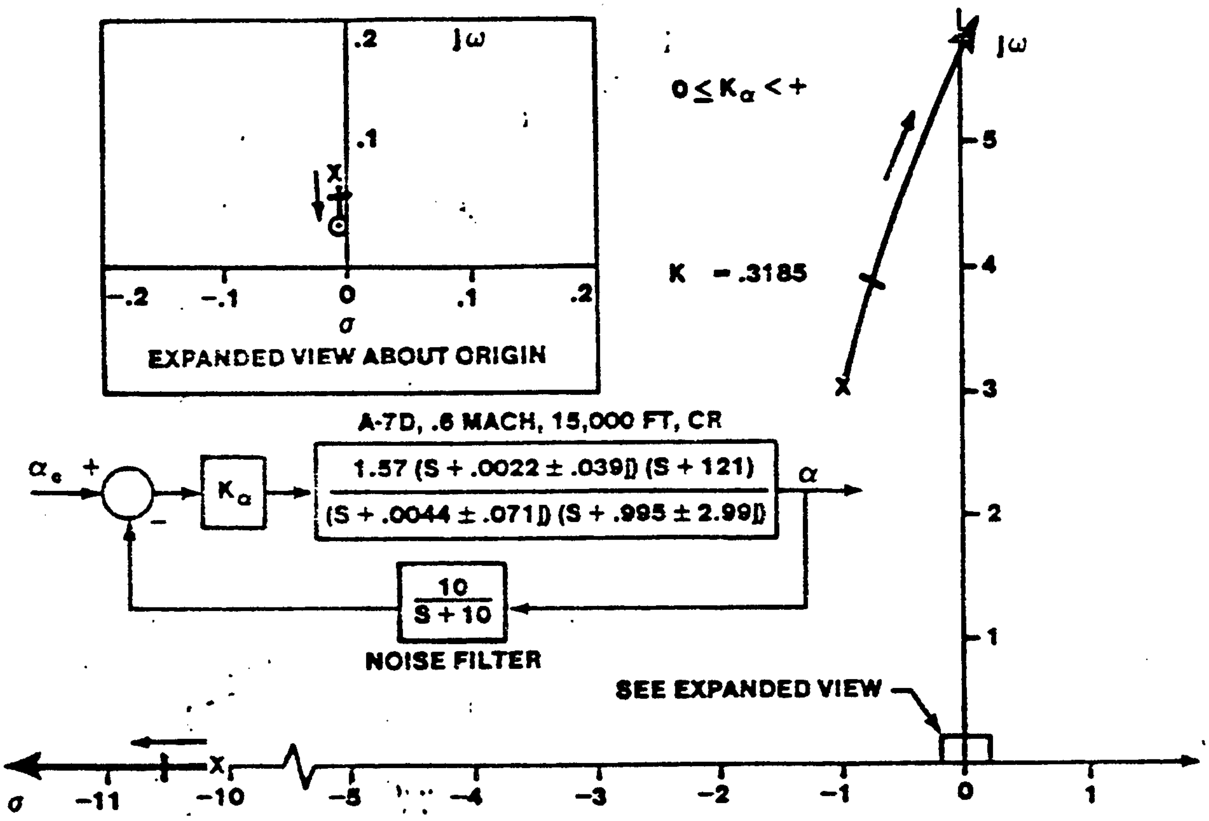

FIGURE 14.116 ROOT LOCUS OF ANGLE OF ATTACK LOOP WITH NOISE FILTER IN THE FEEDBACK PATH

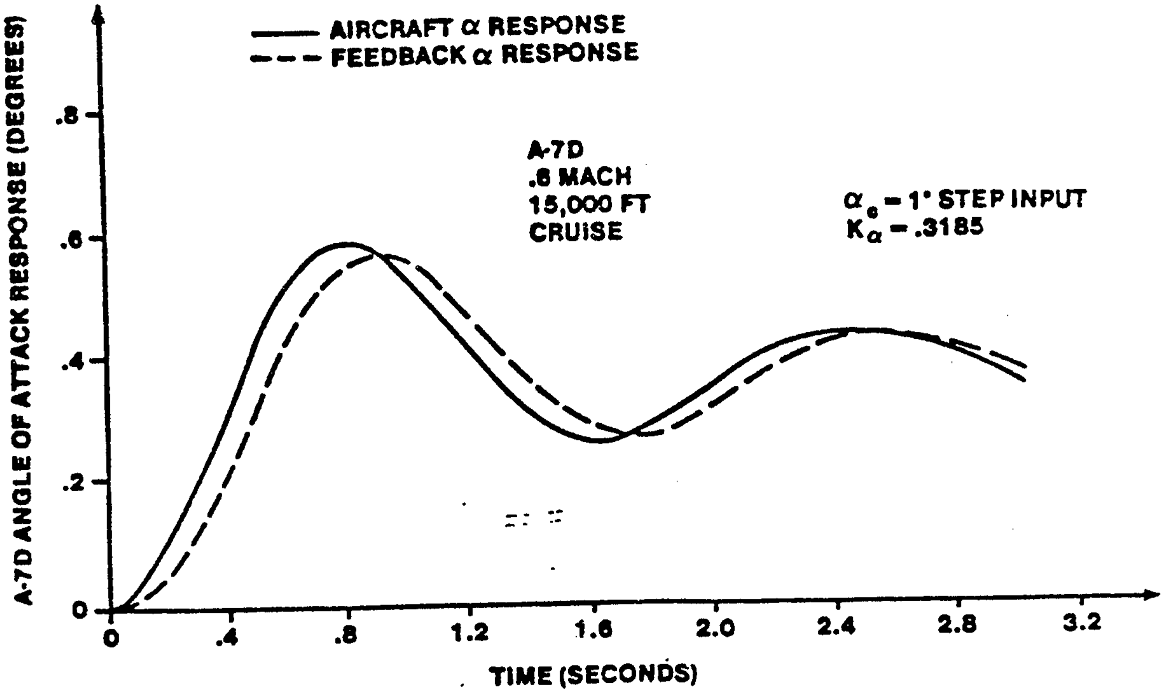

FIGURE 14.117 A-7D ANGLE OF ATTACK RESPONSE OF ANGLE OF ATTACK SYSTEM WITH NOISE FILTER IN FEEDBACK PATH

Noise filters are frequently used on sensors which detect atmospheric turbulence such as angle of attack or sideslip sensors. Another approach is available to provide these signals for control system use -- to computationally derive the signals. This is called a complementary filter approach and is used to provide the flight control system with nearly noise free, turbulence resistant angular and angular rate signals with good high frequency quality for angle of attack or sideslip. This method has been successfully used in the variable stability Learjet and the A-7D Digitac aircraft. The computation scheme used in the A-7D Digitac to provide a high quality angle of attack signal to the directional axis (as part of a computed sideslip rate feedback control law) is shown in figure 14.118.

The angle of attack derivation is based on the normal acceleration equation

$$a_n = U_0 \ (q - \dot{\alpha}) + g \cos \theta \cos \phi \quad \text{(positive up)} \qquad (14.78)$$

where a_n is the acceleration at the center of gravity.

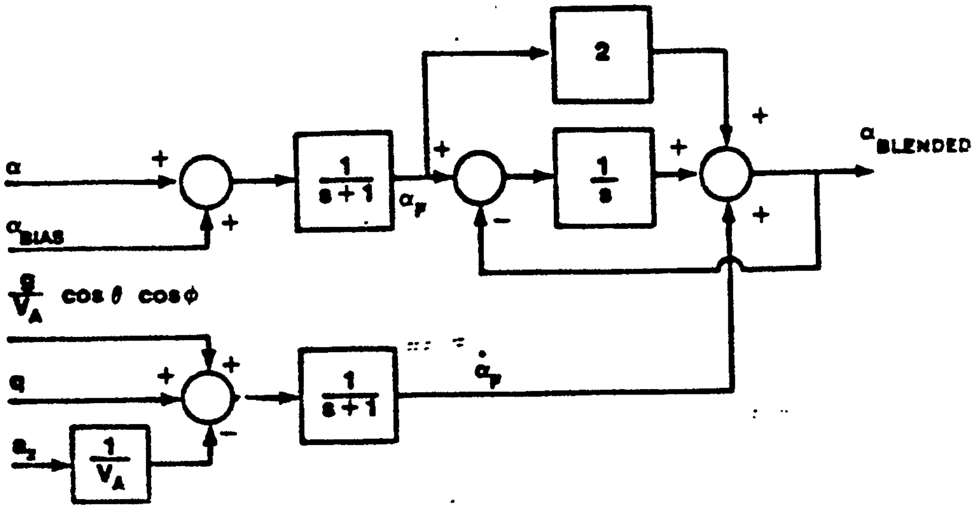

UNITS:
ANGULAR QUANTITIES - RADIANS OR RAD/SEC
ACCELERATIONS - FT/SEC²

NOTE: α_{BIAS} IS A CORRECTION OF REFERENCE TO THE ROLL RATE GYRO PLANE

FIGURE 14.118 ANGLE OF ATTACK COMPLIMENTARY FILTER USED IN THE A-7D DIGITAC

The accelerometer location forward of the center of gravity is neglected since it produces only a small error in the implementation.

The acceleration signal is subtracted from the pitch rate and gravity signals to yield

$$\dot{\alpha} = -\frac{1}{V_A} a_n + q + \frac{g}{V_A} \cos\theta \cos\phi \qquad (U_0 \approx V_A) \qquad (14.79)$$

Neglecting the bias signal, and denoting the signal after the low pass filters as α_F and $\dot{\alpha}_F$ then

$$\alpha_{BLENDED} = \dot{\alpha}_F + 2\alpha_F + \frac{1}{s}(\alpha_F - \alpha_{BLENDED}) \qquad (14.80)$$

or

$$(1 + \frac{1}{s}) \ \alpha_{BLENDED} = (s + 2 + \frac{1}{s}) \ \alpha_F \qquad (14.81)$$

$$\frac{(s + 1)}{s}\,\alpha_{BLENDED} = \frac{(s + 1)^2}{s}\,\alpha_F \qquad (14.82)$$

But

$$\alpha_{BLENDED} = (s + 1)\,\alpha_F = \alpha_F + \dot{\alpha}_F \qquad (14.83)$$

$$\dot{\alpha}_F = \frac{1}{s + 1}\,\dot{\alpha} \qquad (14.84)$$

$$\alpha_F = \frac{1}{s + 1}\,\alpha \qquad (14.85)$$

so that

$$\alpha_{BLENDED} = \frac{1}{s + 1}\,\dot{\alpha} + \frac{1}{s + 1}\,\alpha \qquad (14.86)$$

The angle of attack vane signal provides the low frequency (below 1 radian per second) portion of the signal and the angle of attack rate signal provides the high frequency part of the signal, since

$$\frac{1}{s + 1}\,\dot{\alpha} = \frac{1}{s + 1}\,\alpha \qquad (14.87)$$

Looking at the Bode plot of figure 14.119, it is apparent that high quality

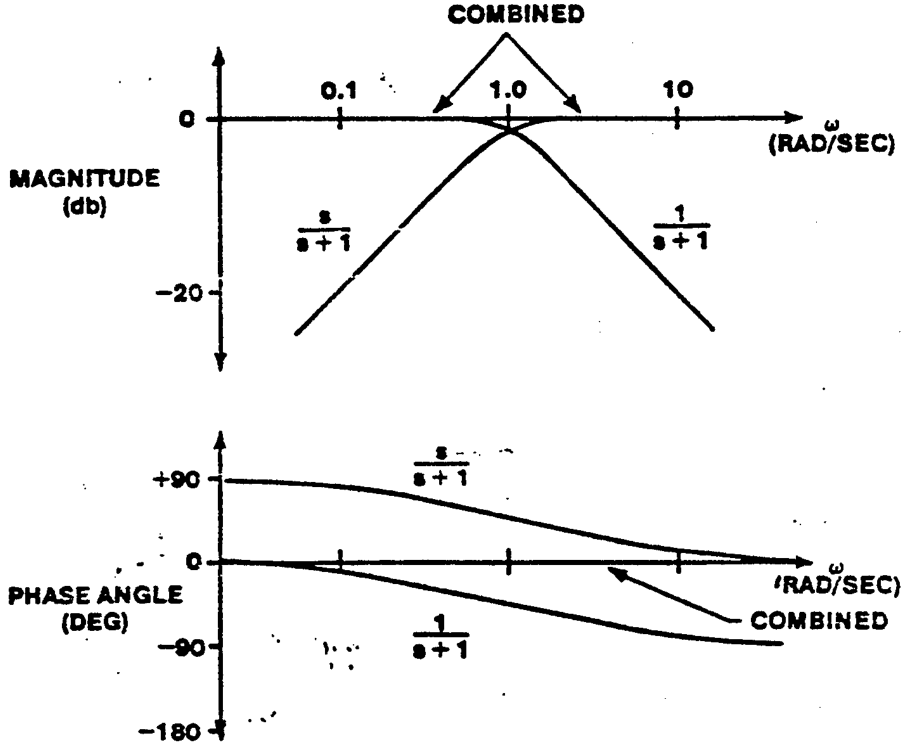

FIGURE 14.119 BODE PLOT FOR ANGLE OF ATTACK COMPLIMENTARY FILTER

angle of attack magnitude information is passed through the filter.

If it is assumed that a signal which is attenuated more than 3 decibels does not contribute to the phase angle, then minimal phase shift is experienced by the output signal across the full spectrum of the angle of attack signal. Complimentary filters have excellent features which are just recently being realized.

14.6.4.2 High Pass Filters in the Feedback Path

Lead compensators are occasionally located in the feedback path and has a similar effect to locating the lead compensator in cascade as shown in the time reponse shown in figure 14.120. The only difference is the proximity of the zero (added to the system by the compensator) to the origin. Note that the response after several seconds is essentially exponential in character. The zero added by the feedback compensator is remote from the origin and the reponse is essentially exponential near the origin. The system is more sluggish than the original system. The cascade compensator zero is much closer to the origin and nearly cancels the exponential response due to the dominant low frequency real root, causing a more abrupt response. The

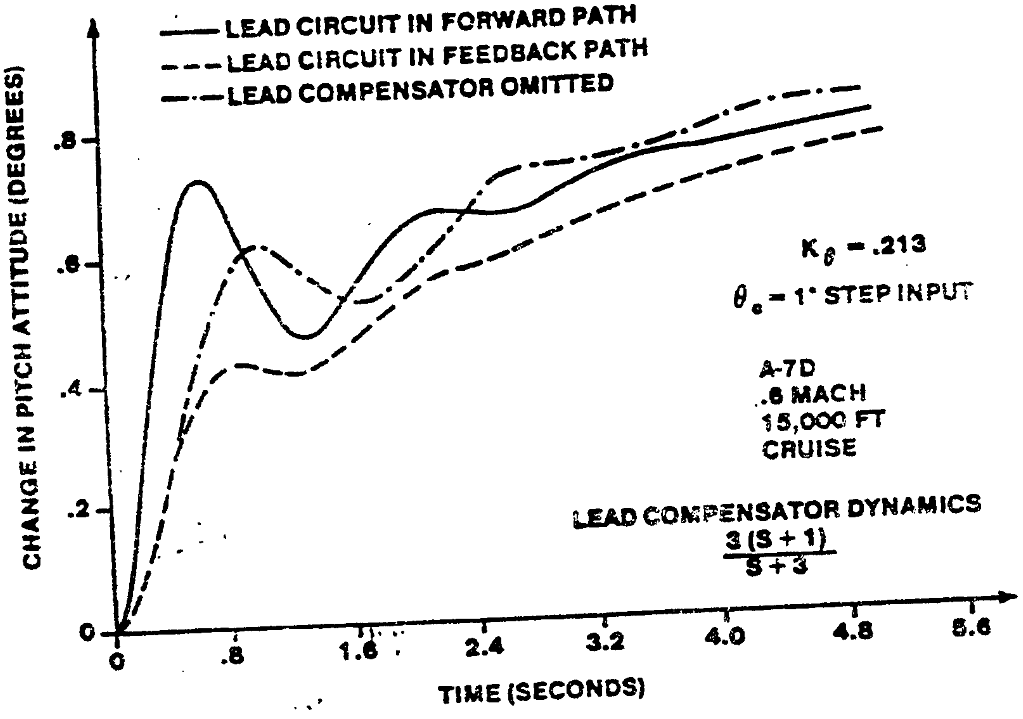

FIGURE 14.120 A-7D PITCH ATTITUDE REPONSE WITH LEAD COMPENSATOR

damping of both compensated systems is higher than the damping of the uncompensated system with the same period. The zero in the cascade compensator reduces the effective damping by causing the initial response overshoot.

A washout filter is very common in the feedback path of yaw damper systems. During a steady state level turn, a steady yaw rate is present. Since the aircraft is in a bank

$$r = \dot{\psi} \cos \phi \tag{14.88}$$

where $\dot{\psi}$ is the heading rate and ϕ is the bank angle. The yaw rate gyro feeds this signal back to the rudder to try to deflect the rudder to oppose the turn. Without a washout filter, a constant rudder deflection would occur which would try to roll the aircraft wings level. This wings level tendency in swept wing aircraft is caused by large sideslip due to rudder deflection and is undesirable during turns. The washout filter prevents the residual rudder deflection during the turn while providing Dutch roll damping during rolling maneuvers.

The s in the numerator represents a differentiation. Therefore, the filter passes only the derivative of the incoming signal, which is zero for a constant amplitude signal. Figure 14.121 shows the washout filter in a pitch rate damper has little effect on the root locus of the pitch rate augmented aircraft. If the pole of the filter were located such that $s < -1.09$, the effect would be slight. If, however, the pole were located where $s << -1.09$, the filter would nearly negate the effect of the feedback since it would pass only very high frequency signals. Figure 14.122 shows the pitch rate response of the pitch damper augmented aircraft to a step pitch rate command. Figure 14.123 shows the output of the washout filter, which goes to zero after a short time.

The use of a washout filter in a command or forward path is inadvisable. The command signal degrades to zero after a short time. For the pitch rate damper, for instance, if a washout filter were added to the command path and the pilot tried to maintain a constant aircraft pitch rate, he would be required to apply a constantly increasing stick force to maintain the rate.

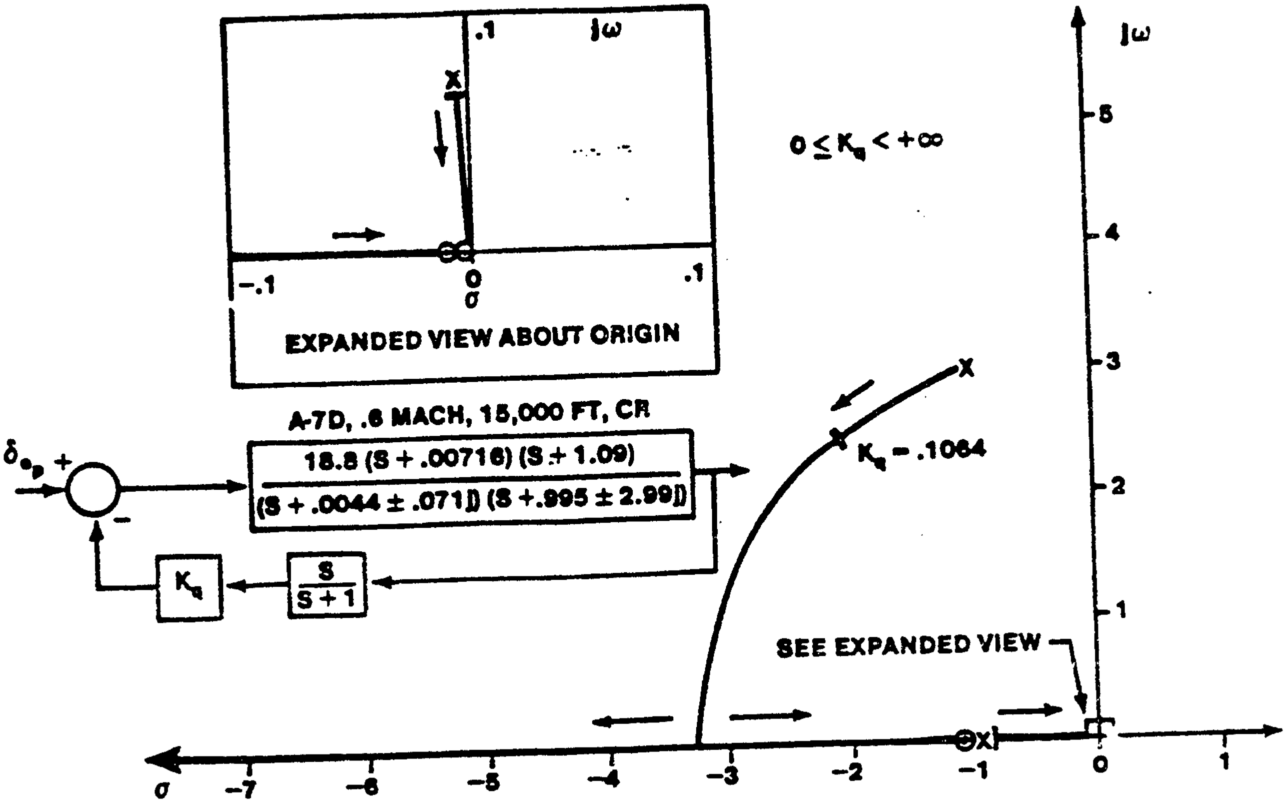
jω
.1
X
−.1
0
σ
.1
EXPANDED VIEW ABOUT ORIGIN
0 ≤ K_q < +∞
A-7D, .6 MACH, 15,000 FT, CR
δ_ep
+
−
18.8 (S + .00716) (S + 1.09)
(S + .0044 ± .071j) (S + .995 ± 2.99j)
K_q
S
S + 1
X
K_q = .1064
SEE EXPANDED VIEW
5
4
3
2
1
σ
−7
−6
−5
−4
−3
−2
−1
0
1

FIGURE 14.121 ROOT LOCUS OF PITCH DAMPER WITH WASHOUT FILTER

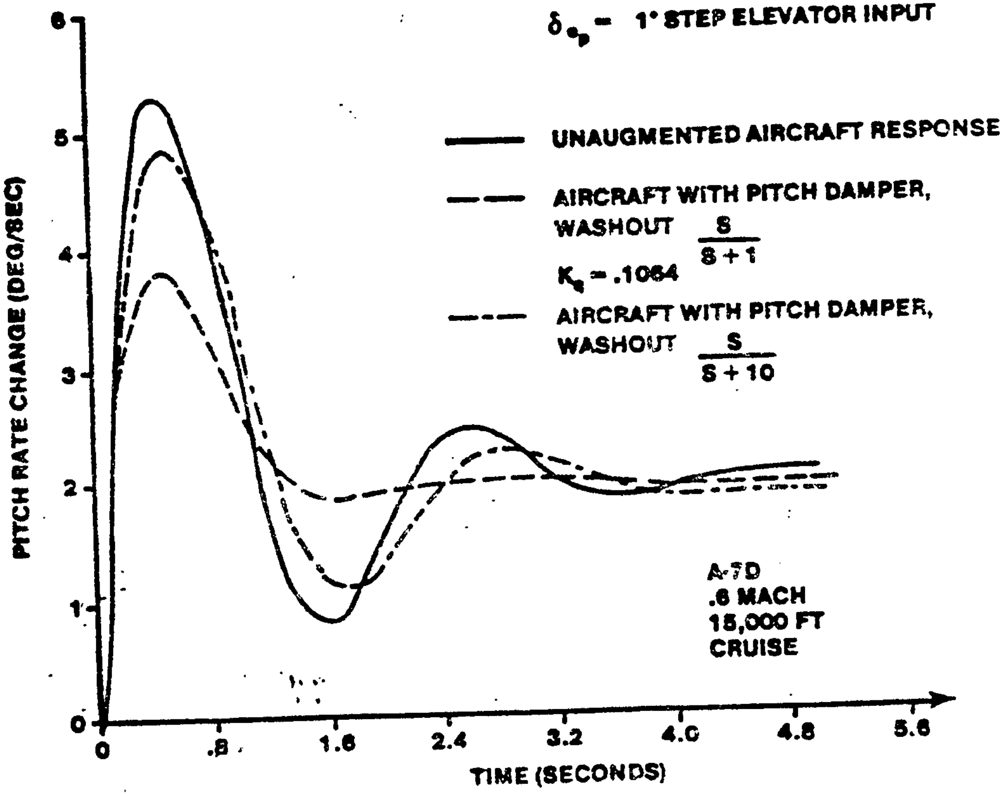

FIGURE 14.122 COMPARISON OF PITCH RATE RESPONSE

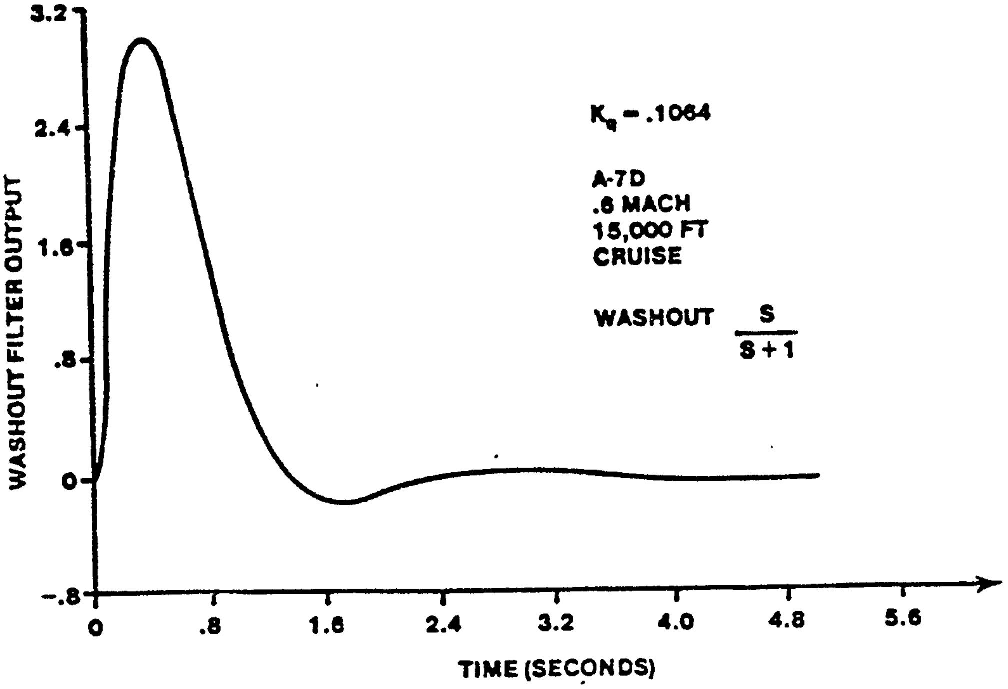

FIGURE 14.123 PITCH DAMPER WASHOUT FILTER OUTPUT TIME RESPONSE

When the pilot reached a force or deflection limit in the feel system the aircraft pitch rate would go to zero and the pilot could no longer pitch the aircraft.

14.7 BASIC AUTOMATIC FLIGHT CONTROL SYSTEMS

During many flight conditions, pilots are very busy carrying out a large variety of tasks. To reduce pilot workload it has been found desirable to provide the pilot with automatic flight control systems. With the automatic flight control systems engaged the pilot needs only to monitor the autopilot operation and is free to perform other tasks.

Autopilots must provide stable roots for all the dynamic modes of the aircraft. In addition, the steady state errors for the controlled variables (such as altitude, pitch attitude or bank angle) must be zero. In this section the basic relief modes (pitch attitude, altitude, bank angle, heading and airspeed hold modes) and navigation mode (lateral beam intercept and hold mode) are discussed. The more sophisticated automated maneuvering systems are covered in section 14.11.

14.7.1 Pitch Attitude Hold

Pitch attitude feedback was seen in section 14.5.1.1.3.1 to be a method of establishing a pitch attitude command system. This is the obvious method of establishing a pitch attitude hold system (with the pitch attitude command θ_c coming from the autopilot system and set by the pilot). This scheme has the disadvantage of a reduction in short period damping. Pitch rate feedback has the advantages of increased short period damping and no effect on the phugoid mode as shown in section 14.5.1.1.1.1.

The typical pitch attitude hold autopilot is, therefore, a multiple loop system with pitch rate feedback as an inner loop and pitch attitude feedback in the outer loop as shown in figure 14.124.

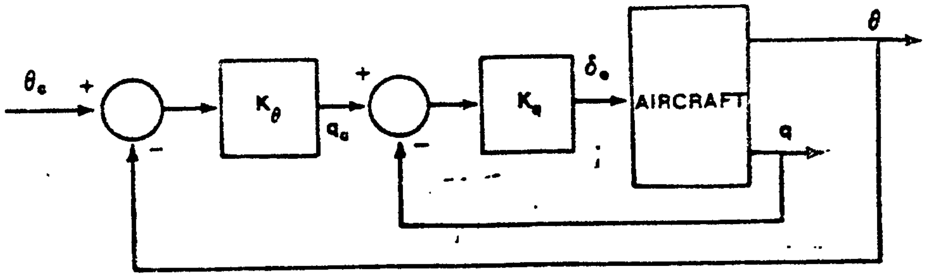

FIGURE 14.124 MULTIPLE LOOP PITCH ATTITUDE HOLD SYSTEM

The composite root locus plot of figure 14.125 clearly shows the advantages of the multiple loop approach over both the single loop approaches for a typical autopilot application. The inner pitch rate loop increases the damping of the short period while not significantly altering the phugoid roots. The pitch attitude outer loop suppresses the phugoid roots. The combined effect yields improved short period damping and well suppressed phugoid motion.

Although this example is for an aircraft that exhibits classical aircraft properties, similar effects can be achieved in the presence of the unstable roots characteristic of the Mach tuck, an aft center of gravity or VTOL transition flight.

This multiple loop pitch attitude hold system is typical of most simple autopilots. Autopilots usually use an angular rate feedback as an inner loop to provide increased damping to the short period or Dutch roll mode and attitude feedback for comparison to the desired reference attitude as an outer loop. The following section will present a detailed analysis of a simple

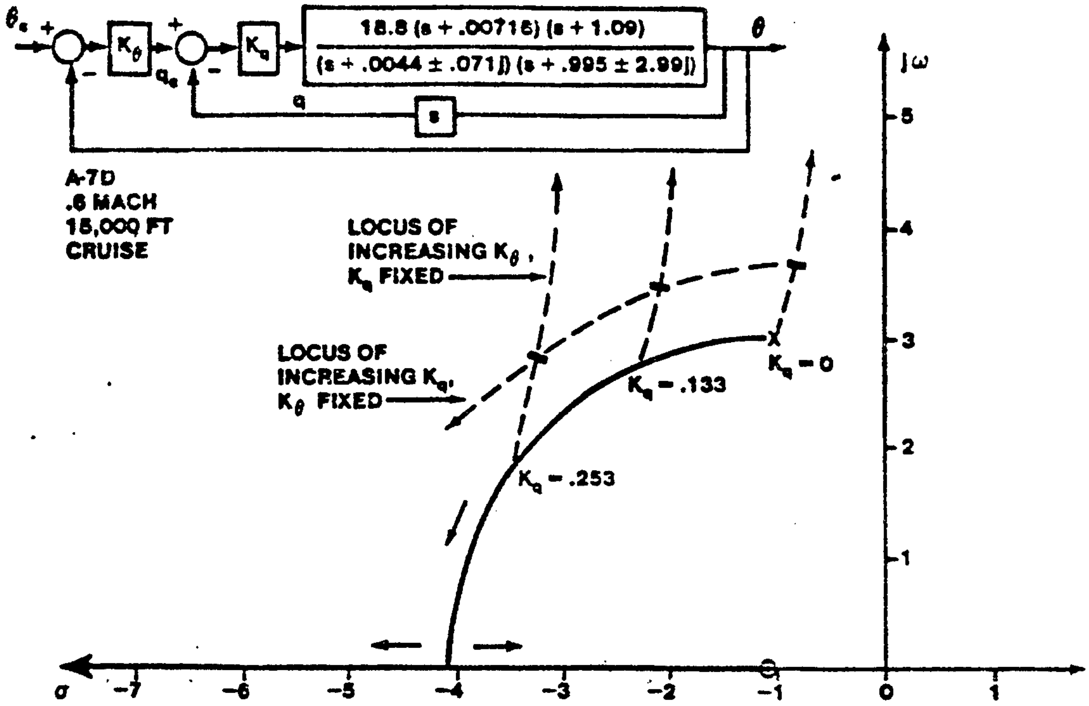

FIGURE 14.125 PITCH RATE AND PITCH ATTITUDE FEEDBACK ROOT LOCUS

pitch attitude hold system. This will be followed by a discussion of methods used to determine the pilot selected reference altitude.

14.7.1.1 Analysis of a Simple Pitch Attitude Hold System

Figure 14.126 presents the pitch attitude hold control system to be analyzed in this section. The block diagram presented, however, is not in a clear format for analysis. It is desirable to reformulate the block diagram to clearly show the multiple loop nature of the system. Figure 14.127 shows

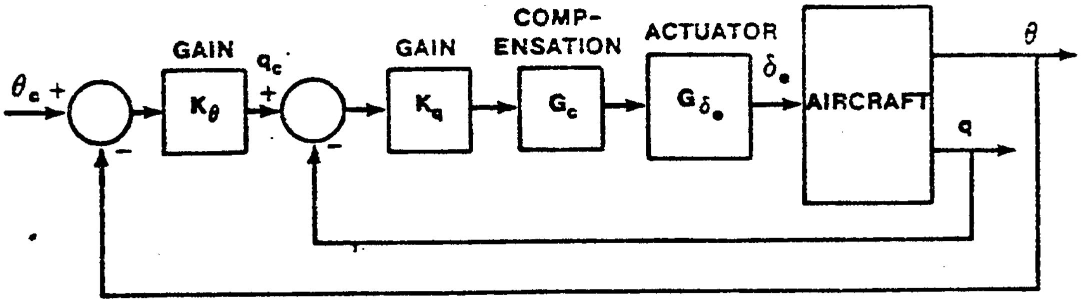
θ_c
+
−
GAIN
K_θ
q_c
+
−
GAIN
K_q
COMPENSATION
G_c
ACTUATOR
G_{δ_e}
δ_e
AIRCRAFT
θ
q

FIGURE 14.126 PITCH ATTITUDE HOLD CONTROL SYSTEM

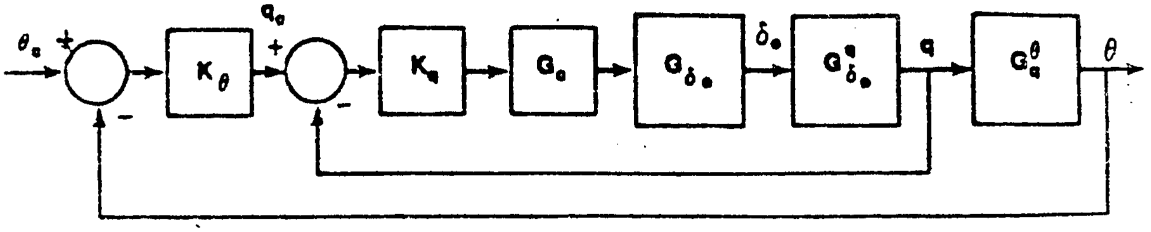

FIGURE 14.127 REFORMULATED PITCH ATTITUDE HOLD CONTROL SYSTEM

the reformulated block diagram. The transfer function relating the pitch attitude to the pitch rate can be found by

$$G^\theta_q(s) = \frac{G^\theta_{\delta_e}(s)}{G^q_{\delta_e}(s)} \tag{14.89}$$

This can be simplified by noting that the denominator of the transfer functions relating θ or q to δ_e is the longitudinal characteristic equation (Δ). This means that the transfer function can be simplfied to the ratio of the two transfer function numerators

$$G^\theta_q(s) = \frac{N^\theta_{\delta_e}(s)}{N^q_{\delta_e}(s)} \tag{14.90}$$

For this case

$$G^\theta_q(s) = \frac{1}{s} \tag{14.91}$$

The block diagram is now in a form which readily lends itself to multiple loop analysis which would proceed as follows.

First, the root locus of the inner pitch rate loop open loop transfer function

$$GH_{q\ \mathrm{loop}} = K_q G_c G_{\delta_e} G^q_{\delta_e} \tag{14.92}$$

is plotted. The pitch rate augmented aircraft roots are then determined from the root locus by selecting a value of K_q which meets the desired pitch rate in terms of response time and damping ratio. The pitch rate augmented aircraft transfer function (inner loop closed) is

$$G^q_{q_c}\Big|_{q\ AUG} = \frac{K_q K_{\delta_e} N_c N^q_{\delta_e}}{\Delta_{q\ AUG}} \tag{14.93}$$

where $\Delta_{q\ AUG}$ is the characteristic equation of the inner loop containing the characteristic roots of the inner loop augmented aircraft determined from the root locus analysis. The block diagram can then be simplified as shown in Figure 14.128.

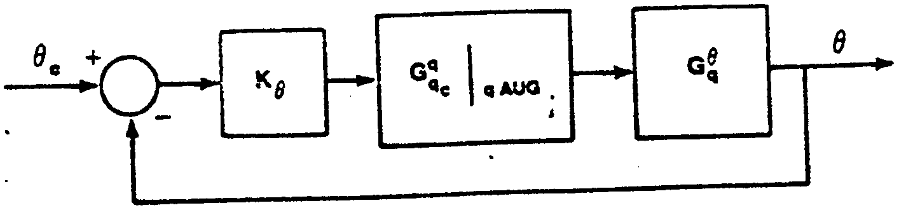

FIGURE 14.128. SIMPLIFIED PITCH ATTITIUDE CONTROL SYSTEM

The outer loop can now be analyzed by forming the open loop transfer function for the attitude hold system augmented aircraft

$$GH_{\theta\ loop} = K_\theta G^\theta_q G^q_{q_c}\Big|_{q\ AUG} \tag{14.94}$$

and plotting the root locus. The closed loop transfer function for the attitude hold system augmented aircraft becomes

$$G^\theta_{\theta_c}\Big|_{q,\theta\ AUG} = \frac{K_\theta N^\theta_q N^q_{q_c}\Big|_{q\ AUG}}{\Delta_{q,\theta\ AUG}} \tag{14.95}$$

where $\Delta_{q,\theta\ AUG}$ are the augmented aircraft characteristic roots with both the pitch and pitch rate feedback loops closed.

This method of analysis can now be used to determine the characteristics of an example pitch attitude autopilot. Figure 14.129 presents a block diagram for a proposed pitch autopilot for the AV-8A Harrier VTOL aircraft. Notice that the cascade compensation consists of a high pass filter (lead compensator) which provides a quicker system response and a low pass fliter (integral plus proportional controller) which eliminates the steady state error in pitch attitude (see section 14.6.1).

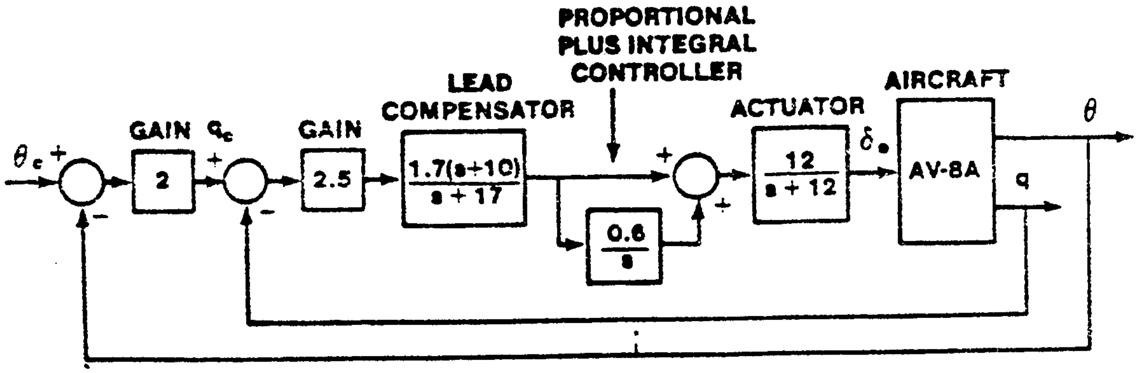
PROPORTIONAL PLUS INTEGRAL CONTROLLER
LEAD COMPENSATOR
AIRCRAFT
ACTUATOR
GAIN
GAIN
q_c
θ_c
+
−
2
+
−
2.5
$\frac{1.7(s+10)}{s+17}$
+
+
$\frac{0.6}{s}$
$\frac{12}{s+12}$
δ_e
AV-8A
θ
q

UNITS: θ_c **DEGREES**
θ **DEGREES**
q_c **DEG/SEC**
q **DEG/SEC**

FIGURE 14.129. PROPOSED PITCH ATTITUDE HOLD SYSTEM FOR THE AV-8A HARRIER FOR THE TRANSITION FLIGHT PHASE

The aircraft transfer function (160 KTAS, sea level, zero engine nozzle angle) is

$$G^{\theta}_{\delta_e}(s) = \frac{6.59\ (s+0.65)\ (s+0.521)}{(s+0.203))\ (s+1.69)\ (2-0.123 \pm 0.364j)}\ (\text{deg/deg}) \quad (14.96)$$

Figure 14.130 shows the block diagram reconfigured for analysis.

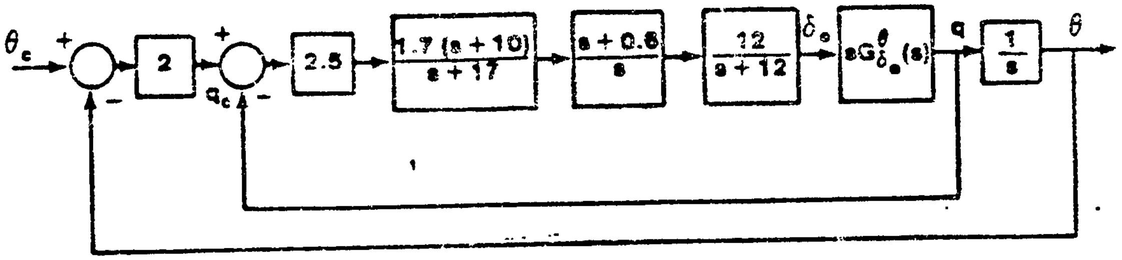
θ_c
+
−
2
+
q_c
−
2.5
$\frac{1.7(s+10)}{s+17}$
$\frac{s+0.6}{s}$
$\frac{12}{s+12}$
δ_e
$sG^{\theta}_{\delta_e}(s)$
q
$\frac{1}{s}$
θ

FIGURE 14.130. REFORMULATED PITCH ATTITUDE HOLD SYSTEM FOR TH AV-8A HARRIER

The inner pitch rate feedback loop is analyzed first. This loop will stabilize the unstable oscillatory root pair of the unaugmented aircraft. The open loop transfer function for the inner loop is formed as

$$GH_{q\ \text{loop}} = \frac{+6.59(2.5)(1.7)(12)\ s\ (s + 0.065)(s + 0.521)(S + 10)(s + 0.6)}{s\ (s + 0.203)(s + 1.69)(s - 0.123 \pm 0.364j)(s + 17)(s + 12)} \quad (14.97)$$

Figure 14.131 presents the root locus plot for the pitch rate feedback loop. The closed loop transfer function characteristic roots corresponding to the design system gain of K_q = 336.09 are found from the root locus analysis. The closed loop transfer function (for the inner loop) zeros are the zeros

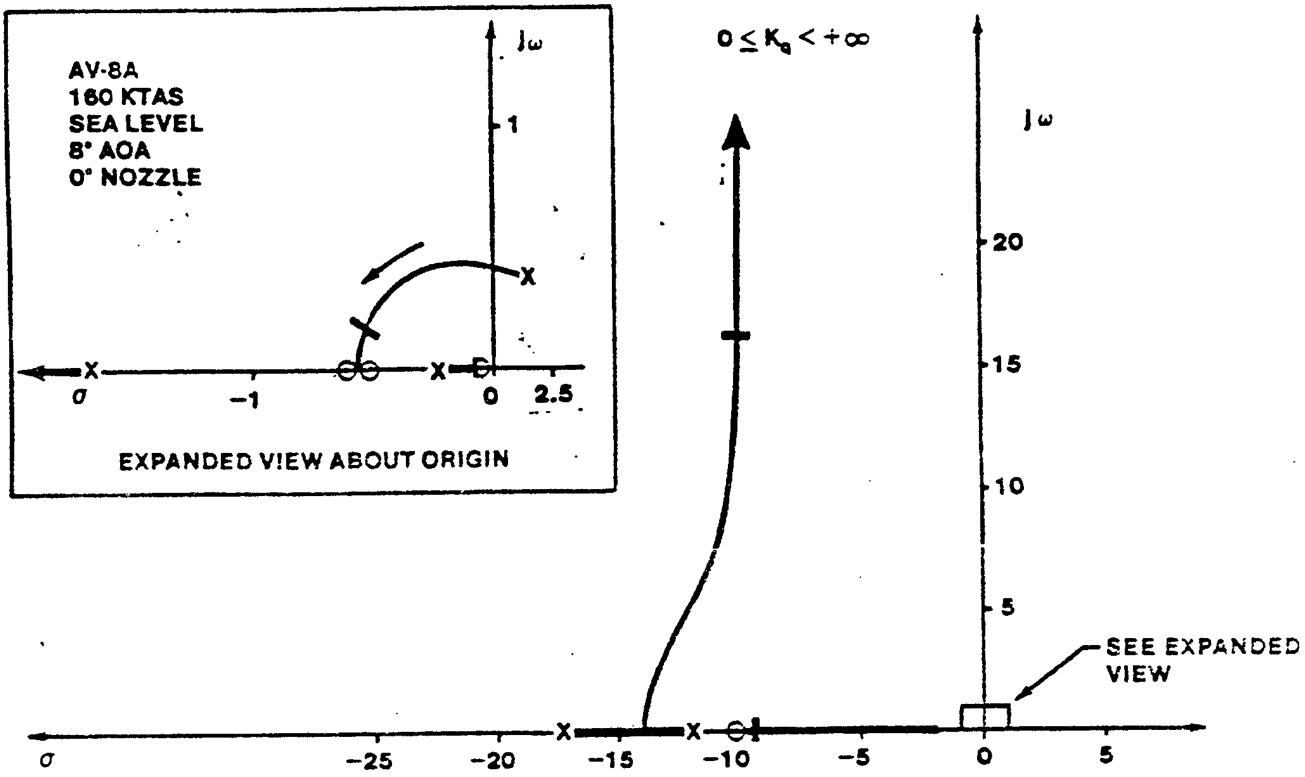

FIGURE 14.131. ROOT LOCUS PLOT FOR PITCH RATE LOOP OF PROPOSED AV-8A ATTITUDE AUTOPILOT

appearing in the forward path of the loop. No other zeros are introduced since no feedback elements exist. The gain of the closed loop transfer function is also found from the forward elements. The closed loop transfer function for the inner loop is

$$G_{q_c}^{q}(s) = \frac{336.09(s + 0.065)\ (s + 0.521)\ (s + 0.6)\ (s + 10)}{(s + 0.074)\ (s + 0.53 \pm 0.165j)\ (s + 9.5)\ (s + 10.0 \pm 16.24j)} \quad (14.98)$$

The inner loop is now replaced by a single block formed by the closed loop transfer function of the inner loop (Figure 14.132).

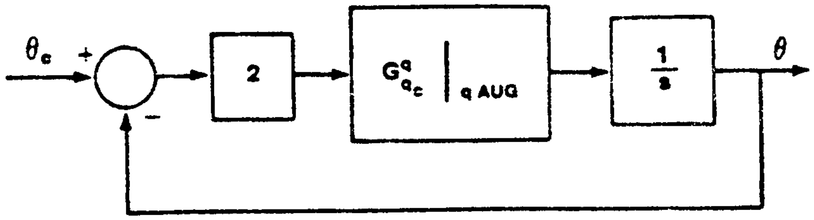

FIGURE 14.132. SIMPLIFIED AV-8A PITCH ATTITUDE HOLD SYSTEM

The open loop transfer function for the outer loop is

$$GH_{\Theta\ loop} = \frac{2}{s}\, G_{q_c}^{q}\ (s)$$

The root locus as K_Θ varies is plotted in Figure 14.133 and the roots for the designed gain of K_Θ = 672.18 are plotted. The closed loop transfer function for the pitch attitude hold system is

$$G_{\Theta_c}^{\Theta}(s) = \frac{672.18\ (s + 0.065)\ (s + 0.521)\ (s + 0.6)\ (s + 10)}{(s+0.065)\ (s+0.71)\ (s+0.47)\ (s+2.09)\ (s+9.32)\ (s+9.0 \pm 15.66j)} \quad (14.99)$$

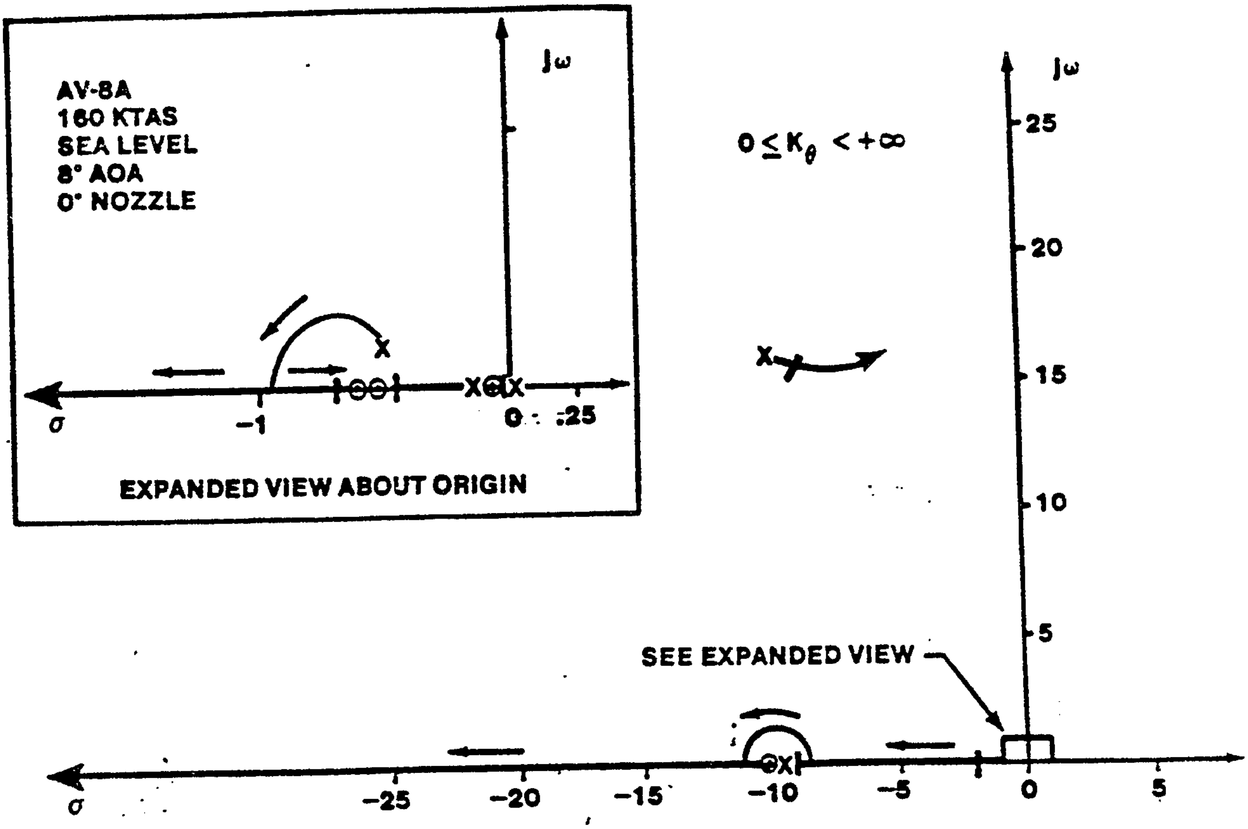
AV-8A
160 KTAS
SEA LEVEL
8° AOA
0° NOZZLE
jω
σ
−1
0
.25
EXPANDED VIEW ABOUT ORIGIN
$0 \leq K_\theta < +\infty$
jω
25
20
15
10
5
SEE EXPANDED VIEW
σ
−25
−20
−15
−10
−5
0
5

FIGURE 14.133. ROOT LOCUS PLOT FOR PITCH ATTITUDE LOOP OF PROPOSED AV-8A ATTITUDE AUTOPILOT

The final value of this system for a unit step pitch attitude change is $\Theta_{ss} = 1°$ which shows that a zero steady-state error exists (as expected for a type 1 system). Notice that all the roots except for the root near $s = -2.1$ and the high frequency roots near $s = -9.0 \pm 15.66j$ are in fairly close proximity to zeros. This implies that they are suppressed and that the dominant root in the aircraft response is $s = -2.1$. The time response of the aircraft to a step input can therefore be closely approximated as $\Theta(t) = 1 - e^{-2.1t}$ as shown in Figure 14.134, where the approximate and the actual responses are compared.

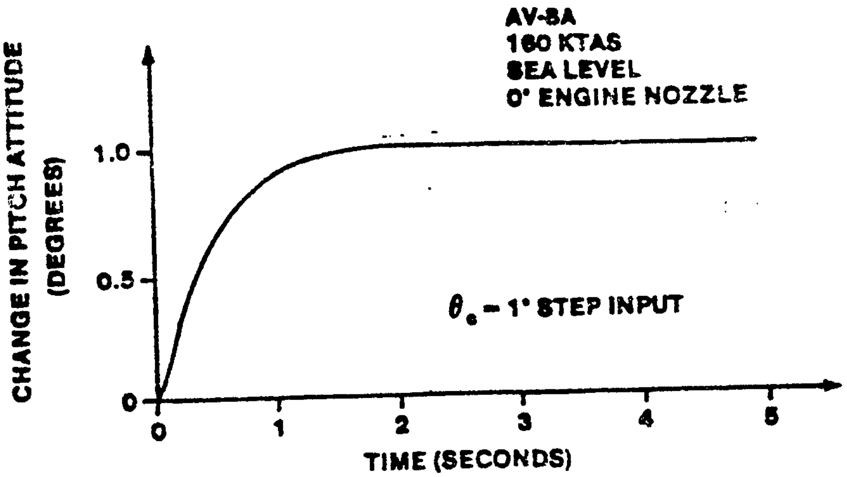

(a). ACTUAL AIRCRAFT RESPONSE

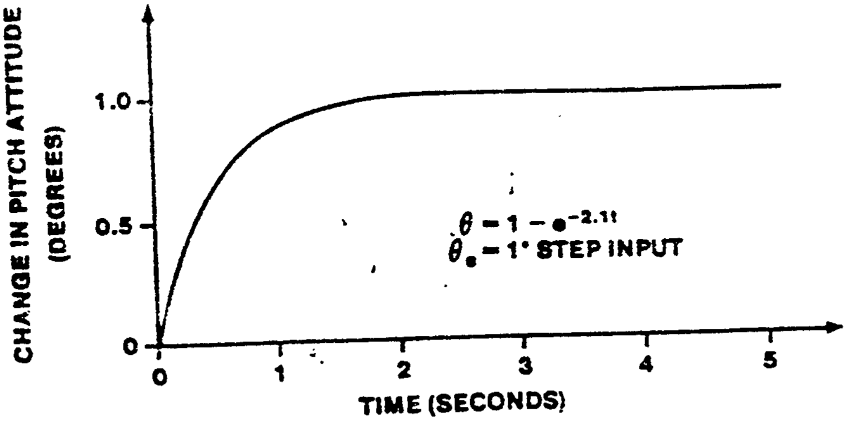

(b). APPROXIMATE AIRCRAFT RESPONSE

FIGURE 14.134. COMPARISON OF ACTUAL AND APPROXIMATE AV-8A PITCH ATTITUDE RESPONSES

14.7.1.2 Determining Pilot Reference Pitch Attitude

Autopilots are often arranged to disengage automatically when the pilot tries to override it (see section 14.7.7 on pilot blending). If this is the case, then some method of resetting the integral output of the proportional plus integral controller (low pass filter) is required. This requirement can be explained as follows. Assume that the reference attitude (Θ_{ref}) is set for 2 degrees. Now suppose the pilot has to make a sudden attitude correction which causes the autopilot to disengage. Assume that as a result of the correction the airplane attitude has changed to $\Theta = -3$ degrees. If the pilot at this point decides to reengage the attitude hold mode, the autopilot would probably try to drive the elevator to the limit of its assigned autopilot authority because of the integrator output. Figure 14.135 shows such an integral plus proportional controller in the feedback path of a pitch attitude hold system (an alternative location then in cascade). Notice that an integrator output canceller circuit is included which acts to reduce the integrator output value to zero when the attitude hold mode in disengaged. In this way there would not be a sudden transient if the attitude hold mode were reengaged.

Notice that this circuit includes a switch that disconnects the Θ feedback path when the pitch attitude hold mode in disengaged. The pilot then commands pitch rate.

Some device must be available in the pitch attitude hold system to remember the pilot selected pitch attitude. This is the purpose of the second integrator. When the pilot supplies enough force to engage the switch (or the pitch attitude hold system is off), the integrator output attempts to match the attitude of the aircraft. The speed at which the integrator output matches the aircraft attitude depends on the integrator gain, which is normally high. When the pilot releases the stick and engages pitch attitude hold, the switch in the integrator path opens and the integrator maintains the last output (desired attitude) prior to the switch opening. Any deviations from this attitude result in a pitch rate command. The integrator is used, therefore, as a memory device.

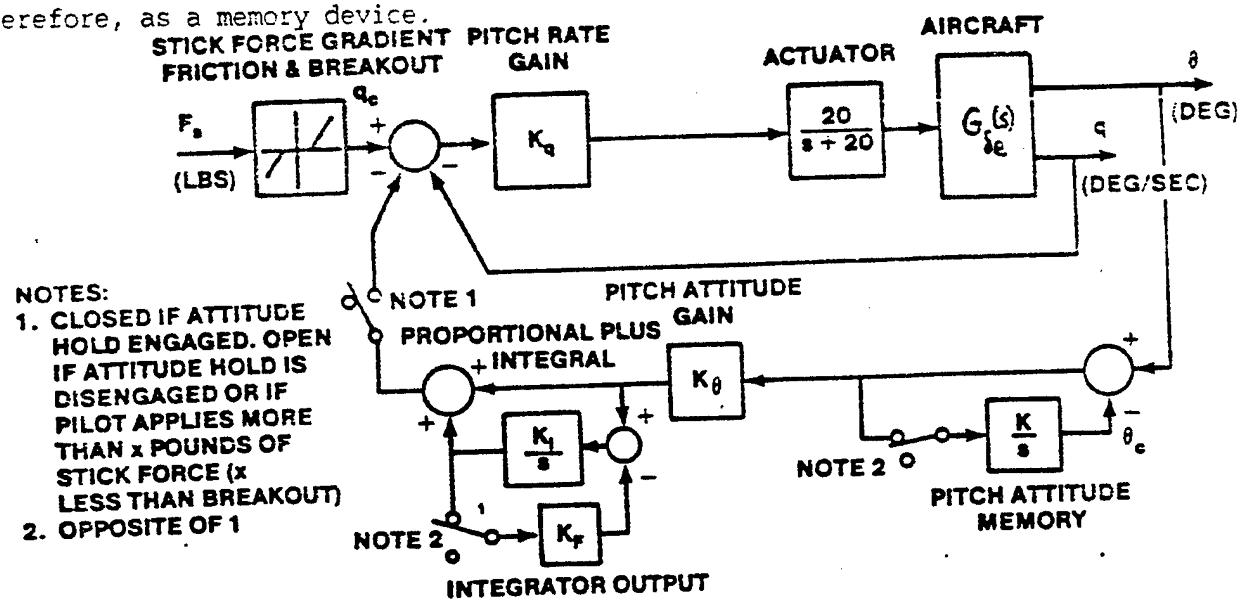
STICK FORCE GRADIENT
FRICTION & BREAKOUT
PITCH RATE
GAIN
ACTUATOR
AIRCRAFT
F_s
(LBS)
q_c
+
−
−
K_q
$\frac{20}{s+20}$
$G_{\delta e}^{\theta}(s)$
θ
(DEG)
q
(DEG/SEC)
NOTES:
1. CLOSED IF ATTITUDE HOLD ENGAGED. OPEN IF ATTITUDE HOLD IS DISENGAGED OR IF PILOT APPLIES MORE THAN x POUNDS OF STICK FORCE (x LESS THAN BREAKOUT)
2. OPPOSITE OF 1
NOTE 1
PITCH ATTITUDE
GAIN
PROPORTIONAL PLUS
INTEGRAL
+
+
+
−
K_θ
$\frac{K_I}{s}$
K_F
1
NOTE 2
0
NOTE 2
$\frac{K}{s}$
+
−
θ_c
PITCH ATTITUDE
MEMORY
INTEGRATOR OUTPUT
CANCELLER

FIGURE 14.135. PITCH ATTITUDE HOLD SYSTEM CONFIGURATION

This same circuit can be used to allow pilot blending if pilot inputs to the stick are used to interrupt rather then disengage the autopilot. The pilot could then reset the reference attitude by moving the aircraft to the desired attitude, with the pitch attitude hold system engaged, and releasing the stick. The system would then automatically hold the new altitude. Pilot blending is discussed more extensively in Section 14.7.7.

The use of devices to remember autopilot commanded attitudes, altitudes, etc., as well as devices to ensure zero steady state error and eliminate engagement/disengagement errors or transients are fundamental parts of all autopilot systems. These are what distinguishes an autopilot from other similar feedback systems that are designed to stabilize the aircraft for improved piloted handling qualities. The following sections discuss other simple autopilot systems and, while these devices are not explicitly mentioned they are always implied.

14.7.2 Altitude Hold

The fundamental part of an altitude hold autpilot is the feedback of altitude to the elevator. The transfer function relating altitude to the elevator deflection can be determined for small perturbation from straight and level flight using figure 14.136. It can be seen from this diagram that the vertical velocity of the aircraft is

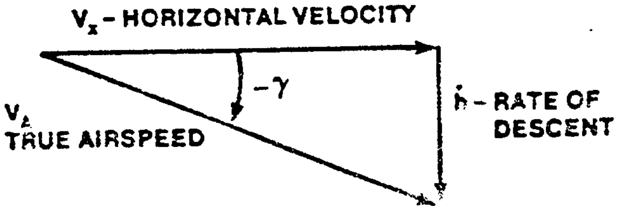

FIGURE 14.136. GEOMETRY FOR ALTITUDE RATE DETERMINATION

$$\dot{h} = V_A \sin \gamma = V_A \sin (\theta - \alpha) \qquad (14.100)$$

using the small angle approximation

$$\dot{h} \approx V_A (\theta - \alpha) \approx U_0 (\theta - \alpha) \qquad (14.101)$$

If the Laplace transform is taken of this equation and it is divided by elevator deflection, the transfer function relating the aircraft altitude to an elevator command becomes

$$\frac{h(s)}{\delta_e(s)} = \frac{U_0}{s}\left(\frac{\theta(s)}{\delta_e(s)} - \frac{\alpha(s)}{\delta_e(s)}\right) \tag{14.102}$$

Because of the free s, the feedback of altitude to the elevator by itself drives the modified phugoid roots into the right half s-plane at very low gains, as can be seen in Figure 14.136. Because altitude control is a long term (navigational) requirement, the phugoid must be stabilized.

A major problem also occurs when the aircraft is on the back side of the thrust required versus airspeed curve. Flight in this regime is accomplished during some approaches to landing (carrier approaches, minimum run landings, and normal landings for some aircraft) or during steep climbs. When on the back side of the power curve, the zero near the origin in Figure 14.137 is in the right half s-plane, causing the pole at the origin to be driven unstable for all closed loop system gains. In principle, the peak of the thrust required curve could be determined and the sign of the gain changed to avoid divergence, but this would cause the phugoid roots to become unstable at very low gain. Altitude control using altitude feedback alone cannot be achieved for flight conditions near the performance reversal airspeed.

Several multiloop system configurations provide possibilities to overcome this instability. A common approach is to feed back altitude as an outer loop parameter with an inner attitude hold loop engaged. Another approach is to feed back a combination of altitude and altitude rate signals. Sensing the rate of climb or descent directly is difficult without excessive lag in the sensor. An alternate method of determining the rate of climb or descent is to compute the signal, using true airspeed from the air data system, pitch angle from the attitude reference system, and angle of attack from the AOA sensor.

As can be seen from Figure 14.138, the inner altitude rate loop has the effect of moving the altitude low frequency roots from the right half well into the left half s-plane. The short period damping has decreased, however.

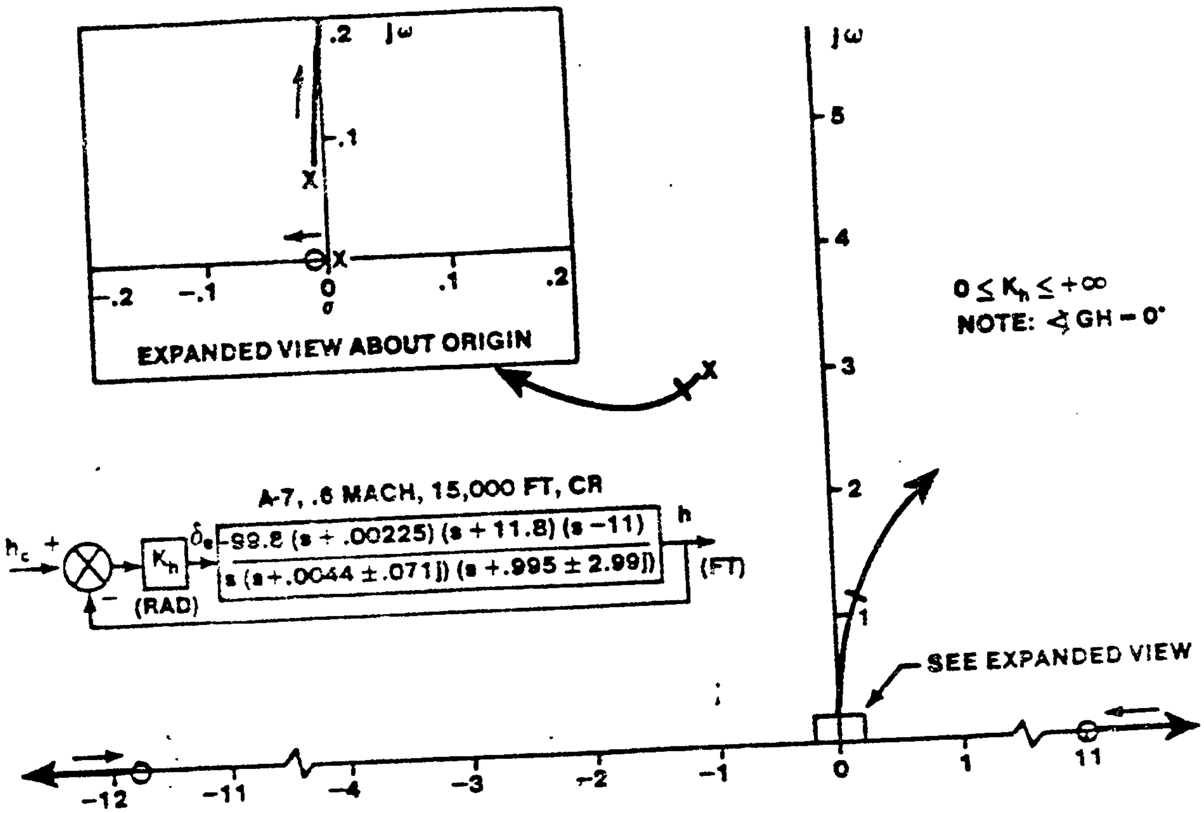

FIGURE 14.137. ROOT LOCUS PLOT OF ALTITUDE HOLD LOOP FOR AN AIRCRAFT WITH GOOD DYNAMICS

Another alternative is to feed back the altitude deviation to a pitch attitude hold system. This can be seen from the following discussion. If altitude rate is computed as

$$\dot{h} = V_A \ (\theta - \alpha) \qquad (14.101)$$

then the perturbed altitude rate becomes

$$\dot{h} = u(\theta_0 - \alpha_0) + U_0 (\theta - \alpha) \qquad (14.103)$$

If the airspeed perturbation is assumed small and the angle of attack is assumed nearly constant (as in the phugoid mode), such that

$$u = 0 \text{ and } \alpha = 0$$

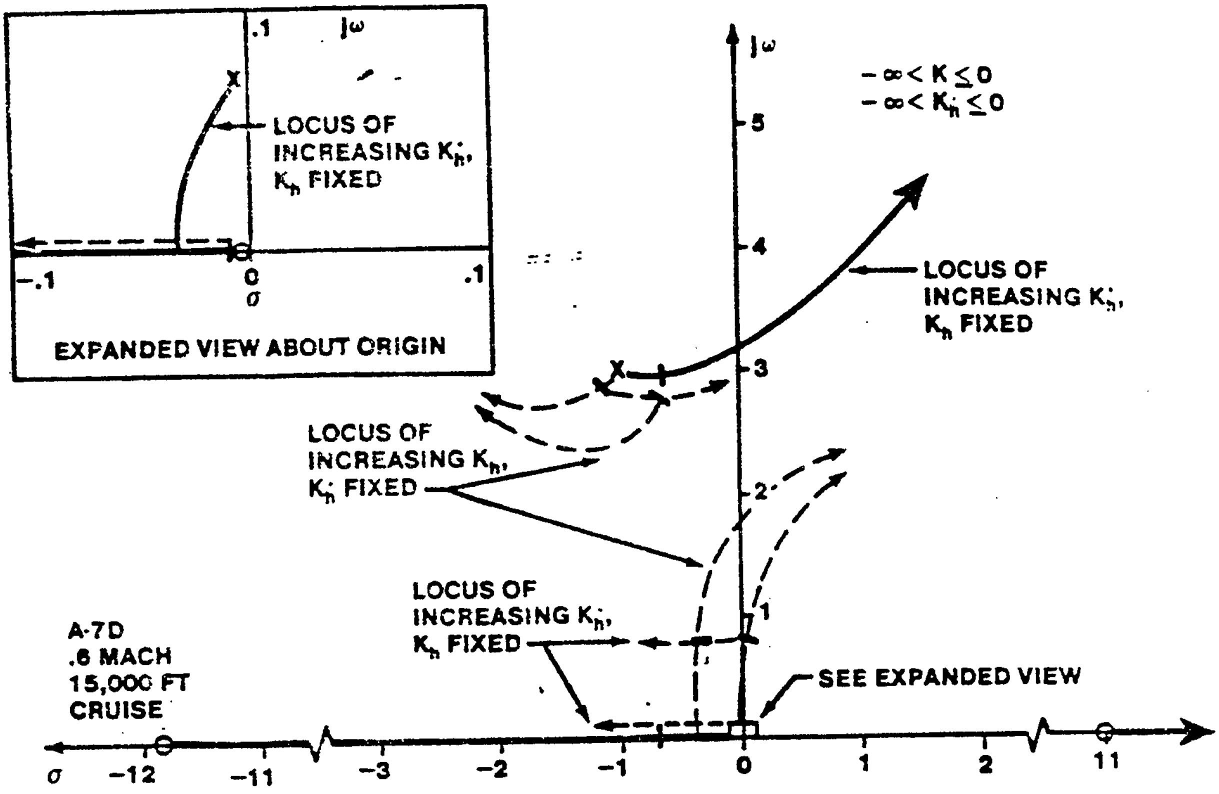

FIGURE 14.138. ROOT LOCUS PLOT OF ROOT MIGRATIONS DUE TO ALTITUDE AND ALTITUDE RATE MULTILOOP FEEDBACK

then the perturbed altitude rate is proportional to the pitch attitude change. The aircraft altitude deviation can be fed back to the input of a pitch attitude hold system through a simple gain to achieve the same effect as the altitude rate plus altitude feedback scheme. A third pitch rate feedback loop could also be added to the pitch attitude system to improve the short period dynamics.

14.7.3 Roll Attitude Hold

The fundamental part of a roll attitude autopilot is the feedback of roll angle to the ailerons. This feedback effectively creates roll static stability and provides a tendency to maintain the roll attitude orientation in turbulence. Figure 14.139 shows the root locus of a bank angle feedback for the A-7D which has good rolling characteristics. The proximity of the numerator zeros to the Dutch roll roots indicates that very little aileron excitation of the Dutch roll dynamics occurs. The performance of the roll attitude hold system shows promise for relatively low gain. The spiral mode of the unaugmented aircraft is slightly stable but unacceptably slow to converge. The augmentation system decreases the convergence time by moving the root further to the left. This is accomplished at the expense of the roll mode time constant, which increases with increasing gain. For somewhat higher gain, the spiral mode and roll mode roots combine and separate from the real axis. For moderate gain, a well damped oscillatory pair are provided, with damping decreasing and natural frequency increasing as the gain increases.

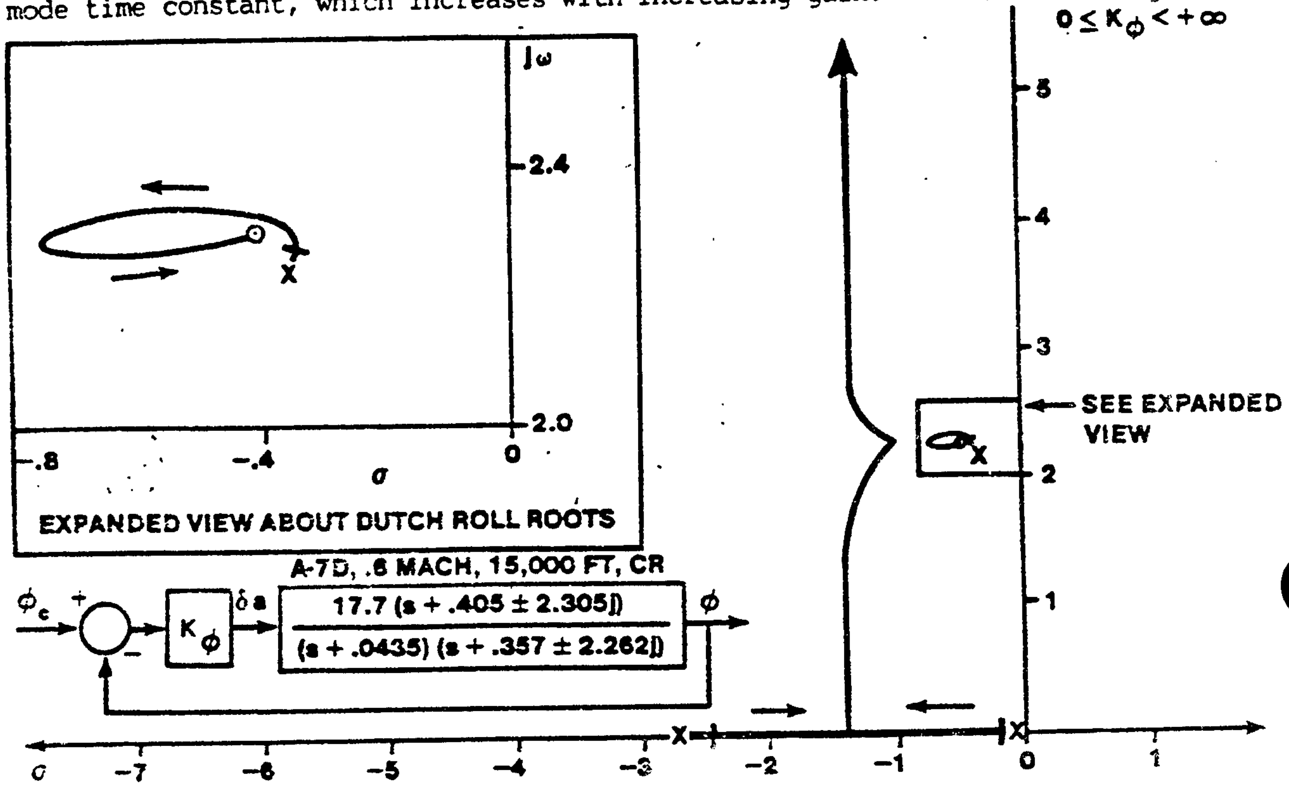

FIGURE 14.139. ROOT LOCUS PLOT OF ROLL ANGLE FEEDBACK TO AILERONS LOOP WITH SUPPRESSED DUTCH ROLL DYNAMICS

Figure 14.140 presents the root locus for the C-5 in which the Dutch roll dynamics are not well suppressed by the numerator zeros. The roll mode and spiral mode roots behave in a similar manner to the previous case for low to moderate gains. The Dutch roll damping increases slightly for low gains, but then decreases steadily as the natural frequency increases with increasing gain. The roll angle feedback is not successful in suppressing Dutch roll dynamics and poor lateral ride quality could be expected.

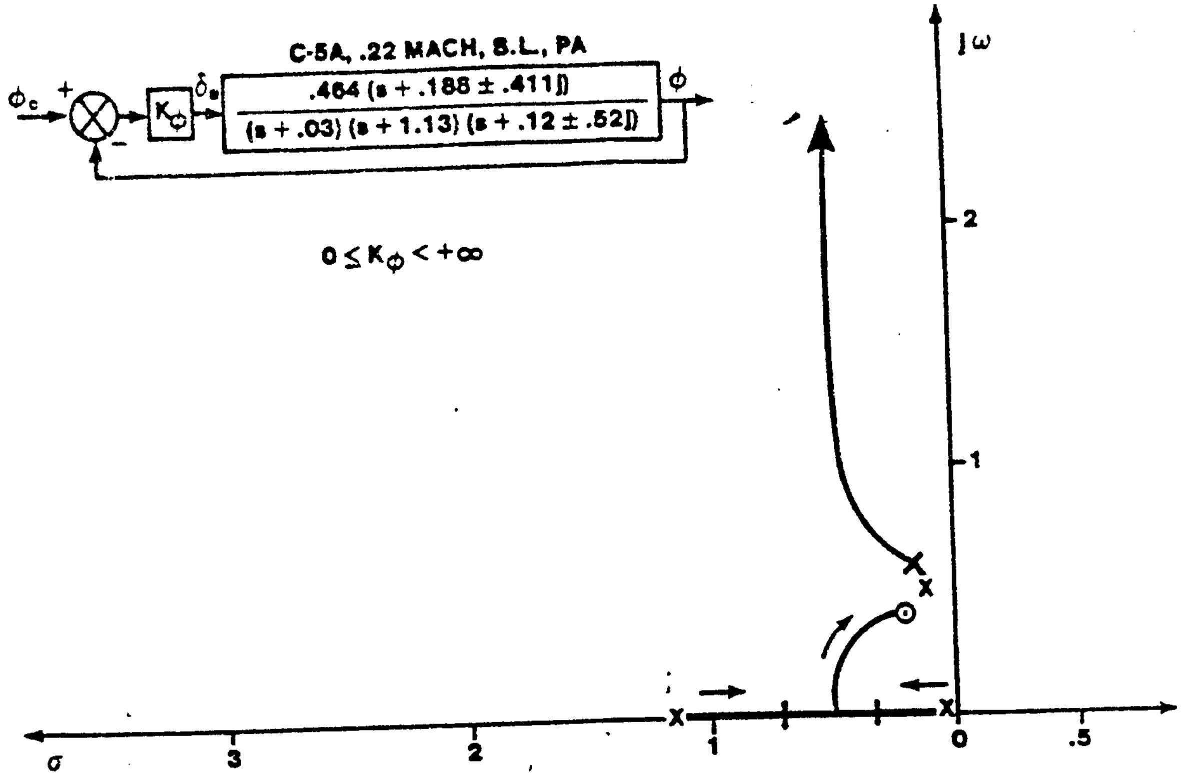

FIGURE 14.140. ROOT LOCUS PLOT OF ROLL ANGLE FEEDBACK TO THE AILERONS LOOP

For a roll attitude hold autopilot to give acceptable flying qualities the Dutch roll must be effectively suppressed and the spiral mode must converge. In cruising flight, the spiral mode time constant is typically very large and the aircraft can be either neutrally stable, slowly convergent, or slightly divergent. The neutrally stable or divergent spiral modes are unacceptable for unattended operation, and the slowly convergent spiral mode is only slightly better. Roll rate feedback was shown to be effective in suppressing the Dutch roll motion which would otherwise be aggravated by aileron deflections. If roll rate is fed back as an inner loop to suppress the bank angle oscillation tendency of the C-5, and roll angle is fed back as an outer loop, the C-5 flying qualities could be improved. This is the typical roll attitude hold scheme as shown in figure 14.141.

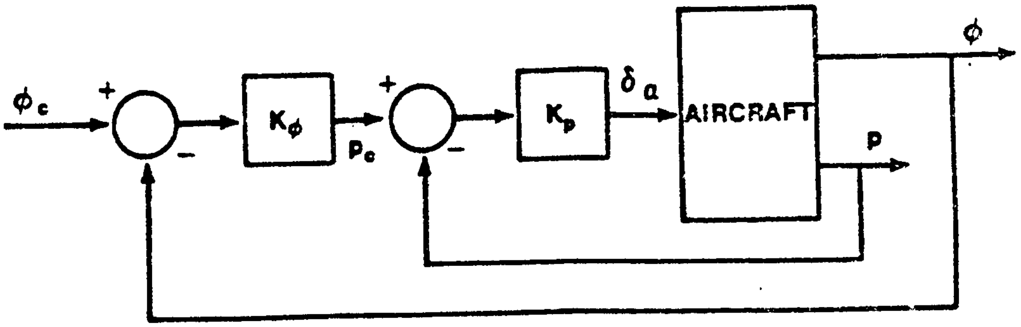

ϕ_c
+
−
K_ϕ
P_c
+
−
K_p
δ_a
AIRCRAFT
ϕ
p

FIGURE 14.141. ROLL ATTITUDE HOLD SYSTEM

14.7.4 Heading Hold

Nearly all autopilot heading hold modes are mechanized with a bank angle control system as the inner loop. The reason for this is found in the following fundamental relationship between bank angle and rate-of-change of heading angle in a steady level turn

$$\dot{\psi} = \frac{g \tan \phi}{U_0} \approx \frac{g\phi}{U_0} \qquad (14.104)$$

Taking the Laplace transform the heading angle to roll angle transfer function is

$$\frac{\psi(s)}{\phi(s)} = \frac{g}{U_0 s} \qquad (14.105)$$

A block diagram for a heading control system is shown is figure 14.142. Precise and comfortable control of heading angle implies some form of turn coordination as discussed in setion 14.5.1.2.4.

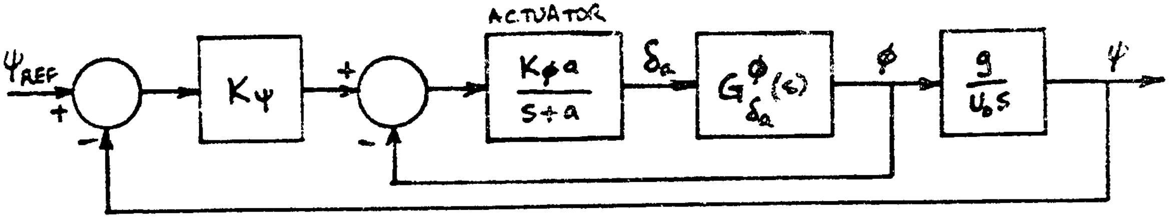

ψ_{REF}
+
−
K_ψ
+
−
ACTUATOR
$\frac{K_\phi a}{s+a}$
δ_a
$G^{\phi}_{\delta_a}(s)$
ϕ
$\frac{g}{U_0 s}$
ψ

FIGURE 14.142 HEADING HOLD SYSTEM

14.7.5 Lateral Beam Intercept and Hold

A heading control autopilot by itself allows a pilot to maintain a given heading only. To fly toward a fixed reference point on the earth requires additional corrections for crosswinds. Intercepting and holding a course to a fixed reference point is required for automatic heading control to fly navigation courses to TACAN or VOR stations, INS courses, or TACAN, VOR or ILS approaches. Autopilot systems capable of lateral beam intercept and hold are also frequently referred to as simpily the navigation mode, or the VOR, TACAN or localizer mode, or as the lateral beam guidance mode. It can serve all these purposes, the only difference being the differences in beam width. For a typical localizer the beam width corresponds to 2-1/2 degrees at full scale indicator deflection. For a typical navigation beam (VOR or TACAN) this is 10 degrees. In both cases the system becomes more sensitive as the aircraft nears the transmitter because the lateral distance off the beam centerline corresponds to a larger error angle, λ, as the transmitter is approached. To avoid this increase in sensitivity it is possible to use gain scheduling as a function of range to the transmitter. This, however, requires distance measuring equipment to be included and represents a system complication. Figure 14.143 shows the geometry of a lateral beam intercept and hold mode.

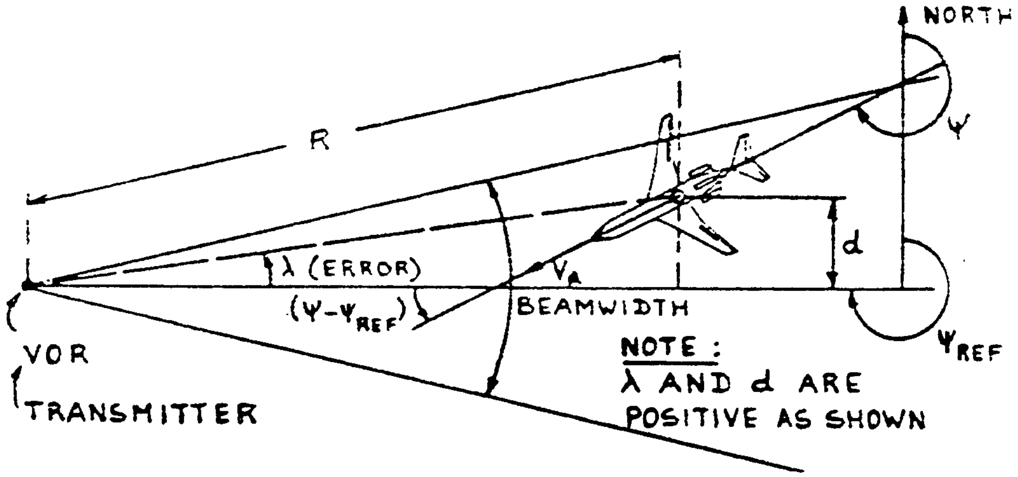

FIGURE 14.143 GEOMETRY OF LATERAL BEAM INTERCEPT AND HOLD MODE

The lateral beam error angle, λ, is given by

$$\lambda \approx \frac{d}{R} \qquad (14.106)$$

From figure 14.143 it can be seen that

$$\dot{d} = V_A \sin(\psi - \psi_{REF}) \approx V_A (\psi - \psi_{REF}) \qquad (14.107)$$

Taking the Laplace transform

$$d(s) = \frac{1}{s} V_p (\psi(s) - \psi_{REF}(s)) = \frac{1}{s} V_p \psi(s) \qquad (14.108)$$

A "geometry transfer function" can now be obtained that relates the heading error $(\psi(s) - \psi_{REF}(s))$ to the error in the course, λ.

$$\frac{\lambda(s)}{\psi(s)} = \frac{1}{(\psi(s) - \psi_{REF}(s))} = \frac{V_p}{SR} \qquad (14.109)$$

Figure 14.144 shows a block diagram relating the error angle, λ to the ψ-control system needed to drive the airplane back to the beam centerline. The required course is given as λ_{REF}.

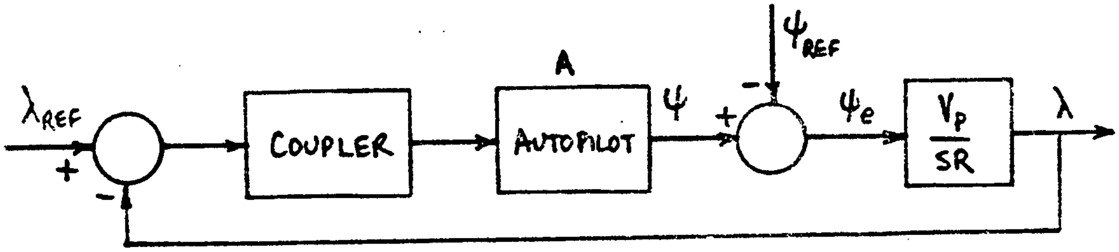

FIGURE 14.144 BLOCK DIAGRAM FOR LATERAL BEAM HOLD SYSTEM

The usual approach is to use a heading hold system for the autopilot in block **A** of figure 14.144. The coupler is a device which operates on the error signal $\lambda - \lambda_{REF}$. The bearing error to the station λ is received by the onboard navigation receiver. The coupler translates λ into a signal which is fed to the aircraft heading angle control system. To allow the coupler to do this even in cross-wind conditions it is found desirable to add an integral plus proportional low pass filter to the coupler. The coupler gain should be high for rapid return to the beam centerline.

Because the gain in these loops is inversely proportional to distance, R, to the transmitter, there is nearly always a stability problem associated with such a loop. The primary method for eliminating such instabilities is to switch gain as a function of range to the station.

14.7.6 Airspeed/Mach Hold

In more sophisticated autopilot systems as well as in high performance aircraft it becomes desirable to also control airspeed. Autopilot modes which accomplish this are called airspeed or Mach hold modes.

Airspeed hold at low speed is a major convenience to pilots when flying coupled (automatic) approaches. There are two popular methods to control speed on final approach

1) Auto-Throttle - using a feedback device to control the throttles
2) Auto-Drag - using a feedback device to control speedbrakes

A block diagram for an auto-throttle system is shown in figure 14.145. Notice that there are lags in the system due to the throttle actuator, the engine response time, and the pitot system response time, which are represented by low pass filters.

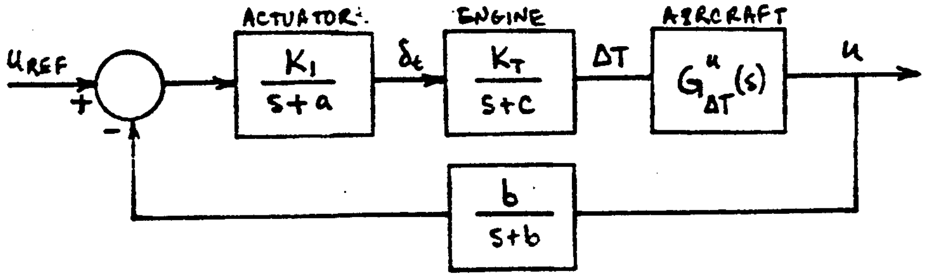

FIGURE 14.145 BLOCK DIAGRAM FOR AUTO-THROTTLE AIRSPEED CONTROL

To derive the required $G^{u}_{\Delta T}(s)$ transfer function, the phugoid approximation can be used. In this system δ_t represents the throttle angle and ΔT represents the resulting change in thrust. If ΔT is divided by the aircraft mass, the longitudinal acceleration can be approximated. The longitudinal axis transfer functions assuming constant angle of attack are

$$\begin{bmatrix} (s - X_u^*) & w_0 s + g\cos\theta_0 \\ -Z_u & -U_0 s + g\sin\theta_0 \end{bmatrix} \begin{bmatrix} u(s) \\ \theta(s) \end{bmatrix} = \begin{bmatrix} \frac{\Delta T}{m} \\ 0 \end{bmatrix} \qquad (14.110)$$

where $X_u^* = X_u + X_{T_u}$. (14.111)

Using Cramer's rule, the transfer function is found as (assuming $\cos\theta_0 \approx 1$ and $\sin\theta_0 \approx \theta_0$)

$$G_{\Delta T}^u(s) = \frac{u(s)}{\Delta T(s)} = \frac{\frac{1}{m}(-U_0 s + g\theta_0)}{-U_0 s^2 + s(g\theta_0 + U_0 X_u^* - Z_u w_0) - X_u^* g\theta_0 + gZ_u} \qquad (14.112)$$

An idealized auto-throttle root locus with no engine lag or pitot lag included usually shows a very fast first order response. Engine response lag, however, can be considerable and must be included in a study of auto-throttle closed loop response.

In some cases the effect of engine lag on the control of airspeed can be severe. This can be overcome by using an auto-drag system. The Dutch F-28 jet transport and the British Hawker-Siddeley (Blackburn) Buccaneer strike fighter are examples of aircraft that used this system. In these cases, speed was controlled by modulating speedbrakes relative to a partially open speedbrake position. Operational experience with this system has been satisfactory. It has two additional advantages: 1) it causes less wear on the engines because these remain at a constant throttle setting, and 2) in a go-around situation, closing the speedbrakes provides an immediate accelerating effect. At the same time the engine speed-up time is reduced because the engine accelerates from a higher RPM.

At high speed, Mach feedback to the elevator is often used to keep the Mach number constant. This type feedback is discussed in section 14.5.1.1.4.1.

14.7.7 Pilot Blending

The controls used by the pilot to engage or disengage autopilots can be mechanized in a variety of different ways. A fundamental requirement for most systems is that the pilot be able to override or disengage the system through controls on the stick or throttle ("hands on"). Aircraft autopilots are often mechanized to disengage if the pilot applies control stick force outside a set stick force breakout. This mechanization is, however, a safety hazard because the autopilot can be inadvertently disengaged which may result in the pilot not knowing he needs to resume aircraft control. An example of such a system is found in the F-4 where a caution light notifying the pilot that the autopilot is disengaged was found to be necessary. Even this warning is sometimes inadequate as shown by aircraft accidents (including large commercial airliners) due to inadvertent autopilot disengagement while the crew was distracted with other tasks. Another disadvantage of this type arrangement is that there are no provisions for the pilot to blend with the autopilot to fly the aircraft to a different condition and to reset the autopilot to these conditions or to return to the original conditions, unless the pilot is given additional controllers to adjust the autopilot settings.

One possible alternative arrangement was shown in section 14.7.1.2 where a memory device (integral plus proportional controller) in the feedback path was engaged whenever the pilot made stick force inputs (outside a set breakout). If these pilot inputs interrupted, but did not disengage the autopilot, the pilot could fly the aircraft to new conditions, release the stick and the autopilot would then maintain these new conditions. This is known as control stick steering and is a superior mechanization to a system that disengages with pilot input because it is safer. It has, however, two disadvantages. First, the pilot cannot return to the original set conditions automatically once he has blended with the system and second, inadvertent pilot stick inputs could cause the system to be reset when this is not desired.

Recent aircraft have been mechanized with an arrangement which allows pilot blending with the autopilot and positive hands on control over the autopilot. Such a system is found in the F-16. In the F-16 the pilot engages attitude, altitude or heading select autopilot modes with switches on the instrument panel. Without known flight control system faults these are the only means of turning off the autopilot. The pilot must, therefore, take his hands off the throttle or stick in order to turn the system off. The autopilot, however, automatically disengages when the landing gear handle is lowered, the air refueling door is open or the aircraft trim system is turned off.

With the F-16 autopilot engaged the pilot can fly the aircraft to any condition desired by blending his commands with that of the autopilot. The stick forces are higher than with the autopilot off but are tolerable. If the pilot releases the stick after blending with the autopilot the aircraft returns to the original autopilot engagement conditions. Inadvertent pilot blending will not, therefore, cause the autopilot to reset to new conditions.

The pilot can, however, interrupt autopilot operation with a paddle switch located on the back side of the stick. When the paddle switch is depressed all autopilot controls are interrupted and the pilot has full command authority at normal stick forces. The pilot can then fly the aircraft to new conditions, release the paddle switch and the autopilot will maintain these new conditions.

Autopilot disengagement, blending and reset capabilities as mechanized in the F-16 have been shown to be a safer and more versatile arrangement than that found in other autopilot arrangements.

14.8 SENSORS AND NONLINEAR ELEMENTS

To utilize airframe output quantities (u, v or β, w or α, p, q, r and their time derivatives) for aircraft flight control systems, they must be sensed, or "picked up," by some means. This section presents a discussion of some of the devices used for this purpose.

The first part of this section will describe each type of sensor while the second part will discuss the importance of sensor placement which will include a discussion of the effects of fuselage structural bending. A brief description of nonlinear elements will be presented at the end of this section.

Table 14.5 lists the most important output quantities used in flight control systems and their usual sensors.

Some discussion of sensor dynamics is included in the following sections but a detailed discussion of sensor dynamics is beyond the scope of this text. These dynamics are usually negligible for the analysis of aircraft control systems since the sensors are selected to be sufficiently fast (very high natural frequencies) so as to add a negligible small amount of lag to the system.

TABLE 14.5 SENSOR APPLICATION

	Basic Output Quantity	Sensor
	Longitudinal	
U_A, u	Forward velocity	Accelerometer; Airspeed detector
w	Vertical velocity	Accelerometer; Local flow detector
q	Pitching velocity	Rate gyro
$\dot{u} = n_x$	Forward acceleration *	Accelerometer
$\dot{w} = n_z$	Vertical acceleration	Accelerometer
α	Angle of attack	Accelerometer; Local flow direction detector
Θ	Pitch angle	Stabilized gyro
$\dot{q} = \ddot{\Theta}$	Pitching acceleration	Angular accelerometer; Two linear accelerometers
h	Altitude	Altitude sensor, Air data computer
	Lateral-Directional	
v	Side velocity	Accelerometer; Local flow direction detector
p	Rolling velocity	Rate gyro
r	Yawing velocity	Rate gyro
$\dot{v} = n_y$	Side acceleration *	Accelerometer
ψ	Yaw angle	Stabilized gyro
$\dot{r} = \ddot{\psi}$	Yaw acceleration	Angular accelerometer; Two linear accelerometers
ϕ	Roll angle	Stabilized gyro; Rate gyro
$\dot{p} = \ddot{\phi}$	Roll acceleration	Angular accelerometer; Two linear accelerometers
β	Sideslip angle	Accelerometer; Local flow direction detector

* NOTE: Angle of attack rate an be derived from $\dot{\alpha} = \dot{w}/u_o$
Sideslip angle rate can be derived from $\dot{\beta} = \dot{v}/u_o$

14.8.1 Sensor Types

The following discussion will present a brief description of gyroscopes, accelerometers, flow incidence angle sensors, airspeed sensors and altitude sensors.

14.8.1.1 Gyroscopes

Among the airframe output quantities listed in Table 14.5 available for use in the flight control system are the aircraft Euler angles (ψ, Θ, ϕ) and angular rates (p, q, r). The device which has been universally used for sensing these quantities is the gyroscope.

14.8.1.1.1 Measurements of Angular Displacements

If no torques are applied to the spin axis, the gyro angular orientation remains fixed with respect to inertial (celestial) space, and in this configuration it can be used to measure angular displacement of its case, when suitable pickoff devices are used to measure the angles between the case and the spin axis. Gyroscopes of this type are commonly used to measure the angular orientation of the airframe, the "vertical" gyro being used measure pitch and roll angle (θ and ϕ) and the "directional" gyro being used to measure airframe heading (ψ).

14.8.1.1.1.1 Vertical Gyros - The vertical gyro is oriented with the gyro spin axis aligned with the airframe z axis. The gimbal orientations are assumed to correspond to level flight. Vertical gyros are always supplied with an erection mechanism whose purpose is to keep the spin axis aligned with the local vertical. The erection mechanism is required for several reasons. First, since the spin axis tends to remain fixed with respect to inertial space, the gyro would sense the rotation of the earth and the curvature of the earth as the airplane is flown at constant altitude. One purpose of the erection mechanism then, is to change the gyro reference from inertial to local vertical. Another reason for requiring an erection mechanism is that it is impossible to fabricate gyros with frictionless gimbals. Thus, as the airplane rotates about either the x or y axis, torque is applied to the spin axis through the friction in the gimbal bearings, causing the gyro to process about the other gimbal axis. This would cause an unpredictable wander of the gyro spin axis. Erection is normally cut out during a coordinated turn to prevent the gyro from erecting to an acceleration vector not representing gravity.

To minimize the coupling effects between the dynamics of the erection system and those of the aircraft, and to minimize the effects of transient accelerations along the x and y airframe axes, the erection mechanism is designed to operate slowly, rates of two to six degrees per minute being typical. Many vertical gyros have two erection rates, the faster of which is used to provide quick erection to minimize the time required for the gyro to become operable after the system is first turned on.

For those cases where the erection system natural frequency is much lower than that of the airframe phugoid, the gyro can be represented as a pure gain and its transfer function becomes

$$\frac{V_G}{\Theta \text{ or } \phi} = K_g \qquad (14.113)$$

where V_G is the voltage from the gyro pickoff, K_g is a constant of proportionality and Θ or ϕ are aircraft attitude angles to be measured.

14.8.1.1.1.2 Directional Gyros - Two degrees of angular freedom are also used for the directional gyro. In this case, however, the gyro spin axis is maintained in a horizontal plane by one of the torquing motors and aligned with some specific compass direction (usually north and south) by the other torquing motor. The latter torque motor is usually energized by the error voltage originating in a synchro transmitter whose rotor is attached to the gyro outer gimbal and whose stator is attached to the gyro case. The stator windings are excited by a remote compass transmitter.

In actual practice both the vertical and directional gyros give accurate indications only when the gimbal axes are orthogonal. For example, for a pitch angle of 90°, the condition known as "gimbal lock" occurs wherein the outer gimbal axis is aligned with the gyro spin axis. For this condition the gyro is not sensitive to roll angle. In the case of the directional gyro, errors are introduced whenever yawing occurs in the presence of a roll angle, such as during a coordinated turn.

14.8.1.1.2 Measurements of Angular Rates

The rate gyro measures the torque which is generated by the gyro due to an angular velocity input. A single degree of freedom gyro is used for this purpose, and the generated torque is normally absorbed by means of a spring which restricts the motion of the gimbal.

If an electrical pickoff is attached to the gyro to measure the gimbal rotation, the rate gyro transfer function is

$$\frac{V_G(s)}{\omega(s)} = \frac{K}{s^2 + 2\zeta\omega_n + \omega_n^2} \qquad (14.114)$$

This transfer function neglects any gyro threshold due to Coulomb friction. Such a friction threshold must obviously be kept to a minimum. Resolution of potentiometers or thresholds of other types of pick offs must be added to the Coulomb friction threshold to obtain the total minimum detectable signal.

Two forms of geometrical cross-coupling occur in rate gyros, one caused by gimbal rotation when the gyro is indicating an angular rate and the other caused by the effects of the airframe angle of attack upon the axis about which the airplane rotates. Both effects introduce error in the measurement of the desired rate and introduce gyro outputs in response to rotation of the airframe about other axes.

14.8.1.2 Accelerometers

Accelerometers are used to sense the linear and angular accelerations of the airframe. They consist almost universally of a mass of relatively high density which is constrained to translate or rotate against a restraining force or torque (usually a spring) as a result of applied acceleration. The mass is usually a solid. Although accelerometers differ in construction details, the behavior of most of them can be adequately described by a second order equation.

It is of some interest to note the behavior of the accelerometer for various forcing frequencies. When the frequency of the applied acceleration is much less than ω_n, the phase lag of the unit is approximately 90° and the output is proportional to the velocity of the accelerometer case. Similarly, when the frequency of the case motion is much higher than ω_n, the phase lag is approximately 180° and the output is therefore proportional to the input displacement.

When properly oriented and located at the airframe center of gravity, accelerometers can be used to measure $a_x = \dot{u} = \ddot{x}$ the forward acceleration, $a_y = \dot{v} = \ddot{y}$ the side acceleration, and $a_z = \dot{w} = \ddot{z}$ the vertical acceleration.

An accelerometer can also be used to give a reasonably accurate indication of sideslip angle. It can be shown that an approximate expression for the a_y/δ_R transfer function is

$$\frac{a_y(s)}{\delta_R(s)} = Y_\beta \frac{\beta(s)}{\delta_R(s)} + Y_{\delta_R} \tag{14.115}$$

Which can be rewritten as

$$a_y(s) = y_\beta \ \beta(s) + Y_{\delta_R} \ \delta_R(s) \tag{14.116}$$

If a signal proportional to δ_R is subtracted from a_y, the resulting signal is proportional to sideslip angle. Since sideslip angle and side velocity are related by the expression

$$v = U_0 \beta \tag{14.117}$$

side velocity can also be obtained by this method.

In a similar manner, the airframe angle of attack can be obtained by means of a normal accelerometer. This relationship is sometimes used to compute angle of attack for fire control purposes.

14.8.1.3 Flow Incidence Angle Sensors

It is desirable in many cases to sense directly the airframe sideslip angle, β, and angle of attack, α, so that these airframe output quantities can be used by the flight control system. Because these angles are defined in terms of the relative wind, their direct measurement involves measurement of the relative wind direction, or the direction of relative motion of the air as it passes over the airframe. This is usually accomplished by means of a vane, a probe, dual pressure pick-ups, or some similar device.

Direct measurement of these quantities, however, suffers from the rather serious disadvantage that the direction of the local flow is not a direct indication of the desired airframe output quantities because of the disturbances which exist near the airframe. At subsonic speeds, these disturbances extend for some distance ahead of the airframe. Consequently, the true angle of attack or sideslip must be computed from the indicated angle. Additional data, such as indicated airspeed and Mach number, are usually required to perform this computation.

The sensitivity of these flow sensors to turbulence and other flow disturbances make their signals unsuitable for differentiation. Because of this, local flow sensors cannot be used for determination of $\dot{\beta}$ or $\dot{\alpha}$ without the introduction of considerable noise into the system.

14.8.1.4 Airspeed Detectors

Local flow magnitude detectors are actually pressure sensors and are used to give an indication of the velocity at which the airframe is moving through the air. Depending on the equations to which these sensors are mechanized, their outputs are proportional in the steady state to indicated airspeed, true airspeed, Mach number, or differential pressure. These devices are used as primary sensing units when airspeed or Mach number is being controlled directly, or as a means of changing controller characteristics as a function of airspeed to compensate for changes in airframe characteristics.

Since the dynamic characteristics of local flow magnitude detectors depend to a large extent upon the characteristics of the pitot static system into which they are connected, it is not considered practical to present a detailed discussion here. However, it can be said that these sensors can often be approximated by the following transfer function

$$\frac{V(s)}{p(s)} = \frac{K}{\left(\frac{s^2}{\omega_n^2} + \frac{2\zeta s}{\omega_n} + 1\right)(T_s s + 1)} \qquad (14.118)$$

where V is the sensor output, p is the pressure presented to the sensor by the pitot-static system, ζ and ω_n are constants describing the sensor mechanical system, and T_s is the time constant describing the sensor pressure system. Usually, the dynamics associated with ζ and ω_n are unimportant, but the time lag T_s may become large enough to require consideration. In addition, the characteristics of the pitot-static system should be carefully analyzed because this system is often characterized by an even larger time lag than T_s.

14.8.1.5 Altitude Sensors

Pressure altitude sensors indicate altitude by measuring the static air pressure. When used as primary sensors for automatic control, they must have an extremely low threshold if the altitude control loop is to be easily stabilized. Like most pressure sensors, the sensing element usually consists of an aneroid bellows; the requirement for low threshold is often met by repositioning the bellows by servo action after a change in altitude. Care should be taken in mounting these units in the airframe, for they are sometimes sensitive to linear and angular accelerations. In addition, the static air line connected to the unit should be carefully selected to minimize the time lag in the pressure changes presented to the sensor. The static pressure system should also be studied to determine effect of airframe angle of attack on the pressure in the system.

14.8.2 Sensor Placement

The following sections will discuss sensor placement first with the aircraft assumed to have a rigid airframe and then with fuselage structural bending considered.

14.8.2.1 Sensor Placement in a Rigid Aircraft

The location of an angle of attack sensor must minimize local flow disturbances near the sensor so as to obtain steady measurements. As noted earlier, since flow near the aircraft is affected by upwash, the angle of attack measurement from the vane in not true angle of attack, and must be corrected to indicate the true angle of attack. This correction may be determined experimentally during tower flyby pitot-static tests for subsonic speeds or computed for supersonic speeds. The correction may be a function of altitude or Mach.

The placement of rate gyros is not critical in rigid aircraft. They are usually aligned to measure rotational motion about the aircraft body axes.

Accelerometers, however, must be located carefully. The acceleration at locations other than the aircraft center of gravity is computed as

$$\bar{a}_{ACCEL} = \bar{a}_{cg} + \dot{\bar{\omega}} \times \ell \qquad (14.119)$$

where ω is the angular acceleration of the aircraft and ℓ is the location of the accelerometer relative to the center of gravity, expressed in the aircraft body axis system.

An accelerometer sensing normal acceleration should be located along the aircraft centerline (to avoid sensing roll accelerations) and ahead of the center of gravity of the aircraft. As noted in section 14.5.3.1 it is impractical to locate an accelerometer at the c.g. because of c.g. shifting during flight. Locating the normal accelerometer ahead of the c.g. moves the zeros in the

$$G_{\delta_e}^{a_z}(s)\Big|_{ACCEL}$$

transfer function move towards the short period roots, in a load factor command system. This increases system stability and provides a quicker response. Moving the normal accelerometer aft of the c.g. causes a destabilizing effect on the short period roots and lowers the maximum gain

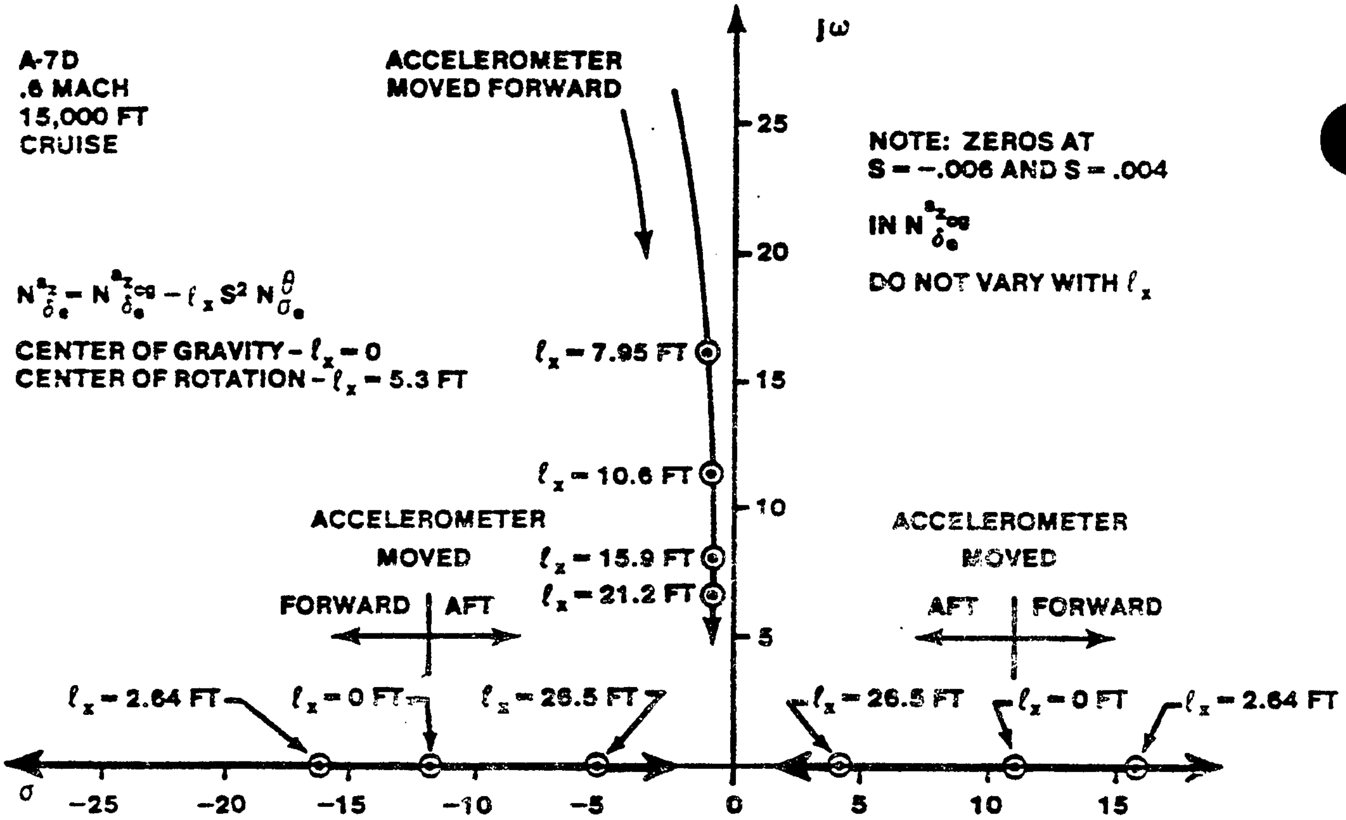

FIGURE 14.146. EFFECT OF NORMAL ACCELEROMETER LOCATION ON ZEROS OF ACCELERATION TRANSFER FUNCTION

that can be used (increasing steady state error). Figure 14.146 shows the effect of normal accelerometer placement on the zeros of the acceleration transfer function.

Figure 14.147 shows the effect of accelerometer location on the short period roots for three otherwise identical acceleration feedback systems. Actuator dynamics are included. As the accelerometer location moves aft of the center of gravity, the short period roots migrate to the right half s-plane at a much lower gain than if the sensor were at the center of gravity. At a relatively low gain, the system with the sensor at the center of gravity will also be driven unstable. With the accelerometer well in front of the center of gravity the system cannot cause the short period roots to become unstable for any gain.

The placement of lateral accelerometers is also important if the destabilizing influence of the acceleration transfer function zeros on the Dutch roll roots is to be minimized so that higher feedback gains can be realized. Figures 14.148 and 14.149 show the migration of the acceleration

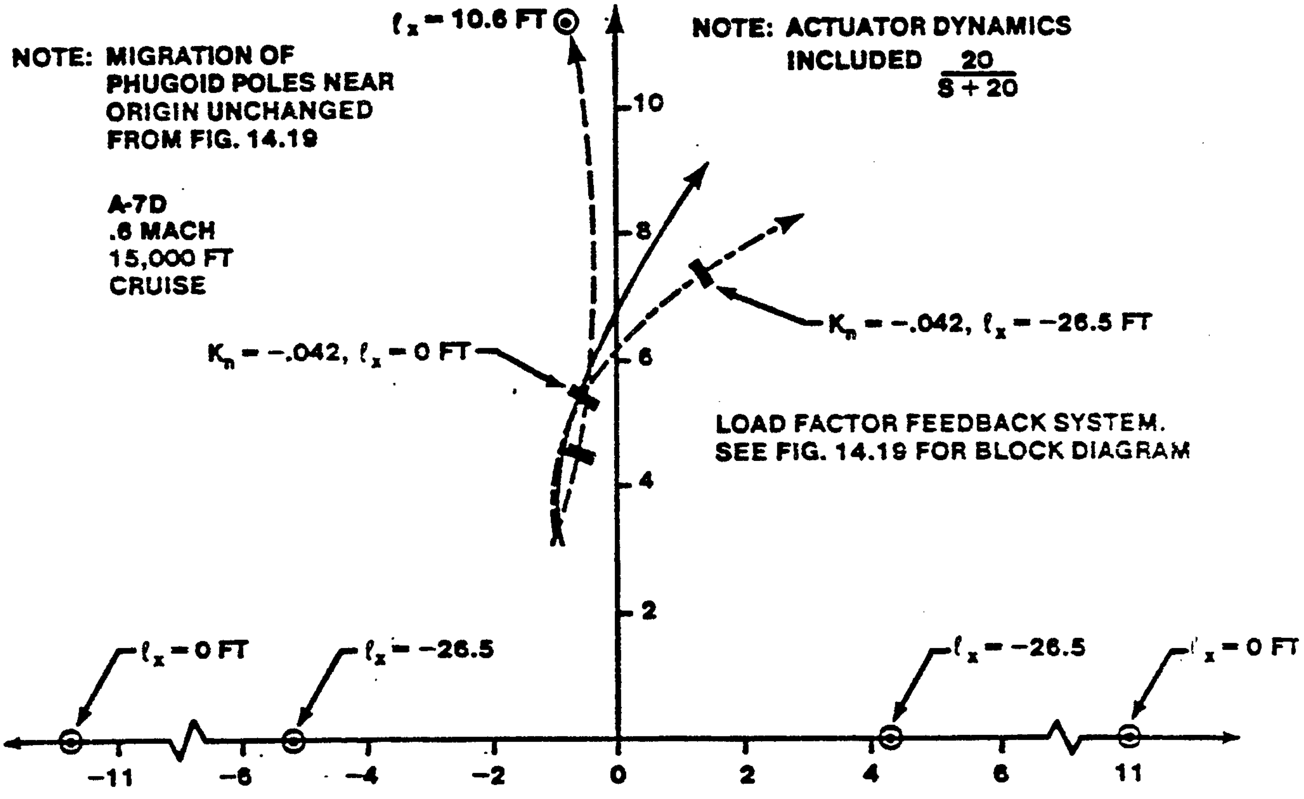

FIGURE 14.147. COMPARISON OF SHORT PERIOD ROOT MIGRATION DUE TO ACCELEROMETER LOCATION

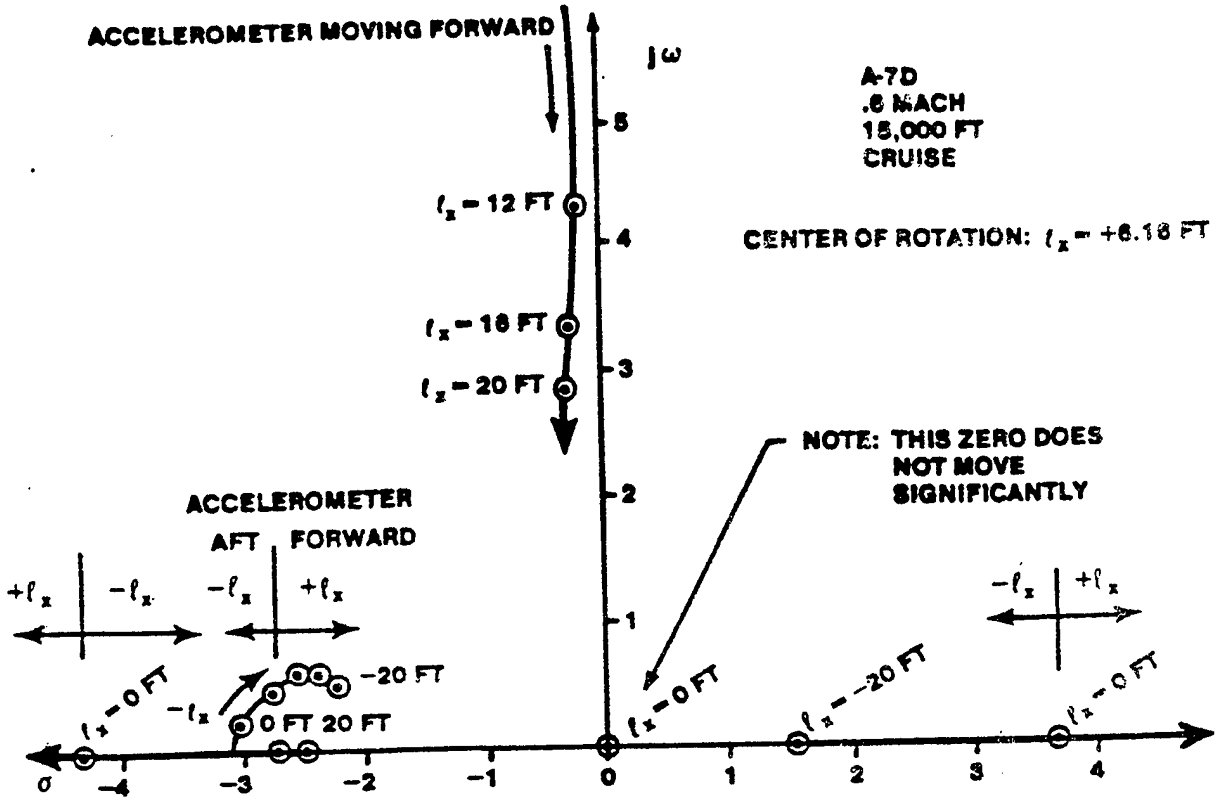

FIGURE 14.148. EFFECT OF LATERAL ACCELEROMETER LOCATION ON ZEROS OF LATERAL ACCELERATION TRANSFER FUNCTION

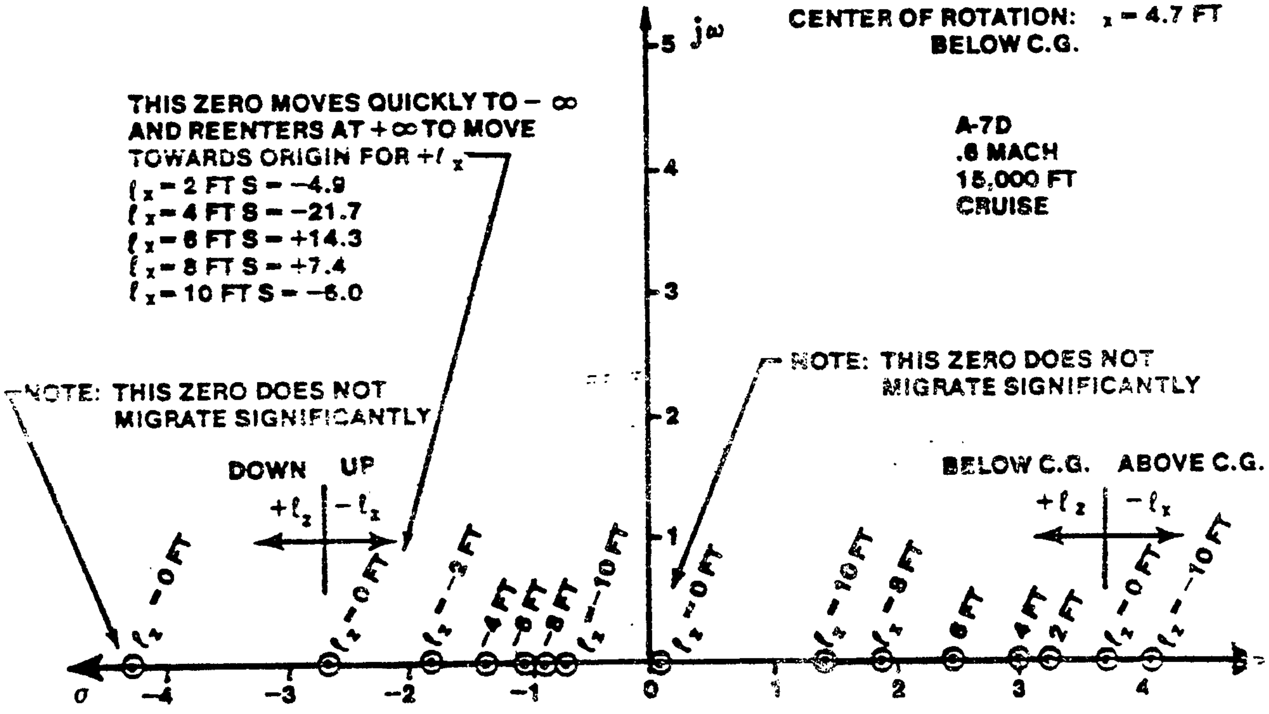

FIGURE 14.149. EFFECT OF LATERAL ACCELEROMETER LOCATION ON ZEROS OF LATERAL ACCELERATION TRANSFER FUNCTION

transfer function zeros with longitudinal and vertical displacement of the accelerometer, respectively. The lateral accelerometer should be located well forward of the center of rotation for the directional axis (ahead of the center of gravity). Locating the lateral accelerometer above the aircraft center of gravity will also minimize the number of zeros in the right half s-plnane and minimize the destabilizing influence of these zeros on the Dutch roll roots. Locating the lateral accelerometer ahead of the directional center of rotation and above the center of gravity combines these two effects.

14.8.2.2 Fuselage Structural Bending

Fuselage bending is sensed by rate gyros and accelerometers at frequencies below the cut-off frequency of the aircraft control system (the maximum frequency at which the flight control system sensors can detect motion). The effects of aeroelastic coupling due to the intermingling of the aircraft structural motions with the rigid body motions, therefore, can produce extraneous control signals which can degrade handling qualities or controllability and may even cause the flight control system to drive the structural motions unstable.

Figure 14.150 shows a representation of the fundamental longitudinal structural bending modes. In reality the number of mode shapes are infinite but the first, second, and third bending modes of the fuselage and the first bending mode of the stabilator are usually the only significant modes (other modes have frequencies too high to be sensed by flight control system elements).

Structural bending effects are usually only of significance to the longitudinal axis, but lateral-directional effects are becoming more of a problem in modern aircraft as improved materials allow a more flexible aircraft. This is seen in such aircraft as the F-16.

14.8.2.2.1 Accelerometer and Rate Gyro Sensor Placement

The ideal location for a normal accelerometer (from a structural point of view) is where the measured normal accelerations from the aircraft bending modes are zero. The ideal placement for a pitch rate gyro is where the slopes of the bending modes are zero. All the structural bending variables are not all zero at the same point. If the structural mode shapes are accurately represented by simple harmonic motion (sinusoidal in nature) then a reduction of structural mode coupling may be obtained by locating accelerometers on nodal points, or points of zero deformation η_1', η_2', $\eta_3' = 0$ where the bending

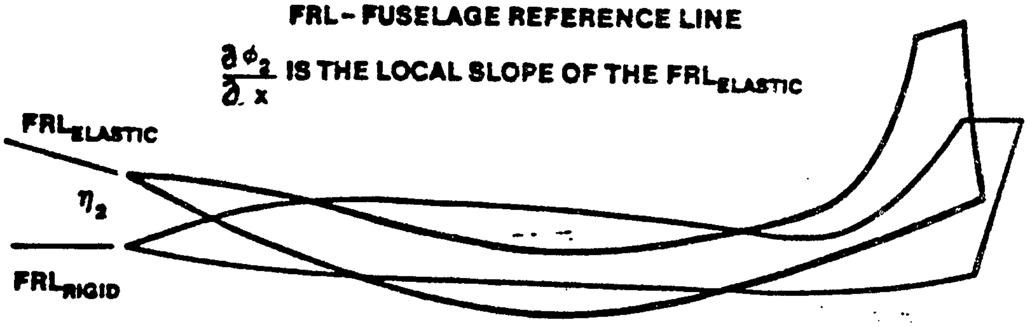
FRL - FUSELAGE REFERENCE LINE
$\frac{\partial \phi_2}{\partial x}$ IS THE LOCAL SLOPE OF THE $FRL_{ELASTIC}$
$FRL_{ELASTIC}$
η_2
FRL_{RIGID}

(a). FIRST FUSELAGE BENDING MODE

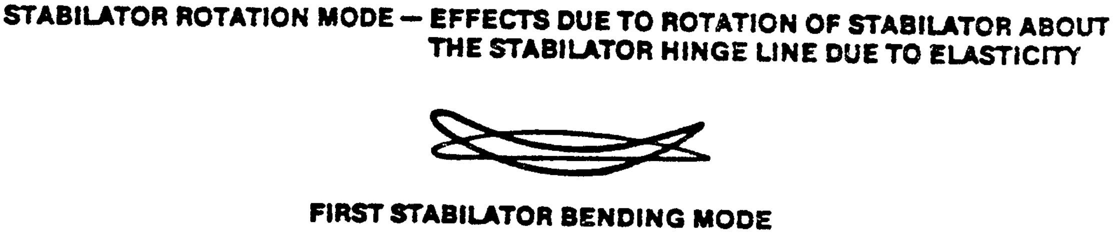
STABILATOR ROTATION MODE — EFFECTS DUE TO ROTATION OF STABILATOR ABOUT THE STABILATOR HINGE LINE DUE TO ELASTICITY
FIRST STABILATOR BENDING MODE

(b). ELASTIC STABILATOR MODES

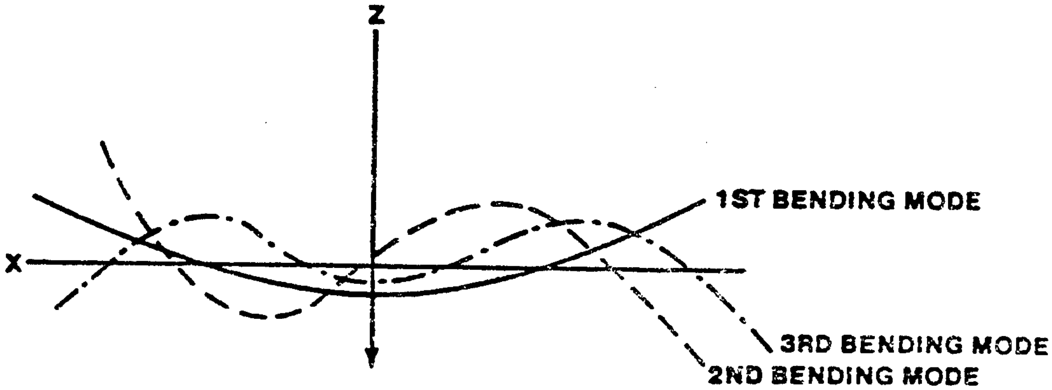
Z
X
1ST BENDING MODE
3RD BENDING MODE
2ND BENDING MODE

(c). BENDING MODE SHAPES

FIGURE 14.150. AEROELASTIC MODE AND VARIABLE DEFINITIONS

mode shapes in Figure 14.149c cross the x axis and by locating rate gyros on anti-nodal points, or points of zero slope, where $\partial\phi_1/\partial x$, $\partial\phi_2/\partial x$, $\partial\phi_3/\partial x = 0$.

Design compromises are necessary due to interference of the bending and rotation modes and due to limitations on available space for sensor location. The normal accelerometer location is usually ahead of the aircraft center of rotation and close to the node of the first fuselage structural mode. The rate gyro is normally located close to the anti-node of the first fuselage bending mode. Rate gyros located forward of this point have a destabilizing effect on the structural mode, which may require compensation to prevent driving the structural mode unstable. Rate gyros located aft of the anti-node have a stabilizing effect on the structural mode.

14.8.2.2.2 Structural Filter Compensation

The proper placement of sensors will not entirely eliminate adverse structural effects in the flight control system. Often structural filters are required to provide structural mode attentuation. A simple first order lag filter, similar to the noise filter previously discussed, or a notch filter are commonly used for this purpose.

Aircraft structural resonance is characterized by a sustained high frequency oscillation of a control surface at a resonant structural frequency, usually above 10 Hertz (62.8 radians per second). It is usually caused by control system sensors (such as rate gyros) sensing small vehicle structural vibrations (caused by control surface movement) and feeding these signals back to the control surface through the flight control system. At structural resonant frequencies, these signals are amplified and a phase lag of 180° may occur through the control system alone. If the phase lag from the sensor to the control surface is 180° and the total system gain is high enough, the surface motion will sustain itself and structural resonance will occur.

An example of the use of such a structural filter can be found in the C-star (C*) command system designed for a proposed fly-by-wire F-4E aircraft. The block diagrams of this system are shown in Figure 14.151. C* is defined as

$$C^* = -n_{z_{\text{ACCEL}}} + Kq \qquad (14.120)$$

This blended pitch rate and normal acceleration system was a common control law strategy in the late sixties and early seventies (the A-7D used a C* control law), but was found to be difficult to design for level 1 flying qualities.

The transfer function

$$\frac{C^*}{\delta_e} = \frac{1355.7(s + 2.63 \pm 5.05j)(s + 0.52 \pm 65.75j)}{(s + 4)(s + 2.08 \pm 7.02j)(s + 1.19 \pm 02.01j)} \quad \text{(g's/radian)} \qquad (14.121)$$

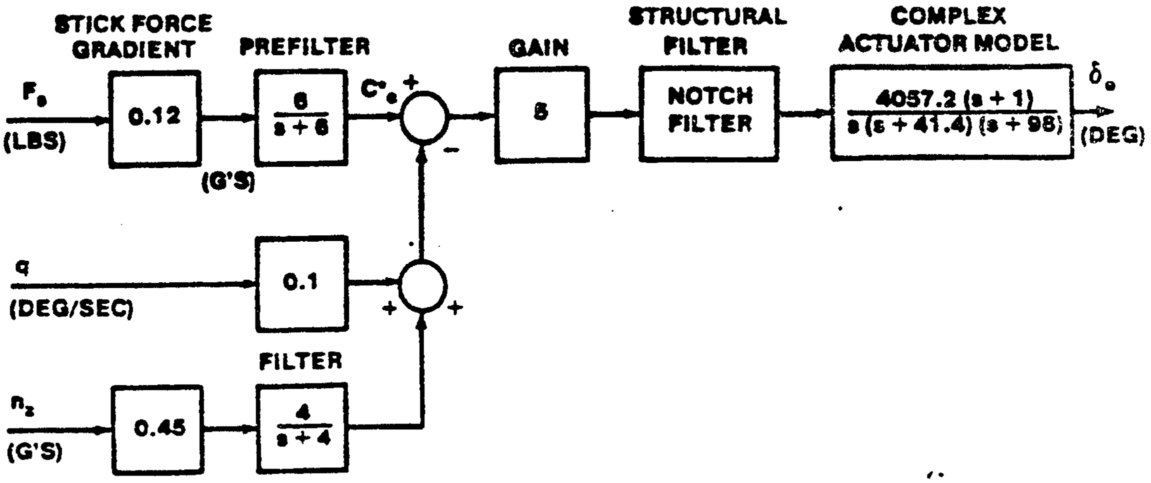
STICK FORCE GRADIENT
PREFILTER
GAIN
STRUCTURAL FILTER
COMPLEX ACTUATOR MODEL
F_s
(LBS)
0.12
$\frac{6}{s+6}$
(G'S)
C^*_c
+
−
5
NOTCH FILTER
$\frac{4057.2(s+1)}{s(s+41.4)(s+98)}$
δ_e
(DEG)
q
(DEG/SEC)
0.1
+
+
FILTER
n_z
(G'S)
0.45
$\frac{4}{s+4}$

FIGURE 14.151. PROPOSED FLY-BY-WIRE LONGITUDINAL FLIGHT CONTROL SYSTEM FOR THE F-4E AIRCRAFT

was found using the longitudinal aeroelastic matrix equation of motion (not covered in this text) for the 1.2 Mach, 5000 foot flight condition. The system designers minimized structural coupling through the pitch rate gyro by locating the gyro at a point where the first fuselage bending mode slope was essentially zero. However, the accelerometer detected some structural mode acceleration. Notice the poles and zeros at very high frequencies which result from the first fuselage bending mode and notice also that a complex actuator model is used.

The control system block diagram may be redrawn for analysis, as shown in Figure 14.152. If the notch filter is neglected, the Bode diagram of Figure 14.153 and the root locus plot of Figure 14.154 result. Notice the instability near 92 radians per second which occurs due to the structural coupling between the first fuselage bending mode and the flight control system (zero gain or phase margin in the Bode diagram and a pair of high frequency oscillatory roots in the right half s-plane in the root locus plot). This instability is due to the accelerometer sensing structural bending mode accelerations and feeding the signals back to the stabilator through the flight control system to further excite the bending mode. The overall gain of the control system must be reduced by a minimum of 15 decibels (a factor of 5.6) to maintain stability, with an accompanying degredation of handling qualities due to a reduced bandwidth and poor short period damping, unless a filter can be added to the system to suppress the coupling.

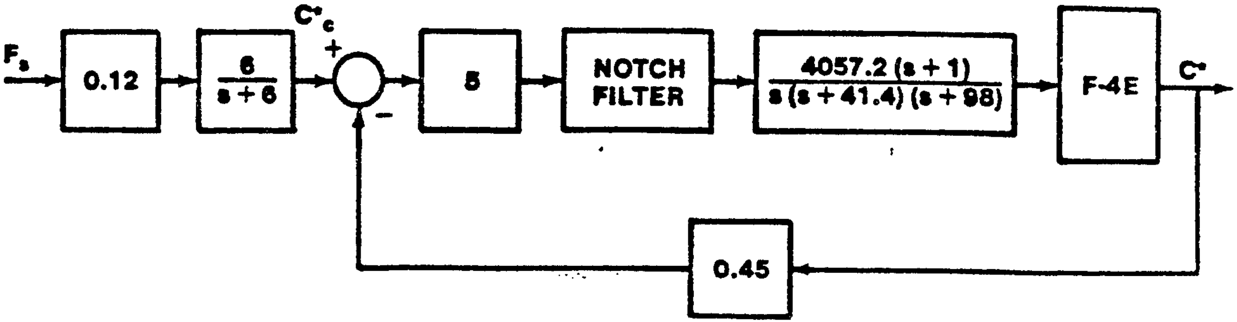

FIGURE 14.152. SIMPLIFIED LONGITUDINAL FLIGHT CONTROL SYSTEM PROPOSED FOR THE F-4E AIRCRAFT

The designers added a notch filter

$$G_{NF}(s) = \frac{0.96(s + 4.3 \pm 85.6j)}{s + 50.4 \pm 67.2j} \qquad (14.122)$$

to the system. Figure 14.155 plots a Bode diagram for this filter. The magnitude plot displays a large reduction in the ratio of the output signal to the input signal near the structural bending mode frequency of 92 radians per second, forming a notch. The magnitude ratio at low frequencies (less than about 16 radians per second) is essentially unaffected so that the short period response is not distorted by the filter. A very slight bit of phase lag occurs in the short period frequency region (about 5°) which causes a slight increase in the response time.

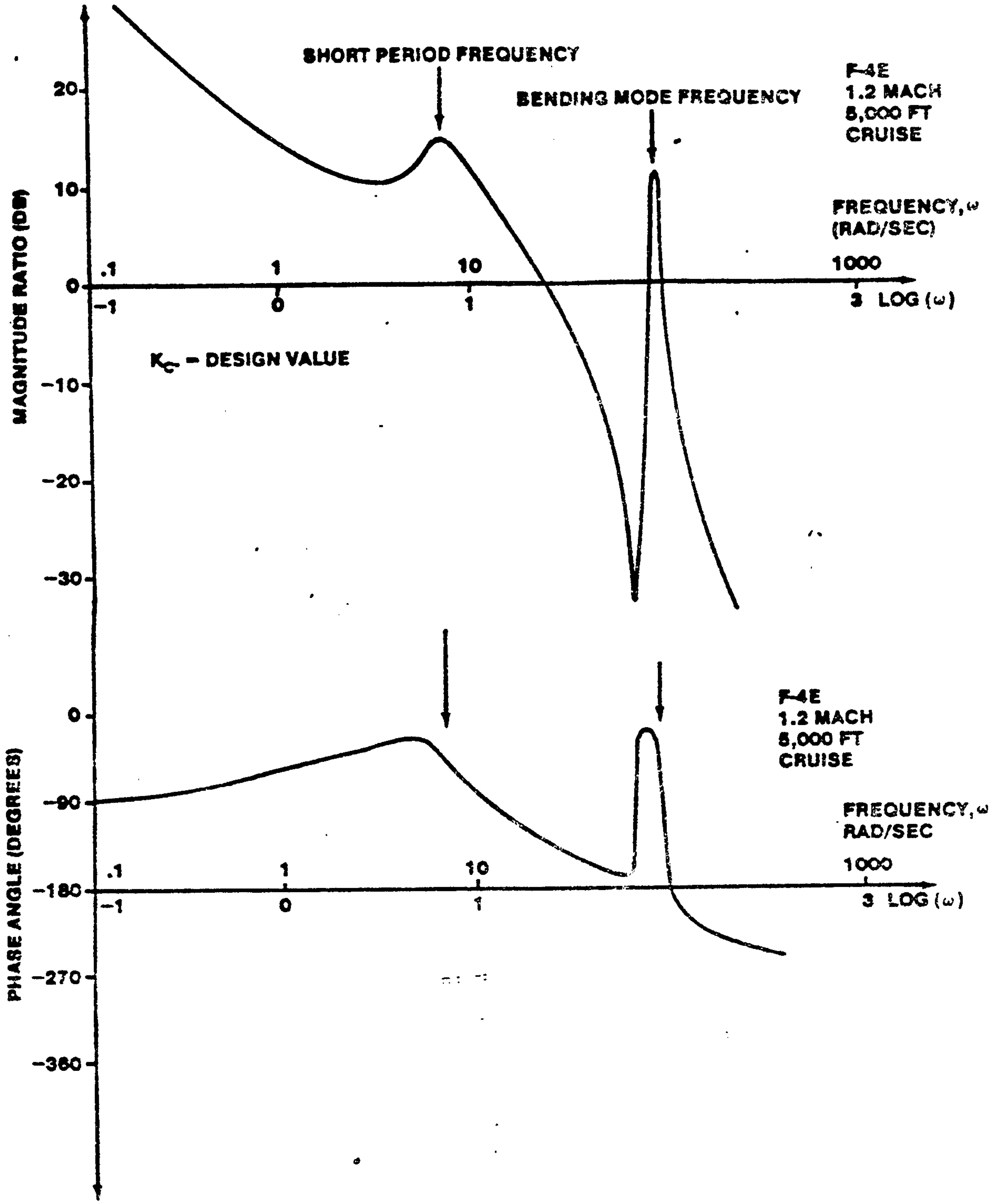

FIGURE 14.153. BODE PLOT OF C* COMMAND SYSTEM FOR F-4E SHOWING EFFECTS OF FIRST FUSELAGE BENDING MODE

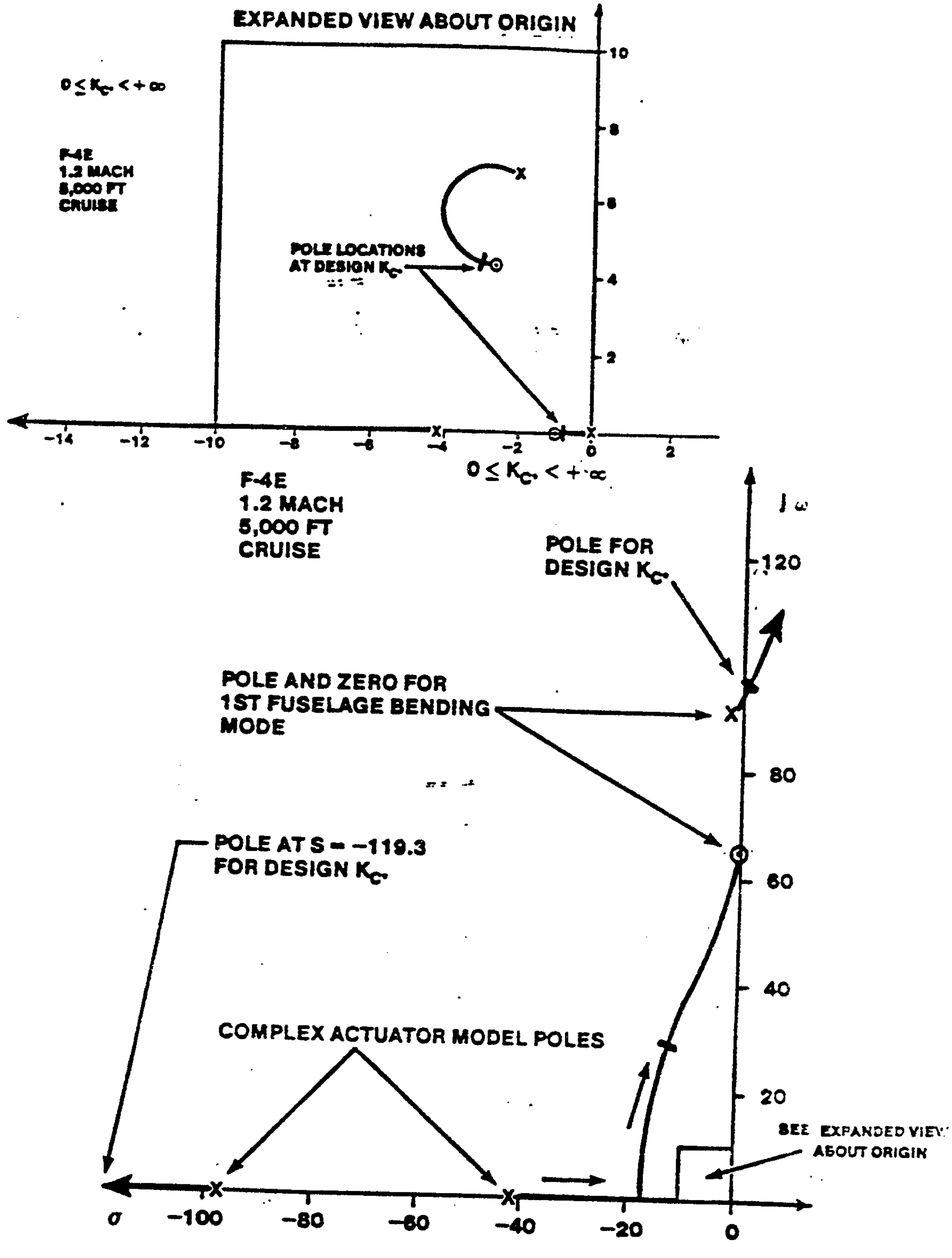

FIGURE 14.154. ROOT LOCUS OF C* COMMAND SYSTEM FOR THE F-4E SHOWING EFFECTS OF FIRST FUSELAGE BENDING MODE

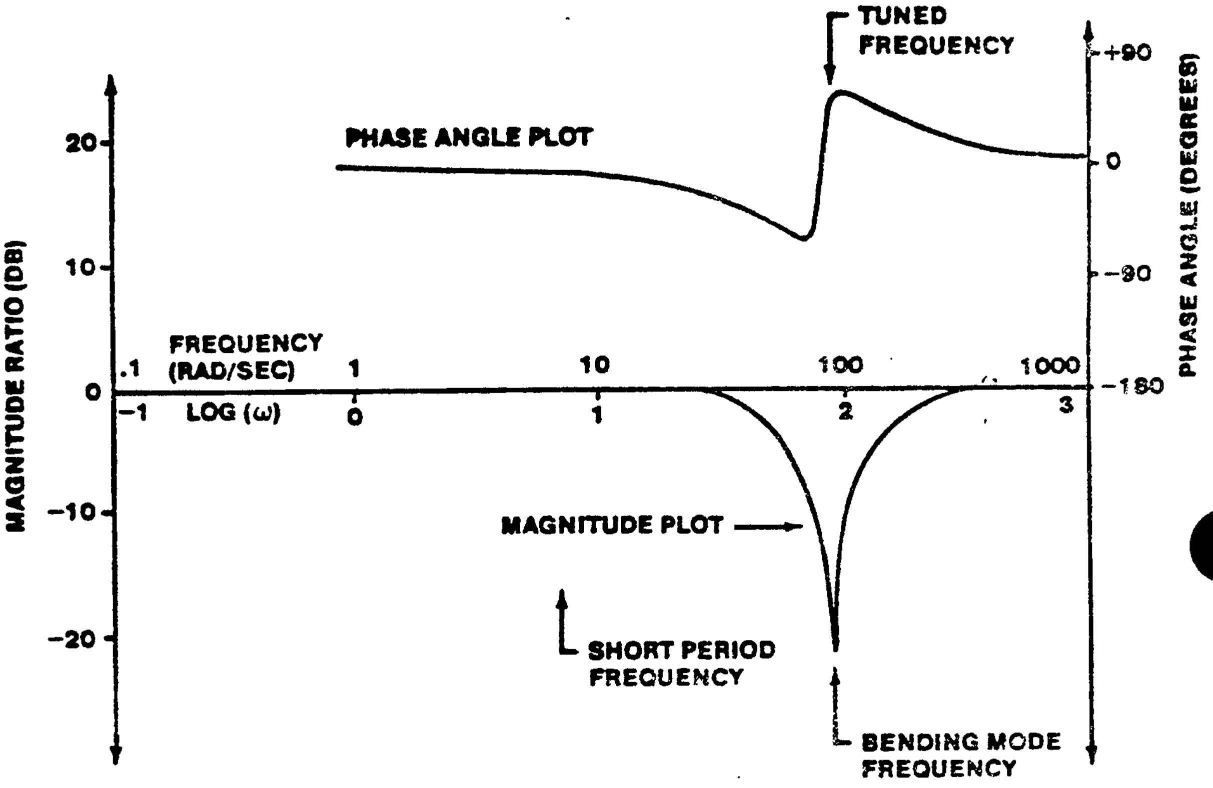

FIGURE 14.155. BODE PLOT OF NOTCH FILTER USED IN F-4E C* COMMAND FLIGHT CONTROL SYSTEM

Figure 14.156 shows the effect of the notch filter on the proposed F-4E fly-by-wire flight control system. Notice the magnitude ratio is suppressed in the vicinity of the bending mode natural frequency. Figure 14.157 presents the root locus plot for the system incorporating the structural filter. Notice that all the augmented roots of the aircraft are stable.

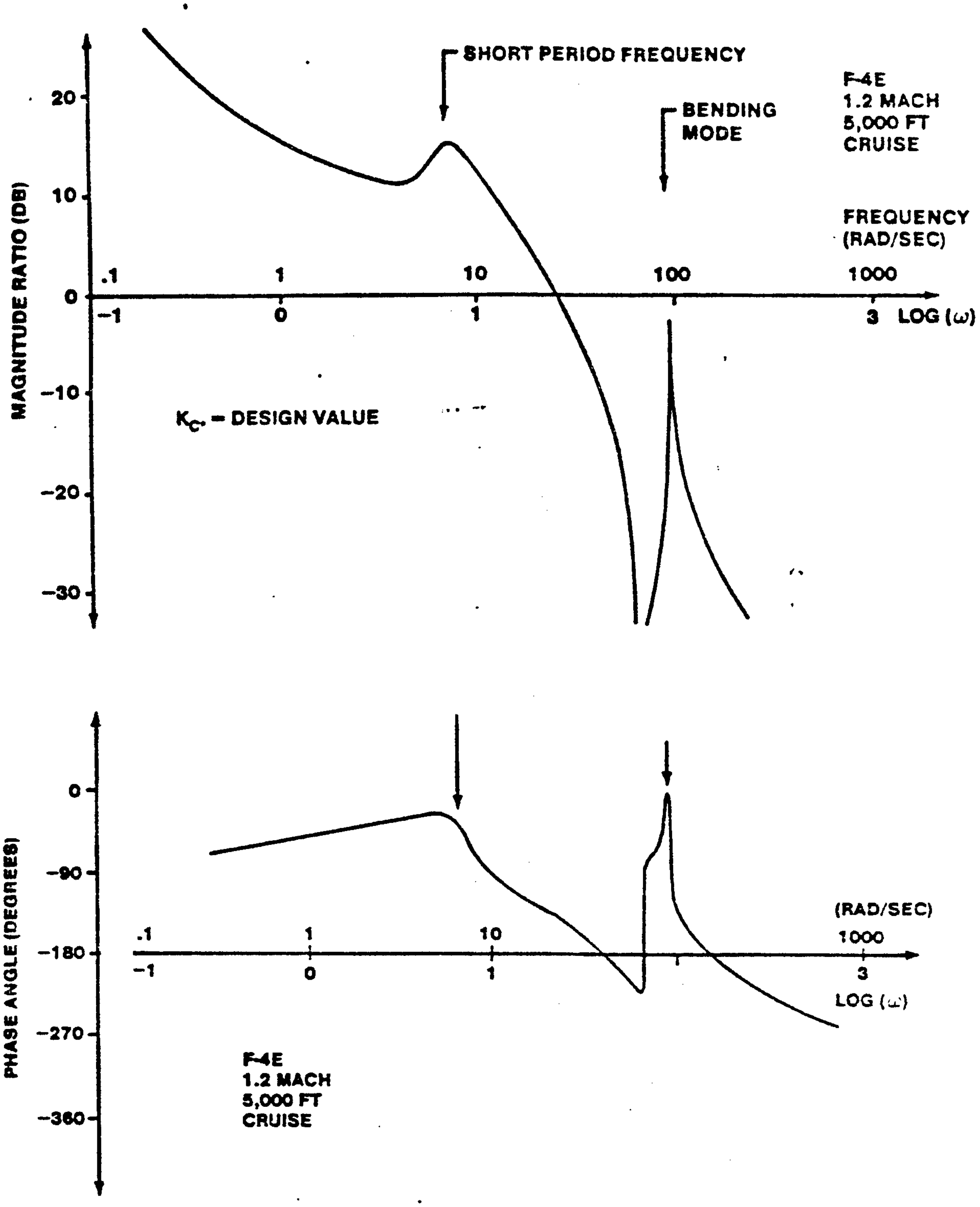

FIGURE 14.156 BODE PLOT OF C* COMMAND SYSTEM FOR F-4E SHOWING SUPPRESSION OF BENDING MODE BY STRUCTURAL FILTER

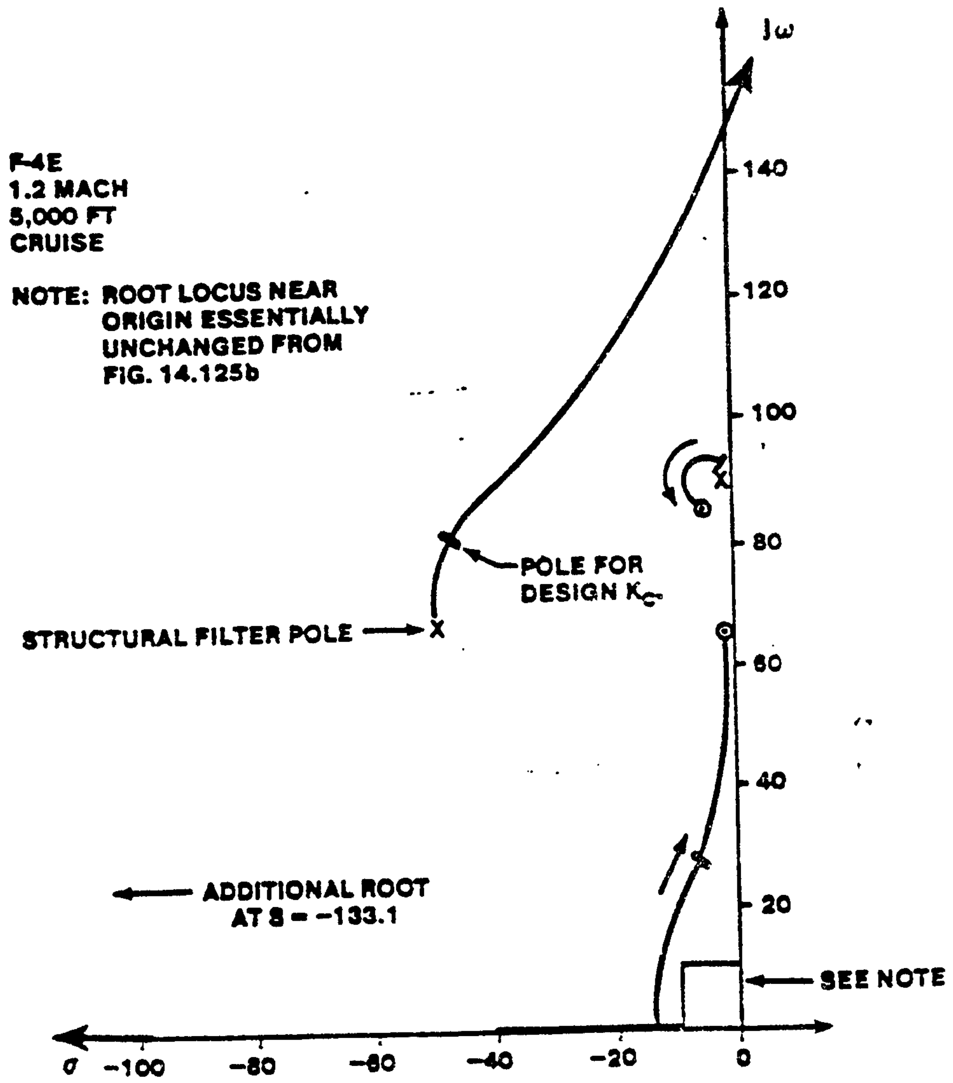

FIGURE 14.157. ROOT LOCUS PLOT OF F-4E WITH C* SYSTEM INCLUDING STRUCTURAL FILTER

14.8.3 Nonlinear Elements

Simplified linear analysis of complex systems often ignores important nonlinear effects which can greatly alter the response characteristics of closed loop control systems and may cause significant adverse or even catastrophic results. Nonlinearities in system elements, such as actuator rate limits, control surface deflection limits, mechanical hysteresis or friction, can cause system instabilities which are not evident from linear analysis.

Figure 14.158 presents four common nonlinearities encountered in flight

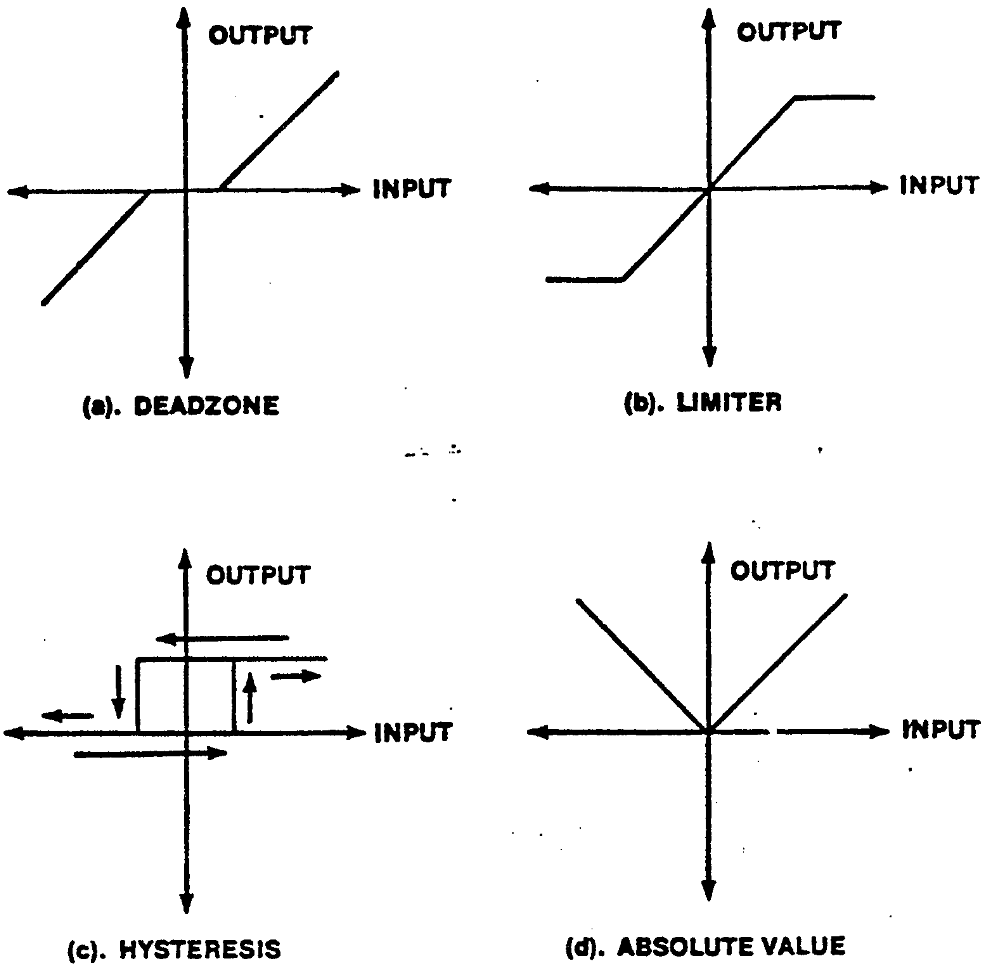
OUTPUT
INPUT
(a). DEADZONE
OUTPUT
INPUT
(b). LIMITER
OUTPUT
INPUT
(c). HYSTERESIS
OUTPUT
INPUT
(d). ABSOLUTE VALUE

FIGURE 14.158. TYPICAL NONLINEARITIES

control systems. The convention used for graphically representing nonlinear effects plots the input variable along the x axis and the output variable along the y axis. The input-output relationship must be understood when examining nonlinear elements.

The deadzone effect is typical of friction and breakout forces present in conventional pilot controller feel systems and occurs to some degree in most mechanical systems. The stick force is plotted as the input variable and the stick displacement is the output variable.

The limiter effect is typical of hydraulic actuators which can deflect an aerodynamic surface at a rate less than commanded depending on the surface aerodynamic hinge moment. Actuators also have limited motion authority due to piston movement capacity. Mechanical stops are usually provided to limit aerodynamic surface range of motion.

Hysteresis is quite common and often undesirable in pitot static instruments. Hysteresis may be useful for other applications. The A-7D maneuvering flaps display hysteresis which was intentionally designed into the system to prevent premature flap extension or retraction. When increasing angle of attack past 14 units the flaps fully extend. As angle of attack is reduced past 11 units they retract.

The absolute value nonlinearity causes a signal to pass which is of the same magnitude as the input regardless of the sign of the input.

In designing primary flight control systems it is of utmost importance to keep friction low, to avoid backlash and to prevent elastic distortions by keeping overall system stiffness as high as possible within reasonable weight constraints. Nonlinear elements in the flight control system or nonlinear operation of control system elements can lead to a limit cycle. A limit cycle is a sustained closed loop oscillation of a control surface at a frequency usually less than 5 Hertz (31.5 radians per second). It occurs when the phase margin of the flight control system loop (consisting of the aircraft, motion sensors and control system elements) is zero degrees (180 degrees of phase lag) and the control system gain is high.

Two types of limit cycles occur—stable and unstable. Stable limit cycles are low amplitude oscillations of the control surface as a result of nonlinearities about null position, such as hysterisis or deadzones. Unstable limit cycles are a result of system saturation such as actuator rate limiting, and are large amplitude divergent oscillations of a control surface, which eventually cause the surface to oscillate between the mechanical limits at the maximum actuator rate. The low amplitude oscillation is undesirable in general, but is usually not catastrophic. The large amplitude oscillation is catastrophic in that loss of control could occur at low speed and structural failure will occur at high speed.

The limit cycle problem can be alleviated by lead compensation to increase the phase margin of the control system in the susceptible frequence range. Another approach to alleviate or reduce limit cycle problems is to reduce the system gain. The lead compensation is usually used so that a sufficiently high gain is maintained to provide the desired handling qualities, that would normally be degraded by a system gain reduction.

14.9 DIGITAL CONTROL SYSTEMS

The methods used in the augmentation systems presented in sections 14.5 to 14.8 were all based on the assumption that the flight control systems were analog (continuous signal). Many modern flight control systems, in reality, have digital components or processors. One distinct advantage of digital controllers or a complete digital flight control system is that they are more versatile than analog systems. The program which characterizes a digital system can be modified to accommodate design changes without any variations in the hardware. Digital components in the form of electronic parts, transducers and encoders, are often more reliable, more rugged in construction, and more compact in size than their analog equivalents. Other advantages include improved sensitivity, no drift, less cost and less effect due to noise and disturbance.

With all these advantages of digital systems over analog the reader may well ask: why then the continued heavy emphasis on synthesis methods which are valid only for analog type systems? The answer is to be found in the fact that as long as the sampling frequency and speed of computation are high compared with the highest break-frequency in the airplane open loop transfer functions, the analog based analysis methods are a perfectly good approximation.

This points out, however, the fundamental problem associated with digital systems: the lag introduced by the sampling process. A sampled (digitized) signal is required because a digital system uses discrete (not analog) signals. The amount of lag introduced by the sampling process (a low pass filter) is a direct function of the frequency of the sampler (sampling rate). Care must be given in selecting a sampling frequency. It must be high enough to provide a stable system (not introduce excessive lag) but low enough to allow the system to perform all the necessary digital calculations between samples.

Compromises are often required when selecting sampling rate. For example the Advanced Fighter Technology Integration (AFTI)/F-16 digital flight control system operates on the fundamental frequency of 64 cycles per second (Hertz). This is sufficient to ensure system stability. Because of limitations on the speed of computations, however, some inputs to the flight control system, such as altitude, are sampled at a lower rate—as low as 4 Hz. These low sample rates have resulted in flight control system problems as the capabilities of the flight control system have been increased from the original design. Increases in the speed of computation which are expected in future systems will allow higher sampling frequencies and therefore increase system stability.

The following sections will briefly describe the fundamentals of analog-to-digital (sampling) and digital-to-analog conversion. From this, an appreciation for the restrictions on sampling frequency can be seen. A more extensive discussion of digital control systems and their analysis is beyond the scope of this text.

14.9.1 Analog-to-Digital Conversion

The A/D (analog-to-digital converter) device is essentially a data sampling device. The A/D converter translates an analog signal into a digital signal. The first step in the A/D process is to sample the signal through a process illustrated schematically in Figure 14.159.

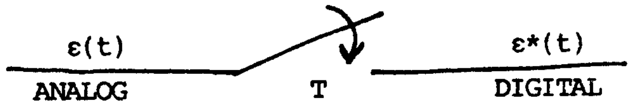

FIGURE 14.159. SYMBOLIC REPRESENTATION OF A SAMPLER OPERATION

A sampler takes an analog signal $\varepsilon(t)$ and translates it into a digital signal $\varepsilon^*(t)$. The sampler may be thought of as a device which multiples a unit-impulse train $\delta_T(t)$ by the analog signal $\varepsilon(t)$ to obtain the digital signal $\varepsilon^*(t)$:

$$\varepsilon^*(t) = \varepsilon(t)\ \delta_T(t) \tag{14.123}$$

where the unit-impulse train $\delta_T(t)$ is a train of impulses with unity area given by

$$\delta_T(t) = \sum_{n=-\infty}^{\infty} \delta(t-nT) \tag{14.124}$$

such that $\delta(t-nT)$ represents an impulse of unit area at time nT. The quantity T is referred to as the sampling period. In practical airplane systems T ranges from roughly 1 sec to .001 sec, depending upon the application. It is fair to assume that systems dealing with rapidly time-varying phenomena need faster sampling (and computing) than do systems with slowly time-varying phenomena.

Combining the above equations yields

$$\varepsilon^*(t) = \varepsilon(t) = \sum_{n=-\infty}^{\infty} \delta(t-nT) = \sum_{n=-\infty}^{\infty} \varepsilon(nT)\delta(t-nT) \qquad (14.125)$$

In nearly all airplane applications it is reasonable to assume $\varepsilon(t) = 0$ for $t < 0$ so that the equation may be written as

$$\varepsilon^*(t) = \sum_{n=0}^{\infty} \varepsilon(nT)\delta(t-nT) \qquad (14.126)$$

An illustration of how a sampler works in accordance with this equation is shown in Figure 14.160.

An A/D converter usually is designed to maintain the last sampled value between sampling intervals—this gives rise to a series of steps instead of impulses as illustrated in figure 1.161. This is known as a hold device which simply maintains or "freezes" the value of the pulse or digital signal between the sampling intervals. In a majority of the practical digital operations, sample and hold are performed by a single unit, and the device is known commercially as sample-and-hold, or S/H.

Sampling the signal is only the first step in analog-to-digital conversion. The second step is to give the sampled signal a discrete value which can be used for digital computation. To do this the range of possible signal outputs is divided into discrete intervals, assigned values, and compared to the sampled signal. A discrete value chosen and is then available for input into the digital computer. This last step is termed encoding and completes the A/D conversion.

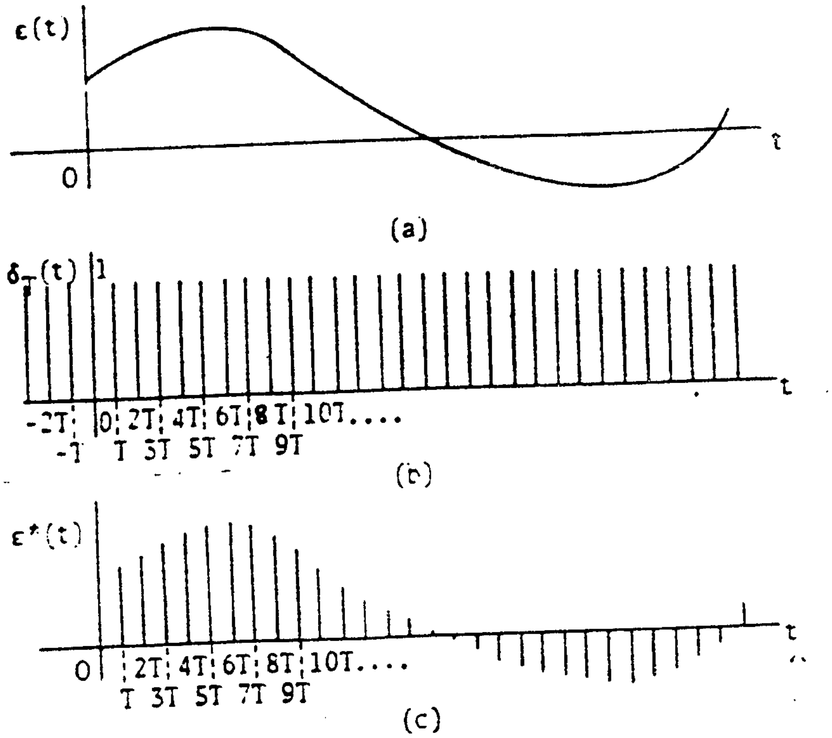
ε(t)
t
0
(a)
δT(t)
1
t
-2T -T 0 T 2T 3T 4T 5T 6T 7T 8T 9T 10T....
(b)
ε*(t)
t
0 T 2T 3T 4T 5T 6T 7T 8T 9T 10T....
(c)

FIGURE 14.160. SIGNAL FORMS ILLUSTRATING THE SAMPLING OPERATION OF AN IDEAL SAMPLER, (A) ANALOG INPUT SIGNAL TO SAMPLER, (B) UNIT-IMPULSE TRAIN (TRAIN OF IMPULSES WITH UNITY AREA), (C) DIGITAL OUTPUT SIGNAL OF SAMPLER

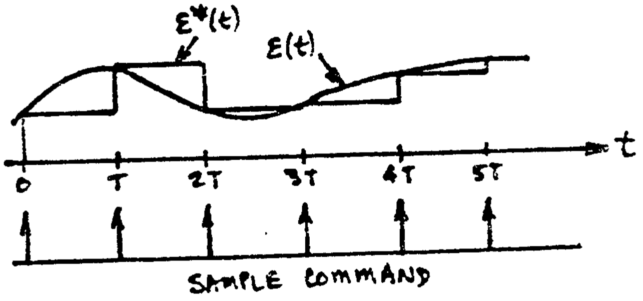
ε*(t)
ε(t)
t
0
T
2T
3T
4T
5T
SAMPLE COMMAND

FIGURE 1.161 INPUT AND OUTPUT SIGNALS OF AN IDEAL S/H

It should be noted that the output signal ε*(t) describes the value of ε(t) only at the sampling instants nT. It does not contain any information on the value of ε(t) during the sampling period from nT to (n+1)T. Figure 14.162 illustrates the consequence of this: two rather different signals have the same digital (sampled) signals. In practical systems this is not a problem as long as T is sufficiently small generating a frequency near the fundamental

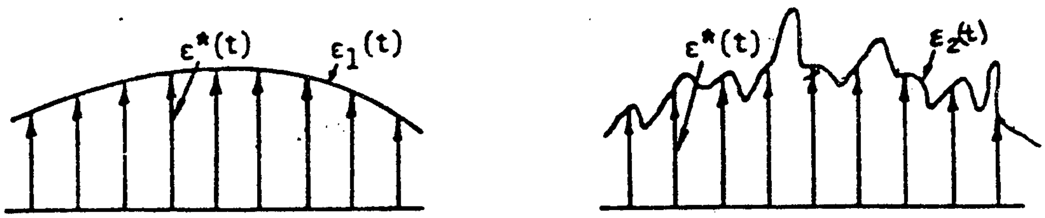

FIGURE 14.162. EXAMPLE OF DIFFERENT ANALOG SIGNALS WITH THE SAME SAMPLED SIGNAL VALUES

frequencies of the input or very high frequencies signals are intentionally being eliminated. It is obvious, however, that no matter how high the frequency of the sampler, some high frequencies are lost which shows how an A/D converter is a low pass filter. An A/D conversion is sometimes referred to as encoding or modulation.

14.9.2 Digital-to-Analog Conversion

Before a digital signal can be used in a practical analog control situation, such as an input to an actuator, it is necessary to reconfigure it into an analog signal. This is because most control systems have components which are designed to be actuated by continuous-date (analog) signals. The smoothing of the pulse signals is, therefore, necessary. Otherwise these analog components may be subject to excessive wear. This is done with a digital-to-analog (D/A) converter.

In order to reconstruct an analog signal an assumption must be made about the signal value between sampling intervals. A device called a zero order hold assumes that the value is constant which gives an output from the D/A converter similar to an S/H output of an A/D converter as shown in Figure 14.163.

Another common D/A device is called a first order hold and assumes that the values of the signal at the current and previous sample can be used to direct a slope indicating the value at the next sample period. The output value of the first order hold is shown in Figure 14.164. Higher under hold devices are possible but are not often used.

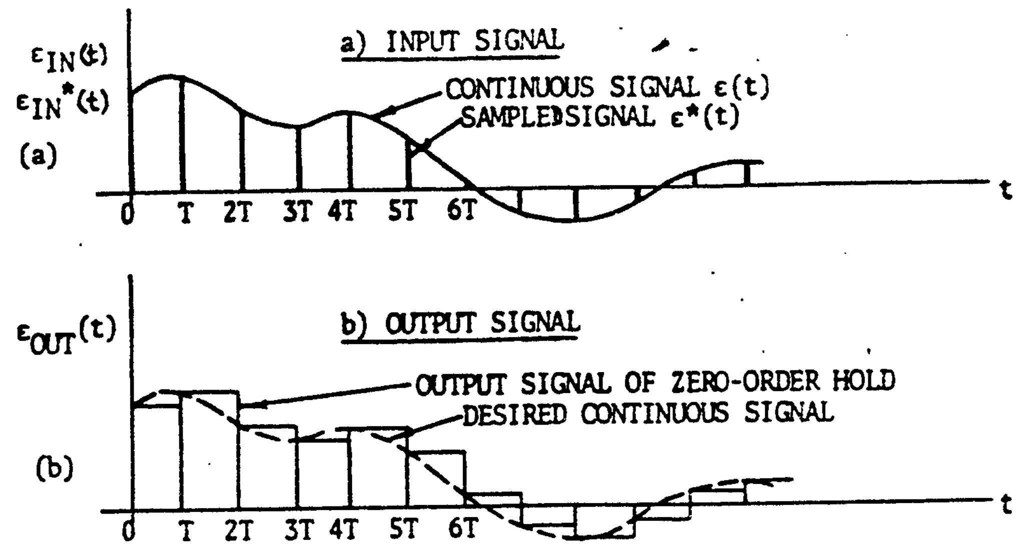

FIGURE 14.163 ZERO ORDER HOLD IN THE TIME DOMAIN, (a) INPUT SIGNAL ε(t), AND SAMPLED SIGNAL ε*(t), (b) OUTPUT WAVEFORM OF ZERO-ORDER HOLD CIRCUIT AND CONTINUOUS SIGNAL ε(t)

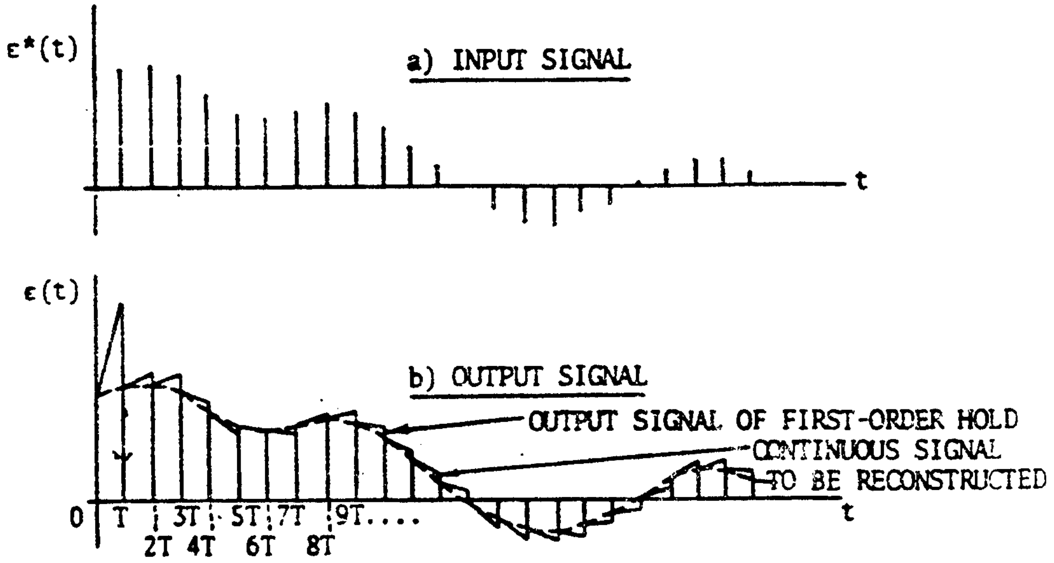

FIGURE 14.164 EXAMPLE OF FIRST-ORDER HOLD OPERATION IN THE TIME DOMAIN

14.10 FLY-BY-WIRE FLIGHT CONTROL SYSTEMS

The most modern flight control systems have replaced the mechanical linkages between the pilot controllers and the control surface with wires carrying electrical actuation signals from flight control computers. The flight control computers are basically control augmentation system with 100% control authority. Systems of this type have come to be known as fly-by-wire flight control systems.

14.10.1 Advantages of Fly-by-Wire Control

Fly-by-wire flight control systems generally have four advantages over more traditional mechanical system with augmentation:

1. Reduced weight - the electrical components and wiring weigh considerably less than equivalent mechanical components. This translates into greater range, payload or maneuverability.

2. Increased Capabilities - Because the fly-by-wire system has greater authority than a SAS or CAS, and is not influenced by a parallel mechanical system it is capable of more sophisticated control, such as load factor limiting or departure prevention. It also has more consistent operation throughout the flight envelope.

3. Greater Combat Survivability - A mechanical flight control system generally has only one set of mechanical linkages from the pilot. If one of these cables is damaged in combat the result could be the loss of aircraft. Fly-by-wire systems tend to have three to four separate command paths (wires) to each actuator. If one of these wires is damaged in combat the full flight control system will still be operating through the other wires.

4. Easier Modification - Since there are not mechanical elements to the flight control system (other than actuators), modifications are easier because it can be accomplished by reprogramming the flight control computers. This is easier in a digital system because it involves software changes while analog systems involve wiring or component changes.

Fly-by-wire control systems, because of their increased capabilities, tend to be more complicated than control augmentation systems. They are made up of the basic stability augmentation, control augmentation, compensation devices and sensors that have been discussed. It is interesting to note, however, that some of the advanced aircraft with fly-by-wire control systems have elected not to use the conventional pilot control system with artificial feel. This allows a more efficient use of cockpit space and a more comfortable positioning of the controls. For example, the F-16 uses isometric force controllers and lacks an artificial feel system, although some movement in the controller (proportional to the pilot force) has proven to be helpful in reducing pilot-induced oscillation tendencies, especially in the roll axis.

14.10.2 Analysis of a Simplified Fly-by-Wire Control System

Effective flight control testing depends on a thorough understanding of the flight control operation. This section provides the test pilot and flight test engineer a background in flight control system simplification and analysis. A simplified F-16 multiloop longitudinal flight control system will be used as an example.

Figure 14.165 presents a block diagram for the F-16 flight control system simplified for linear analysis (leading edge flaps locked up). Gains F2 and F3 are scheduled with the flight condition, gain F2 being a function of dynamic pressure divided by static pressure and gain F3 being a function of dynamic pressure alone. The gains shown are for the flight condition to be analyzed (0.6 Mach at sea level). The aircraft transfer functions are:

$$\Delta(s) = (s - 0.087)\ (s + 2.373)\ (s + 0.098 \pm 0.104j) \tag{14.125}$$

$$N^{\alpha}_{\delta_e}(s) = 0.203\ (s + 0.0087 \pm 0.067j)\ (s + 106.47) \text{ deg/deg} \tag{14.126}$$

$$N^{q}_{\delta_e}(s) = 21.516\ s\ (s + 0.0189)\ (s + 1.5) \text{ deg/sec/deg} \tag{14.127}$$

$$N^{n_z}_{\delta_e}(s) = 0.0889\ s\ (s + 0.0158)\ (s + 1.165 \pm 11/437j) \text{ g's/deg} \tag{14.128}$$

where

$$G^{\alpha}_{\delta_e} = \frac{N^{\alpha}_{\delta_e}(s)}{\Delta(s)} \tag{14.129}$$

and similarly for

$$G^{q}_{\delta_e}(s) \text{ and } G^{n_z}_{\delta_e}$$

The load factor transfer function is for the accelerometer location.

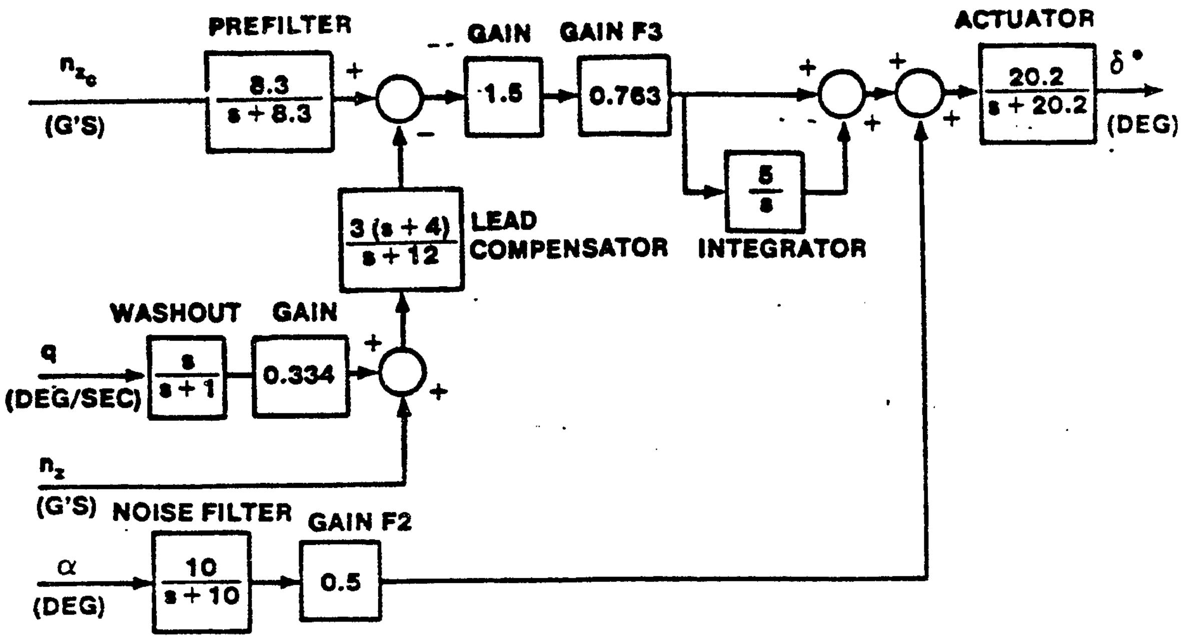
PREFILTER
GAIN
GAIN F3
ACTUATOR
n_{z_c}
(G'S)
$\frac{8.3}{s+8.3}$
1.5
0.763
$\frac{20.2}{s+20.2}$
δ_e
(DEG)
$\frac{5}{s}$
INTEGRATOR
$\frac{3(s+4)}{s+12}$
LEAD COMPENSATOR
WASHOUT
GAIN
q
(DEG/SEC)
$\frac{s}{s+1}$
0.334
n_z
(G'S)
NOISE FILTER
GAIN F2
α
(DEG)
$\frac{10}{s+10}$
0.5
+
-
+
+
+
+
+
+
+

FIGURE 14.165 SIMPLIFIED F-16 LONGITUDINAL AXIS FLIGHT CONTROL SYSTEM, 0.6 MACH AT SEA LEVEL

Prior to analyzing any block diagram it is necessary to perform a units check to make sure the diagram is consistent for the desired inputs and outputs. It is very common to have unit errors in block diagrams. These errors are usually manifested as unit conversion errors and will result in gain errors, e.g. 32.2 ft/sec^2/g (gravitational acceleration) or 57.3 deg/rad (angular relationship). Before investing a lot of work, determine and check the units at the summing functions to ensure the units match. If a flight control system report is to be made, it is useful to include units on the block diagram.

The next step is to determine the sign convention used in the block diagram. The sign convention is often that of the contractor's and it is important to be able to work with different sign conventions in order to fully understand control diagrams from various sources. It is also not uncommon to find sign errors in block diagrams. The two most common sign conventions (TPS and NASA) were given in Table 14.1

One way to determine which sign convention is used in a block diagram is to assume an aircraft motion which in turn produces a given sense to the control surface movement feedback variables. In almost all cases the feedback signal for a stability augmentation system (SAS) should attempt to move the control surface in a direction to counteract the assumed aircraft motion. As noted in section 14.3.5 the sign of the $G_{\delta_e}^{q}$, $G_{\delta_a}^{p}$ and $G_{\delta_R}^{r}$ gain terms also indicate the sign convention.

Once the sign convention and units are determined, the block diagram can be redrawn to clearly see the feedback loops. Figure 14.166 presents the block diagram in a clearer format. The forward path gains have been combined and the integral plus proportional paths have been added together. Although this diagram shows the relationship of the feedback loops in a clearer format (since the angle of attack loop is clearly shown to be the innermost feedback loop) it is still not completely satisfactory for analysis purposes. The aircraft block needs to be simplified so that the elements of each loop analysis are clearly defined and the lead filter must be relocated so that the pitch rate and load factor feedback paths add directly to the forward path. Two options are possible for the lead filter: adding it into the forward path, in which case a compensating filter must be added to the command path in accordance with block diagram reduction procedures (the inverse of the lead filter must be added), or adding the lead filter to each of the feedback paths which pass through it (pitch rate and load factor feedbacks) but separating the two feedback paths for clarity. The second option is chosen as being the most logical since the command path is left unchanged and all elements in each feedback path are accurately shown. Figure 14.167 shows the simplified block

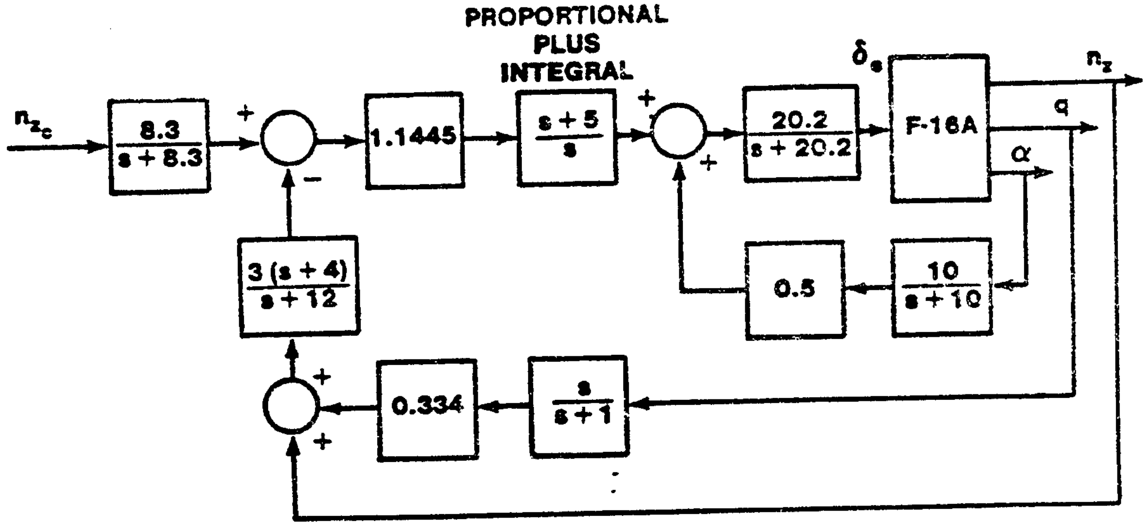

FIGURE 14.166 SIMPLIFIED F-16 LONGITUDINAL AXIS FLIGHT CONTROL SYSTEM SHOWING FEEDBACK LOOPS

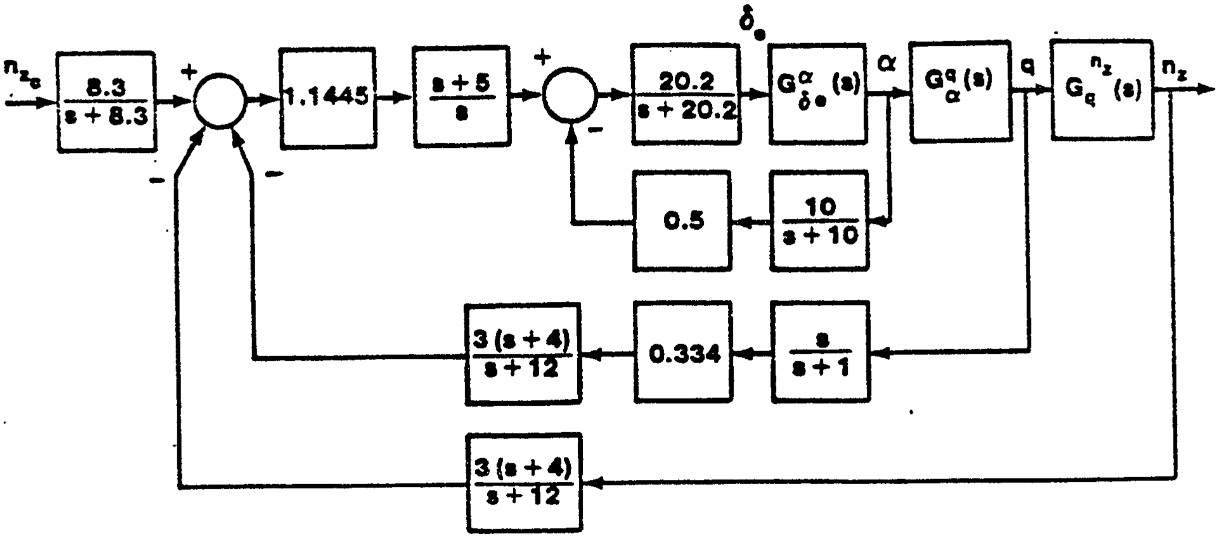

FIGURE 14.167 SIMPLIFIED F-16 LONGITUDINAL FLIGHT CONTROL SYSTEM IN FORMAT FOR ANALYSIS

diagram for the analysis. The pitch rate and load factor loops could have been interchanged (pitch rate outer loop, load factor inner loop) with a corresponding change in the aircraft block diagrams, but the load factor loop is selected as the outermost loop since the pilot commands load factor.

The angle of attack feedback loop, being the innermost loop, is analyzed first. Looking at the characteristic roots of the aircraft transfer function and realizing that the F-16 is statically unstable due to an aft center of gravity, the angle of attack feedback will stabilize the aircraft roots and should separate the nondistinct short period and phugoid characteristics into the more conventional configuration. It was noted earlier that angle of attack feedback augments the M_α stability derivative which tends to stabilize a statically unstable aircraft and moves the short period to a higher natural frequency.

The open loop transfer of the innermost loop is

$$GH_{\alpha \text{ loop}} = \underbrace{\frac{0.203\ (s + 0.0087 \pm 0.067j)\ (s + 106.47)}{(s - 0.087)\ (s + 2.373)\ (s + 0.098 \pm 0.104j)}}_{\text{Aircraft}} \ \underbrace{\frac{20.2}{s + 20.2}}_{\text{Actuator}} \ \underbrace{\frac{5}{s + 10}}_{\text{Feedback Elements}} \tag{14.130}$$

and the root locus is plotted in Figure 14.168. The closed loop transfer function characteristic equation (denominator poles) is found from the root

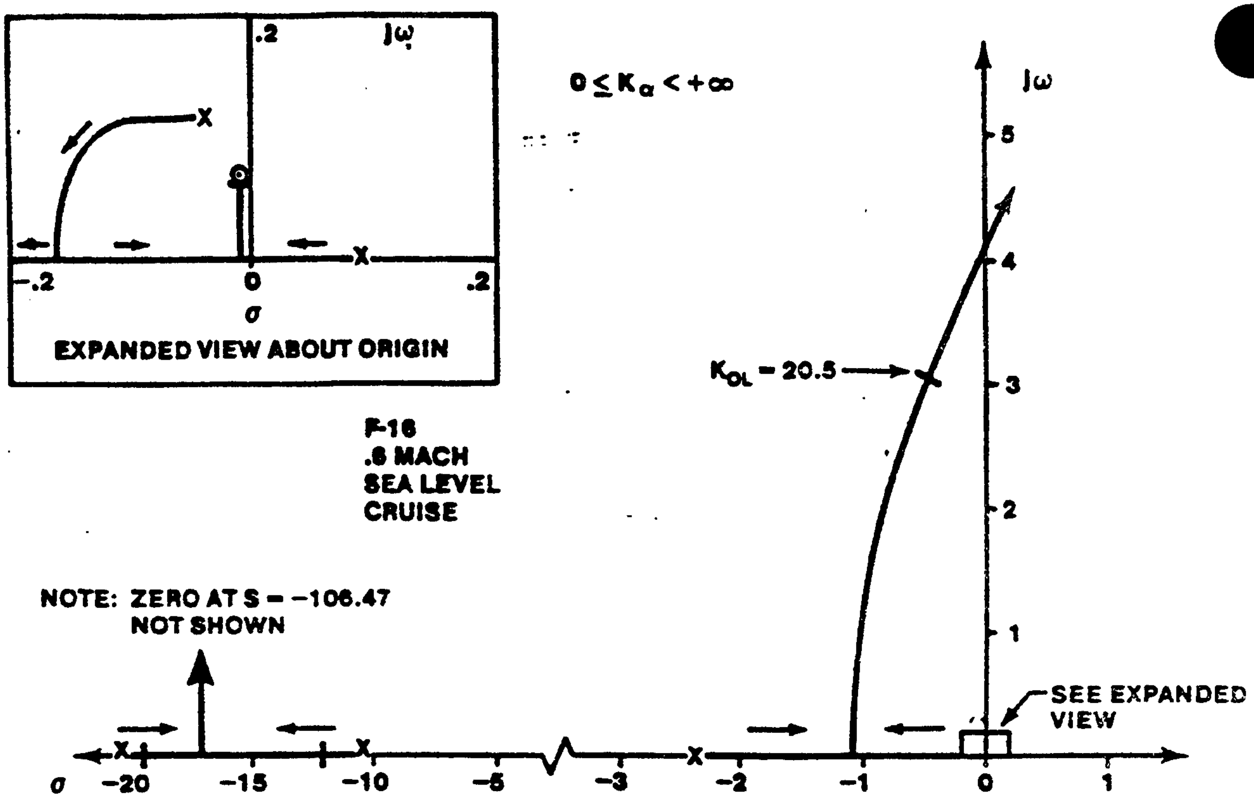

FIGURE 14.168 ROOT LOCUS PLOT OF ANGLE OF ATTACK FEEDBACK LOOP FOR THE F-16A AIRCRAFT

locus analysis. The open loop gain is $K_{\alpha\ \text{loop}} = 20.5$. The points on the root locus corresponding to this gain are the closed loop characteristic roots. The closed loop gain is equal to the forward path gain, and the closed loop zeros are the forward path open loop zeros and the feedback path open loop poles. The closed loop transfer function becomes, for the design gains

$$G^{\alpha}_{\alpha_c}\Big|_{\text{loop closed}} = \frac{4.1\ (s + 0.0087 \pm 0.067j)\ (s + 106.47)\ (s + 10)}{(s + 0.0083 \pm 0.0643j)\ (s + 0.478 \pm 3.03j)\ (s + 12.1)\ (s + 19.6)} \qquad (14.131)$$

where the (s + 10) zero is from the feedback path. Notice the roots at $(s + 0.478 \pm 3.03j)$. These roots are the short period roots and, as a result of the angle of attack feedback, the aircraft has effectively acquired longitudinal static stability and looks like a conventional aircraft. The short period damping, however, is low, being $\zeta_{sp} = 0.156$ and must be augmented. The short period natural frequency is

$$\omega_{n_{sp}} = 3.07 \text{ rad/sec} \quad (n/\alpha = 29.6 \text{ g's/rad})$$

which is at the boundary between level 1 and level 2 in MIL-F-8785C. Pitch rate feedback is used to improve the short period damping but should not change the short period natural frequency significantly. The analysis thus far has indicated a potential handling qualities problem due to a low short period natural frequency.

Figure 14.167 can now be simplified further resulting in Figure 14.169.

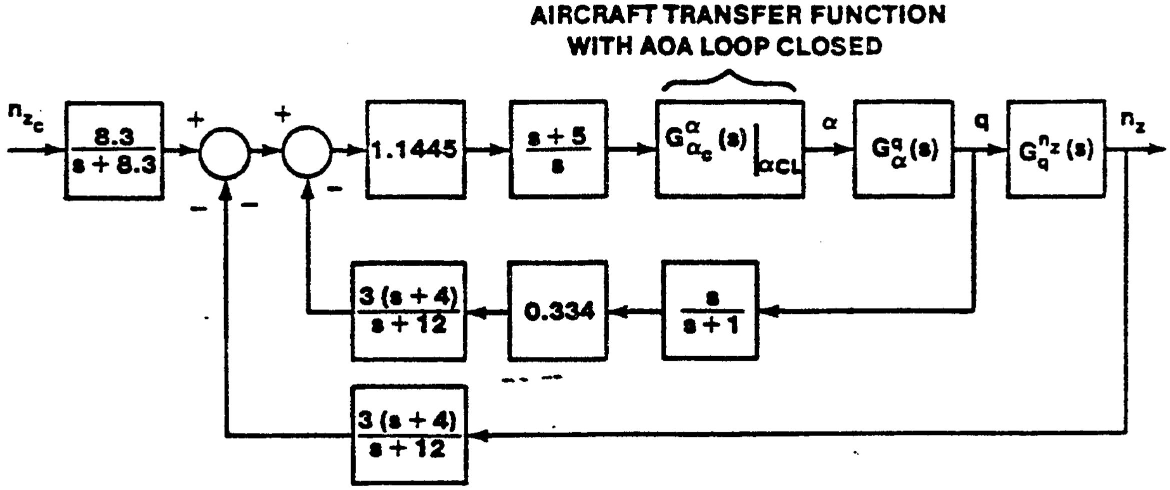

AIRCRAFT TRANSFER FUNCTION
WITH AOA LOOP CLOSED
n_{z_c}
$\frac{8.3}{s+8.3}$
+
-
-
+
-
1.1445
$\frac{s+5}{s}$
$G^{\alpha}_{\alpha_c}(s)\Big|_{\alpha CL}$
α
$G^{q}_{\alpha}(s)$
q
$G^{n_z}_{q}(s)$
n_z
$\frac{3(s+4)}{s+12}$
0.334
$\frac{s}{s+1}$
$\frac{3(s+4)}{s+12}$

FIGURE 14.169 SIMPLIFIED F-16 FLIGHT CONTROL SYSTEM WITH ANGLE OF ATTACK CLOSED LOOP TRANSFER FUNCTION REPLACING ANGLE OF ATTACK LOOP

Next, the transfer function

$$G^{q}_{\alpha_c}(s)\Big|_{\alpha \text{ loop closed}} = G^{\alpha}_{\alpha_c}\Big|_{\alpha \text{ loop closed}} G^{q}_{\alpha}(s) \qquad (14.132)$$

is formed, where

$$G^{q}_{\alpha}(s) = \frac{N^{q}_{\delta_e}(s)}{N^{\alpha}_{\delta_e}(s)} \qquad (14.133)$$

Notice that the zeros and gain of the pitch rate numerator replace the zeros and gain of the angle of attack closed loop transfer function, but that the zero which resulted from the noise filter on the angle of attack signal and the gain of the actuator remain. The open loop transfer function of the pitch rate loop becomes

$$GH_{q\ \text{loop}} = \underbrace{\frac{434.6232\, s(s + 0.0189)\ (s + 1.5)}{(s + 0.0083 \pm 0.0634j)\ (s - 0.478 \pm 3.03j)\ (s + 12.1)\ (s + 19.6)}}_{\text{Pitch Rate Transfer Function with a Loop Closed}}$$

$$\times \underbrace{\frac{1.1445\ (s + 5)}{s}}_{\substack{\text{Forward Path}\\ \text{Elements}}} \times \underbrace{\frac{1.002\, s(s + 4)}{(s + 1)\ (s + 12)}}_{\substack{\text{Feedback}\\ \text{Elements}}} \qquad (14.134)$$

where $K_{OL} = 498.42$.

Once again plotting the root locus (Figure 14.170) and selecting the roots matching the design open loop gain, the closed loop transfer function for the system with both the angle of attack and pitch rate feedback loops closed becomes

$$G^{C}_{q_c}(s)\Big|_{\alpha,q\ CL} = \frac{497.43\ (s + 0.0189)\ (s + 1.5)\ (s + 10)\ (s + 5)}{(s + 0.0093 \pm 0.023j)\,(s + 1.33)\,(s + 3.78 \pm 2.68j)\,(s + 10.2)}$$

$$\times \frac{(s + 1)\ (s + 12)}{(s + 13.3 \pm 20.2j)} \qquad (14.135)$$

The phugoid roots are altered slightly. Because of the zeros at (s + 4) and (s + 5) in the open loop equation, the frequency of the short period roots, (s + 3.78 ± 2.68j), has been increased significantly from $\omega_{n_{sp}} = 3.07$ rad/sec to 4.63 rad/sec as well as the short period damping, from $\zeta_{sp} = 0.156$ to 0.816. The pitch rate feedback loop has moved the short period natural frequency further into the level 1 area, but the frequency is still somewhat low and remains an area of concern for high gain tracking tasks. A new significant root has appeared at (S + 1.33). The effects of this root are of concern due to its low frequency. A zero is close by at (s + 1), but not really close enough to cancel completely the effects of the pole. This root

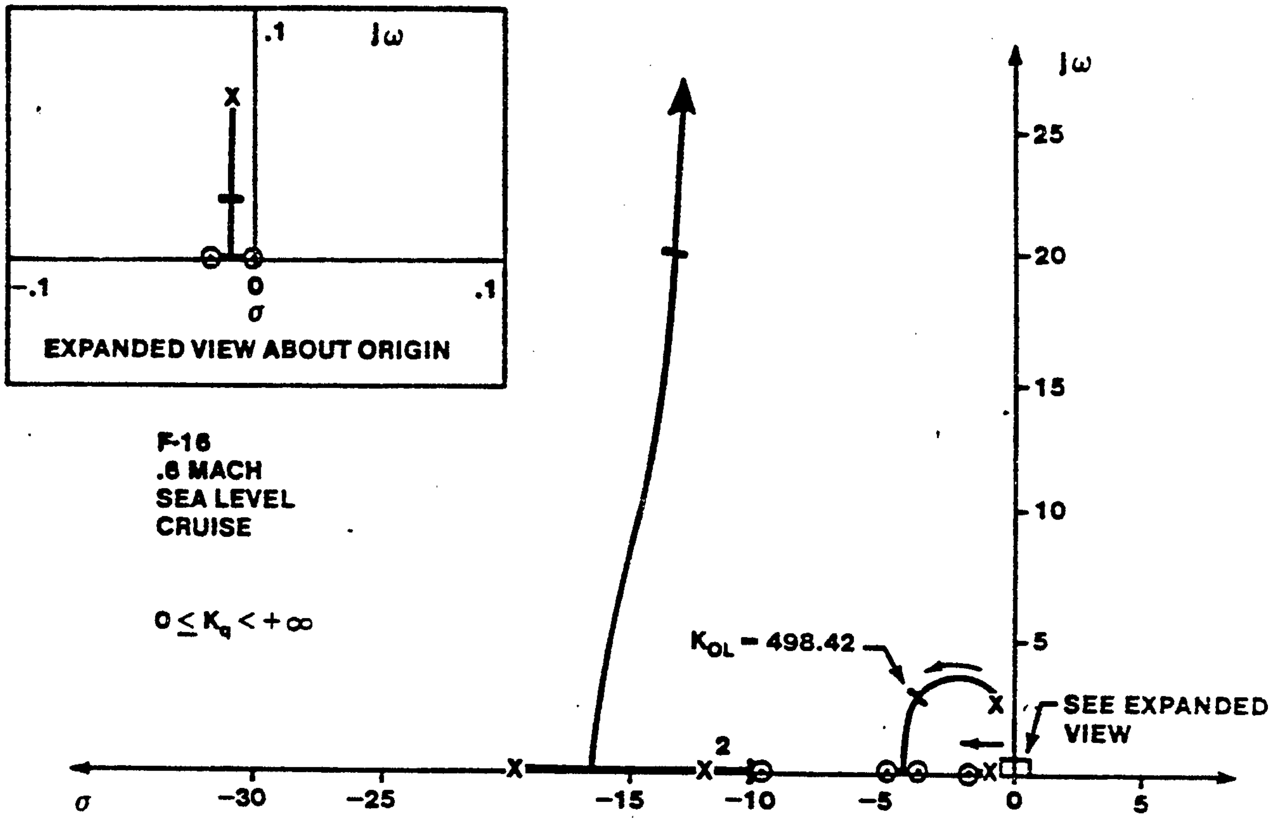

FIGURE 14.170. ROOT LOCUS PLOT FOR WASHED OUT PITCH RATE FEEDBACK LOOP FOR THE F-16A AIRCRAFT

should be kept in mind during the analysis of the outermost loop, the load factor feedback path. Figure 14.171 shows the reduced block diagram for the analysis conducted thus far.

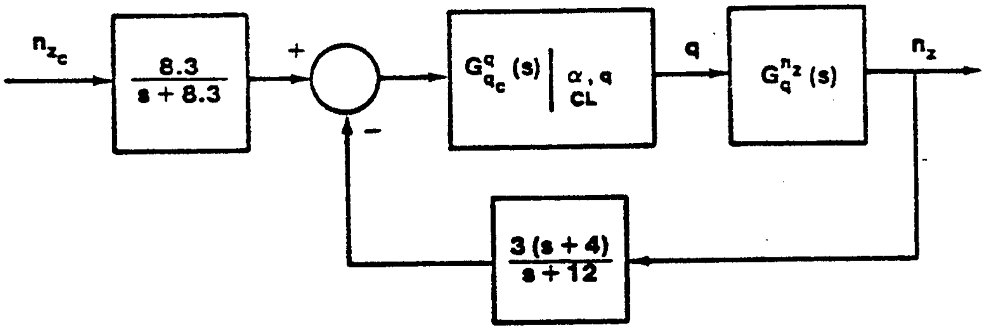
n_{z_c}
$\frac{8.3}{s+8.3}$
+
-
$G^{q}_{q_c}(s) \Big|_{\substack{\alpha, q \\ CL}}$
q
$G^{n_z}_{q}(s)$
n_z
$\frac{3(s+4)}{s+12}$

FIGURE 14.171 SIMPLIFIED F-16 LONGITUDINAL FLIGHT CONTROL SYSTEM WITH THE TWO INNER LOOPS CLOSED

The open loop transfer function for the outer loop becomes

$$GH_{n_z}\text{ loop} = \underbrace{\frac{2.055\ (s + 0.0058)\ (s + 1.165 \pm 11.437j)\ (s + 10)\ (s + 5)\ (s + 1)}{(s + 0.0093 \pm 0.023j)\ (s + 1.33)\ (s + 3.78 \pm 2.68j)\ (s + 10.2)}}_{\text{Forward Path Transfer Function}}$$

$$\times \underbrace{\frac{s + 12}{(s + 13.3 \pm 20.2j)}}_{\text{Forward Path Transfer Function}} \times \underbrace{\frac{3(s + 4)}{(s + 12)}}_{\text{Feedback Elements}} \qquad K_{OL} = 6.165 \qquad (14.136)$$

From the root locus (Figure 14.172) it appears that the short period roots have moved to a slightly higher natural frequency and somewhat reduced damping. However, additional roots have appeared near the origin on the real axis which threaten to become dominant. The closed loop transfer function becomes

$$G_{n_{z_c}}^{n_z}(s)\Big|_{\alpha,q,n_z\ CL} = \frac{2.055\ (s + 0.0158)\ (s + 1.165 \pm 11.437j)\ (s + 10)}{(s + 0.0164)\ (s + 1.74)\ (s + 3.86 \pm 3.32j)\ (s + 0.637)}$$

$$\times \frac{(s + 5)\ (s + 1)\ (s + 12)}{(s + 10.3)\ (s + 15.7 \pm 17.6j)} \times \underbrace{\frac{8.3}{(s + 8.3)}}_{\text{Prefilter}} \qquad (14.137)$$

Two real roots have appeared in the denominator at (s + 1.74) and (s + .637). These roots are not well suppressed by any nearby zeros and represent the dominant short period roots in addition to the short period roots at (s + 3.84 ± 3.32j). The high frequency roots have little impact on the aircraft response since their effects die out rapidly. The two real roots dominate the aircraft response. The initial response lag will be significant with this many unsuppressed roots dominating the response and may hinder tracking tasks. The natural frequency of the short period root (at s = -1.74) fails to meet the level 1 requirements of MIL-F-8785C. The steady state value to a step acceleration input is (final value theorem)

$$n_{z_{ss}} = \lim_{s \to 0} G_{n_{z_c}}^{n_z}(s)\Big|_{\alpha,q,n_z\ CL} = 0.96 \text{ g's} \qquad (14.138)$$

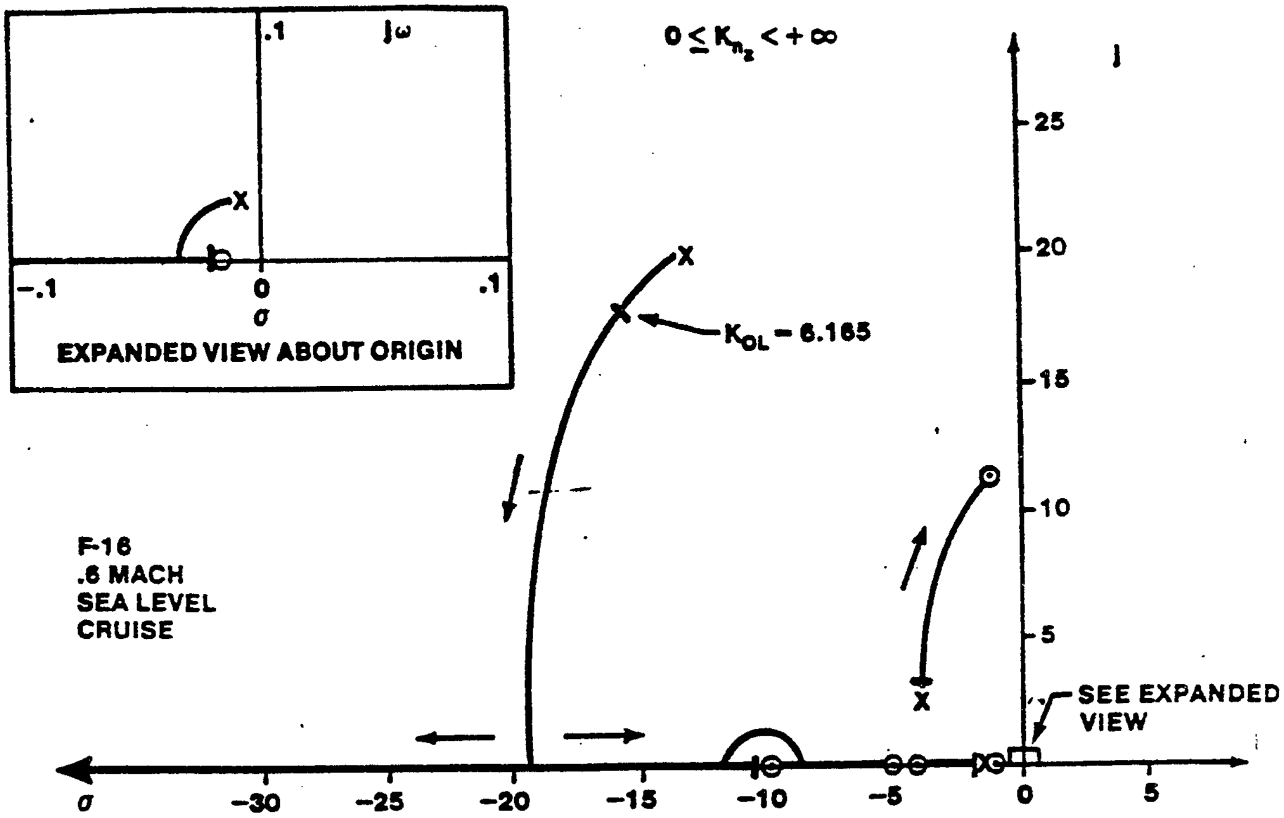

FIGURE 14.172. ROOT LOCUS PLOT OF LOAD FACTOR FEEDBACK LOOP FOR THE F-16A AIRCRAFT

The load factor time response of the aircraft with and without the prefilter in the command path are shown in Figures 14.173 and 14.174. With a prefilter, the response is relatively slow and exponential with the root at (s + 1.74) dominating the short term response and the root at (s + 0.637) dominating the longer term response. Significant time delay occurs initially, which is apparent from the plot. Without the prefilter, the initial response is slightly more abrupt. The pitch rate time response of the aircraft is shown in Figure 14.175 using the closed loop pitch rate transfer function

$$G^{q}_{n_{z_c}}(s)\Big|_{\alpha,q,n_z CL} = \frac{497.43\ (s + 0.0189)\ (s + 1.5)\ (s + 10)\ (s + 5)\ (s + 1)}{(s + 0.0164)\ (s + 1.74)\ (s + 3.86 \pm 3.32j)\ (s + 0.637)} \tag{14.139}$$

$$\times \frac{(s + 12)}{(s + 10.3)\ (s + 15.7 \pm 17.6j)}$$

No initial overshoot of the final pitch rate value occurs. Inflight investigations using variable stability aircraft have shown that heavy suppression of the pitch rate overshoot tendency (present in conventional aircraft) results in objectionable handling qualities.

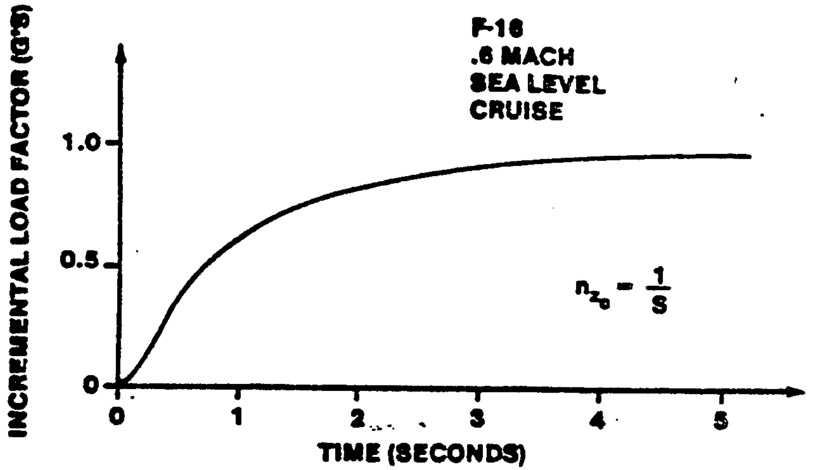

(a) ACTUAL AIRCRAFT LOAD FACTOR RESPONSE

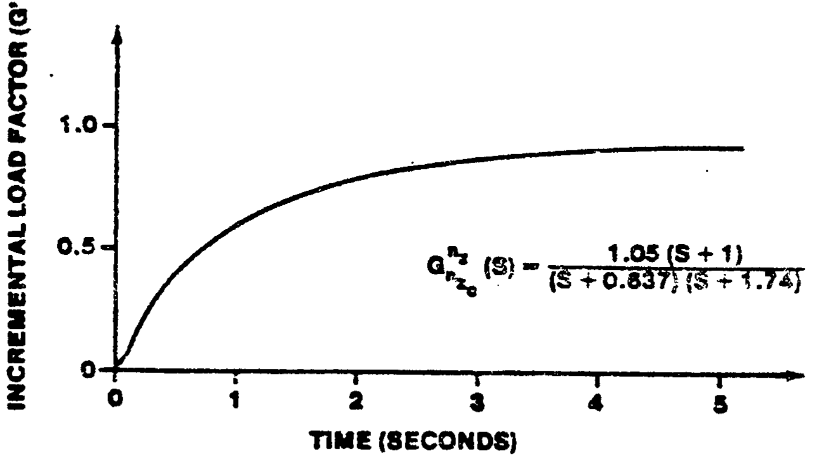

(b) APPROXIMATE AIRCRAFT LOAD FACTOR RESPONSE

FIGURE 14.173 F-16A LOAD FACTOR RESPONSE, PREFILTER EFFECTS OMITTED

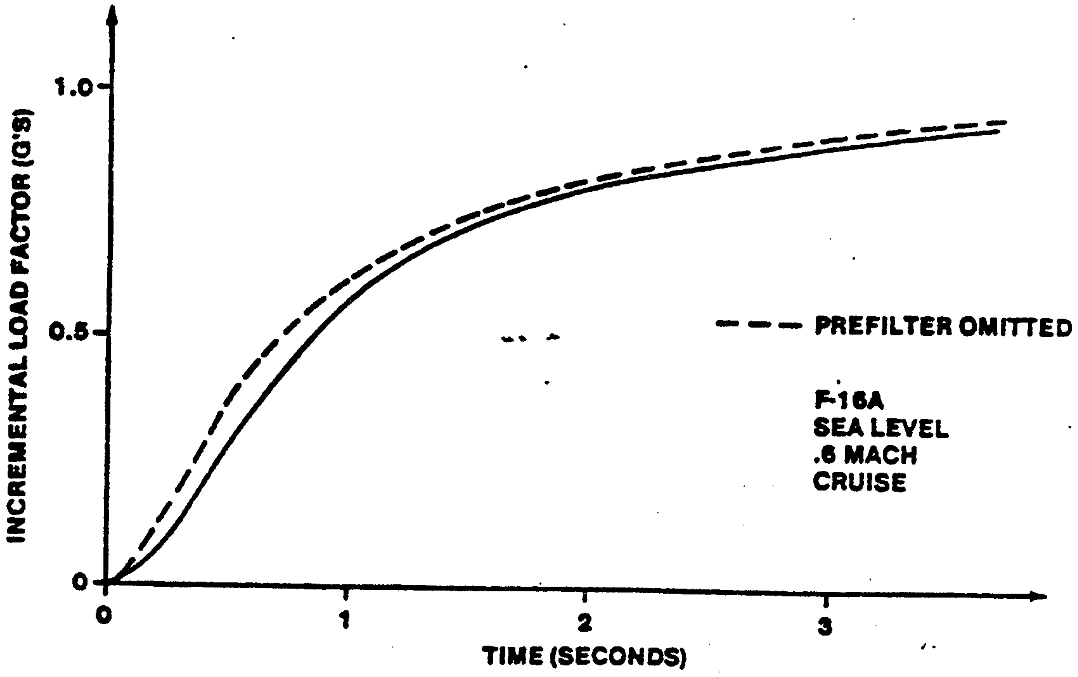

FIGURE 14.174. F-16A LOAD FACTOR RESPONSE, PREFILTER EFFECTS INCLUDED

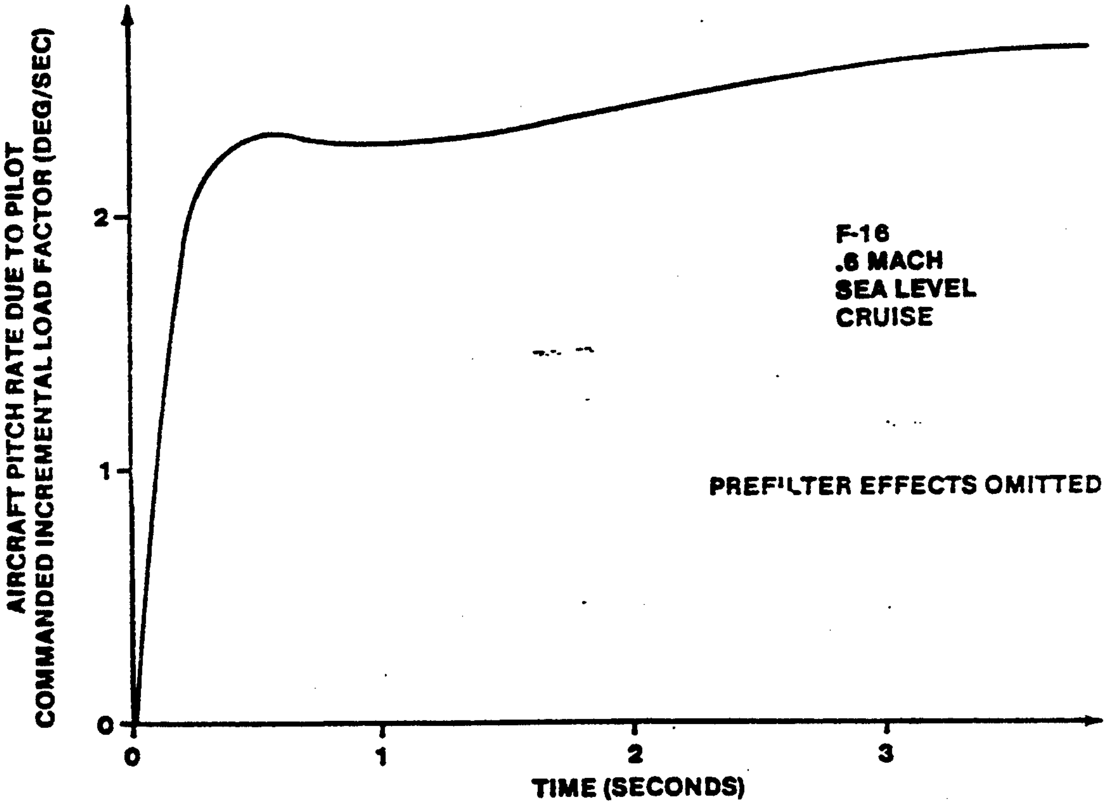

FIGURE 14.175. F-16A PITCH RATE RESPONSE FROM STEP LOAD FACTOR COMMAND

The handling qualities of the aircraft with the flaps locked up are suspect at this flight condition since the load factor response is slow and the pitch rate overshoot tendency is suppressed. Figure 14.176 shows the block diagram of the system if the maneuvering flaps are allowed to move. The angle of attack is fed back to the leading edge flap actuator through a lead compensator and a gain. The analysis of this block diagram is more complex due to its multi-input character.

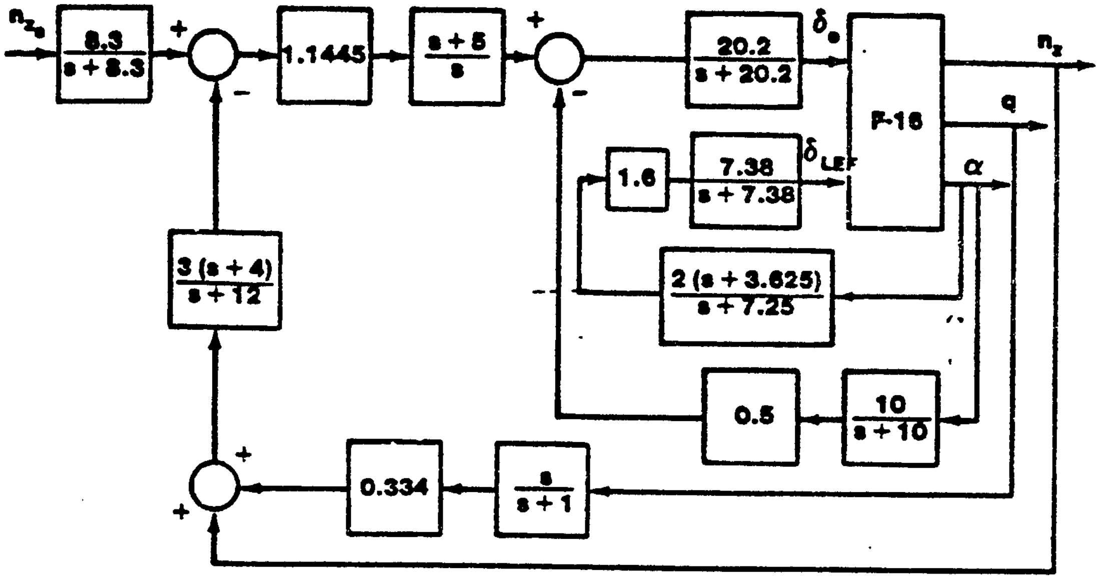

FIGURE 14.176. LONGITUDINAL FLIGHT CONTROL SYSTEM WITH LEADING EDGE FLAP SYSTEM ENGAGED

The aircraft lift coefficient may increase or decrease slightly as a result of the leading edge flap deflection, with total lift being reduced at very low angles of attack. At moderate to high angles of attack, the aircraft lift coefficient is increased. The stall angle of attack is higher with the leading edge flaps deflected. The airflow over the wing stays attached to the wing surface to a higher angle of attack with the leading edge flaps deployed, postponing separation buffet onset (stall warning). Leading edge flaps also aid directional stability at high angles of attack. While the pitching moment coefficient is reduced (slightly more negative) with the leading edge flaps deflected at low to moderate angles of attack, a noticeable positive pitching moment contribution occurs at high angles of attack, reducing the static and dynamic stability of the aircraft.

Modifying the aircraft equations of motion to account for the leading edge flaps (after obtaining leading edge flap stability derivative data from lift and moment coefficient curves for 0.6 Mach) yields

$$\begin{bmatrix} s + 0.0177 & 0.0269 & 0.048 \\ 0.095 & s + 1.479 & -s \\ 0 & 0.221\,s - 0.906 & s^2 + 0.752s \end{bmatrix} \begin{bmatrix} U(s) \\ \alpha(s) \\ \Theta(s) \end{bmatrix} = \begin{bmatrix} 0.022 & 0 \\ -0.203 & -0.052 \\ -21.544 & -2.819 \end{bmatrix} \begin{bmatrix} \delta_e(s) \\ \delta_{LEF}(s) \end{bmatrix} \qquad (14.190)$$

The leading edge flaps provide a small positive contribution to aircraft lift, but also provide a net nose down pitching moment increment at the 1 g flight condition of interest.

In a similar manner to the coupled analysis conducted for the lateral-directional axis, the first step in analyzing the F-16 longitudinal axis is to assume that $\delta_e = 0$ and perform a root locus analysis of the aircraft leading edge flap loop (see Figure 14.175). The aircraft transfer function is

$$G^{\alpha}_{\delta_{LEF}}(s) = \frac{0.052\,(s + 0.009 \pm 0.067j)\,(s + 54.96)}{(s - 0.087)\,(s + 2.373)\,(s + 0.098 \pm 0.104j)} \text{ deg/deg} \qquad (14.141)$$

The open loop transfer function for the leading edge flap loop is

$$GH_{\delta_{LEF}} = \frac{1.228\,(s + 3.625)\,(s + 0.009 \pm 0.067j)\,(s + 54.96)}{(s - 0.087)(s + 2.373)(s + 0.098 \pm 0.104j)(s + 7.38)(s + 7.25)} \qquad (14.142)$$

The root locus is plotted in Figure 14.177 as $K_{\alpha\delta_{LEF}}$ varies. Notice that the leading edge flaps effectively stabilize the aircraft.

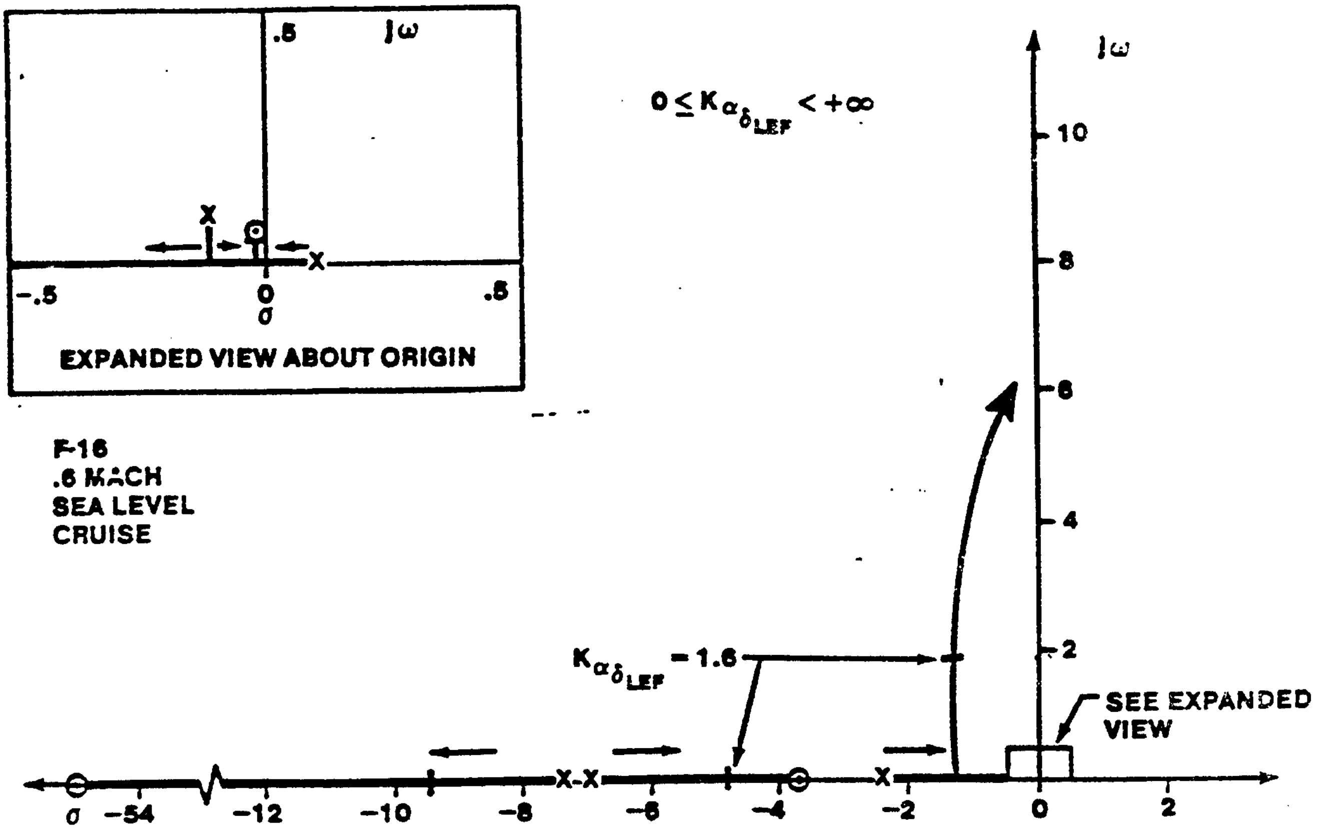

FIGURE 14.177. ROOT LOCUS PLOT OF F-16 LEADING EDGE FLAP CONTROL SYSTEM

The aircraft transfer functions

$$G^{\alpha}_{\delta_e}(s), \quad G^{q}_{\delta_e}(s) \quad \text{and} \quad G^{n_z}_{\delta_e}(s)$$

must be modified to account for the simultaneous leading edge flap deflections. For the angle of attack transfer function

$$\alpha = G^{\alpha}_{\delta_e}\delta_e + G^{\alpha}_{\delta_{LEF}}\delta_{LEF} \tag{14.143}$$

where (from Figure 14.152)

$$\delta_{LEF} = K_{\alpha_{\delta_{LEF}}} H_{c_{\delta_{LEF}}} G_{\delta_{LEF}} \alpha \tag{14.144}$$

where

$$K_{\alpha_{\delta_{LEF}}} = 1.6$$

$$H_{c_{\delta_{LEF}}} = \frac{2(s + 3.625)}{s + 7.25} \qquad (14.145)$$

$$G_{\delta_{LEF}} = \frac{7.38}{s + 7.38} \qquad (14.146)$$

so that

$$\alpha = G^{\alpha}_{\delta_e}\delta_e + G^{\alpha}_{\delta_{LEF}} K_{\delta_{LEF}} H_{\delta_{LEF}} G_{\delta_{LEF}} \alpha \qquad (14.147)$$

yielding

$$\frac{\alpha}{\delta_e} = \frac{G^{\alpha}_{\delta_e}}{1 - K_{\alpha_{\delta_{LEF}}} G_{\delta_{LEF}} H_{c_{\delta_{LEF}}} G^{\alpha}_{\delta_{LEF}}} \qquad (14.148)$$

or, after simplifying

$$\frac{\alpha}{\delta_e} = \frac{N^{\alpha}_{\delta_e} D_{c_{\delta_{LEF}}} D_{\delta_{LEF}}}{\Delta D_{\delta_{LEF}} D_{c_{\delta_{LEF}}} - K_{\alpha_{\delta_{LEF}}} N^{\alpha}_{\delta_{LEF}} N_{c_{\delta_{LEF}}} K_{\delta_{LEF}}} \qquad (14.149)$$

The aircraft angle of attack due to an elevator deflection transfer function includes two additional zeros (the poles of the leading edge flap actuator and lead compensator) as well as the closed loop poles obtained from the leading edge flap system analysis, yielding

$$G^{\alpha}_{\delta_e}(s)\Big|_{\delta_{LEF}\ CL} = \frac{0.203\ (s + 0.0087 \pm 0.067j)\ (s + 7.25)\ (s + 7.38)}{(s + 0.0083 \pm 0.058j)\ (s + 1.39 \pm 1.92j)\ (s + 4.8)\ (s + 9.53)} \qquad (14.150)$$

The pitch rate transfer function for the aircraft is found by writing the equations

$$q = G^{q}_{\delta_e}\delta_e + G^{q}_{\delta_{LEF}}\delta_{LEF} \qquad (14.151)$$

$$\alpha = G_{\delta_e}\delta_e + G_{\delta_{LEF}}\delta_{LEF} \tag{14.152}$$

substituting in the expression for δ_{LEF} and writing the matrix equation

$$\begin{bmatrix} 1 - G^{\alpha}_{\delta_{LEF}} K_{\alpha_{\delta_{LEF}}} G_{\delta_{LEF}} H_{c_{\delta_{LEF}}} & 0 \\ - G^{q}_{\delta_{LEF}} K_{\delta_{LEF}} G_{\delta_{LEF}} H_{c\delta_{LEF}} & 1 \end{bmatrix} \begin{bmatrix} \alpha \\ q \end{bmatrix} = \begin{bmatrix} G^{\alpha}_{\delta_e} \\ G^{q}_{\delta_e} \end{bmatrix} \delta_e \tag{14.153}$$

yields

$$G^{q}_{\delta_e}\Big|_{\delta_{LEF}\,CL} = \frac{G^{q}_{\delta_e} - K_{\alpha_{\delta_{LEF}}} G_{\delta_{LEF}} H_{c_{\delta_{LEF}}} sG^{\beta\ \alpha}_{\delta_e \delta_{LEF}}}{\Delta_{\delta_{LEF}}\,CL} \tag{14.154}$$

where $\Delta_{\delta_{LEF}\,CL}$ are the roots of the leading edge flap system augmented aircraft, already obtained.

Simplifying yields

$$G^{q}_{\delta_e}\Big|_{\delta_{LEF}\,CL} = \frac{N^{q}_{\delta_d} D_{\delta_{LEF}} D_{c_{\delta_{LEF}}} - K_{\alpha_{\delta_{LEF}}} K_{\delta_{LEF}} N_{c_{\delta_{LEF}}} sN^{\theta\ \alpha}_{\delta_e \delta_{LEF}}}{\Delta_{\delta_{LEF}}\,CL} \tag{14.155}$$

Similarly

$$G^{n_z}_{\delta_e}\Big|_{\delta_{LEF}\,CL} = \frac{N^{n_z}_{\delta_e} D_{c_{\delta_{LEF}}} D_{\delta_{LEF}} - K_{\alpha_{\delta_{LEF}}} K_{\delta_{LEF}} N_{c_{\delta_{LEF}}} N^{n_z\ \alpha}_{\delta_e \delta_{LEF}}}{\Delta_{\delta_{LEF}}\,CL} \tag{14.156}$$

Since $n_z = \frac{1}{(57.3)\ (32.2)} [U_0\ (\dot{\alpha} - q) - \ell_x \dot{q}]$ g's/deg and

$$N^{n_z\ \alpha}_{\delta_e \delta_{LEF}} = N^{n_z}_{\delta_e} N^{\alpha}_{\delta_{LEF}} - N^{\alpha}_{\delta_e} N^{n_z}_{\delta_{LEF}} \tag{14.157}$$

$$N_{\delta_e \ \delta_{LEF}}^{n_z \ \alpha} = \frac{\ell_x}{(32.2)\ (57.3)} s\ s + \frac{U_0}{\ell_x} N_{\delta_e \delta_{LEF}}^{\theta \ \alpha} = 0.0042\ s(s + 0.007)\ (s + 45.44) \tag{14.158}$$

from the aircraft equations of motion since the normal accelerometer is located at $\ell_x = 14$ feet.

The aircraft pitch rate and normal acceleration transfer functions become

$$G_{\delta_e}^{q}\Bigg|_{\delta_{LEF}\ CL} = \frac{21.516\ (s + 0.018)\ (s + 1.6)\ (s + 7.26 \pm 1.033j)}{(s + 0.0083 \pm 0.058j)\ (s + 1.39 \pm 1.92j)\ (s + 4.8)\ (s + 9.53)} \tag{14.159}$$

$$G_{\delta_e}^{n_z}\Bigg|_{\delta_{LEF}\ CL} = \frac{0.0889\ s(s + 0.0155)\ (s + 6.36)\ (s + 8.46)\ (s + 1.07 \pm 11.594j)}{(s + 0.0083 \pm 0.058j)\ (s + 1.39 \pm 1.92j)\ (s + 4.8)\ (s + 9.53)} \tag{14.160}$$

The effects of the leading edge flap system are accounted for in the

$$G_{\delta_e}^{\alpha}\Bigg|_{\delta_{LEF}\ CL} \quad G_{\delta_e}^{q}\Bigg|_{\delta_{LEF}\ CL} \quad \text{and} \quad G_{\delta_e}^{n_z}\Bigg|_{\delta_{LEF}\ CL}$$

transfer functions. Now, all the modified aircraft transfer functions are available to repeat the previous analysis. The closed loop transfer function for the aircraft load factor response becomes

$$G_{n_{z_c}}^{n_z}\Bigg|_{\substack{FULL\\AUG}} = \frac{2.055\ (s + 0.0155)\ (s + 1)\ (s + 5)\ (s + 6.36)\ (s + 8.46)\ (s + 10)}{(s + 0.0164)\ (s + 0.58)\ (s + 1.7)\ (s + 10.24)\ (s + 5.87)\ (s + 7.97)} \times \frac{(s + 1.07 \pm 11.594j)\ (s + 12)}{(s + 4.29 \pm 4.022j)\ (s + 15.77 \pm 17.55j)} \tag{14.161}$$

and the final load factor is

$$\lim_{s \to 0} \left[G_{n_{z_c}}^{n_z}\Bigg|_{\substack{FULL\\AUG}} \right] = 0.95 \text{ g's} \tag{14.162}$$

which is close to one, as expected (the error is due to round-off errors in the analysis introduced by the root locus factoring scheme). Notice that the dominant poles at (s + 0.58) and (s + 1.7) are nearly identical to the dominant poles at (s + 0.637) and (s + 1.74) obtained earlier. This indicates that the aircraft response with the leading edge flaps is nearly the same as with the flaps locked up (for the low angle of attack flight condition analyzed). This would not be true at high angles of attack, where the leading edge flaps would provide improved lift characteristics and a pronounced destabilizing pitching moment.

14.10.3 Advanced Flight Control System Analysis Programs

The analytical techniques discussed in this chapter, are often laborious, especially if a large number of flight conditions are to be considered. Fortunately, sophisticated flight control system analysis programs are available to greatly simplify the process. Programs available at the Flight Test Center use matrix techniques and state space formulation of the aircraft equations of motion to allow the linearized aircraft model and the complete linearized control system to be programmed on the computer. Test inputs can be applied to the flight control system model. Several aircraft parameters and control surface motions can be recorded simultaneously. Bode and root locus plots of the various aircraft transfer functions, as specified by the user, are also easily obtained.

14.11 INTEGRATED FLIGHT CONTROL SYSTEMS

Aircraft flight controls, propulsion, avionics, and sensors have traditionally been separate components of an aircraft which only interact (or are integrated) through control by the pilot. With recent advances that have resulted in fly-by-wire and digital flight control systems, integration of flight controls with propulsion, avionics and sensors is now possible. The flexibility of such a system is a means of providing significant improvements to capabilities in a relibale and cost effective manner.

Integration of flight controls with avionics and sensors gives the capability of automated air-to-surface and air-to-air weapons deliveries with significant reduction in pilot workload. It also provides the capability for automated ground collision avoidance systems which significantly enhance safety. Integration of flight controls with the propulsion system promises increased capability for range-payload performance and maneuverability.

Integration of flight controls with the airframe itself through systems to detect damage to flight control system surfaces gives the ability to have a self-repairing flight control system with increased combat survivability and reduced cost.

Integration of flight controls with other aircraft systems requires some means of artificial redundancy for single-thread avionics and sensors that are coupled to the highly-redundant flight control system. This will be discussed in the following section on the Advanced Fighter Technology Integration (AFTI)/F-16 Automated Maneuvering Attack System. This will be followed by brief discussions of integrated propulsion and flight controls (NASA HIDEC program) and self-repairing flight controls.

14.11.1 Integrated Avionics, Sensors and Flight Controls

The AFTI/F-16 experimental aircraft has been used to develop an Automated Maneuvering Attack System (AMAS) for both air-to-air and air-to-surface attack. This system integrates avionics and sensors with the flight control system. We can expect this type of integration on aircraft in the near future in order to provide AMAS as well as other capabilities, such as automatic ground collision avoidance. This section will use the air-to-surface AMAS tested on the AFTI/F-16 from 1984 to 1987 as an example of this type of integrated flight control system.

The AFTI/F-16 AMAS was an outgrouwth of the F-15 Integrated Fire and Flight Control (IFFC/Firefly III) system tested from 1981 to 1983. Both of these systems provided automated air-to-air and air-to-surface attack. Unlike the AFTI/F-16 AMAS, however, the IFFC F-15 provided no artificial redundancy for non-redundant avionics and sensors. The System-Wide Integrity Management (SWIM) system on the AFTI/F-16 provided this artificial redundancy by monitoring all components for proper operation and providing automatic ground collision avoidance.

The air-to-surface AMAS was termed AMAS pre-planned target or APPT. Target acquisition for an APPT delivery was initiated by inertial navigation positioning of sensors with visual or radar refinement. This was followed by target search and track with the conformally mounted sensor tracker which contained an infrared tracker, laser ranger, and target state estimator (Kallman filter). Automated maneuvering consisted of ingress steering (as low as 200 feet AGL), curvilinear weapons delivery (lateral toss up to 5 g's), and target area egress as shown in Figure 14.178.

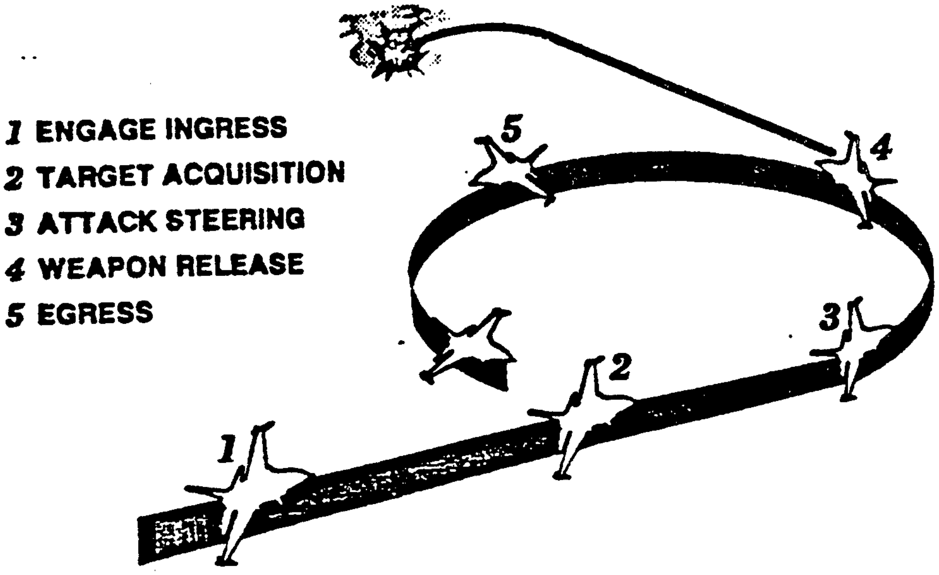

FIGURE 14.178 AIR-TO-SURFACE AMAS

Computations for the delivery were made in the fire control computer (FCC) using inputs received through the aircraft multiplex bus system from sensors, avionics, and flight controls. The FCC determined the required flight path from target state, current aircraft state, ballistic trajectories, and the desired profile. The FCC then commanded aircraft load factor and bank angle with signals sent through the multiplex bus to the digital flight control system (DFCS). The DFCS took these commands and blended them with pilot inputs in order to adjust the control surfaces to follow the commanded sum.

The pilot controlled the APPT profile by setting a release range between 3,000 and 20,000 feet, engaging AMAS at the desired ingress altitude, and manually flying the desired airspeed. Short release ranges and high airspeeds tended to give level or diving deliveries while long release ranges and lower airspeeds gave lofting deliveries.

AMAS was a closed-loop control system as shown in Figure 14.170. Through this system many single-thread (non-redundant) sensors were used for aircraft control. The traditional approach in design of flight controls is to have redundancy in all parts of the system, including sensors, such as in the AFTI/F-16 triplex DFCS. Other aircraft sensors and avionics, however, are not normally redundant.

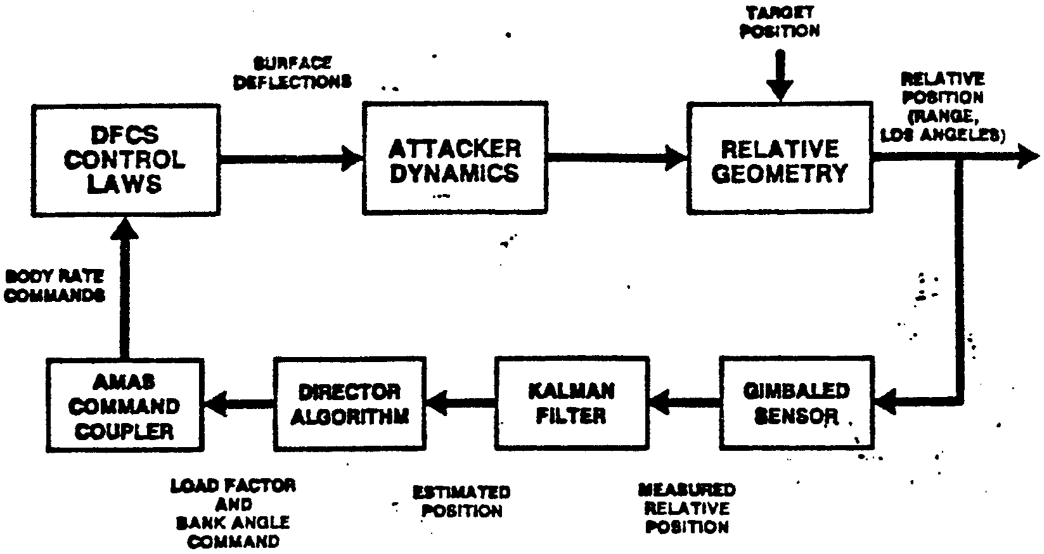
TARGET POSITION
SURFACE DEFLECTIONS
RELATIVE POSITION (RANGE, LOS ANGELES)
DFCS CONTROL LAWS
ATTACKER DYNAMICS
RELATIVE GEOMETRY
BODY RATE COMMANDS
AMAS COMMAND COUPLER
DIRECTOR ALGORITHM
KALMAN FILTER
GIMBALED SENSOR
LOAD FACTOR AND BANK ANGLE COMMAND
ESTIMATED POSITION
MEASURED RELATIVE POSITION

FIGURE 14.179 AMAS CLOSED-LOOP CONTROL

The SWIM system on the AFTI/F-16 artificially provided the required avionics and sensor redundancy. The concept of artificial redundancy is essential in a highly integrated system like the AFTI/F-16 where many of the feedback elements are single thread. The need for redundancy in these elements can no more be ignored than redundancy in the standard rate gyros and accelerometers used by the flight controls.

The SWIM system used a combination of interactive built-in test, continuous inflight integrity testing, and automatic enforcement of established operating restrictions in order to provide a measure of system operating integrity and safety against failures and improper operation. SWIM had four functional areas: 1) ground collision avoidance, 2) flight-critical sensor fusion, 3) physical constraint monitors, and 4) AMAS fault processing.

14.11.1.1 Ground Collision Avoidance

The ground collision aviodance function was a backup to the AMAS primary guidance algorithms and represented the last line of defense against hardware or software hazards which might cause the automated system to penetrate the pilot-selected minimum descent altitude (MDA). It also cued the pilot in both manual and automated modes as to when a flyup was required to prevent MDA penetration. The SWIM ground collision avoidance function was performed simulataneously by both the DFCS and the FCC.

The ground collision avoidance system predicted when current aircraft conditions constituted an imminent penetration of the MDA based upon above ground level (AGL) altitude from the radar altimeter. At that time the aircraft automatically performed a recovery maneuver (flyup). The aircraft was commanded to a roll rate equal to twice the absolute value of the bank angle, and the load factor was commanded to -1 g inverted and 5 g's when less than 90 degrees of bank angle. Automatic control was continued until the flight path angle was greater than three degrees and the wings were level. A derivative of this system is now scheduled for production on the F-16 and being considered for production on the F-18 and other aircraft.

14.11.1.2 Flight-Critical Sensor Fusion

Communications to the flight controls from flight critical sensors and avionics were carefully scrutinized by the triply redundant DFCS. Attitude information from the inertial navigation system (INS) was compared with body rates of the flight control rate gyros for gross anomalies. The DFCS checked the integrity of the FCC by requiring the FCC to provide a checksum and the answers to alternating problems. The FCC in turn checked the integrity of the other avionics subsystems by comparing similar inputs form different sources. The FCC then fused their inputs to provide valid estimates of AGL altitude, AGL rate, roll attitude, roll rate, and load factor.

14.11.1.3 Physical Constraint Monitors

The physical constraint monitors consisted of the operational mission restructions (OMR). These monitors detected conditions that were, by definition, outside the established limits (such as airspeed, altitude, etc.) for AMAS operation. Also, mode protocol checks assured that all critical subsystems were operating in consistent modes that could support AMAS operation.

OMRs were found to be very useful and could be incorporated on any aircraft where known hazards exist. An OMR is a simple software flag helping avoid those known hazards.

14.11.1.4 AMAS Fault Processing

Upon detection of a fault, AMAS operation was suspended and a flyup was executed if required. In addition, the process, subsystem or function in error was isolated and catalogued for fault reporting and an AMAS-disengage warning light and warning tone were activated. The nature of the fault was then displayed on a multifunctional display in the cockpit.

14.11.1.5 AMAS Test Results

The air-to-surface AMAS test program was completed in 1987 and the results showed that integration of avionics, sensors and flight controls could be used to reduce pilot workload (automate flying) in order to allow the pilot to perform other required tasks such as target acquisition and threat detection and avoidance. This integration also allowed increased capability (curvilinear weapons delivery, for example) and increased safety (automatic ground collision avoidance). A more detailed discussion of integration of avionics, sensors and flight controls will be given in the integrated avionics course. This course will also discuss the unique methods used to test these systems.

14.11.2 Integrated Propulsion and Flight Controls

The highly integrated digital electronic control (HIDEC) project flown at NASA Ames-Dryden showed that the integration of flight controls with the propulsion system had significant performance benefits. The benefits of this integration are based upon a tradeoff of engine stall margin for thrust.

In engines not integrated with flight controls an adequate stall margin must be maintained in order to accommodate maneuvering of the aircraft. Rapid changes in Mach, altitude, angle of attack (α) and sideslip (β) will decrease engine stall margin. An adequate stall margin must, therefore, include an "extra" stall margin to protect against sudden changes that might cause an engine stall. Because of this, the engine stall maring on aircraft where flight controls are not integrated with propulsion is larger than required for current conditions. This translates into reduced engine efficiency and performance. If a lower stall margin could be maintained, this would translate to a higher thrust capability (higher maximum level of thrust for conditions) or to a decreased fuel flow (higher temperature for constant thrust which gives more engine efficiency).

The HIDEC test aircraft was a highly modified F-15 with a digital electronic engine control (DEEC), and a digital CAS coupled through the aircraft multiplex bus system to the engine. Figure 14.180 shows a schematic of the HIDEC.

In the HIDEC system, engine pressure ration (EPR) was used as a measure of engine stall margin. The flight control computer continuously adjusted EPR (generated a ΔEPR) in order to keep the stall margin at a minimum and consequently the thrust at a maximum, or the fuel flow at a minimum. Prior to any augmentation by the flight control computer the DEEC determined the original EPR from safety schedules. This EPR would then be modified by the

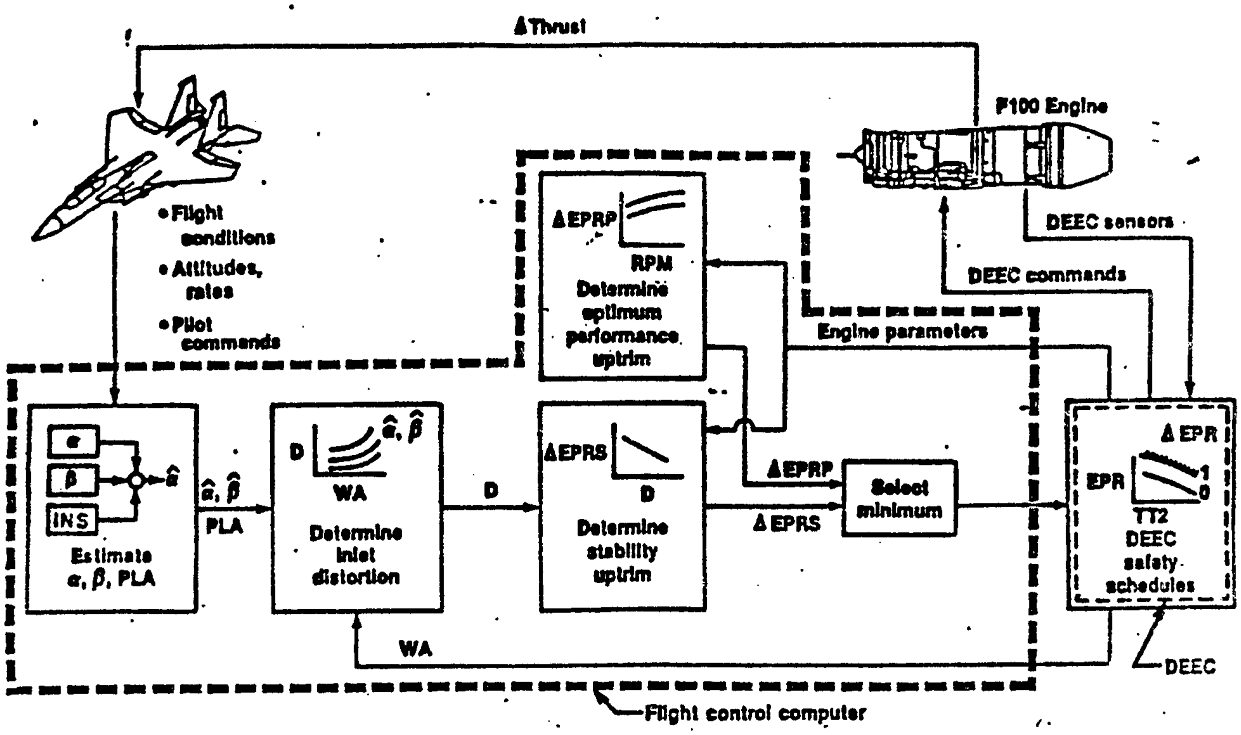
ΔThrust
F100 Engine
DEEC sensors
DEEC commands
Engine parameters
•Flight conditions
•Attitudes, rates
•Pilot commands
ΔEPRP
RPM
Determine optimum performance uptrim
α
β
INS
α̂
α̂, β̂
PLA
Estimate α, β, PLA
D
α̂, β̂
WA
Determine inlet distortion
D
ΔEPRS
D
Determine stability uptrim
ΔEPRP
ΔEPRS
Select minimum
ΔEPR
EPR
1
0
TT2
DEEC safety schedules
DEEC
WA
Flight control computer

FIGURE 14.180 HIDEC ADAPTIVE ENGINE CONTROL SYSTEM

flight control computer with a ΔEPR.

The ΔEPR was determined by the flight control computer in the following manner. First, current flight conditions (Mach, altitude, α, and β) were combined with current pilot commands (stick, rudder, and throttle position) and current attitude rates (from the INS) in order to estimate the values of α, β, and throttle setting (power level angle, PLA) one half second into the future. These were then used (along with airflow form the DEEC) to determine probable inlet distortion one half second in the future. The flight control computer then determined the proper value for uptrimming the EPR from an engine stability (stall margin) point of view (ΔEPRS). Simultaneously the optimum uptrim of EPR from an engine performance point of view (ΔEPRP) was determined by including feedback of engine parameters. The lower of these two values (one giving higher stall margin) was then used as ΔEPR to retrim the engine.

The benefits of the HIDEC can be seen in Figure 14.181 and 14.182 which show predicted increases in thrust and decreases in fuel flow. For example, at 40,000 feet the predicted increase in MIL thrust is 7 to 8 percent (Figure 14.181), while max thrust fuel flow can be reduced (at the same thrust) from 3 to 18 percent.

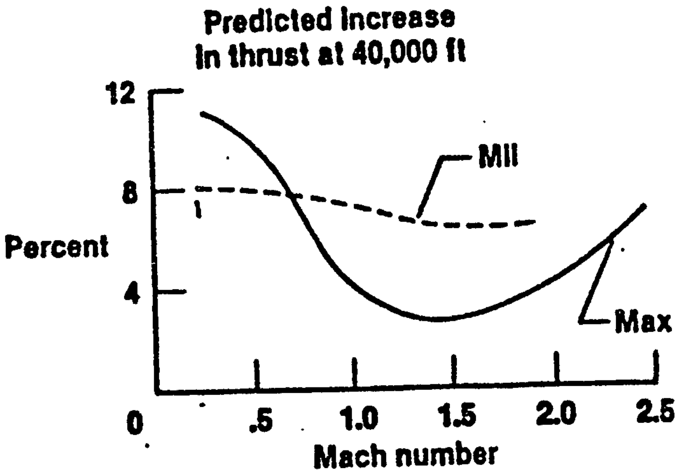

FIGURE 14.181 HIDEC PREDICTED THRUST INCREASES

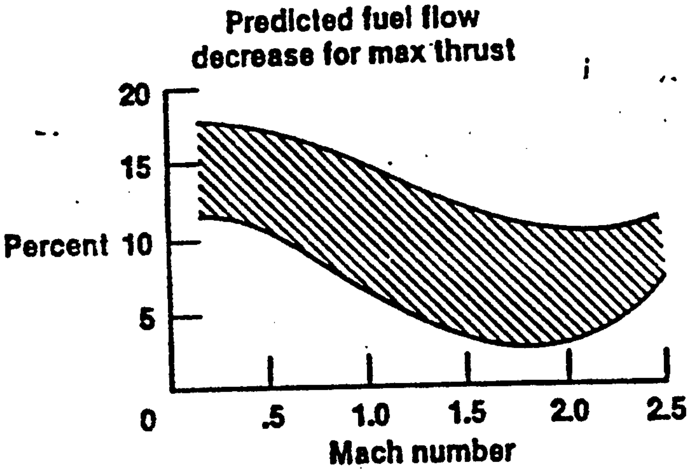

FIGURE 14.182 HIDEC PREDICTED FUEL FLOW DECREASES AT CONSTANT THRUST

14.11.3 Self-Repairing Flight Control Systems

A self-repairing flight control system is one which is capable of reconfiguring the aircraft flight control system to compensate for lost or impaired aerodynamic control surfaces. This is accomplished by using combinations of other available control surfaces to provide the desired control action. Self-repairing systems have the potential to provide two primary enhanced capabilities: a) aerodynamic control surface damage tolerance, and b) reduced flight control system complexity.

Self-repairing systems have obvious advantages for battle damaged aircraft, but also have applications for aircraft damaged in weather or mid-air collision. The type of damage that these systems are designed to compensate for include the loss of all or part of an aerodynamic surface or the loss of the control of a surface.

Increased flight control system complexity has been required because of the need to avoid the loss of the control for an aerodynamic surface at all costs. In today's aircraft, the components that move the surfaces represent sources of single-point failures because many of them are flight critical. The need to prevent them from failing has led control system designers to build in high levels of redundancy in order to meet requirements on aircraft flight safety. The impact on life-cycle costs and system reliability have been high. Reducing the complexity of flight control systems is, therefore, the second goal of a self-repairing flight control system.

Simpler flight control systems are possible if aircraft are designed such that the effect of each surface can be replicated by some combination of the others. This "aerodynamic redundancy" allows the aircraft to tolerate the loss of a surface. Thus, the aircraft can also tolerate the loss of any flight control element in that surface's control path. By careful design choices, therefore, the designer may use less reliable (and consequently less expensive) components leading to a reduction in the number and complexity of some of the most expensive components in the system.

The first challenge in the design of a self-repairing flight control system is to develop the capability to reliably determine when a flight control impairment has occurred and then to isolate the fault to a specific surface. Sensing of surface position and hinge movements and comparing them to expected values is one of the techniques used for this.

The general strategy of self-repairing reconfiguration is to guarantee safe operation and recover full performance if possible. The first is intended to be sufficient to allow a reduction of flight control system complexity while the second goes on to exploit the full potential of self-repairing flight control technology through maintenance of combat capability even with flight control failures.

There are three common ways a control system can deal with detected control surface degradations. It can use robust feedback to simply tolerate (mask) their effects, it can adapt to them by continuously adjusting its parameters (changes in gain, for example), or it can identify them and switch to an alternate control law. One problem associated with self-repairing systems is that the loss of a critical surface (horizontal tail) may preclude the recovery of full performance. Another possibility is to have more surfaces to utilize. For example, horizontal canards could be added to supplement the horizontal tails. The size of the surfaces could then be reduced which would minimize the impact of the additional surfaces on performance (drag). The system would then be more tolerant to the loss of a surface.

14.12 FLIGHT CONTROL SYSTEM TESTING OF HIGHLY AUGMENTED AIRCRAFT

The ultimate goal of both the aircraft designer and tester is to ensure that aircraft are provided to operational units which can efficiently accomplish their design missions — aircraft that are simple and easy to fly so that the pilot can devote his attention to accomplishing his mission objectives. The more thoroughly the tester understands flight control theory, the better the tester can communicate with the designer and the earlier the tester can become involved in the development of the flight control system. The closer the understanding between the tester and the designer, and the greater the extent to which both realize they share a common objective, the more efficiently and effectively the communication loop between them will be, resulting in a satisfactory flight control system for the aircraft.

Up to this point, the textbook has emphasized the analysis of aircraft flight control systems and their effects upon the handling qualities of the aircraft. This knowledge is essential to the design of a test plan which can verify the performance of the flight control system, as well as uncover and correct important handling qualities deficiencies. Figure 14.183 presents a schematic of a flying qualities flight test program for a modern, highly augmented aircraft. Simplified linear analysis and detailed block diagram analysis have been the subject of the earlier sections of this textbook. The purpose of this section is to provide a general guideline to considerations which should be made during the test program planning stage, and to point out mandatory ground tests and possible test procedures. Many of the flight test techniques used for testing flight control systems, such as open loop static stability or dynamics tests have been addressed in earlier chapters. In this section, flight test techniques will be discussed which are available to evaluate the closed loop handling qualities of modern, highly augmented aircraft.

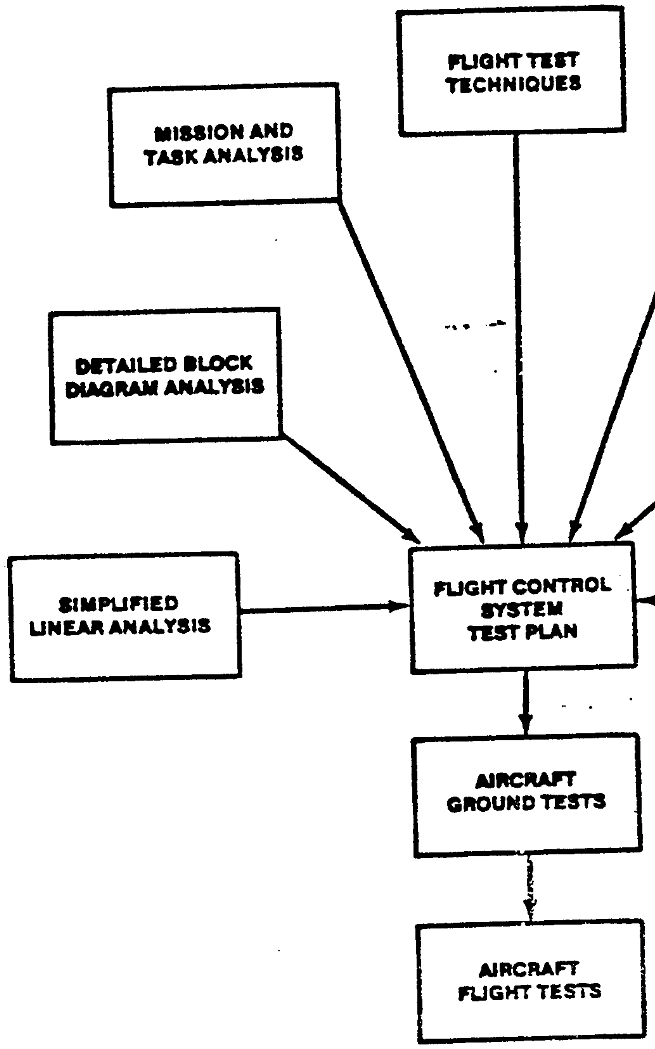
FLIGHT TEST TECHNIQUES
MISSION AND TASK ANALYSIS
GROUND SIMULATIONS
DETAILED BLOCK DIAGRAM ANALYSIS
INFLIGHT SIMULATIONS
SIMPLIFIED LINEAR ANALYSIS
FLIGHT CONTROL SYSTEM TEST PLAN
HARDWARE AND SOFTWARE VERIFICATION
AIRCRAFT GROUND TESTS
AIRCRAFT FLIGHT TESTS

FIGURE 14.183 FLIGHT CONTROL SYSTEM TEST PLANNING CONSIDERATIONS AND TEST CONDUCT

14.12.1 Flight Control System Requirements

Flight control systems must meet the following requirements:

a) Military Specifications MIL-F-8785C and MIL-F-9490

b) Special performance requirements of the procurment detail specification

c) The requirements of the flight control system specification

The latter two requirements come from program derectives and contracts, and will often require unique tests which will not be addressed in this text.

MIL-F-8785C and, to a lesser extent, MIL-F-9490 contain detailed handling qualities requirements for flight control system testing.

14.12.1.1 MIL-F-8785C, "Flying Qualities of Piloted Aircraft"

This specification applies to the flying qualities of fixed wing aircraft in conventional modes of flight (requirements for V/STOL aircraft in transition are covered in MIL-F-83300 and for helicopters in MIL-F-8501A). The requirements are written in terms of the cockpit controls which produce conventional pitching, rolling, or yawing motions. No specific requirements are currently provided for unconventional flight modes — such as direct lift, sideforce or fuselage pointing — although these modes are not precluded. The handling qualities are specified for four classes of aircraft (the classes being divided by mission group). Also, three phases or types of tasks are defined which further delineate handling qualities requirements. Three levels of handling qualities are defined — corresponding to three of the four primary categories of the Cooper-Harper rating scale (not including Cooper-Harper ratings of 10) as follows:

1. Level 1. Flying qualities which are adequate for the mission flight phase (Cooper-Harper ratings of 1 to 3).
2. Level 2. Flying qualities which are adequate to accomplish the mission flight phase but some increase in pilot workload or some degradation in mission effectiveness, or both, exists (Cooper-Harper ratings of 4 to 6).
3. Level 3. Flying qualities such that the airplane can be controlled safely, but pilot workload is excessive or mission effectiveness is inadequate, or both (Cooper-Harper ratings of 7 to 9).

The requirements of the specification apply to the full range of operational center of gravity and gross weight conditions, including external store configurations (symmetric and asymmetric) as well as all aircraft configurations used in operational tasks. Requirements for both normal operation and failure states are provided and aircraft operation, service and permissible flight envelopes are defined. Level 1 flying qualities are required within the service flight envelope and during some failure state operation (based on the probability of the failure occurring). Other failure states require level 2 or 3 flying qualities.

These requirements are based to a large extent on flight experiments conducted in variable stability aircraft using well-defined, precision, high gain tasks. Cooper-Harper ratings of the defined tasks were correlated to the aircraft characteristics to determine the characteristics which result in level 1, 2, or 3 flying qualities. Open loop tests determine the test aircraft's characteristics, which are compared to the data derived from the flight experiments to determine the adequacy of the closed loop handling qualities. In theory this method should work — and it was reasonably successful for conventional unaugmented or slighty augmented aircraft. The use of these requirements to assure adequate flying qualities for modern, highly augmented aircraft has been unsuccessful for two reasons:

1. The flight control system effectively masks or alters the basic aerodynamic characteristics of the aircraft so the aircraft do not respond to pilot inputs with classical second order short period or Dutch roll characteristics.
2. Flight control system engineers have not used the requirements of the specification as design guidelines.

To overcome the inadequacies of the specification when dealing with these aircraft, several new criteria have been proposed during the past several years. Two of the criteria are the equivalent lower order system approach and the bandwidth criteria. Several other criteria are available, such as C*, Neal-Smith, and time response characteristic envelopes, and are useful as design criteria.

14.12.1.1.1 Equivalent Lower Order Systems

The equivalent lower order systems approach attempts to fit the Bode gain and phase angle plots of a high order augmented aircraft transfer function (aircraft pitch rate response due to a pilot stick force input, for example) with an equivalent lower order transfer function (a transfer function which nearly matches the Bode gain and phase angle curves over a wide range of frequencies, typically 0.1 to 20 radians per second). The approach concentrates on those characteristics which greatly influence aircraft handling qualities — the short period, Dutch roll, and roll mode parameters. Once the equivalent lower order system is obtained, the requirements of MIL-F-8785C are applies to the aircraft parameters, such as short period damping ratio and natural frequency, as identified from the equivalent lower order transfer functions.

Equivalent lower order transfer functions are derived from classical aircraft dynamics theory which, for example, provides a second order transfer function relating the aircraft pitch rate response to the elevator deflection of the form

$$\frac{\dot{\theta}(s)}{\delta_e(s)} = \frac{K_\theta \; (s + 1/T_{\theta_2})}{s^2 + 2\zeta_{sp}\omega_{n_{sp}} \, s + \omega_{n_{sp}}^2} \tag{14.163}$$

where $1/T_{\theta_2}$ is a parameter which relates to the aircraft's load factor change to an angle of attack change (n/α) as

$$\frac{n}{\alpha} = \frac{V(1/T_{\theta_2})}{g} \tag{14.164}$$

The above equation is limited in its ability to match phase angle shifts of an actual aircraft transfer function which are due to the compensators, actuators, integrators, filters and other elements present in the flight control system. The equivalent system procedure augments the equation with the addition of a time delay factor to introduce phase lag without affecting the gain characteristics. The resulting system transfer function is

$$\frac{\dot{\theta}(s)}{\delta_e(s)} = \frac{K_\theta \; (s + 1/T_{\theta_2}) \, e^{-\tau s}}{s^2 + 2\zeta_{sp}\omega_{n_{sp}} \, s + \omega_{n_{sp}}^2} \tag{14.165}$$

where τ is equivalent time delay, in seconds. Requirements are being established for the time delay parameter (MIL-F-8785C places a limit on the apparent time delay as seen by the pilot).

The primary advantage of the equivalent lower order systems approach is the retention of the current MIL-F-8785C requirements with minor additions to account for the equivalent time delay due to the flight control system dynamics. The data on aircraft handling qualities obtained through years of inflight experimentation are retained. Good correlation has been obtained using these criteria and comparing them to flight test data. The importance, however, of the effective time delay (no actual time delay occurs in analog flight control systems, only in digital systems) has been demonstrated and shown to have significant effects on aircraft handling qualities.

The equivalent lower order systems approach is not yet completely accepted by the aerospace industry. Much disagreement exists concerning the best way to achieve the curve fit to the actual aircraft transfer function.

14.12.1.1.2 Bandwidth Criteria

The bandwidth requirement is a task oriented criterion motivated by the hypothesis that each aircraft task can be accomplished well if the aircraft has good response characteristics over a sufficiently wide range of pilot control input frequencies. This is essentially what MIL-F-8785C attempts to achieve through open loop test requirements. It is especially applicable to highly augmented aircraft.

Two criteria are specified: an equivalent time delay to account for the higher order dynamics of the aircraft, and the bandwidth of the aircraft transfer function. The bandwidth is calculated two ways. The frequency and gain where the phase angle is -180°, ω_{180} is determined. The frequency at the gain which is 6 db above the ω_{180} gain is defined as the bandwidth $\omega_{BW_{GAIN}}$ due to the gain margin. The frequency at a phase margin of 45° $\omega_{BW_{PHASE}}$ is found and is defined as the bandwidth due to the phase margin. The lesser of $\omega_{BW_{GAIN}}$ and $\omega_{BW_{PHASE}}$ is the bandwidth of the aircraft (see figure 14.184).

To determine the level of compliance with the proposed MIL-F-8785C criteria, the equivalent time delay is also needed. This is computed using the formula

$$\tau_p = -\frac{(\phi_{2\omega_{180}} + 180)}{2(57.3)(\omega_{180})} \qquad (14.166)$$

where $\phi_{2\omega_{180}}$ is the phase angle at twice the frequency where -180° of phase angle occurs.

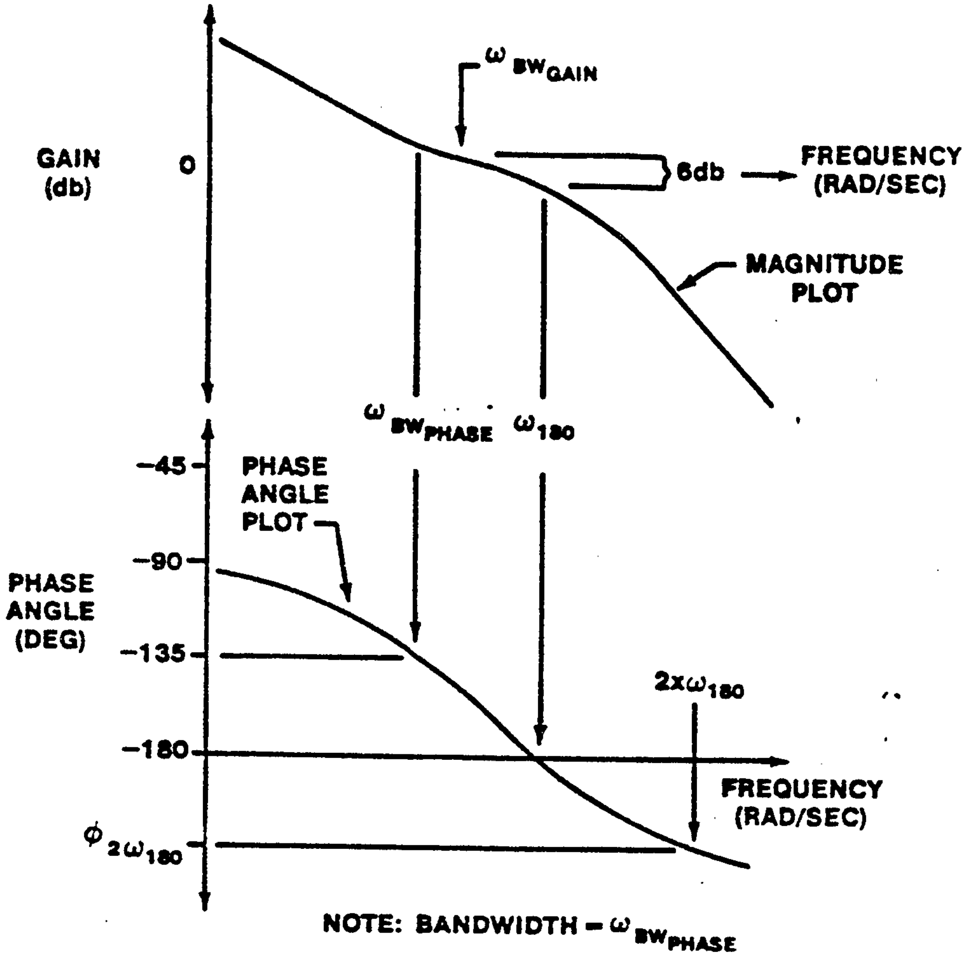
$\omega_{BW_{GAIN}}$
GAIN (db)
0
6db
FREQUENCY (RAD/SEC)
MAGNITUDE PLOT
$\omega_{BW_{PHASE}}$
ω_{180}
-45
PHASE ANGLE PLOT
-90
PHASE ANGLE (DEG)
-135
$2x\omega_{180}$
-180
FREQUENCY (RAD/SEC)
$\phi_{2\omega_{180}}$
NOTE: BANDWIDTH = $\omega_{BW_{PHASE}}$

FIGURE 14.184 DEFINITION OF BANDWIDTH

Figure 14.185 shows an example of the proposed bandwidth criteria, which have been correlated to pilot ratings during flight tests. The advantage of the bandwidth criteria is its simplicity of application, both for the flight control engineer and the flight test organization. The basic assumptions of the criteria are widely accepted in industry, but some controversy exists as to its exact application, especially the lack of any specification on the control sensitivity of the aircraft (gain margin criteria). The major disadvantage is that new criteria are required for MIL-F-8785C since the current criteria do not relate to the bandwidth hypothesis. This negates a large store of acquired knowledge and requires research to ensure that the criteria developed are adequate.

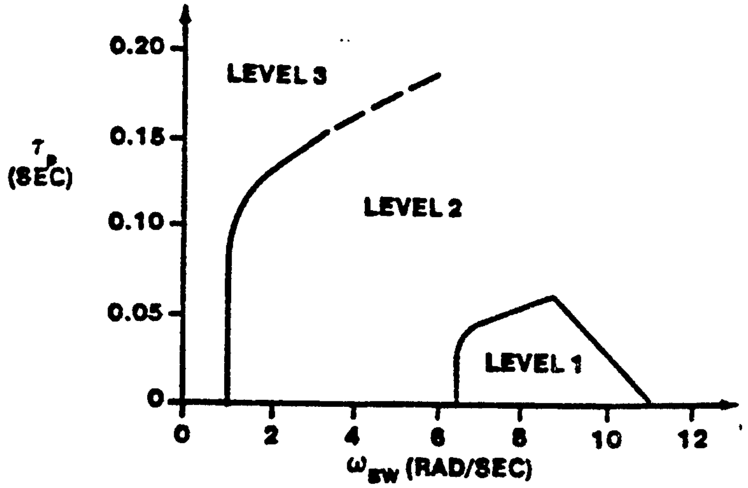

a. REQUIREMENTS FOR CATEGORY A FLIGHT PHASES

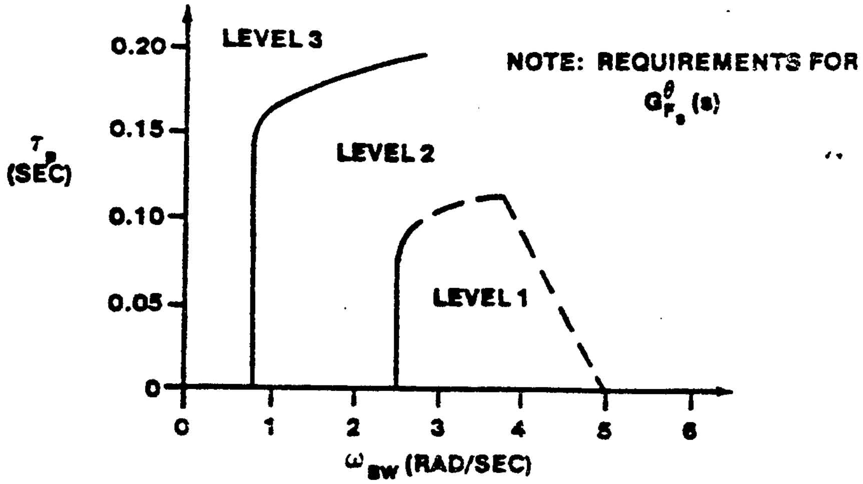

b. REQUIREMENTS FOR CATEGORY C FLIGHT PHASES

FIGURE 14.185 PROPOSED BANDWIDTH REQUIREMENTS FOR CLASS IV AIRCRAFT (PITCH ATTITUDE CHANGE DUE TO PILOT STICK FORCE)

14.12.1.2 MIL-F-9490 "Flight Control Systems - Design, Installation and Test of Piloted Aircraft, General Specification For"

This specification applies to the general performance of flight control systems in Air Force piloted aircraft. This includes specifications for flight control system design, survivability, maintenance, structural integrity, pilot controls and displays, sensors, computers, actuators, and quality assurance. In addition, MIL-F-9490 contains detailed requirements for autopilot performance.

Methods for demonstrating compliance with the requirements of the specification fall into the following categories:

1. Analysis
2. Inspection
3. Test
    a. Laboratory (including piloted simulations)
    b. Airplane ground
    c. Airplane flight

To the maximum extent possible, compliance with quantitative requirements must be demonstrated by actual tests.

14.12.2 Ground Tests

The flight control system and related subsystems should be thoroughly tested on the ground prior to the start of flight testing. This is critical in the case of flight control systems since the pilot's ability to fly the aircraft is directly dependent upon the proper operation of the flight control system. A comprehensive ground test phase will ensure that the flight control system is installed correctly and functioning properly, and will reveal some flying qualities or flight control system design deficiencies which can impact flight safety. All system components must be tested to demonstrate their satisfactory performance and operation under the environmental extremes expected to be encountered during the flight test program. Some of these tests will be the responsibilty of other organizations, such as the contractor. The results of these mandatory tests should be reviewed, however, by the flight test organization. A summary of the mandatory ground test requirements (detailed in MIL-F-9490) is given in the following sections.

14.12.2.1 Ground Simulation Tests

The complete flight control system must pass the following tests, either on an "Iron Bird" mockup coupled to a computer aerodynamic simulation of the aircraft (where the flight control system is functionally, statically, and dynamically duplicated), or on the actual aircraft.

1. Power supply variation tests
2. Limited fatigue tests - to ensure the structural integrity of the flight control system mechanical elements

3. Stability margin tests — which cannot be economically or safely tested in flight
4. Flight control system failure tests — to determine the effects of single and multiple flight control system component failures on the performance, safety, or mission accomplishment reliability of the aircraft as well as to develop emergency procedures to counteract the effects of failure
5. Flight control system wear life tests - to identify areas where component wear is likely and where frequent inspection may be required
6. Temperature variation tests
7. Integration tests - to determine the compatability of flight control system elements with interfacing systems, such as navigation, pitot static, or weapons delivery systems

Analog and digital flight control computer program operation should be thoroughly tested using ground simulations, the "Iron Bird" mockup, and the aircraft, and should include simulated support system and flight control system failures. A real danger exists in the area of digital systems, where insidious programming bugs may occur, endangering flight safety.

14.12.2.2 Ground On-Aircraft Tests

The following ground tests must be performed on the test aircraft:

1. Limit cycle tests (see section 14.12.5.2 for test techniques)
2. Structural resonance tests (see section 14.12.5.3 for test techniques)
3. Functional checks - to ensure proper flight control system operation in the aircraft as well as check that test instrumentation does not impact flight control system performance (see section 14.12.5.1 for test techniques)
4. Electromagnetic interference tests
5. Integrity tests - to ensure soundness of components and connections as well as the adequacy of component clearences and proper operation
6. Taxi tests
7. Flight control system failure tests

14.12.3 In-Flight Simulation

During a flight control system development effort, in-flight simulation of the aircraft and flight control system should be seriously considered. Ground simulations are most deficient in areas where pilots make high frequency inputs to the aircraft, such as during landings, fingertip formation, air refueling, air-to-air and air-to-ground tracking, or other maneuvers where the pilot relies on visual or motions cues. Time delays due to digital sampling and computation which appear in the visual systems of ground simulators preclude the use of these simulations as a viable method for handling qualities determination and refinement during high gain piloting tasks.

An in-flight simulation effort, if pursued, should occur relatively early in the flight control system development — shortly after the major control system configuration decisions are finalized based on ground simulations, and as soon as adequate wind tunnel data are available to provide a realistic simulation of the aircraft. The idea is to perform inflight simulations early enough so that handling qualities deficiencies, especially in those flight phases which are not well simulated on the ground simulators, can be identified and corrected.

Current in-flight simulators include:

1. The Total Inflight Simulator (TIFS), a six degree of freedom variable stability C-131 which is capable of purely digital, purely analog, or hybrid flight control simulations

2. The variable stability NT-33, a three degree of freedom aircraft with analog or digital control system capabilities

3. The variable stability X-22 Vertical Takeoff and Landing aircraft for V/STOL simulations

4. Two variable stability Navions, one with a six degree of freedom capability

5. A variable stability Learjet with three degrees of freedom and similar capabilities as the NT-33. This aircraft is not normally available for inflight simulations due to its use for student test pilot instruction at the Air Force and Naval Test Pilot Schools

6. A variable stability F-16 is being planned for future use

A major limitation of airborne simulations is an inability to completely simulate the test aircraft, particularly aircraft performance, structural effects or cockpit environment of the test aircraft. It is essential to minimize the effect of those characteristics of the simulation aircraft which interfere with the desired evaluation.

14.12.4 Flight Tests

Flight testing ensures that the aircraft flight control system meets the following general criteria:

1. Contractual specifications
2. Adequate flying qualities for mission accomplishment
3. Proper system operation under a variety of flight conditions and situations
4. Flight safety considerations

Preparation for the flight test requires a consolidation of experience from the following areas:

1. A thorough knowledge of the flight control system operation and design. Analysis of the flight control system block diagram will aid in understanding the system in detail and will help identify specific test objectives. Computer analysis programs available at the Air Force Flight Test Center, as well as analysis methods discussed in this text, should be used.
2. Consideration of the results obtained during ground and airborne simulations. The limitations of each simulation method used must be kept in mind when evaluating the results of handling qualities tests.
3. Analysis of the results obtained during ground tests conducted on the flight test article.
4. Advantages and disadvantages of the various test methods available to determine the adequacy of the aircraft's handling qualities for the required mission phases.

When testing the handling qualities of an aircraft, a thorough knowledge of the aircraft's design missions and required mission elements is essential. The test pilot often makes qualitative decisions regarding the mission suitability of the aircraft. He can only assess the suitability of the aircraft based on his flight experience, his training, and his understanding of the intended mission. Sometimes an aircraft must be evaluated against a new mission, and the pilot must rely heavily upon his understanding of the tasks required to accomplish that mission rather than upon his personal flight experience. Table 14.6 provides a list of tasks that are elements of a multi-role fighter mission. A listing of this type is a first step in the design of a handling qualities test program. After the mission tasks are

TABLE 14.6 TYPICAL FIGHTER MISSION PROFILE

MISSION EVENTS

- Ground Checks
- Taxi
- Takeoff
  - Rotation
  - Gear and Flap Retraction
  - Acceleration
- Climb
- Level Off
- Cruise
  - Steady Turns
- Mission Tasks
  - Subsonic, Transonic, Supersonic Flight
  - Acrobatics
    - Lazy 8
    - Loop
  - Air Refueling
  - Air-to-Air Combat
    - Gunnery
    - Missiles
    - Break Turns
    - Jinkout Maneuvers
  - Air-to-Ground Combat
    - Roll-ins
    - Strafe
    - Dive Bomb
    - Pop-ups
    - Rolling Pull-offs
  - Low Level
  - Formation
    - Fingertip
    - Trail
    - Fighting Wing
    - Tactical
- Descent
- Approach
  - IFR
  - VFR
  - Information
- Landing
  - Normal
  - Minimum Run
  - Crosswind
  - Wet or Icy Runway
  - Emergency
  - Formation

defined, the specific elements of each task should be determined to clearly define important considerations which contribute to task accomplishment (Table 14.7 shows an example). Once the specific elements of a task are defined, flight test maneuvers may be specified to thoroughly evaluate the handling

TABLE 14.7 DETAILED TASK ANALYSIS

TASK: APPROACH AND LANDING

ELEMENTS:

Airspeed (Angle of Attack) Control
- Speed Stability
- Slow Speed Cue
- Flight Path Stability
- Engine Response
- Turbulence Effects

Flight Path Control
- Longitudinal Attitude Control, Predictability and Precision
- Aim Point Predictability and Precision
- Short Period Dynamics (High Gain Task)
- Control of Runway Alignment

Attitude Control
- Control Harmony
- Control Sensitivity
- Friction and Breakout
- Predictability and Precision
    - Touchdown
    - PIO Tendency
    - Float and Balloon Tendency
    - Turbulence Effects
    - Aerobraking

Touchdown Point Predictability, Precision and Repeatability
Gear Dynamics at Touchdown
Crosswind Effects
IFR (Hood) Approaches
- Heading Control

Overhead Traffic Patterns
- Maneuvering Gradient

Heads-Up Display and Instrument Lag Effects
- Angle of Attack
- Attitude Reference
- Flight Path Reference
- Readability

Approach Techniques
- Constant Angle of Attack to Touchdown
- Flare
- Wing Low
    - Lateral-Directional Stability
- Crab

Pilot Visibility

qualities of the aircraft (see Section 14.12.5.4 for specific flight test techniques).

In developing a test plan particular attention should be given to the following flight control system areas:

1. Variable gain scheduling operation.
2. Single point failures and resulting flight control characteristics.
3. Effect of programmed control system reconfigurations, such as switch position gauges and feedback control law alteration (change from pitch rate feedback to blended rate and load factor feedback, for instance).
4. Failure mode tests, concentrating on transients, proper operation of the degraded system and the adequacy of aircraft handling qualities.
5. Operation of automatic limiters, such as load factor or angle of attack limiters, during both slow and rapid maneuvers.
6. Operation of special features such as roll coupling prevention features during aileron and rudder rolls, under varying load factor conditions.
7. Effects of actual weapons employment on handling qualities, especially gun firing.
8. High angle of attack maneuvers including stall warning or prevention features incorporated into the flight control system. These should be tested during 1 g and accelerated maneuvers as well as during very slow flight conditions such as resulting from nose high zooming flight at speeds below the stall speed. Departure and spin characteristics with the flight control system engaged should be investigated as well as transients due to partial or complete flight control system disengagements as high angle of attack flight is approached (disengagement of the A-7 roll CAS at 22 units angle of attack, for example).
9. Pilot relief mode operation (autopilot features). These must meet the requirements of MIL-F-9490.
10. Engagements and disengagement transients during autopilot operation.
11. Operation of warning systems to advise the pilot of inadvertent autopilot disengagements.
12. Effects of atmospheric turbulence, jet wash and runway crosswinds on the aircraft's handling qualities.
13. Verification of gound test data concerning limit cycle gain margins and structural resonance.

14. Effect of asymmetric store loads on all aspects of the control system operation and performance, especially regarding adequacy of control authority, automatic maneuver limiter operation and high angle of attack characteristics.

15. Effects of center of gravity location and gross weight on handling qualities.

16. Trim system rates and authority (including auto-trim features).

17. Electrical power transients or voltage reduction effects on control system operation and flying characteristics.

18. Hydraulic system failure effects.

19. Fault tolerance (ability to reconfigure or compensate for detected system failures) and redundancy management (voting schemes to detect faults).

20. Human factors associated with flight control system operation, pilot control actuation techniques, control harmony, friction, breakout, and control forces.

21. Operational environmental effects on control system components and overall system operation.

22. Environmental control system capabilities to provide adequate cooling for flight control system avionic components.

23. Operation of unconventional flight modes as well as associated human factors and handling qualities.

24. Structural implications of control system operation. This is critical in programs like the AFTI/F-16 where the control surface motions are changed relative to the F-16 to provide unconventional flight modes.

25. Effects of non-flight control system failures (such as engine failures in various configurations) on the handling qualities of the aircraft. These failures should be tested in conjunction with a fully operational flight control system (compatible with the failure) as well as with partial or complete flight control system failures.

26. Flight control system operation during maneuvers typical of the aircraft operational mission, including training maneuvers. The A-10 Beta-dot stability augmentation system (SAS) provides rudder inputs during maneuvers which pass through 90° of pitch (loops) and during turns when the SAS gain is suddenly changed according to a discrete, rather than a continuous gain schedule with airspeed.

27. Effects of nonlinear force gradients on pilot-in-the-loop tasks, especially near gradient slope changes

14.12.5 Test Techniques

The following discussion of flight control system test techniques has been divided into four sections: Ground Functional Test Techniques, Limit Cycle Test Techniques, Structural Resources Test Techniques, and Handling Qualities Test Techniques.

14.12.5.1 Ground Functional Test Techniques

Functional tests should be accomplished on the aircraft prior to flight to ensure proper flight control system implementation. Control force and deflection gradients can be verified (irreversable controls) by measuring pilot applied forces and the resulting control deflections and then comparing these to the signals applied to the flight control system. A similar technique could be used on a mechanical system with hydraulically actuated control surfaces that do not allow access to components within the system, the control input to control surface position output can be used to verify the force gradient.

Frequency response can be used to determine the open loop transfer functions of the flight control system or to obtain transfer function data on individual components within the system, such as actuators, filters or compensators. The procedure is shown in Figure 14.186. A sinusoidal test signal (from a calibrated oscillator) is applied to a given path of the flight control system (stick force input to control surface deflection or feedback sensor output to control surface deflection). The input and output sinusoidal signals are recorded. The amplitude ratio of the output to the input is computed, as well as the phase shift between the input and the output. A Bode plot of amplitude ratio versus frequency and phase shift versus frequency is constructed and compared directly with block diagram computed data. Transfer function testers are available to perform the frequency response tests and compute the transfer function Bode diagram automatically. However, if the flight control system has nonlinear elements which are frequency dependent (where exciting the system at a particular frequency changes the gain at all frequencies — such as the Space Shuttle Pilot-Induced Oscillation suppressor) the results can be misleading. Another approach uses the Frequency Response Analysis (FRA) program available at the Air Force Flight Test Center and applies a standard input test signal to the flight control system. Output parameters are recorded at various points in the flight control system and the FRA program reduces the data and provides Bode plots of the transfer

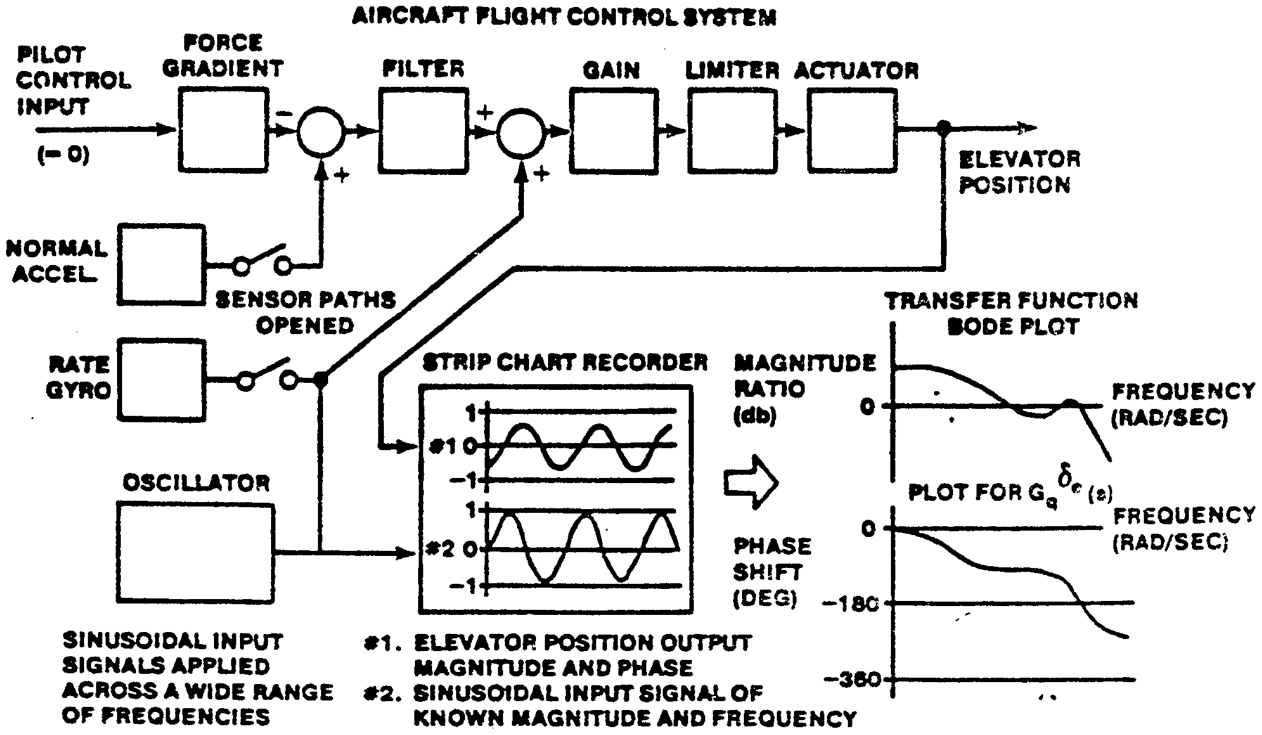
AIRCRAFT FLIGHT CONTROL SYSTEM
PILOT CONTROL INPUT
(= 0)
FORCE GRADIENT
FILTER
GAIN
LIMITER
ACTUATOR
ELEVATOR POSITION
NORMAL ACCEL.
RATE GYRO
SENSOR PATHS OPENED
OSCILLATOR
STRIP CHART RECORDER
#1
#2
1
0
−1
MAGNITUDE RATIO (db)
PHASE SHIFT (DEG)
TRANSFER FUNCTION BODE PLOT
FREQUENCY (RAD/SEC)
PLOT FOR $G_q^{\delta_e}(s)$
0
−180
−360
SINUSOIDAL INPUT SIGNALS APPLIED ACROSS A WIDE RANGE OF FREQUENCIES
#1. ELEVATOR POSITION OUTPUT MAGNITUDE AND PHASE
#2. SINUSOIDAL INPUT SIGNAL OF KNOWN MAGNITUDE AND FREQUENCY

FIGURE 14.186 FREQUENCY RESPONSE TEST PROCEDURE

functions. The test signals are of small enough amplitude to avoid saturating system limiters and the effects of deadzones are considered or bypassed. The effects of nonlinearities in the flight control system can be obtained by varying the amplitude of the input test signals and recording the outputs. The flight control system configuration must be the same as the configuration at the flight condition of interest.

Gain schedules which depend on pitot static inputs are verified using pitot static test equipment. The static ports are connected to a vacuum pump and the ram air port is connected to a pressure source. A particular altitude is simulated by lowering the static pressure and an airspeed is simulated by increasing the pressure at the ram air port. This procedure is used during pitot static system leak checks. The airspeed and altitude combination are determined from the cockpit instruments. The control system gains (voltage outputs) are recorded for a number of flight conditions and compared to the design values. Wheels on the ground switches and other switches in the flight control system may have to be artificially placed in the flight position to obtain proper flight control system operation.

An end-to-end check is performed to determine flight control system operation under simulated dynamic conditions. The pitot static system simulates a particular flight condition to set scheduled gains at the appropriate values. A computer simulation simulates aircraft aerodynamic responses to control surface inputs. These responses are applied to the flight control system where the sensor outputs interface with the flight control system. The actual control surface positions are provided to the simulation, closing the complete flight control system loop. Pilot inputs are applied through the control path and parameters in the flight control system recorded. Comparing actual flight control responses to engineering simulations for similar inputs provides a good check on the system implementation across a wide range of aerodynamic conditions.

14.12.5.2 Limit Cycle Test Techniques

Perform limit cycle tests on each axis separately unless coupling of the control system axes occurs, in which case multiple, or even all, axes should be tested simultaneously as well as separately.

14.12.5.2.1 Limit Cycle Ground Tests

The equipment and instrumentation necessary to conduct ground limit cycle tests include: an analog computer in which the appropriate aircraft aerodynamic equations of motion are programmed, position transducers on the control surfaces, and strip recorders to document control surface position limit cycle amplitudes and frequencies.

Extreme care is required when using a digital aircraft simulation since the sampling and computation lag in the simulation may alter the limit cycle characteristics of the aircraft. An analog simulation is usually preferred for limit cycle tests.

A simulated aerodynamic loop is closed on the aircraft by sending the control surface position to the analog computer (in which the aerodynamic transfer functions of the aircraft are programmed for the simulated flight condition). The outputs of the analog computer are the dynamic motion parameters, such as pitch rate, angle of attack, or normal acceleration, and are scaled and fed back into the flight control system at the point where the sensor output occurs, thus completing the control system loops. The actual sensors should be disconnected since actual aircraft motions (due to the control surface motions) would be added to the system, altering the limit cycle characteristics. Ensure the flight control system configuration (gain schedules, switch positions, etc.) is consistent with the simulated aerodynamic flight conditon.

Small, (less than one degree control surface command) and larger (greater than one degree) amplitude step inputs are applied to the control system at the point where the pilot input is summed to the feedback paths. Alternate inputs are applied where the sensor inputs are provided to the flight control system. Small and large inputs should be applied to the system at progressively increasing values of total loop gain. The loop gain may be adjusted at any point in the loop — in the flight computer for digital system and in the analog computer simulation of the aircraft in the case of hardwired analog flight control computers. Limit cycle amplitudes and frequencies are recorded at each gain setting by recording the control surface deflection on a strip chart recorder. The loop gains should be increased until a divergent oscillation is obtained.

Based on experience obtained during test programs conducted at the Air Force Flight Test Center, a gain margin criterion has been established for limit cycle phenomenon. With a gain margin of 6 decibels used (double the normal system gain at any flight condition), no limit cycle is allowed which has an amplitude greater than 0.5° of control surface deflection, peak-to-peak, in any axis. The maximum speed envelope is restricted to ensure the gain margin is provided during initial flights, if necessary. This criterion is conservative to provide a safety margin due to the many uncertainties which exist in predicting limit cycle characteristics. For aircraft which schedule control system gains with airspeed, Mach, or dynamic pressure, the high speed condition may not be the most critical in terms of encountering a limit cycle. The high speed condition will, however, be critical from the structural integrity point of view if a limit cycle is encountered.

14.12.5.2.2 Limit Cycle Flight Tests - Initial flights should use large gain margins for suspected limit cycle conditions by restricting the maximum speed using the ground test results. Before the flight envelope is expanded, carefully controlled inflight tests should determine the actual limit cycle characteristics of the aircraft and flight control system combination. Inflight tests are conducted by applying small, sharp step or pulse inputs into each axis of the flight control system at incrementally increasing stabilized airspeeds. Real time control surface data should be recorded at each flight condition. If no limit cycle tendency exists, the aircraft is cleared to the next point. This procedure is continued until a tendency toward a large amplitude limit cycle is observed. At all times, the test pilot must be ready to disconnect the control system, reduce speed or reduce the control system gain, if possible, should a control system instability occur. The results obtained from inflight tests establish the maximum allowable control system gain or maximum allowable flight speed.

14.12.5.3 Structural Resonance Test Techniques

Structural resonance occurring in flight can be destructive and result in the loss of the aircraft. The Air Force Flight Test Center policy is to conduct ground tests on the actual flight control system and structure of a new aircraft (as opposed to mathematically modelling the aircraft control system and structure). This eliminates many uncertainties concerning control system response characteristics, structural model response and sensor location with regard to the structural wave shapes.

14.12.5.3.1 Structural Response Ground Tests

Structural resonance for the worst case is assumed to be independent of aerodynamic flight conditions. No aerodynamic computations, such as those needed for limit cycle tests, are required. The tests apply relatively large, sharp inputs into each axis of the flight control system just prior to the surface servo actuators. The aircraft should be as close as possible to the actual flight configuration. All flight hardware and aircraft structure should be installed and secured. The landing gear struts should be deflated to a minimum allowable value to reduce gear frequencies as much as possible so that they will have minimal influence on the structural resonance frequencies. Tests should be performed on a range of fuel and external store configurations. The control surface frequency and amplitude for each axis are recorded to identify any structural resonance. The flight control system gains should be increased gradually to at least twice the maximum total system gain to be used inflight without encountering resonance.

Structural resonance can damage the aircraft even during ground tests. The flight control system must be disengaged as soon as resonance occurs. A good way to disengage the system is to disconnect the sensor by opening the sensor feedback path. For fly-by-wire aircraft, disconnect switches may be added to prevent feedback to the surface if resonance is encountered. The disconnect capability should be remote from the aircraft since large aircraft motions can be encountered during these tests. If a structural resonance problem is encountered, an aircraft flight control system redesign or gain reduction may be required.

The current structural resonance criterion requires that all three axes of the flight control system (six degrees-of-freedom for control configured vehicles) be capable of operating on the ground at twice the maximum total axis gain to be used in flight without sustaining structural mode vibrations. This conservative criterion was established due to the many uncertainties in predicting structural resonance. These uncertainties include inaccuracies in theoretical or experimental predictions of aeroelastic effects, atmospheric turbulence and variations in inertia and structural characteristics due to changes in fuel loads. It is therefore highly desirable to establish large gain margins for the first flight(s) where unexpected problems are likely to surface. As the system characteristics become known or actual inflight structural resonance characteristics are determined, this criterion may be relaxed somewhat.

14.12.5.3.2 Structural Resonance Taxi Tests

Obtaining structural resonance data should definitely be an objective of any taxi test. For example, the structural filter of the B-1 was modified as a result of structural resonance encountered during the initial high speed taxi tests conducted prior to its first flight.

14.12.5.3.3 Structural Resonance Flight Tests

Structural resonance flight tests are performed using sharp pulse inputs through the flight control system or by using a structural mode exciter system. These tests may be conducted in conjunction with limit cycle tests or during aeroelastic testing. Structural resonance may be distinguished from limit cycle by the frequency of the control surface oscillation. A careful buildup test procedure should be used.

14.12.5.4 Handling Qualities Test Techniques

Table 14.8 contains a list of flight test techniques available to determine the adequacy of flight control system performance. Open loop (non-task related) techniques are useful for aircraft which are not highly augmented, and respond to a pilot input with essentially a classical second order short period or Dutch roll. Static tests are useful for maneuvering force gradient testing and determining apparent static stability. A pilot control frequency sweep can generate time history data (similar to the tracking test technique data) which can be reduced to obtain Bode plots of the aircraft or flight control system transfer functions. Open loop tests provide data which can be compared to MIL-F-8785C requirements, and are thereby compared to characteristics experimentally determined to provide adequate handling qualities in various mission tasks. Even for classical aircraft, however, open loop tests cannot be relied on exclusively to determine the adequacy of the aircraft's handling qualities to accomplish mission related tasks. Open loop techniques were presented in earlier chapters and are not discussed in this text.

TABLE 14.8 HANDLING QUALITIES FLIGHT TEST TECHNIQUES

OPEN LOOP TEST TECHNIQUES

Longitudinal Static Stability
    - Stabilized Method
    - Accel-decel Method
Maneuvering Stability
    - Stabilized 'g' Method (Pull-up Technique)
    - Slowly Varying 'g' Method
Lateral-Directional Stability
    - Stabilized Sideslip Method
    - Slowly Varying Sideslip Method
Roll Performance (1 g and Loaded)
Dynamics
    - Doublet Inputs
    - Step Inputs
Trim Change Tests
Sinusoidal Stick Pump (Frequency Sweep)

CLOSED LOOP TEST TECHNIQUES

HQDT
    - Air-to-Air
    - Air-to-Ground
Fingertip Formation
Air Refueling
Spot Landings
Precision Approaches
    - Meatball (Carrier Landing System)
    - ILS
Precision Attitude Changes
Horizon Tracking

Open loop test techniques to identify the dynamic response characteristics of an aircraft do not adequately evaluate the dynamic modes of the aircraft.

This is particularly true in two situations:

1. High gain pilot-in-the-loop mission related tasks, such as formation, air refueling, precision landings, air-to-air or air-to-ground target tracking.
2. Highly augmented aircraft where the aircraft response is more dependent on the characteristics of the flight control augmentation system than on the aerodynamic characteristics of the aircraft.

Closed loop testing, where the pilot accomplishes a precision, well-defined, mission-related task, is essential. Closed loop testing can be divided into handling qualities during tracking techniques (HQDT) and handling qualities during mission elements techniques. HQDT techniques are currently the only methods available which can reveal handling qualities deficiencies in highly augmented aircraft (those in which the dynamic response characteristics of the aircraft are governed by the flight control system more so than by the aircraft aerodynamics).

The specific elements of closed loop handling qualities tests are:

1. Pilot flying the aircraft.
2. Mission oriented tasks.
3. Repeatable test maneuvers.
4. Rapid operational envelope scan.
5. Clearly defined performance standards and control strategies. Well-defined tracking tasks are normally used for test maneuvers.
6. Control stargegies which are operationally significant but which possess adequate frequency content so as to excite the aircraft and flight control system dynamics over a wide frequency range. To ensure adequate frequency content in the aircraft response, the pilot must immediately, positively, and continuously correct any tracking errors which occur, no matter how small the errors are. This aggressive piloting technique increases the pilot's gain (assuring adequate frequency content) while amplifying the adverse impact of handling qualities deficiencies upon task accomplishment.
7. Adequate duration to separate transient and steady state residual motions and to provide adequate frequency resolution. In analyzing time history data, the frequency resolution and the lowest identifiable frequency are inversely proportional to the duration of the test maneuver.
8. Separation of the effect of noise variables, such as atmospheric turbulence or aerodynamic buffet.

14.12.5.4.1 Handling Qualities During Tracking (HQDT) Test Techniques

The handling qualities during tracking (HQDT) test techniques were developed to excite dynamic modes that are not adequately excited by traditional open or closed loop test techniques. Tracking test techniques are a powerful tool for identifying handling qualities deficiencies, and were specifically developed to obtain engineering data to support pilot rating and comment data. An air-to-air tracking test is the most satisfactory precision tracking task, in terms of obtaining both qualitative pilot ratings and comments as well as quantitative time history data, although other tests are possible, such as air-to-ground tracking, precision formation flying or precision spot landings, as dictated by the aircraft's mission or flight phase. It is very important not to confuse tracking test techniques with the operational tracking and gun firing techniques associated with air-to-air combat. While it is expected that the results of tracking tests will provide information on the pilot's ability to precisely control the aircraft's attitude or flight path during combat maneuvers, the data gathered cannot be extrapolated to reflect specific operational mission effectiveness (such as kill ratios to be expected against typical adversaries).

The tracking test technique is philosophically based on the idea that a pilot performing a precision tracking task will be able to easily identify flying qualities deficiencies which make the task difficult to perform well. The pilot is in the loop, not merely providing a test input to obtain open loop data. The task is well defined and the pilot must perform aggressively to obtain the desired degree of precision.

Experience has shown that pilots who are unfamiliar with tracking test techniques or with the test aircraft and its flying qualities may require several familiarization maneuvers before good quality pilot comments and tracking data are obtained.

Precision tracking is the most important element of HQDT test techniques. HQDT precision tracking has a specific meaning that ensures that the combined airframe and flight control system dynamics are initially and continually excited during the tracking task. Precision tracking does not necessarily result in the best tracking of the target, and this is not even an objective.

Precision tracking begins with an acquisition task used to initially excite the augmented aircraft dynamics. For the remainder of the tracking task (20 to 30 seconds) the precision tracking technique serves to continually excite the combined pilot-aircraft dynamics.

The precision tracking technique used in flying qualities evaluations uses a fixed (noncomputing) gunsight. Computing gunsights are unacceptable since the gunsight dynamics may completely mask the actual aircraft handling qualities during aggressive tracking or the pilot may revert to operational tracking techniques which do not adequately excite the pilot-aircraft system dynamics. The gunsight pipper depression angle should be as nearly aligned with the roll axis as possible. It may be desirable to set the pipper depression angle to correspond to the actual roll axis for the test load factor (constant angle of attack tests).

For air-to-air tracking tests, a prominent feature should be selected on the target aircraft to be the precision aimpoint (like a tailpipe). During a tracking test, the tracking pilot must devote his entire mental concentration and physical effort to keeping the pipper on the precision aimpoint. Even the smallest pipper excursion from the precision aimpoint must be immediately, positively and aggressively corrected. The pipper must not be allowed to float near the target, or to stabilize in order to facilitate returning the pipper to the aimpoint. The tracking pilot must use the selected precision aimpoint and resist the tendency to aim at the "center" of the target aircraft. The result of this technique is to make the tracking errors worse than if the pipper were allowed to float undisturbed near the target, especially if the aircraft exhibits poor flying qualities. Despite the reduced tracking accuracy, the precision tracking technique perpetuates the initial perturbation of the combined airframe, control system and pilot dynamics, and has proved to be the most effective test technique for uncovering and magnifying flying qualities deficiencies.

With certain exceptions, tracking tests must be accomplished without using the rudder (pilot's feet on the floor). This is due to the ability of some pilots to completely mask flying qualities deficiencies through rudder coordination. There are two exceptions to this general rule. First, if the pilot is relatively unfamiliar with the aircraft, he may be allowed to use the rudder during the early stages of tracking tests. Serious flying qualities deficiencies will still become apparent despite the rudder coordination while increasing the pilot's familiarity with the aircraft. Second, after flying qualities deficiencies have been discovered using the "feet on the floor" method, the tracking test should be conducted allowing the pilot to use the rudder. This aids in determining the effectiveness of using the rudder during tracking and in proposing modifications to correct the handling qualities deficiencies.

The aircraft must be trimmed prior to starting the tracking maneuver and must not be retrimmed during the tracking test. During the early phases of flight control testing, tracking tests should begin near the middle of the flight envelope. As experience with the aircraft and control system accumulates, tracking test points where handling qualities deficiencies are expected or near the boundaries of the envelope (see Figure 14.187) are investigated. Knowledge of the aircraft's design mission role and mission flight arena will aid in test point selection. Also, a thorough knowledge of the flight control system operation, such as flight conditions where gains change, nonlinearities are encountered, or the control system configuration changes will help define additional test points.

Initial flight control system optimization should be conducted at a limited number of mission relevant test points — a representative air combat point (0.85 Mach at 15,000 ft) or a typical supersonic point (1.2 Mach at 30,000 ft), for example. Once acceptable handling qualities are achieved at these typical flight conditions a survey of the remainder of the flight

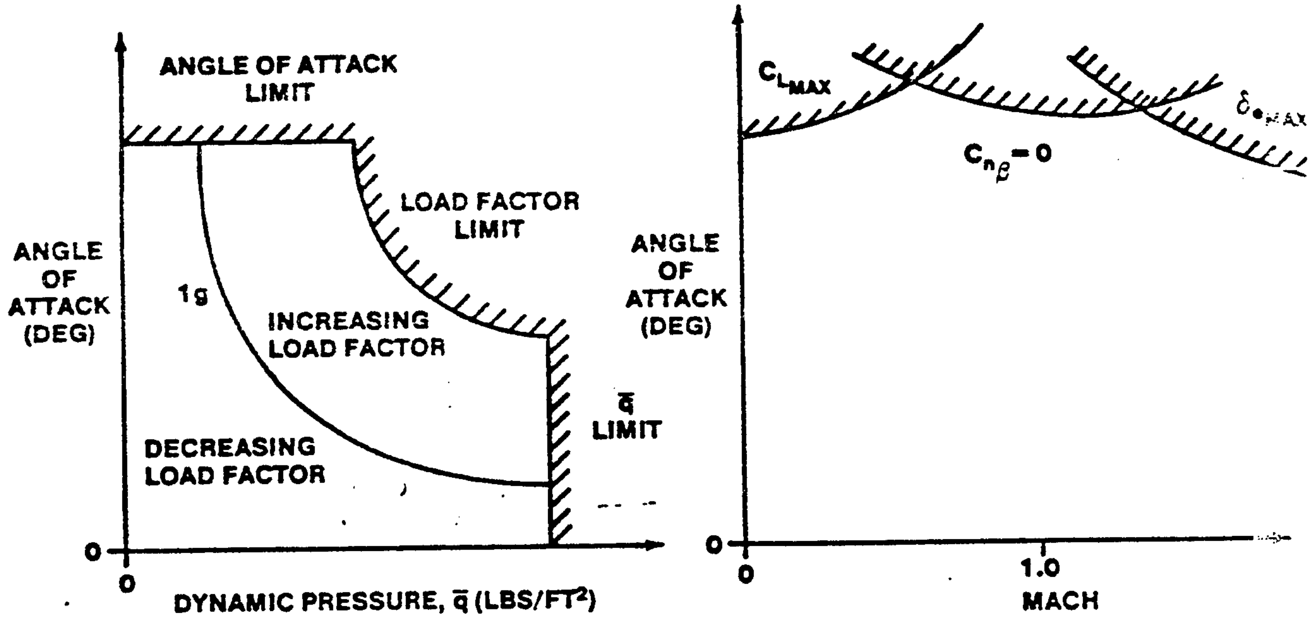

FIGURE 14.187 FLIGHT ENVELOP LIMITS OF AN AIRCRAFT AS FUNCTIONS OF ANGLE OF ATTACK VERSUS DYNAMIC PRESSURE OR MACH

envelope should be accomplished. Selecting a limited number of mission relevant points at which to conduct the bulk of the handling qualities developmental testing will establish a standard of acceptable handling qualities while reducing test time, cost, and uncertainty. Initial tracking tests for large aircraft, or for fighter aircraft in the power approach configuration, may be limited to precision tracking of mountain peaks or the horizon while in level flight. For aircraft which are not normally equipped with a gunsight, a series of reference lines should be provided on the windscreen to provide a reference for precision tracking. Heads Up! Testing in the proximity of other aircraft or the ground are hazardous since poor handling qualities could cause a PIO, mid-air collision or loss of control.

14.12.5.4.1.1 Air-to-Air Tracking Test Maneuvers - Target aircraft tracking maneuvers can be tailored to the specific handling qualities data to be investigated, but must possess two important characteristics:

1. The maneuver must be repeatable. It must be simple enough so that airspeed and load factor combinations can be easily and accurately repeated from day to day and from target pilot to target pilot.
2. The maneuver must require the tracking pilot to excite the aircraft and flight control system dynamics to be investigated.

Unless a specific problem is to be investigated, wind-up turns are recommended as the first tracking maneuvers to be performed. These maneuvers will allow the test team to quickly examine the aircraft's handling qualities throughout the useful range of angle of attack at various Mach and dynamic pressure test conditions. Wind-up turns may be followed by constant angle of attack tests.

14.12.5.4.1.1.1 Wind-Up Turns - Once the desired Mach and altitude are attained, two techniques may be used to initiate the maneuver:

1. The target establishes a 30° bank at the tracker's command with the tracker in trail. The tracker turns on the data systems (gun camera and onboard data acquisition system) and clears the target to maneuver. The target initiates the wind-up turn.
2. The tracker aircraft is aligned slightly below and inside (the designated turn direction) with the target in 1 g wings-level flight. After turning on the data systems, the tracker clears the target to maneuver. The target initiates the wind-up turn.

In either case, after being cleared to maneuver, the target pilot increases the angle of attack in the wind-up turn at approximately one degree every two seconds while the evaluation pilot performs the acquisition maneuver. The tracker tries to precisely track the aimpoint throughout the remainder of the maneuver. One acquisition maneuver used requires the tracker to place the target on an outer ring of the gunsight reticle and then as rapidly as possible move the target to the pipper, where precision tracking is immediately begun.

The optimum tracking range is 1500 feet, plus or minus 500 feet. This range keeps the tracker close enough to the target to clearly distinguish the precision aimpoint to the pilot and on the gun camera record, and far enough back to keep the tracker from entering the target's jetwash. If possible, ranging radar or transponder data may be displayed in the tracker's gunsight. The target's wingspan may also be used to estimate and control the tracking range.

The maneuver is terminated on command of the tracker after the target aircraft calls that he has reached the maximum test angle of attack, when the tracker aircraft handling qualities deteriorate to the point that precision tracking is not possible at maximum pilot effor, anytime flight safety considerations dictate, or when the desired test condtion Mach and altitude tolerance bands are exceeded.

Tests conducted at supersonic speeds may require the sacrifice of altitude to maintain Mach, especially at high load factors. Mach can decrease rapidly in a poorly performed maneuver, and "transonic dig-in", a sudden increase in load factor as airspeed decreases through the Mach 1 region, may cause and aircraft overstress and should be avoided.

14.12.5.4.1.1.2 Constant Angle of Attack Tests - Camera, time history and pilot comment data from wind-up turns will allow the test team to identify angle of attack and Mach combinations which warrant further testing.

The procedure used to accomplish constant angle of attack tests is similar to the wind-up turn. Upon command of the tracker, the target establishes a 30° banked turn at the test Mach and altitude. The tracker sets up approximately 1500 feet in trail. When the data systems have been turned on, the tracker clears the target to maneuver. The target smoothly increases angle of attack (load factor) at the desired Mach. The tracker moves the target to the desired location in the gunsight for the acquisition maneuver. The target calls when he is established at the desired Mach and angle of attack. The tracker begins precision tracking for 20 to 30 seconds.

If the effect of large perturbations on the pilot's ability to precisely track the target are desired, rapid constant laod factor barrel-rolling reversals of the turn direction may be incorporated into the constant angle of attack tracking turns. These reversals are performed at near combat reversal rates. A rolling reversal may be sandwiched between two constant angle of attack tracking maneuvers.

14.12.5.4.1.1.3 Transonic Tests - If the target and tracker aircraft each have sufficient engine thrust to maintain transonic speeds and angles of attack, tracking tests in the transonic region may be performed in a manner similar to subsonic tests. If insufficient thrust is available, transonic handling qualities can be examined using the constant angle of attack technique by starting the maneuver supersonic and permitting the Mach number to slowly decay through the transonic region while continuing to track.

14.12.5.4.1.2 Air-to-Ground Tracking Test Maneuvers - The techniques used for air-to-air tracking tests can be successfully used in air-to-ground tests when a target aircraft is not available. The disadvantages of air-to-ground tests are that only points near 1 g flight (load factor equals the cosine of the dive angle) can be investigated and the target range cannot be held constant. Strafing gunsight settings and shallow dive angles are preferred to steep dive angles or large gunsight depressions. Strafing passes allow more tracking time and better airspeed control. Tests should be conducted as close to a constant airspeed as possible in a shallow dive. A range of test airspeeds should be selected. The ground target selected should be prominent and well defined. The test aircraft should set up on the test condition with the target offset in the gunsight. The pilot attempts to rapidly acquire the target to excite the flight control dynamics. Precision tracking of the target should then be accomplished for 10 to 20 seconds. The tracking pilot must be cognizant of the hazards of target fixation during these tests. If desirable, the target may be changed after tracking the initial target. An initial acquisition maneuver is performed to move the pipper to the new target followed by precision tracking of the new target. This allows further investigation of the handling qualities in either the longitudinal or lateral axis by additional excitation of a particular axis of the aircraft.

14.12.5.4.2 Handling Qualities During Mission Elements Test Techniques

The mission elements commonly used for handling qualities investigations are formation, air refueling, and approach and landing.

14.12.5.4.2.1 Formation - Fingertip is the preferred formation for handling qualities investigation for formation tasks. The fingertip position should be well defined and adequate visual references should be provided to define the position accurately. The test aircraft should be flown to remain in the desired position precisely. Level flight, steady turns and Lazy 8 type maneuvers over a range of airspeed and load factors should be performed. Pilot comments, Cooper-Harper ratings and time history data should be collected throughout the maneuver. The precision formation task is a high pilot gain task. Fingertip formation in the power approach configuration is an excellent way to uncover handling qualities deficiencies associated with approach and landing.

14.12.5.4.2.2 Air Refueling - Proximity tests should be performed initially without trying for an actual hook-up. This will reveal the effects of the refueling aircraft's wake on the handling qualities of the receiver. Precise positioning should be achieved by visual cues and boom operator direction. Once the general handling qualities near the tanker are understood, the aircraft should be flown to an actual hook-up to investigate the effects of the boom proximity to the aircraft as well as the handling qualities during precision formation (trail formation) flying. For tankers, the effects of various large receiver aircraft in the air refueling position (such as the B-52 or C-5) should be investigated to determine the change in handling qualities associated with these aircraft during refueling operations.

14.12.5.4.2.3 Approach and Landing - Precision approaches can be flown using a Navy optical landing system or instrument landing system (ILS) approach. These tasks provide general handling qualities information for landing tests and reveal handling qualities deficiencies associated with instrument approaches. The optical landing system suffers due to lack of trend information as well as a changing vertical position sensitivity with decreasing range from touchdown. The ILS approach suffers in that the dynamics of the approach system indicators in the cockpit are included in the pilot loop. Another test technique available to evaluate handling qualities during the approach phase is the air-to-air tracking test technique at constant angle of attack in the power approach configuration.

Precision landing tests should be performed using spot landings. These tests reveal handling qualities deficiencies associated with precise pitch attitude and airspeed control, ground effect, and touchdown. Spot landings are difficult to perform in aircraft that require an extensive flare prior to touchdown. Several practice approaches must be performed to determine the aircraft performance characteristics during the flare and landing phase before meaningful pilot rating data can be obtained. It is essential to establish desired and acceptable touchdown zones and to award ratings according to the performance actually achieved during the spot landings.

14.12.6 Pilot Ratings

Pilot ratings are meaningful only for closed loop task performance. Pilot ratings are not assigned during classical open loop stability and control tests, nor are they assigned to aircraft performance characteristics. Specific closed loop tasks must be devised to determine how stability and control characteristics obtained during open loop testing affect pilot task accomplishment. These are the Cooper-Harper rating, the pilot induced oscillation (PIO) susceptibility rating and the turbulence effect rating. All three ratings should be given when appropriate along with a confidence level rating if desired.

14.12.6.1 Cooper-Harper Rating Scale

The Cooper-Harper rating is a numerical assessment of the aircraft's handling qualities as they affect the pilot's ability to perform a specific task (Figure 14.188).

The consistency of the ratings between pilots requires a clear understanding of the definition of the key decision making terms. The determination of aircraft controllability (first decision block in the scale) must be made withing the framework of the defined mission or intended use. An example of considerations which must be addressed when deciding if the aircraft is controllable might occur during an evaluation of fighter handling qualities during air-to-air tracking. The pilot encounters a situation in which aircraft control could be maintained only by devoting his complete and undivided attention to flying the aircraft. In this situation, the aircraft is controllable in the strict sense, but the pilot maintains control only by restricting the tasks he can perform and by giving the flying of the aircraft his undivided attention. For the pilot to answer that the aircraft is

HANDLING QUALITIES RATING SCALE

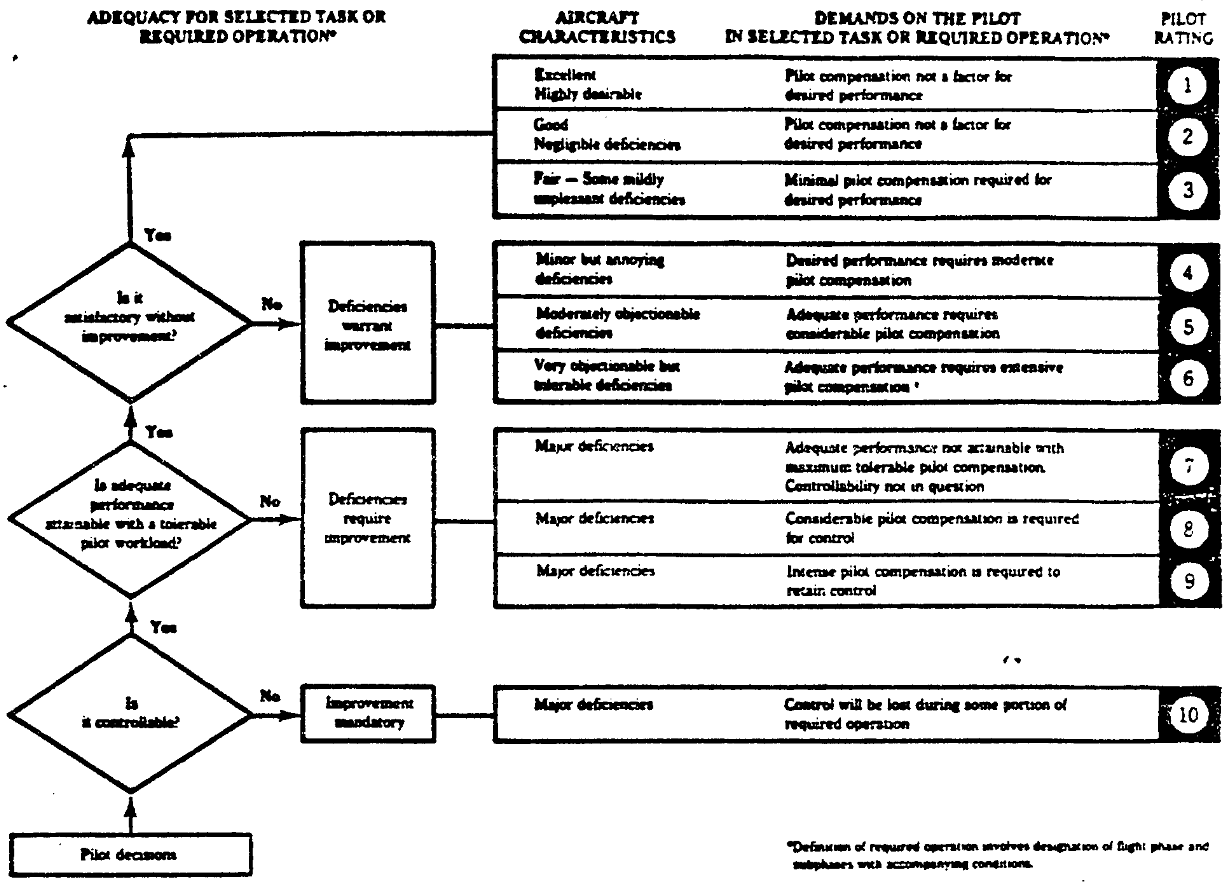
ADEQUACY FOR SELECTED TASK OR REQUIRED OPERATION*
AIRCRAFT CHARACTERISTICS
DEMANDS ON THE PILOT IN SELECTED TASK OR REQUIRED OPERATION*
PILOT RATING
Excellent Highly desirable
Pilot compensation not a factor for desired performance
1
Good Negligible deficiencies
Pilot compensation not a factor for desired performance
2
Fair – Some mildly unpleasant deficiencies
Minimal pilot compensation required for desired performance
3
Yes
Is it satisfactory without improvement?
No
Deficiencies warrant improvement
Minor but annoying deficiencies
Desired performance requires moderate pilot compensation
4
Moderately objectionable deficiencies
Adequate performance requires considerable pilot compensation
5
Very objectionable but tolerable deficiencies
Adequate performance requires extensive pilot compensation
6
Yes
Is adequate performance attainable with a tolerable pilot workload?
No
Deficiencies require improvement
Major deficiencies
Adequate performance not attainable with maximum tolerable pilot compensation. Controllability not in question
7
Major deficiencies
Considerable pilot compensation is required for control
8
Major deficiencies
Intense pilot compensation is required to retain control
9
Yes
Is it controllable?
No
Improvement mandatory
Major deficiencies
Control will be lost during some portion of required operation
10
Pilot decisions
*Definition of required operation involves designation of flight phase and subphases with accompanying conditions.

FIGURE 14.188 HANDLING QUALITIES RATING SCALE

controllable in this task, he must be able to retain control in all mission required tasks. Therefore, in the example discussed, the appropriate decision is that the aircraft is not controllable (control will be lost during some portion of the required operations) since all tasks could not be performed and those that could be performed required all the pilot's attention and effort, forcing him to neglect elements of his overall duties. Major aircraft deficiencies exist which require mandatory improvement.

Aircraft adequacy (second decision block in the scale) must be determined within the context of the task to be accomplished and the level of effort (pilot workload) that must be expended. A yes answer at this decision point in the rating scale means that the flight phase or task can be adequately accomplished, that the evaluation pilot would agree to use the aircraft for the designated role and that the deficiencies which exist can be tolerated.

Although the task can be accomplished with adequate precision, its accomplishment may require considerable effort and concentration on the part of the pilot. However, the workload required to achieve adequate precision in the task is tolerable and not unreasonable in the context of the aircraft's intended use. A no answer does not necessarily mean that the task cannot be achieved or that the pilot workload necessary to accomplish the task are of such a magnitude that the pilot rejects the aircraft for this aspect of the mission. It means instead that deficiencies and objectionable characteristics exist which require improvement.

The determination of whether the aircraft's handling qualities are satisfactory (third decision block in the scale) must be made in the context of the level of precision with which the required task can be performed and the workload required to attain the level of precision. The pilot's judgement of desired versus adequate performance must be considered. Satisfactory handling qualities does not imply that the aircraft is perfect, but rather that desired task performance is achievable without aircraft improvement. Unsatisfactory handling qualities imply that although the task can be adequately accomplished, the desired level of precision cannot be achieved (Cooper-Harper ratings of 5 and 6). A rating of 4 implies that although desired performance is achievable, it is attained at a higher than desired pilot workload.

The rating scale includes further subdivisions of quality within each of the primary categories. These subdivisions provide descriptions to define quality differences separating each numerical rating. The pilot should not award ratings of 3.5, 6.5 or 9.5 since this indicates a reluctance to make fundamental decisions with respect to a primary category, nor should he break his ratings down any finer than half ratings. The proper use of the rating scale requires the pilot to refer to the rating scale itself and sequentially answer each question.

14.12.6.2 Pilot Induced Oscillation (PIO) Rating Scale

The PIO rating scale (figure 14.189) is useful in conjunction with the Cooper-Harper rating scale to provide further insight into the aircraft handling qualities.

DESCRIPTION	NUMERICAL RATING
No tendency for pilot to induce undesirable motion.	1
Undesirable motions tend to occur when pilot initiates abrupt maneuvers or attempts tight control. These motions can be prevented or eliminated by pilot technique.	2
Undesirable motions easily induced when pilot initiates abrupt maneuvers or attempts tight control. These motions can be prevented or eliminated, but only at sacrifice to task performance or through considerable pilot attention and effort.	3
Oscillations tend to develop when pilot initiates abrupt maneuvers or attempts tight control. Pilot must reduce gain or abandon task to recover.	4
Divergent oscillations tend to develop when pilot initiates abrupt maneuvers or attempts tight control. Pilot must open loop by releasing or freezing the stick.	5
Disturbance or normal pilot control may cause divergent oscillation. Pilot must open control loop by releasing or freezing the stick.	6

FIGURE 14.189 PIO RATING SCALE

A pilot induced oscillation is an unwanted, inadvertent and atypical closed loop coupling between the pilot and the aircraft response. Factors which contribute to PIO include:

1. Excessive stick force to control surface lag
2. Rate saturated controls
3. High stick force friction
4. High bobweight friction
5. High bobweight contribution to stick force per g
6. Low short period damping
7. Low stick force per g or elevator deflection per g
8. Excessive control sensitivity

The PIO tendency will increase pilot workload to accomplish a given task, force the pilot to divert his attention from task accomplishment to aircraft control, or cause the pilot to lose control of the aircraft. If aircraft control is lost, the only successful recovery technique is for the pilot to either freeze or release the flight controls.

The PIO rating scale should be used in conjunction with the Cooper-Harper scale to rate the aircraft handling qualities during high gain pilot-in-the-loop tasks such as air-to-air tracking, precision formation flying or spot landings. The pilot should physically refer to the rating scale descriptions after completing a given task and award a PIO numerical rating along with a Cooper-Harper rating. These two ratings provide a more complete picture of the aircraft's handling qualities than either rating standing alone.

14.12.6.3 Turbulence Rating Scale

The turbulence rating scale (Figure 14.190) is designed to show the effect of turbulence on the handling qualities of an aircraft during precision, high gain tasks. If turbulence is encountered during handling qualities testing, this scale should be used in conjunction with the Cooper-Harper and PIO rating scales.

INCREASE OF PILOT EFFORT WITH TURBULENCE	DETERIORATION OF TASK PERFORMANCE WITH TURBULENCE	RATING
No Significant Increase	No Significant Deterioration	A
More Effort Required	No Significant Deterioration	B
	Minor	C
	Moderate	D
Best Efforts Required	Moderate	E
	Major (But Evaluation Tasks Can Still Be Accomplished)	F
	Large (Some Tasks Cannot Be Performed)	G
Unable To Perform Tasks		H

FIGURE 14.190 TURBULENCE RATING SCALE

14.12.6.4 Confidence Factor

A confidence factor scale (figure 14.191) may be used to indicate the level of confidence the pilot has that the task performed during a particular test was representative of the defined task. This factor is not to be used as an indication of the rater's inability to make a decision regarding the test aircraft's handling qualities. It is useful instead in judging the quality of the task performed, since data collected during non-representative tasks may not be useful. Both the tracker and the target pilots may assign confidence factors to the test maneuver to indicate if the task was flown as defined.

DESCRIPTION	CLASSIFICATION
The pilot rating was assigned with a high degree of confidence.	**A**
The pilot rating was assigned with only a moderate degree of confidence because of uncertainties introduced by moderate differences in environmental conditions, or in aircraft configuration or state, or in the task, from what was desired.	**B**
The pilot rating was assigned with minimum confidence because of important differences between the desired and the actual environmental conditions, aircraft configuration or state, or task, requiring considerable pilot extrapolation.	**C**

FIGURE 14.191 CONFIDENCE FACTOR SCALE

14.12.7 Configuration Control

During developmental testing of digital flight control systems it is critical to establish strict software configuration control policies. This is necessary to ensure that:

1. No software change is incorporated which results in the development of a flight safety hazard. Sufficient analysis must be performed to assess the impact of changes on the aircraft flying qualities.
2. The test configuration of the flight control system is known at all times. The configurations should be confirmed prior to flight using ground test procedures discussed in Paragraph 14.12.5.
3. Test results can be correlated to specific configurations.
4. Configuration changes are well documented.

Strict configuration control is required to ensure that proposed software changes are adequately reviewed prior to incorporation into the flight control system, and that the full impact of proposed changes are completely investigated (with adequated simulation, if available).

The procedures established to manage proposed software changes depend on the impact of those changes on the flight control system if the changes do not function properly, if unforeseen program operations occur, or if undesirable operations which already exist are further degraded. Software changes to the flight control program can fall into one of the following categories:

1. Nuisance failures which do not affect flight safety but may cause delays in some test accomplishment.

2. Mission failures which may degrade the flying qualities (reduce the level of flying qualities or cause reversion to backup flight control modes) and result in the loss of effective testing.

3. Flight safety failures which severely degrade flying qualities (cause large aircraft response transients or loss of control) and may result in loss of the aircraft as well as injury or death to the crew.

Flight control software changes are governed by Air Force Class II modification procedures and regulation (AFR 57-4 and AFSCR 80-33). These procedures are often unwieldly in software development efforts and alternate procedures must be established in the test plan. Strict software change review procedures should be used to ensure a complete technical and safety review of proposed changes as well as to formally document all changes (including a complete listing of the most recent software package with the changes incorporated). A possible way to manage this process is to create a software review board to assess the technical and flight safety impact of all software changes. When proposed changes are considered, the changes must be carefully evaluated for the entire envelope for which the aircraft has been previously cleared. Often a change implemented to correct a deficiency at one flight condition can adversely impact the flying qualities in another flight regime. Additionally, attention must be devoted to the effects of changes on limit cycle and structural resonance characteristics.

14.12.8 Flight Test Instrumentation and Data Acquisition

In addition to the data acquisition system configured for stability and control testing, the flight control computer should be instrumented to record:

1. Signals being supplied to the computer by sensors and pilot controllers.

2. Signals being sent by the computer to the actuators.

3. Internal signals within the flight control computer such as:

    a. Filter and integrator inputs and outputs.
    b. Switch positions.
    c. Inputs and outputs of nonlinear elements.
    d. Results of computation as well as signals being supplied to the computational algorithms.
    e. Operation of logic decisions.

A thorough instrumentation of digital flight control computer programs is extremely important during developmental testing. Thorough documentation of the operation of the flight control program will greatly aid data analysis, is essential to detecting and defining glitches in the program operation and is necessary to confirm the proper operation of the flight control system. Without this instrumentation, unexplained anomolies in the aircraft flying qualities will be difficult to explain and correct if they are a result of computer programming bugs.

Three sources of data are necessary to define flying qualities deficiencies using tracking test techniques: Pilot comments and Cooper-Harper ratings, gun camera film records of the pipper position relative to the target, and time history records of aircraft parameters such as pilot control forces and deflections, control surface positions, aircraft motion, and flight control system parameters.

The single most important source of data for discovering handling qualities deficiencies is the pilot comments and Cooper-Harper ratings. The best technique for gathering pilot comments is to record them as the test maneuver is peformed, or as soon as possible after the maneuver is completed. Cooper-Harper numerical ratings must be carefully awarded using the rating scale. Two other rating scales are also useful in defining handling qualities deficiencies: the pilot induced oscillation (PIO) rating scale and the trubulence rating scale. Taken together with the pilot comments, the three rating scales can provide meaningful comparitive data during a flight control optimization.

The gun camera film is a physical measure of what the pilot observes during the tracking test. Taken by itself, pipper motion analysis (figure 14.192) is not a reliable quantitative measure of the aircraft's flying qualities. It supplements pilot comments and ratings. If a video recorder system is used in place of a gun camera, the video may be effectively used during the debrief of each test maneuver and may result in additional pilot comment data.

The time history record of aircraft and flight control system parameters is obtained from the stability and control data acquisition system. These data are important in defining the cause of handling qualities deficiencies, which is essential if design modifications are required.

An accurate method of time correlating all three of the data sources is extremely important. This can be effectively accomplished using a data correlation switch (ideally the gun trigger). Activation of the switch should

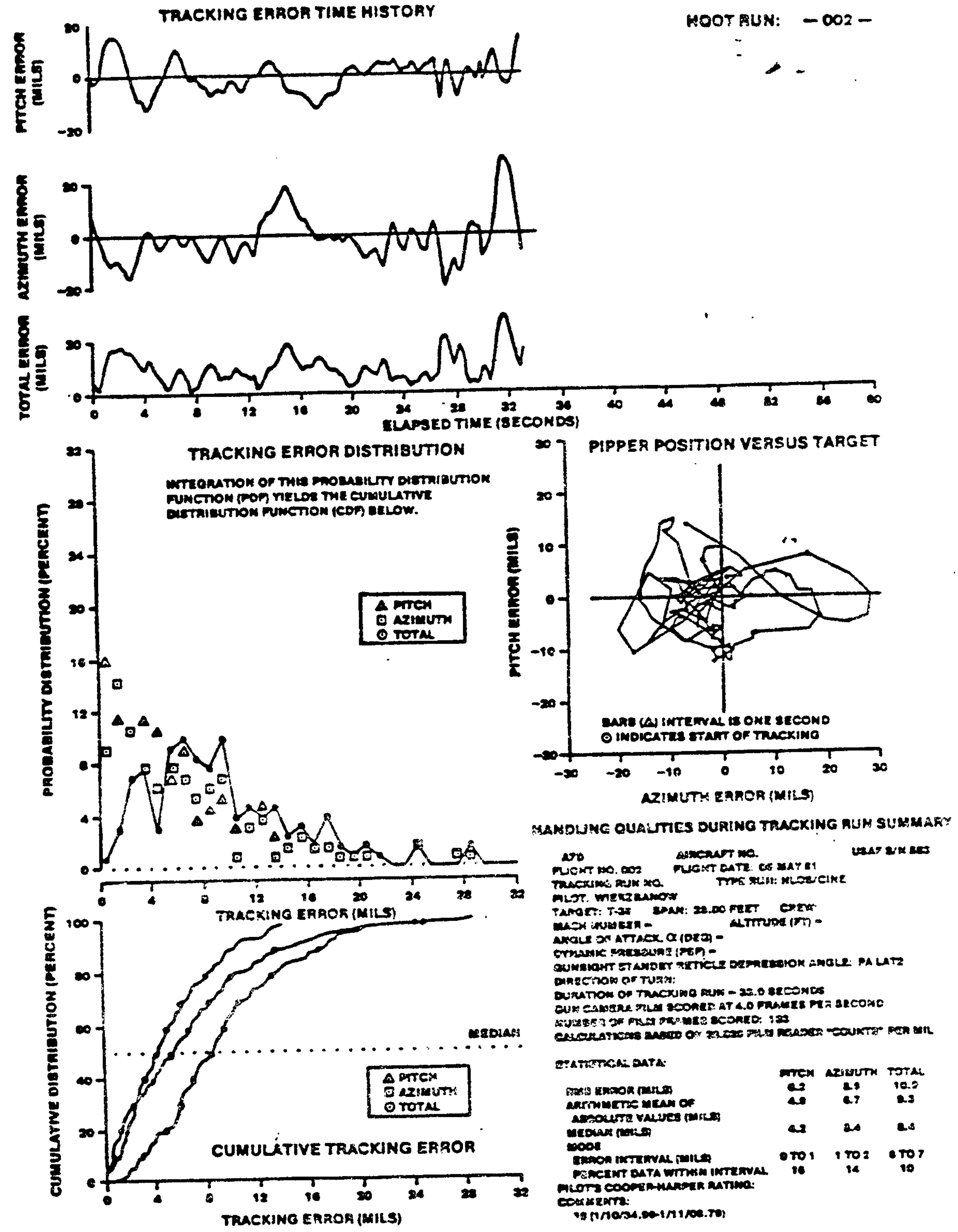

HANDLING QUALITIES DURING TRACKING RUN SUMMARY

A7D AIRCRAFT NO. USAF S/N 583
FLIGHT NO. 002 FLIGHT DATE: 06 MAY 81
TRACKING RUN NO. TYPE RUN: HLOS/CINE
PILOT. WIERZBANOW
TARGET: T-38 SPAN: 25.00 FEET CREW
MACH NUMBER = ALTITUDE (FT) =
ANGLE OF ATTACK, α (DEG) =
DYNAMIC PRESSURE (PSF) =
GUNSIGHT STANDBY RETICLE DEPRESSION ANGLE: PA LAT2
DIRECTION OF TURN:
DURATION OF TRACKING RUN = 32.0 SECONDS
GUN CAMERA FILM SCORED AT 4.0 FRAMES PER SECOND
NUMBER OF FILM FRAMES SCORED: 129
CALCULATIONS BASED ON 30.026 FILM READER "COUNTS" PER MIL

STATISTICAL DATA:

	PITCH	AZIMUTH	TOTAL
RMS ERROR (MILS)	6.2	8.1	10.2
ARITHMETIC MEAN OF ABSOLUTE VALUES (MILS)	4.8	6.7	9.3
MEDIAN (MILS)	4.2	5.4	8.4
MODE			
ERROR INTERVAL (MILS)	0 TO 1	1 TO 2	6 TO 7
PERCENT DATA WITHIN INTERVAL	16	14	10

PILOT'S COOPER-HARPER RATING:
COMMENTS:
18 (1/10/34.90-1/11/06.79)

FIGURE 14.192 CALCOMP PLOT TRACKING ANALYSIS OF AN AIR-TO-AIR TRACKING TASK

turn on a light in the gun camera field of view and provide a signal trace in the data acquisition system. A pilot comment into the tape recorder will correlate a voice recorder other than the voice track of the data acquisition system.

14.12.9 Data Analysis

There are two techniques available for data anlysis of closed loop handling qualities tests: System Identification From Tracking (SIFT) and Dynamic Parameter Analysis.

14.12.9.1 System Identification From Tracking

System Identification from Tracking (SIFT) is a flight test data analysis technique for evaluating the pilot-in-the-loop handling qualities of highly augmented aircraft. Normal stability and control flight test parameters are recorded by the onboard data acquisition system during pilot-in-the-loop, mission oriented, precision tracking maneuvers. Open loop sinusoidal stick pumps (frequency sweeps) may also be used, but tracking tasks are much preferred. The data are analyzed in the frequency domain. The transfer function data of the combined aircraft and flight control system can be used to verify aircraft compliance with the proposed flying qualities requirements using either the equivalent lower order system approach or the bandwidth criteria.

The preferred maneuver for obtianing this data is a constant angle of attack, Mach, and altitude, high gain air-to-air tracking task. Good frequency content in the pilot inputs and controlled test conditions are important to acquiring useful data. Use of the rudder is required if directional axis data are desired.

The quantitative test data, in the form of time histories of aircraft motion, control surface positions or flight control system parameters acquired during the test maneuver are analyzed using the Frequency Response Analysis program available at the Air Force Flight Test Center. This program uses a Fast Fourier Analysis scheme to provide user specified Bode plots. These Bode plots may be specified as the airframe aerodynamics (pitch rate due to elevator input transfer function, for example), the flight control system (elevator deflection due to pitch rate feedback signal transfer function), the overall aircraft (pitch rate due to pilot command input) or some other component or subsystem in the flight control system (elevator actuator displacement due to electrical signal input). An advantage of the Bode plots identified through SIFT, versus aerodynamic data obtained through parameter identification tests, is that the actual system is identified directly rather than using a "best estimate".

The quantitative data obtained during tracking tests have been extremely valuable in isolating the cause of handling qualities deficiencies. An example occurred in the F-15 flight test program. A two to three mil pitch bobble was observed during precision tracking maneuvers. Classical stability and control tests did not uncover the problem. Once observed, several attempts to isolate the cause of the pitch bobble and correct the problem failed. The SIFT technique isolated the pitch bobble frequency at twice the Dutch roll frequency by analyzing the augmented aircraft pitch rate due to elevator input transfer function Bode diagram obtained during precision tracking. The problem was found to be a cross-coupling of the lateral-directional dynamics into the pitch axis due to the rolling tail. Once isolated, the problem was corrected through flight control system redesign.

14.12.9.2 Dynamic Parameter Analysis

The dynamic parameter analysis relies on identification of aircraft stability derivatives from flight test data by using specialized test inputs and maneuvers. Stability derivative data is obtained by reducing flight test data using a maximum likelihood data reduction scheme.

Flight test determined stability derivatives are used to update analytical models (transfer functions) of the aircraft for improved flight control system design and analysis and to improve ground and airborne simulations of the aircraft and the flight control system. The updated aircraft transfer function data can be used to conduct an analysis of the augmented aircraft and a comparison of the results can be made to the requirements of MIL-F-8785C. The SIFT method is greatly preferred over the Dynamic Parameter Analysis technique for flight control system contractual compliance verification and handling qualities evaluation.

14.12.10 Control System Optimization

It is frequently necessary to obtain a concensus of opinion among a group of test pilots when optimizing a flight control configuration. Establishing criteria which the test pilots agree are important to the accomplishment of the required task is imperative.

Suggested criteria:

1. Desired performance limits for the task (these must be specified — for example, track the target within 5 mils of the aimpoint 80% of the time).
2. Adequate performance limits for the task (for example, track the target within 10 mils 50% of the time). Performance outside these limits is, by definition, not adequate and should be accompanied by Cooper-Harper ratings between 7 and 9.
3. Aircraft flight path predictability.
4. Control harmony.
5. Control forces.
6. Control sensitivity.
7. Workload required to accomplish the task.

Additional criteria may be required as problems are identified.

If pilot comments and ratings show a clear preference for a particular configuration then the data is capable of clearly supporting a conclusion. Discussion of the individual impressions of the various configurations is undesirable in general since the results could become biased. However, a clear preference is usually not apparent from the data and a discussion of the results and impressions is necessary to differentiate between the configurations tested.

The first step in arriving at a consensus is to rank the relative importance of the criteria. The test pilots must then discuss the various configurations, their ranking relative to the criteria, and the overall ranking of the configuration options. No one individual or group should dominate this discussion.

14.12.11 Mission Briefing and Debriefing

The following section contain lists of mission briefing and debriefing items for handling qualitities tests.

14.12.11.1 Mission Briefing Items

1. Review of Maneuvers and Test Conditions
   a. Target maneuvers to be flown
   b. Test Conditions
   c. Conditions at which maneuvers will be terminated

2. Review of Test Techniques
   - a. Target pilot responsibilities
   - b. Maneuver initiation technique
   - c. Initial excitation technique
   - d. Trim consideration (trim prior to maneuver initiation)
   - e. Rudder technique (feet on the floor)
   - f. Precision tracking test technique review (aimpoint, aggressive tracking)
   - g. Desired test range
   - h. Duration of the maneuver parts (20 seconds minimum)
   - i. Maneuver termination procedures

3. Pilot Evaluations
   - a. Pilot comment and rating procedures (use of the rating scales)
   - b. Particular aspects of flying qualities or task performance to which the tracking pilot should direct attention

4. Other Considerations
   - a. Gunsight depression angle
   - b. Time correlation procedures for data
   - c. Camera or gunsight filters
   - d. Gun camera and data acquisition system speeds
   - e. Marking of film magazines for identification
   - f. Check film magazine after each maneuver to assure proper operation

5. Safety
   - a. Procedures for avoiding jetwash
   - b. Special considerations (high angle of attack, departure, transonic dig-in)

14.12.11.2 Mission Debriefing Items

1. General Pilot Comments and Impressions

2. Discussion of Each Maneuver
   - a. Were the test conditions met?
   - b. Was the tracking aircraft trimmed for straight and level flight prior to the maneuver?
   - c. Did the tracking pilot retrim during the maneuver?
   - d. Was correct tracking range maintained?
   - e. Were the rudder pedals used?
   - f. Was the precision aimpoint used?
   - g. Was the aimpoint persistently tracked? Was the pipper allowed to float?
   - h. Was jetwash encountered?
   - i. Pilot comments and impressions of task performance and aircraft flying qualities
   - j. Cooper-Harper rating of flying qualities for the maneuver, based on step by step progress through the rating scale
   - k. What flying qualities improvements are desirable?

THIS PAGE LEFT INTENTIONALLY BLANK

FLIGHT CONTROL SYSTEMS

Study Guide

The following defintions apply to the terms "know" and "understand" used in the course objectives found in the study guide.

KNOW

Commit to memory. Be able to define, reproduce, prove, or otherwise demonstrate the concept with minimal information provided.

UNDERSTAND

Be thoroughly familiar with. Be able to use the concept in a reasoning process to draw conclusions. Limited information will be provided usually in one of the following forms:

a. example case
b. block diagram
c. fill-in-the-blank or matching exercise
d. basic functional description

Hour 1

Reading Assignment Prior to Class: pp 14.1 - 14.12
skim pp 14.12 - 14.46

Objective 1:

Understand how modern flight control systems evolved and the flying qualities problems they have introduced.

< 1915 -
1915 → WWII
WWII → present -
Current trend: Design for ____________.

Objective 2:

Know the two basic requirements of the control system of an airplane.

a.

b. Provide pilot with ______________.

Objective 3:

Know the requirements of cockpit control forces and deflections.

a. Pull - _________ nose, __________ speed

b. Push - _________ nose, __________ speed

c. Never reverse, except when ___________________.

Objective 4:

Understand the difference between the TPS and NASA sign conventions for aircraft motion and control displacements.

SIGN CONVENTIONS

(CONVENTIONAL FORMAT)

AFFTC:

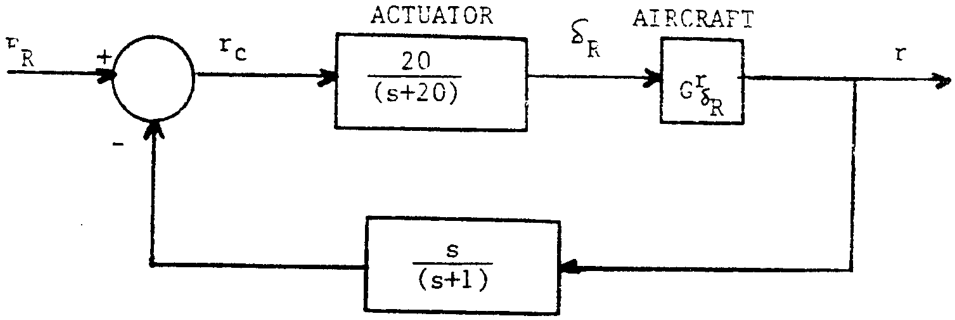

r_R
+
−
r_c
ACTUATOR
$\frac{20}{(s+20)}$
δ_R
AIRCRAFT
$G^r_{\delta_R}$
r
$\frac{s}{(s+1)}$

NASA:

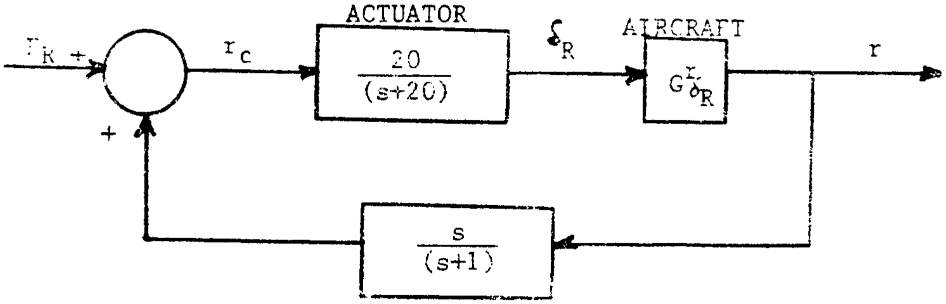

r_R
+
+
r_c
ACTUATOR
$\frac{20}{(s+20)}$
δ_R
AIRCRAFT
$G^r_{\delta_R}$
r
$\frac{s}{(s+1)}$

BLOCK DIAGRAMS

(PITCH RATE COMMAND SYSTEM)

CONVENTIONAL
FORMAT:

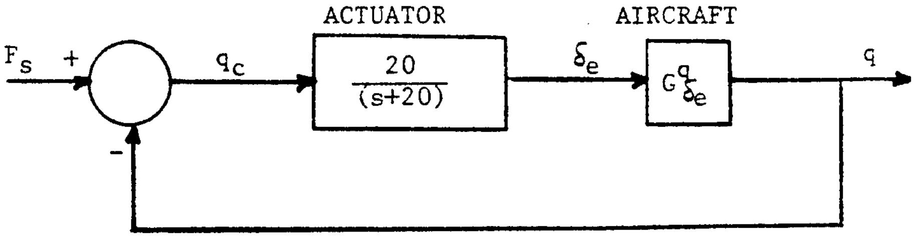
F_s
+
q_c
ACTUATOR
$\frac{20}{(s+20)}$
δ_e
AIRCRAFT
$G^{q}_{\delta_e}$
q
−

FLIGHT CONTROL
SYSTEM FORMAT:

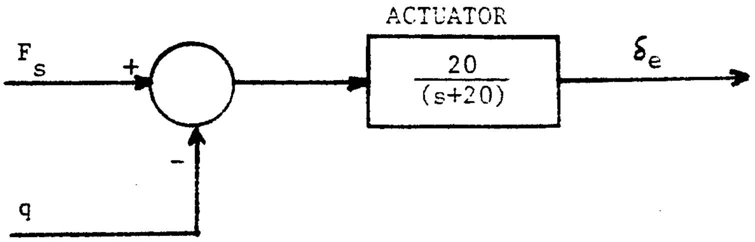
F_s
+
ACTUATOR
$\frac{20}{(s+20)}$
δ_e
−
q

SIGN CONVENTIONS

(FLIGHT CONTROL SYSTEM FORMAT)

AFFTC:

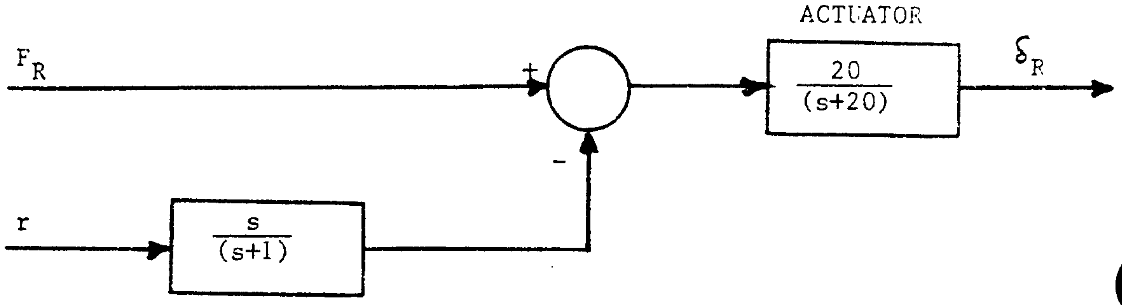
ACTUATOR
F_R
+
−
$\frac{20}{(s+20)}$
δ_R
r
$\frac{s}{(s+1)}$

NASA:

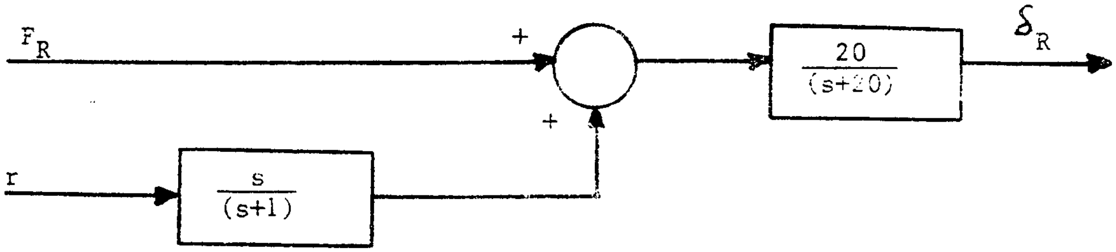
F_R
+
+
$\frac{20}{(s+20)}$
δ_R
r
$\frac{s}{(s+1)}$

CHANGING SIGN CONVENTION

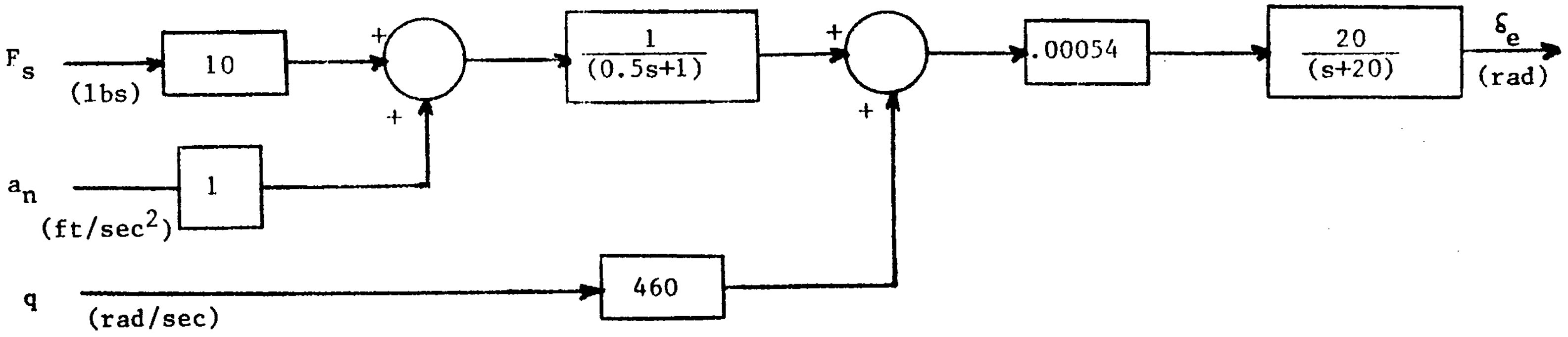
F_s
(lbs)
10
+
+
a_n
(ft/sec²)
1
q
(rad/sec)
1/(0.5s+1)
460
+
+
.00054
20/(s+20)
δ_e
(rad)

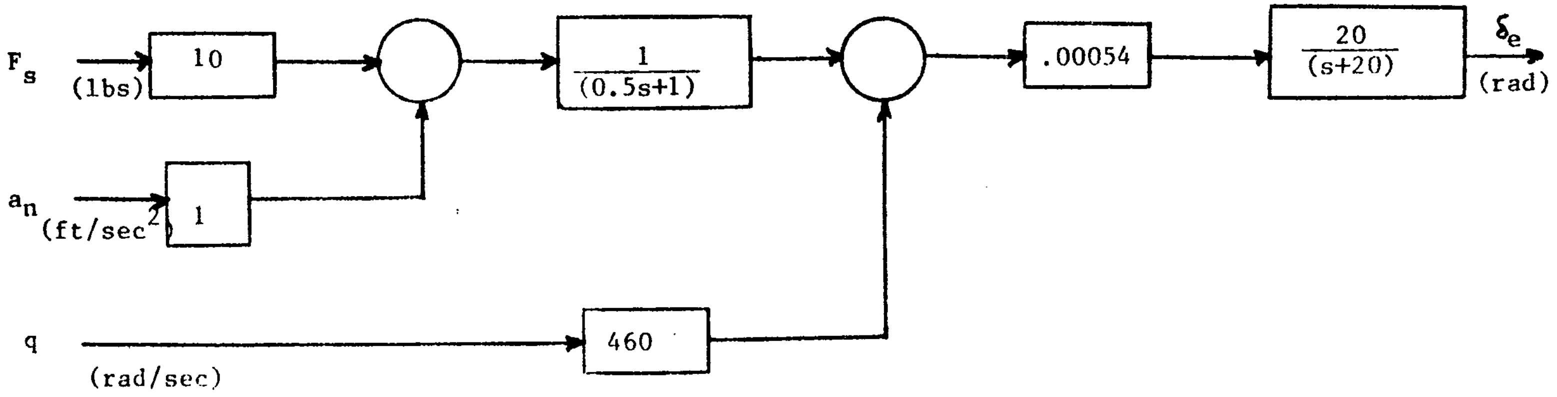
F_s
(lbs)
10
a_n
(ft/sec²)
1
q
(rad/sec)
1/(0.5s+1)
460
.00054
20/(s+20)
δ_e
(rad)

Objective 5:

Know the difference between a reversible and irreversible flight control system.

Reversible FCS:

a. Cockpit controls connected to surface.

b. Movement of surface causes ____________________.

Irreversible FCS:

a. Cockpit controls not connected to surface.

b. Cockpit controls electrically or mechanically connected to ______________.

c. Surface cannot _______________.

Objective 6:

Know the basic transfer function of a hydraulic actuator with feedback and its effect upon control of the aircraft.

$\frac{X_2 (S)}{X_1 (S)} =$ Effect is _____________.

Objective 7:

Know why irreversible controls are used.

a. Transonic speeds cause a wide variation in ___________ and ______________.

b. Augmentation system signals can be combined with ___________________ to provide better feedback control.

c. Can provide ____________________ over entire flight envelope.

Objective 8:

Understand the dynamic effects of artificial feel systems and be able to apply this to the F-4C artificial feel system.

Bellows pressure: prevents lightening of stick forces at _______________.

Bellows spring: provides _____________ and adds a _________________.

Lumped Viscous Damping: prevents ______________ and adds force in proportion to ____________________.

Bobweight: provides ________________.

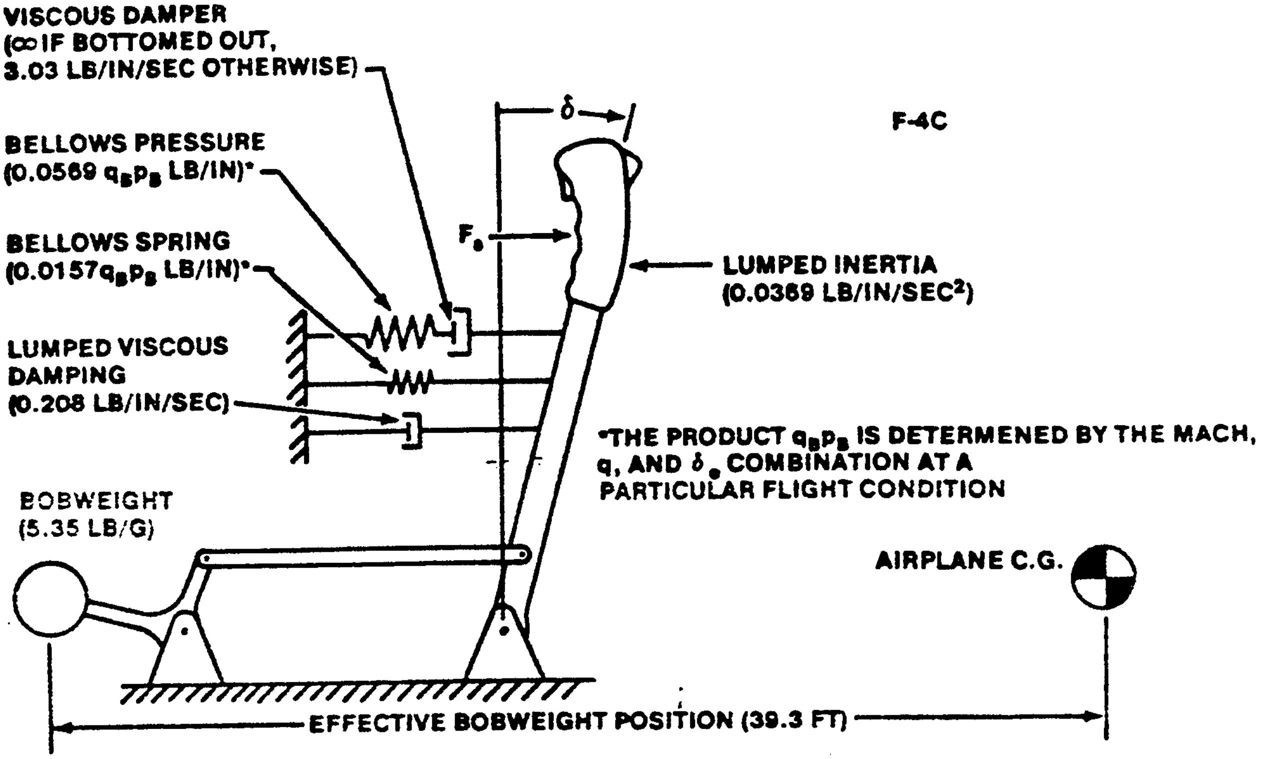
VISCOUS DAMPER
(∞ IF BOTTOMED OUT,
3.03 LB/IN/SEC OTHERWISE)
BELLOWS PRESSURE
(0.0569 $q_B p_B$ LB/IN)*
BELLOWS SPRING
(0.0157 $q_B p_B$ LB/IN)*
LUMPED VISCOUS
DAMPING
(0.208 LB/IN/SEC)
BOBWEIGHT
(5.35 LB/G)
δ
F_s
F-4C
LUMPED INERTIA
(0.0369 LB/IN/SEC^2)
*THE PRODUCT $q_B p_B$ IS DETERMENED BY THE MACH,
q, AND δ_e COMBINATION AT A
PARTICULAR FLIGHT CONDITION
AIRPLANE C.G.
EFFECTIVE BOBWEIGHT POSITION (39.3 FT)

Homework 1-1.

a. What is the sign convention of the following block diagram? NASA/TPS

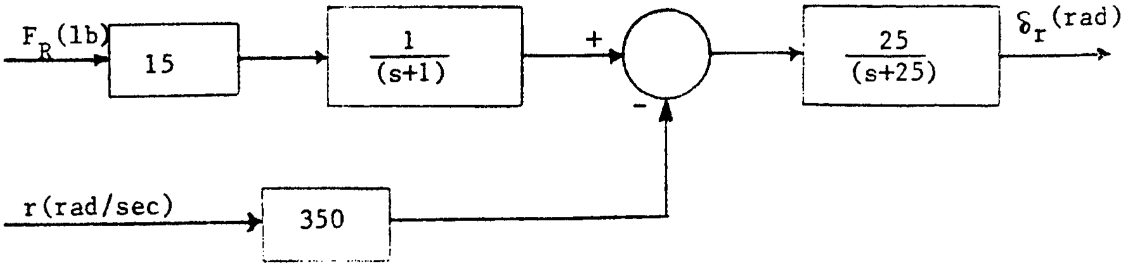
F_R(lb)
15
$\frac{1}{(s+1)}$
+
−
$\frac{25}{(s+25)}$
δ_r(rad)
r(rad/sec)
350

b. Change the above block diagram to TPS sign convention if NASA or NASA sign convention if TPS.

Hour 2 and 3

Reading Assignment Prior to Class: pp 14.47 -14.92

Objective 1: Know the purpose and difference between a SAS and CAS.

SAS:

Purpose: Improves aircraft ______________________.

Characteristics:

a. _____________ control authority

b. Usually non-redundant

CAS:

Purpose:

a. Improves aircraft _________________________.

b. Provides consistent ________________________.

Characteristics:

a. ___________ control authority.

b. Requires redundancy.

Primary difference between SAS and CAS:

Adds _______________ from pilot to augmentor.

Objective 2:

Know the need for good short period dynamics and understand the general characteristics which lead to good dynamics.

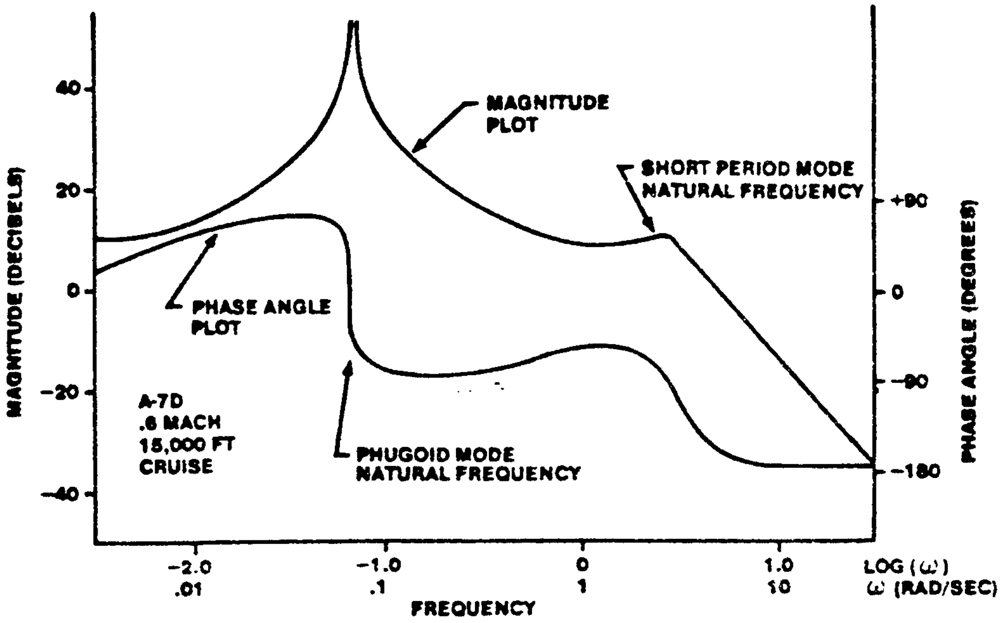

Purpose of acceptable short period dynamics:

a. Performance of ____________________

b. Provide ________________________ to pilot

Characteristics:

a. ____________________ between short period and phugoid natural frequencies.

b. Relative ______________ of short period.

Objective 3:

Know what types of feedback are used to alter the damping ratio of the short period made and be able to describe the feedback effects using a root locus.

a. Feedbacks used to increase short period damping:

1.

2.

Most common method:

A-7 EXAMPLE

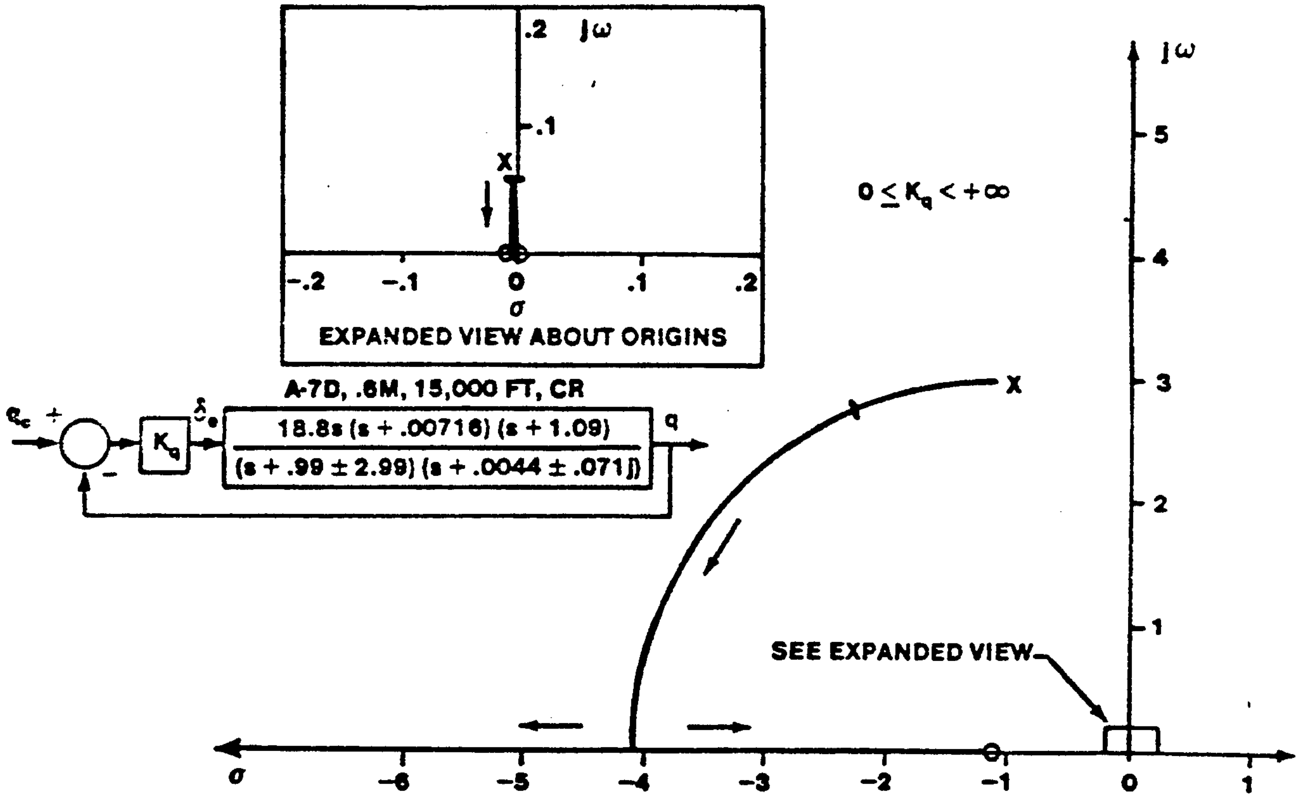

.2 jω
.1
X
-.2 -.1 0 .1 .2
σ
EXPANDED VIEW ABOUT ORIGINS
A-7D, .6M, 15,000 FT, CR
q_c +
−
K_q
δ_e
$\frac{18.8s(s+.00716)(s+1.09)}{(s+.99\pm 2.99)(s+.0044\pm .071j)}$
q
jω
5
4
3
2
1
$0 \leq K_q < +\infty$
X
SEE EXPANDED VIEW
σ
-6 -5 -4 -3 -2 -1 0 1

b. Feedbacks used to Increase Short Period Natural Frequency:

1.

2.

A-7 EXAMPLE

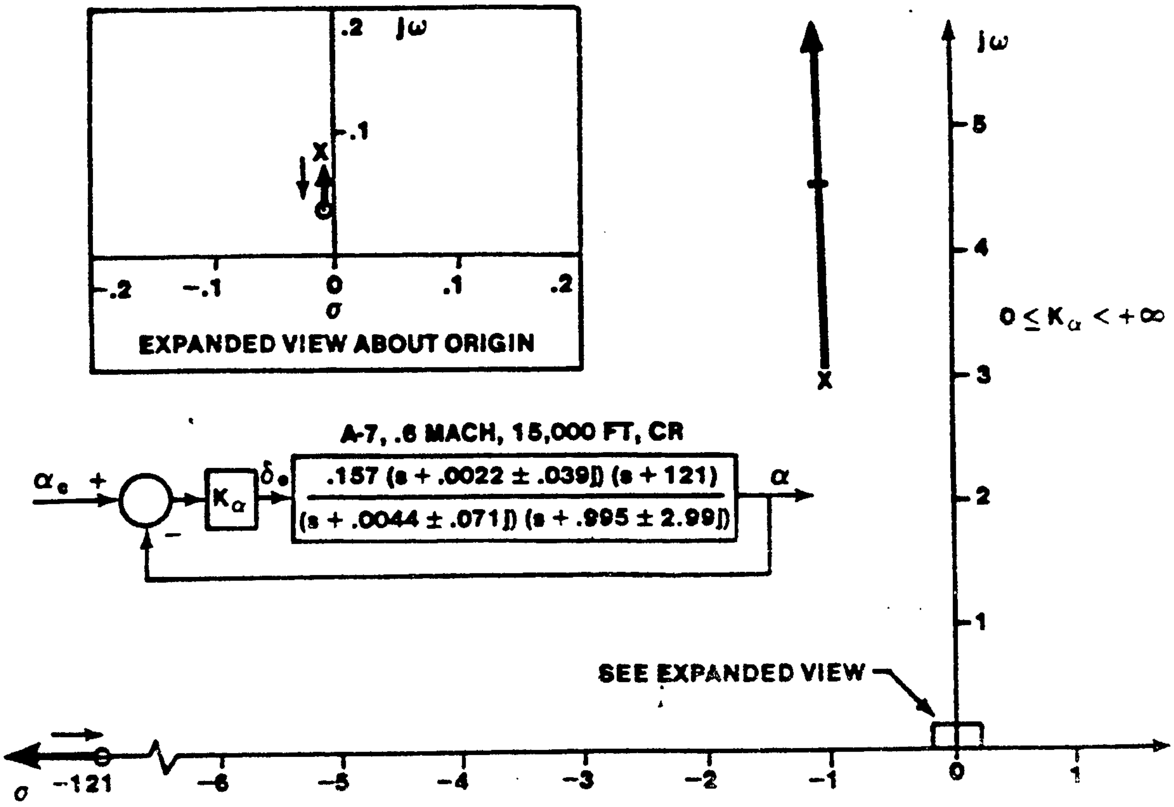
.2
jω
.1
X
O
-.2
-.1
0
.1
.2
σ
EXPANDED VIEW ABOUT ORIGIN
A-7, .6 MACH, 15,000 FT, CR
α_c
+
−
K_α
δ_e
$\frac{.157\,(s + .0022 \pm .039j)\,(s + 121)}{(s + .0044 \pm .071j)\,(s + .995 \pm 2.99j)}$
α
X
jω
5
4
3
2
1
$0 \leq K_\alpha < +\infty$
SEE EXPANDED VIEW
σ
−121
−6
−5
−4
−3
−2
−1
0
1

Objective 4:

Know what type of feedback is used to stabilize an aft c.g. aircraft and be able to describe the feedback effects by using a root locus.

1.
2.
3.

Most Common:

F-16 EXAMPLE (AOA FEEDBACK)

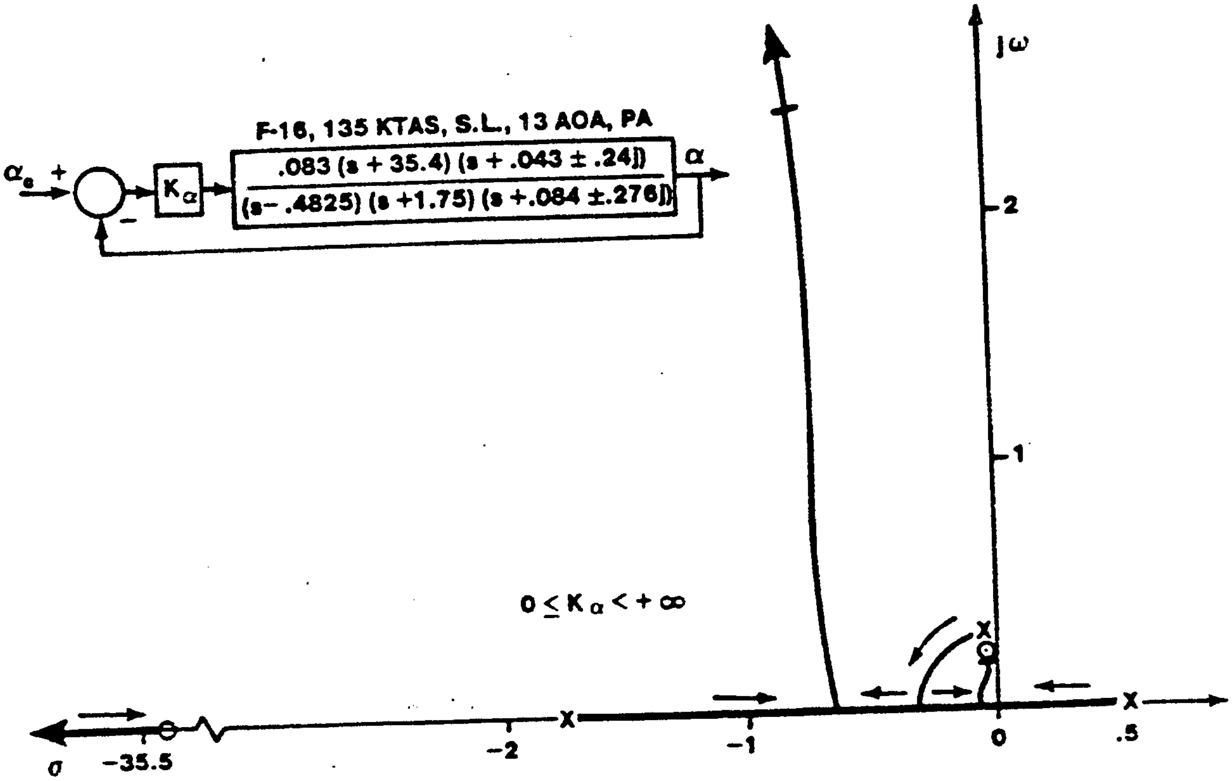
F-16, 135 KTAS, S.L., 13 AOA, PA
α_c
+
−
K_α
$\frac{.083(s+35.4)(s+.043\pm.24j)}{(s-.4825)(s+1.75)(s+.084\pm.276j)}$
α
$j\omega$
2
1
$0 \leq K_\alpha < +\infty$
σ
−35.5
−2
−1
0
.5

Objective 5:

Know what type of feedbacks are used to alter the damping ratio and natural frequency of the Dutch Roll mode and be able to describe the feedback effects by using a root locus.

1.

2.

C-5A EXAMPLE (YAW RATE FEEDBACK)

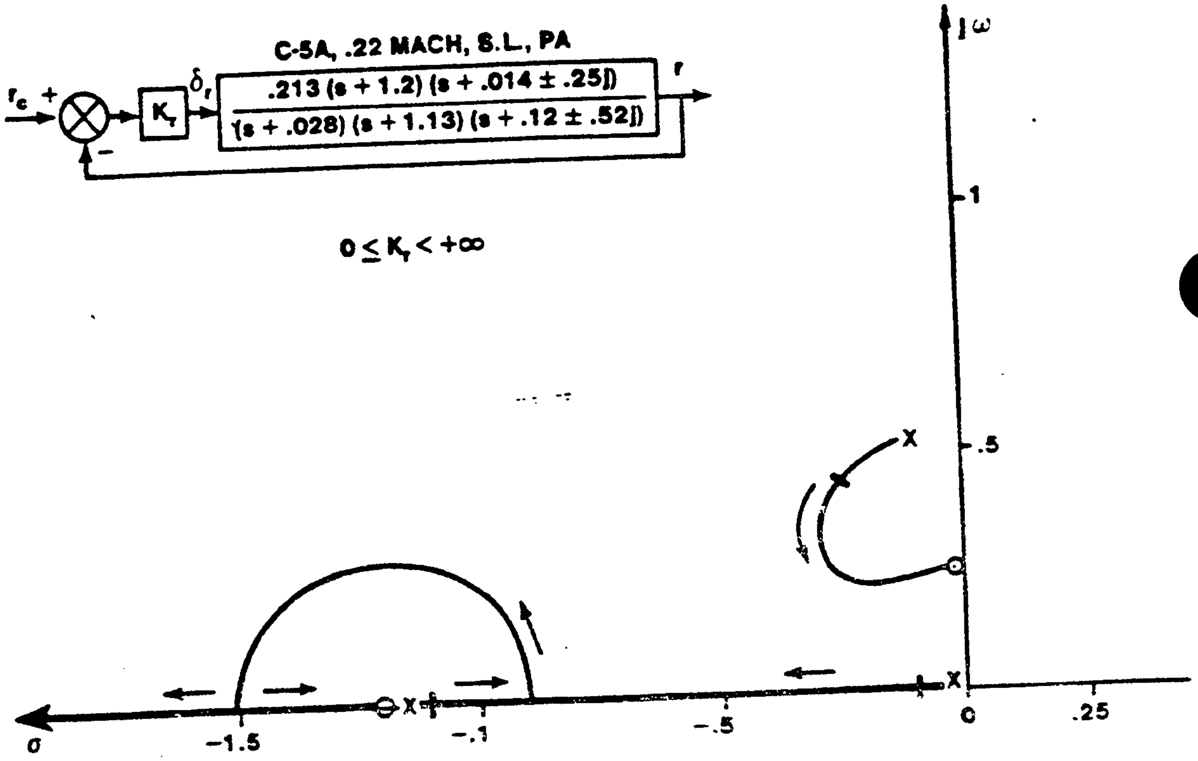
C-5A, .22 MACH, S.L., PA
r_c
+
−
K_r
δ_r
$\frac{.213\,(s + 1.2)\,(s + .014 \pm .25j)}{(s + .028)\,(s + 1.13)\,(s + .12 \pm .52j)}$
r
$0 \leq K_r < +\infty$
jω
1
.5
σ
−1.5
−.1
−.5
0
.25

Objective 6:

Know what type of feedback is used to decrease the roll mode time constant and be able to describe the feedback effects by using a root locus.

1.

C-5A EXAMPLE

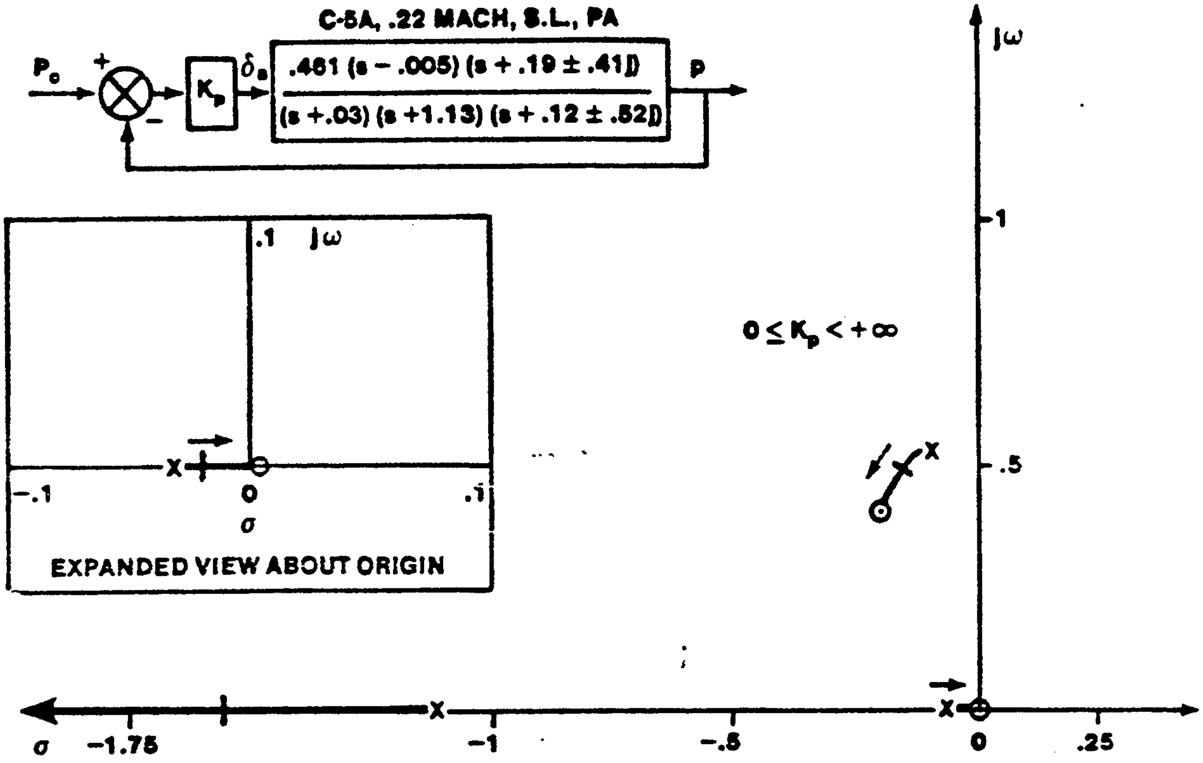
C-5A, .22 MACH, S.L., PA
P_c
+
−
K_p
δ_a
$\frac{.461 (s - .005)(s + .19 \pm .41j)}{(s + .03)(s + 1.13)(s + .12 \pm .52j)}$
p
$0 \le K_p < +\infty$
jω
1
.5
σ
−1.75
−1
−.5
0
.25
.1
jω
−.1
0
σ
.1
EXPANDED VIEW ABOUT ORIGIN

Objective 7:

Understand the general effects of an actuator on a control system.

Objective 8:

Know the advantages that multiple-loop strategies have over compensation devices in designing FCS.

1. Compensation devices (filters) increase ____________.
2. Best FCS are ________________.
3. Take advantage of the feedback parameters influenced on ____.

Objective 9:

Know the general characteristics of a load factor command system.

1. Feedback _______ to elevator.
2. Usually have _____________________.
3. Use forward path integrator to ______________________.
4. Place accelerometer _______________________.

Objective 10:

Understand the reason for gain scheduling.

Provide ________________________________ throughout flight envelope.

Homework 2-1.

Given the following:

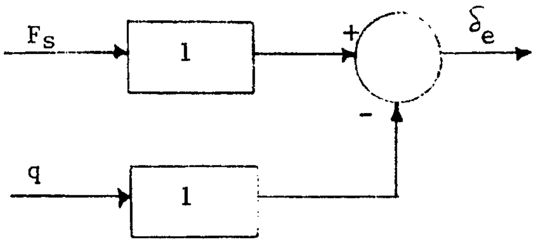

aircraft dynamics:

$$\frac{\theta}{\delta_e} = \frac{1.556(.49962)(.00353)}{[0.09057,0.05844][0.352311,2.82226]}$$

where
(a) represents $(s+a)$
$[\zeta,\omega_n]$ represents $s^2 + 2\zeta\omega_n s + \omega_n^2$

a. Identify the short period and phugoid mode.

b. What is the $q/\delta e$ (pitch rate) transfer function?

c. Redraw the above block diagram to a conventional format (i.e, include the aircraft dynamics).

d. Using cc, draw the root locus of the block diagram.

e. What are the open loop short period natural frequency and damping ratio? Would you expect the open loop characteristics to produce good closed loop handling qualities?

f. From the root locus, determine what value of gain would be required to give a closed loop short period about 0.7. What is the closed loop short period natural frequency? What was the effect on the phugoid mode?

g. Redraw the conventional block diagram with the actuator dynamics included as shown below:

h. Using cc, redraw the root locus of the block diagram including the actuator dynamics.

What effect do the actuator dynamics have on the overall system?

i. Using the same value of gain computed in part "f" what damping ratio would result using the root locus including the actuator dynamics?

j. Close the loop for the transfer function with and without the actuator dynamics for the gain found in part "f". Plot the time responses to see the effect of the actuator (select open loop step response in CC).

Hour 4

Reading Assignment Prior to Class: pp 14.93 - 14.130

Objective 1:

Know why compensation devices are used in flight control systems and how they differ from augmentation systems.

Why:

a. Reshape __________________.

b. Alternative to adding ______________________ to system.

Difference from Augmentation:

Increase ____________________

Objective 2:

List the four compensation types as classified by frequency characteristics.

a.

b.

c.

d.

Objective 3:

Know what each type of filter is called based on its location in a block diagram.

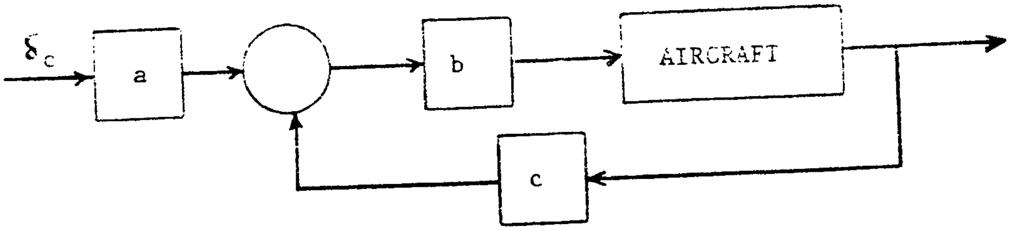

a.

b.

c.

Objective 4:

Know the characteristics of a lead filter.

a. ______________ low frequency signals

b. ______________ high frequency signals

c. Root locus shifted _________________________

d. __________________ ω_n, δ

e. Overall system stabilty _________________

Objective 5:

Know the characteristics of a lag filter.

a. ______________ low frequency signals

b. ______________ high frequency signals

c. Root locus shifted _________________

d. ______________ ω_n, δ

e. _______________ steady state error

f. Overall system stability ______________

Objective 6:

Know the characterisitcs of a lead-lag filter.

a. _________________ of lead and lag filters

b. _________________ steady state error

c. _________________ ω_n

Objective 7:

Know the characteristics of a notch filter.

a. __________________ middle range of frequencies.

b. __________________ high and low frequencies.

Objective 8:

Understand the effect of lead and lag pre-filters on aircraft time response.

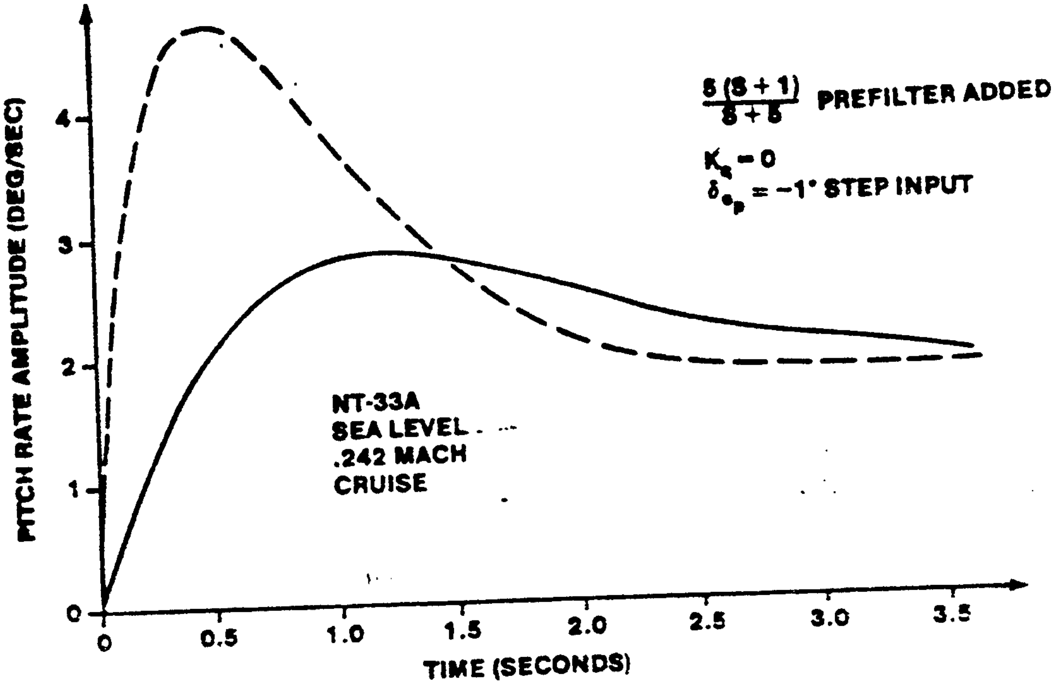

a. Effect of lead pre-filter.

____________________ initial response

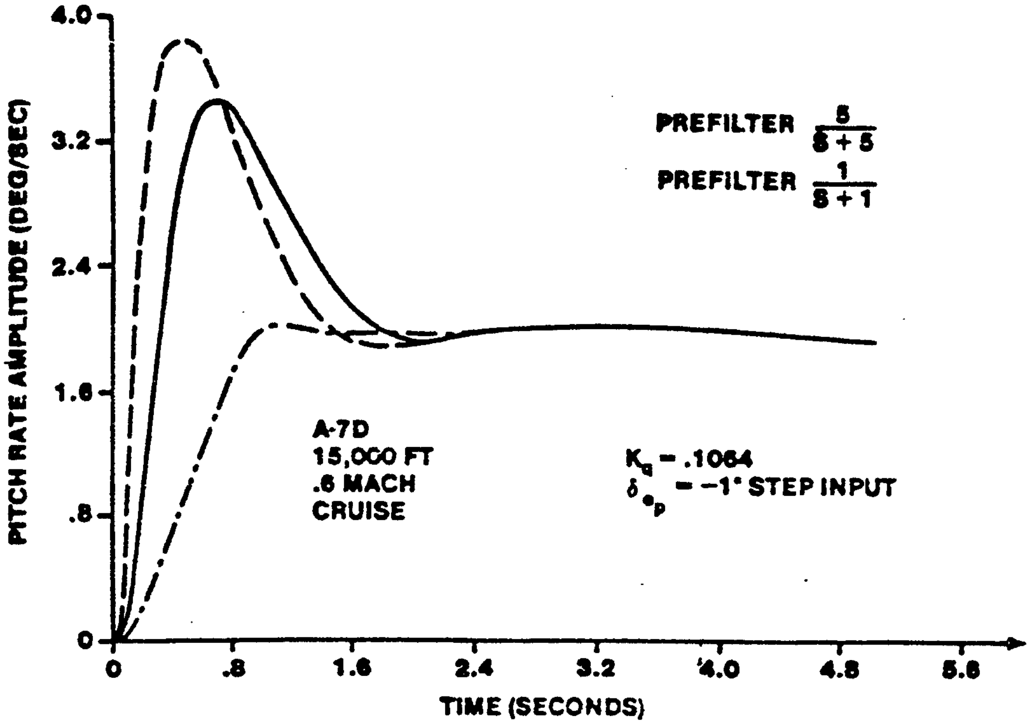

b. Effect of lag pre-filter.

____________________ initial response

Objective 9:

Understand why integral plus proportional control is used in a load factor command system and what advantages it has over pure integral control.

Why? _________________ steady state error (want neutral speed stability)

Advantages

a. Effective time delay ____________________

b. System convergence ______________________

c. Pilot has direct command path.

Objective 10:

Understand why integral plus proportional control is used in a pitch attitude command system and what advantages it has over pure integral control.

Why? Reduce steady state error

Advantages

a. ____________ response than pure integral

b. provides pilot direct path

c. ____________ convergence time

Homework 4-1.

Given the aircraft/actuator dynamics shown below:

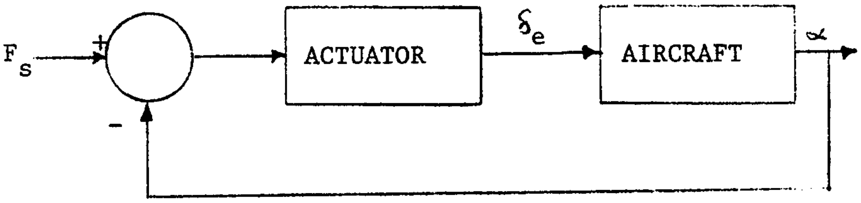

F_s
+
-
ACTUATOR
δ_e
AIRCRAFT
α

$$\text{ACTUATOR} = \frac{20}{(s+20)}$$

$$\frac{\alpha}{\delta_e} = \frac{3.241(202.107)[.04176,.06052]}{[0.05844,0.09057][.35231,2.82226]}$$

Show the effect on the system time responses and root loci of adding the following filters:

a.

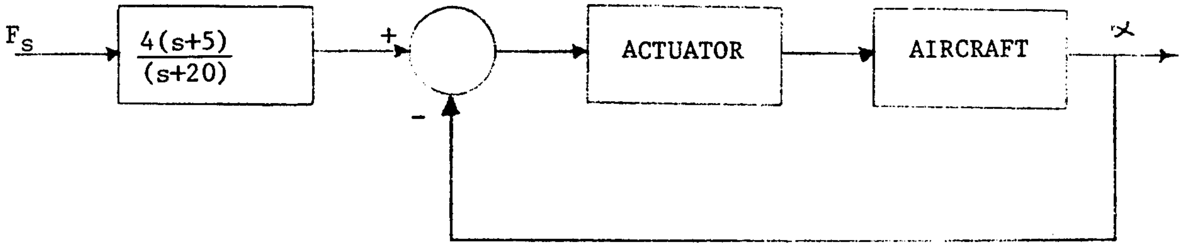

F_s
$\frac{4(s+5)}{(s+20)}$
+
-
ACTUATOR
AIRCRAFT
α

This is a lead/lag filter (circle one).

b.

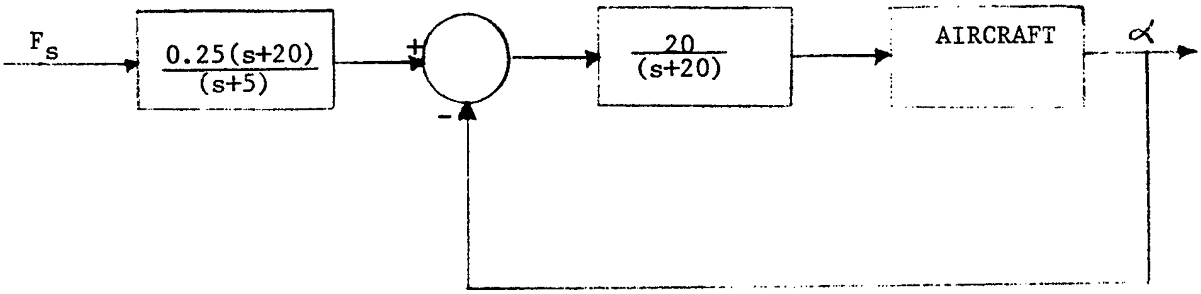
F_s
$\frac{0.25(s+20)}{(s+5)}$
+
-
$\frac{20}{(s+20)}$
AIRCRAFT
α

This is a lead/lag filter (circle one).

c.

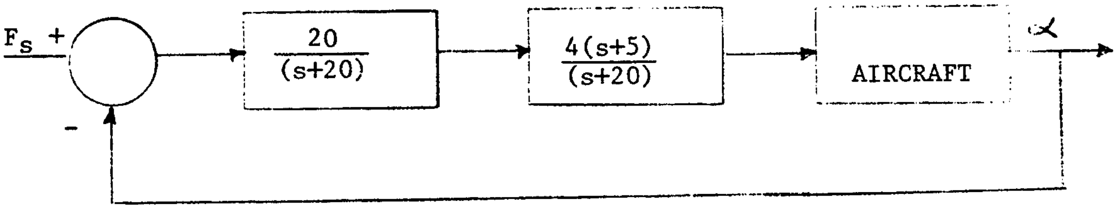
F_s
+
-
$\frac{20}{(s+20)}$
$\frac{4(s+5)}{(s+20)}$
AIRCRAFT
α

This is a lead/lag fileter (circle one).

d.

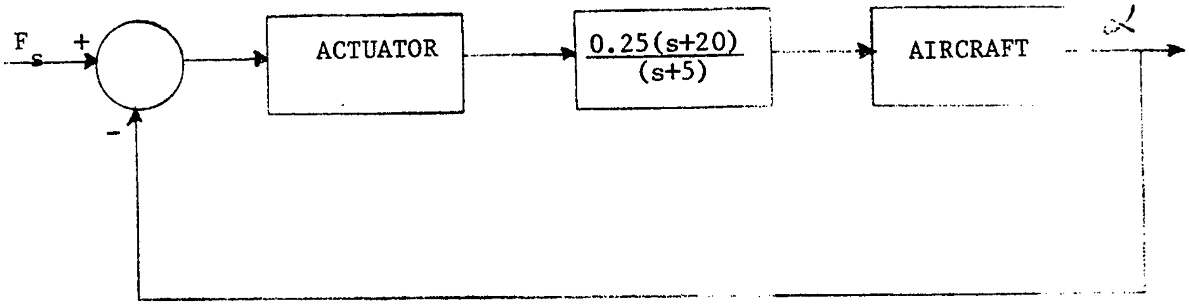
F_s
+
-
ACTUATOR
$\frac{0.25(s+20)}{(s+5)}$
AIRCRAFT
α

This is a lead/lag filter (circle one).

5-1. The following equations are for the acceleration sensed by an accelerometer and the acceleration (at c.g.) and pitch transfer functions of an aircraft.

$$a_z = a_{z_{cg}} - l_x s^2 \theta$$

$$\frac{a_{z_{cg}}}{\delta_e} = \frac{5.36\ (0)\ (3.468)\ (-2.665)(.046)}{[0.15,\ 0.17]\ [0.57, 2.30]}$$

$$\frac{\theta}{\delta_e} = \frac{0.33685(0.085)\ (0.695)}{[0.15,\ 0.17]\ [0.57,\ 2.30]}$$

a. Using CC, draw the root locus of a_z/δ_e for $l_x = 0$ (i.e., accelermoter located at the c.g.)

b. Determine the a_z/δ_e transfer function for $l_x = 6.4$ (forward of c.g.). Draw the root locus of this transfer function. Is it more or less stable than the root locus in a?

c. Determine the a_z/δ_e transfer function for $l_x = -6.4$ (aft of c.g.). Draw the root locus of this transfer function. Is it more or less stable than the root loci in a and b?

Hour 5

Reading Assignment Prior to Class: pp 14.154 - 14.211

Objective 1:

Know what parameters can be measured using each of the following sensors:

a. vertical gyro -
b. directional gyro -
c. single DOF (rate) gyro -
d. linear accelerometer -
e. angular accelerometer -
f. flow incidence angle sensor -

Objective 2:

Understand the placement of the following sensors in a rigid aircraft:

a. angle of attack:
    minimize ______________________________.
b. rate gyros
    placement not critical
c. longitudinal accelerometer
    along aircraft ____________________ __________________
    of center of gravity.

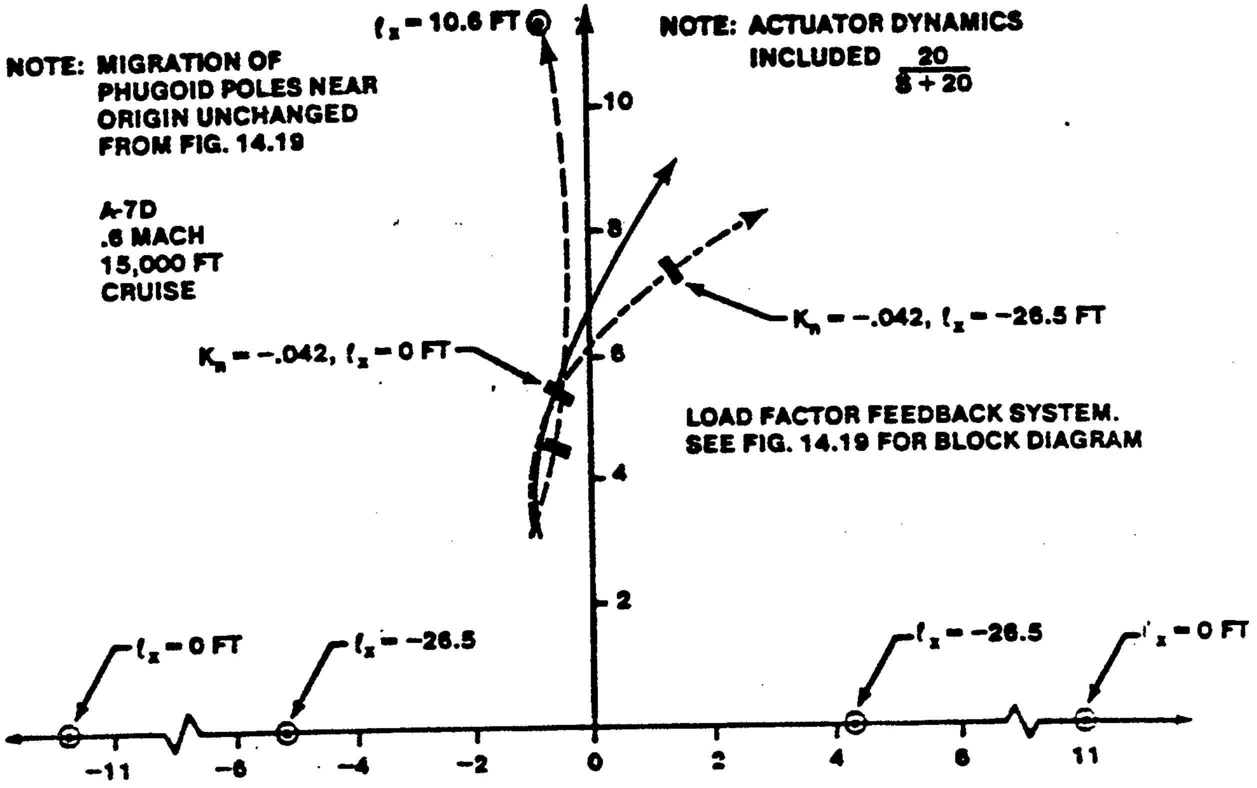

Objective 3:

Understand how fuselage bending affects aircraft flight control systems and what these effects are.

How? Fuselage bending is sensed by ____________________

at frequencies below the flight control system
______________________________.

Effects:

a. May ____________________ handling qualities

b. May cause ______________________.

Objective 4:

Know the characteristics and cause of structural resonance.

a. Sustained high frequency oscillation of ______________.

b. Occurs at a ________________________ frequency.

c. Control system sensors feedback ___________________.

d. Signals are amplied, 180° out of phase, leading to a ________________________.

Objective 5:

Know the major advantages and disadvantage to digital flight control systems.

Advantages:

a. Reduced ______________

b. Increased __________________

c. Greater ____________________

d. Easier ____________________

Disadvantage:

Tend to be ___________________

Objective 6:

Be able to draw a simplified block diagram of a digital flight control system showing the connection between stick inputs and control surface deflections.

Aircraft
Motion
Sensors

Augmentation
System
Computer

Control
Force/Motion
Sensors

Actuator

Objective 7:

Be able to follow through the analysis of a simple fly-by-wire flight control system.

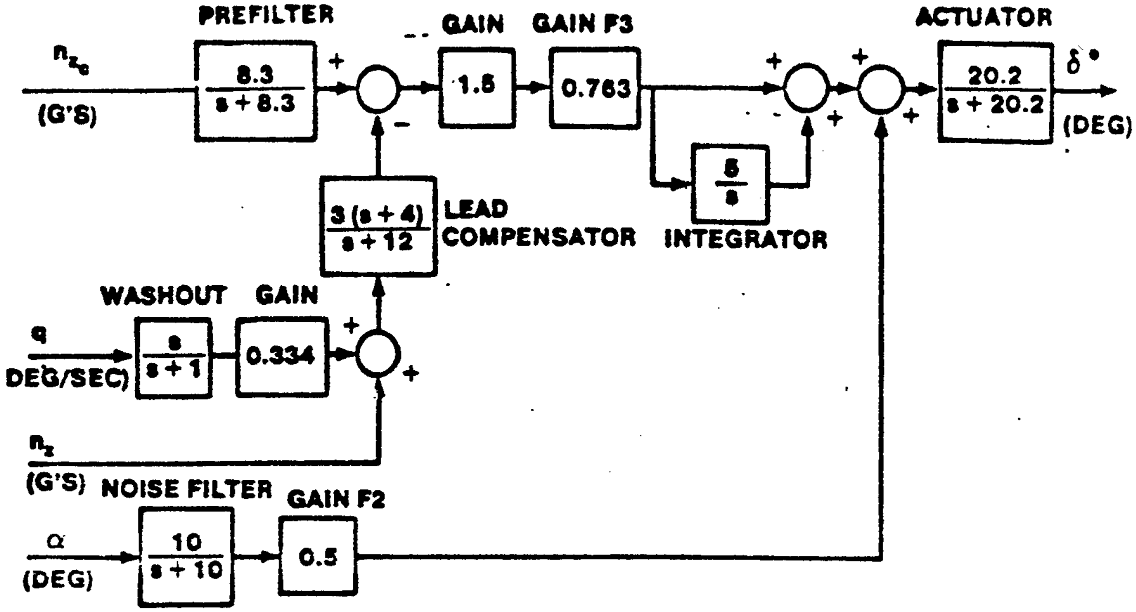
PREFILTER
8.3 / s + 8.3
n_{z_c}
(G'S)
+
−
GAIN
1.5
GAIN F3
0.763
+
−
+
+
+
ACTUATOR
20.2 / s + 20.2
δ°
(DEG)
5 / s
INTEGRATOR
3 (s + 4) / s + 12
LEAD COMPENSATOR
WASHOUT
GAIN
q
DEG/SEC)
s / s + 1
0.334
+
+
n_z
(G'S)
NOISE FILTER
GAIN F2
α
(DEG)
10 / s + 10
0.5

a. Units check

b. Sign convention check

c. Redraw to show feedback loops

d. Simplify to analysis format

TRANSFER FUNCTIONS

$$\Delta(s) = (s - 0.087)\ (s + 2.373)\ (s + 0.098 \pm 0.104j)$$

$$N^{\alpha}_{\delta_e}\ (s) = 0.203\ (s + 0.0087 \pm 0.067j)\ (s + 106.47)\ \text{deg/deg}$$

$$N^{q}_{\delta_e}\ (s) = 21.516\ s\ (s + 0.0189)\ (s + 1.5)\ \text{deg/sec/deg}$$

$$N^{n_z}_{\delta_e}\ (s) = 0.0889\ s\ (s + 0.0158)\ (s + 1.165 \pm 11/437j)\ \text{g's/deg}$$

where

$$G^{\alpha}_{\delta_e} \qquad \frac{N^{\alpha}_{\delta_e}\ (s)}{\Delta(s)}$$

and similarly for

$$G^{q}_{\delta_e}\ (s) \text{ and } G_{\delta_e}^{n_z}$$

e. Analyze angle-of-attack loop (innermost loop)

Purpose of loop:

OLTF =

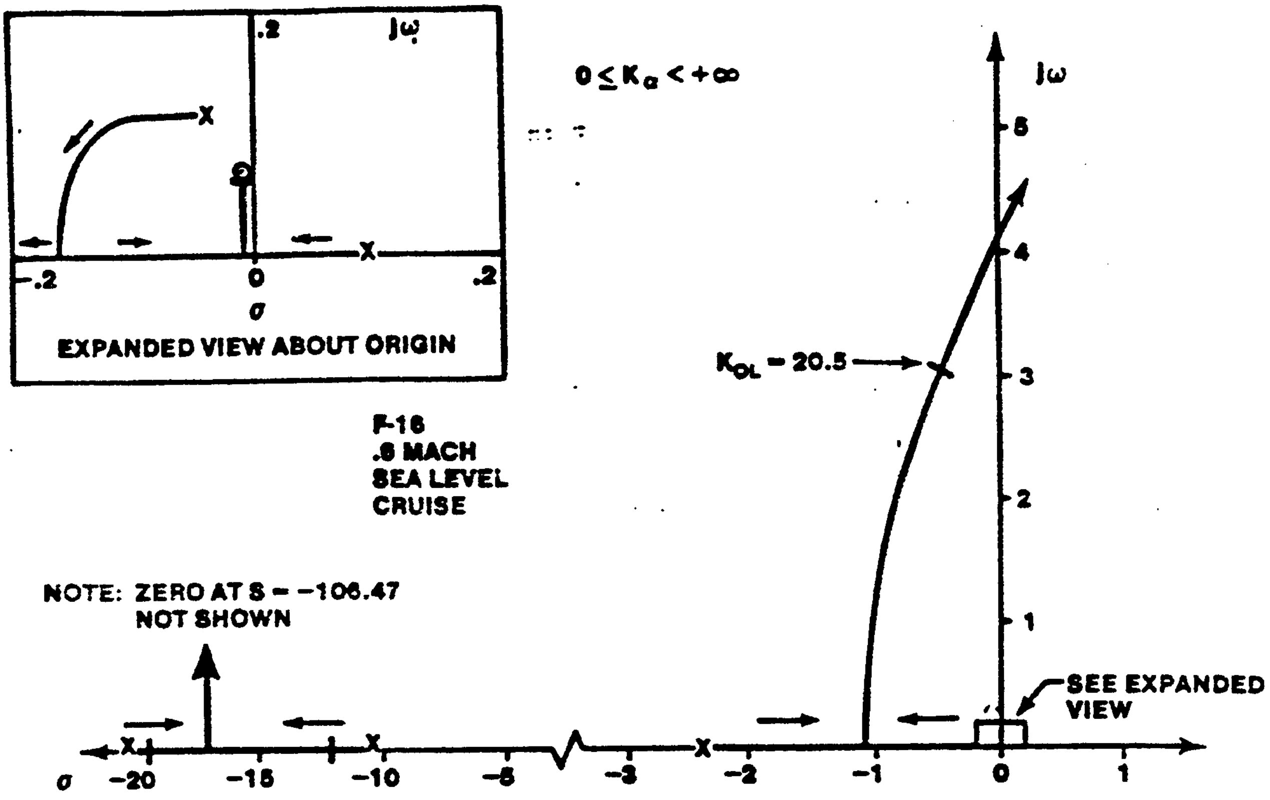

CLTF:

$$G^{\alpha}_{\alpha_c}\Big|_{\alpha_{\text{loop closed}}} = \frac{4.1\ (s + 0.0087 \pm 0.067j)\ (s + 106.47)\ (s + 10)}{(s + 0.0083 \pm 0.0643j)\ (s + 0.478 \pm 3.03j)\ (s + 12.1)\ (s + 19.6)}$$

f. Redraw block diagram with AOA loop closed.

g. Analyze pitch rate feedback loop.

Purpose of loop:

OLTF =

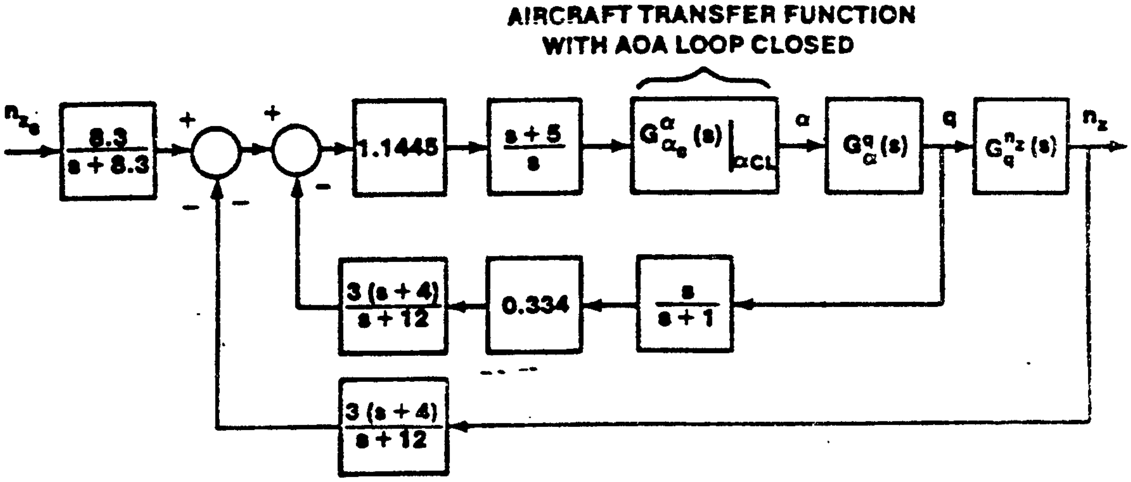
AIRCRAFT TRANSFER FUNCTION
WITH AOA LOOP CLOSED
n_{z_c}
$\frac{8.3}{s+8.3}$
+
+
−
−
−
1.1445
$\frac{s+5}{s}$
$G^{\alpha}_{\alpha_c}(s)\big|_{\alpha CL}$
α
$G^{q}_{\alpha}(s)$
q
$G^{n_z}_{q}(s)$
n_z
$\frac{3(s+4)}{s+12}$
0.334
$\frac{s}{s+1}$
$\frac{3(s+4)}{s+12}$

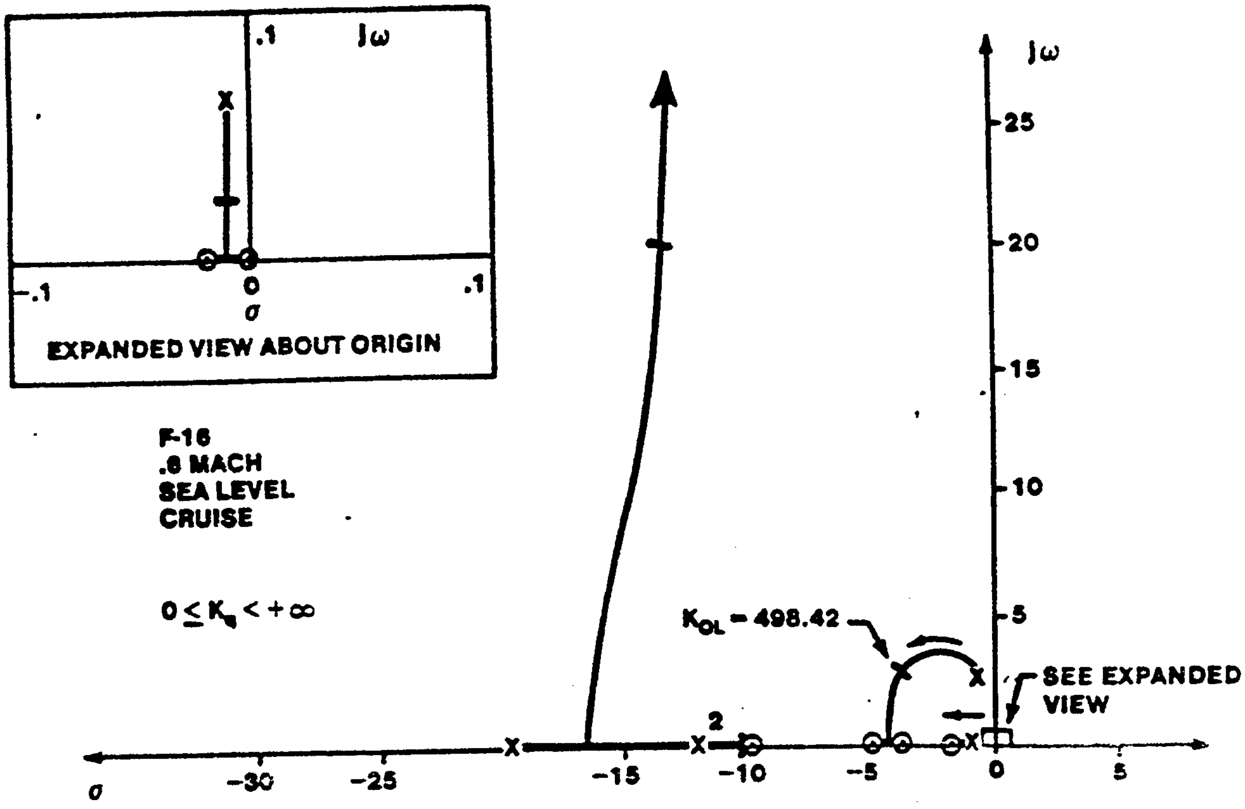

$$G_{q_c}^{q}(s)\Big|_{\alpha,q\ CL} = \frac{497.43\ (s + 0.0189)\ (s + 1.5)\ (s + 10)\ (s + 5)}{(s + 0.0093 \pm 0.023j)\ (s + 1.33)\ (s + 3.78 \pm 2.68j)\ (s + 10.2)}$$

$$\text{CLTF} = \times\ \frac{(s + 1)\ (s + 12)}{(s + 13.3 \pm 20.2j)}$$

g. Redraw block diagram with pitch rate loop closed.

h. Analyze Nz feedback loop.

Purpose of loop:

OLTF

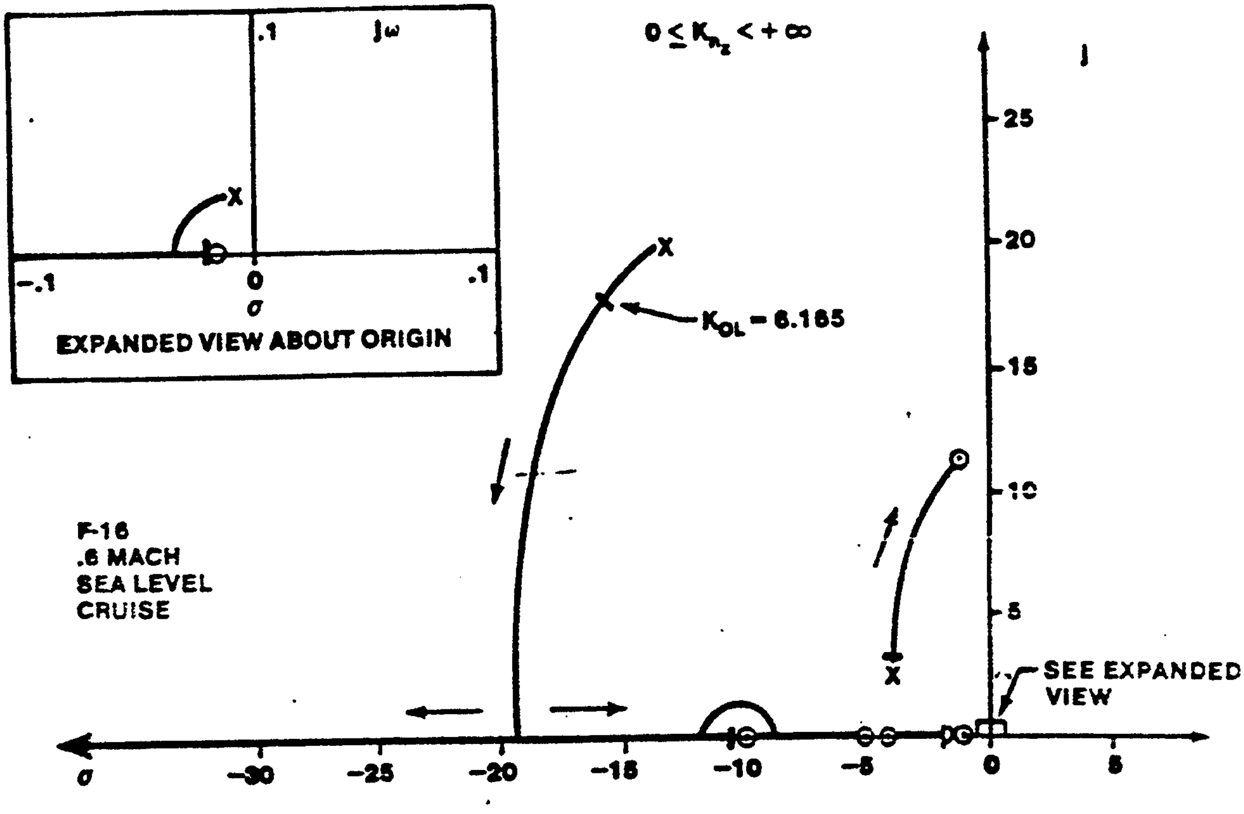

CLTF =

$$G_{n_{z_c}}^{n_z}(s)\Bigg|_{\alpha,q,n_z\ CL} = \frac{2.055\ (s + 0.0158)\ (s + 1.165 \pm 11.437j)\ (s + 10)}{(s + 0.0164)\ (s + 1.74)\ (s + 3.86 \pm 3.32j)\ (s + 0.637)}$$

$$\times \frac{(s + 5)\ (s + 1)\ (s + 12)}{(s + 10.3)\ (s + 15.7 \pm 17.6j)} \times \frac{8.3}{\underbrace{(s + 8.3)}_{\text{Prefilter}}}$$

i. Examine aircraft time responses.

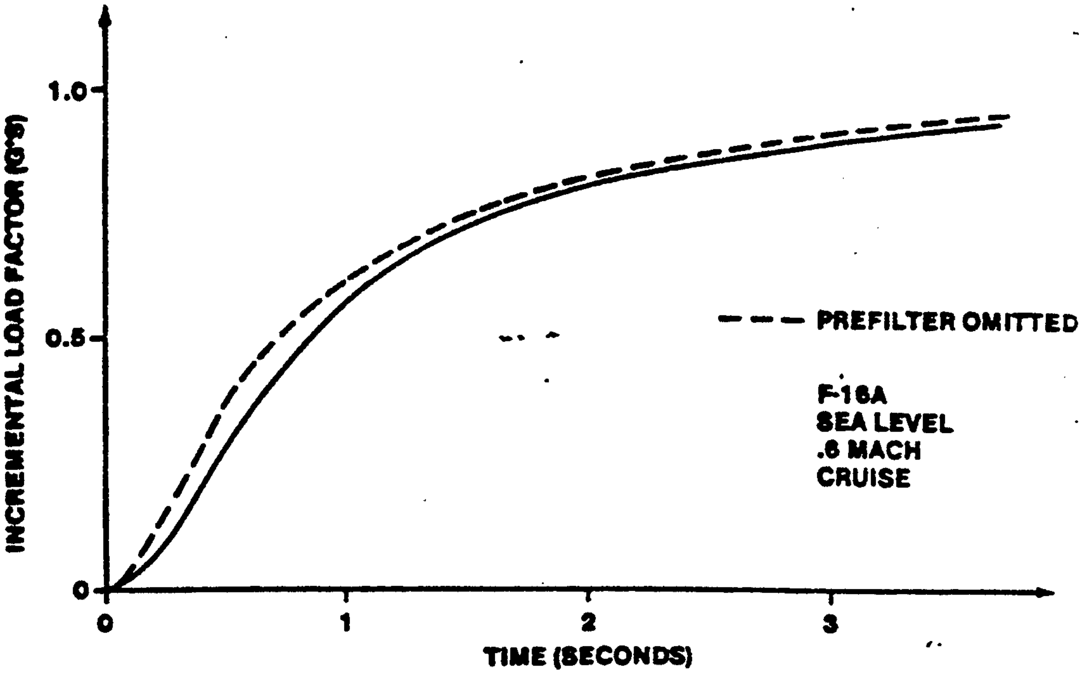

Objective 8:

Understand the reasons for integrating flight control systems with:

a. avionics and sensors

i. Automated ____________________

ii. Automatic ____________________ avoidance

iii. Decreased __________, increased __________

b. propulsion systems

i. ________________ range/payload performance

ii. ________________ maneuverability

Hour 6

Reading Assignment Prior to Class: pp 211 - 253

Objective 1:

Be familiar with the mandatory ground tests which must be performed on flight control system components prior to the start of flight tests.

a.

b.

c.

d.

e.

f.

g.

Objective 2:

Be familiar with the mandatory ground test which must be performed on the test aircraft prior to the start of flight tests.

a.

b.

c.

d.

e.

f.

Objective 3:

Understand the need for inflight simulation of an aircraft flight control system.

a. Ground simulators are usually deficient because ________ ______________.

b. Inflight simluation can simulate ______________________ tasks.

c. If performed early, results can be used to refine FCS _________________________.

Objective 4:

Know what can be tested during ground functional test techniques.

a. Control force and deflection __________________.

b.

c. Frequency responses-used to determine _________________.

d. Simulate _____________ conditions

Objective 5:

Know why open loop tasks cannot adequately evaluate the dynamic modes of a highly augmented aircraft.

The response of a highly augmented aircraft is more dependent on ______________________ than on ______________________.

Objective 6:

Understand the elements of closed loop handling qualities tests.

a. Pilot ________________

b. ________________ tasks

c. ________________ test maneuvers

d. Clearly defined ________________ standards and
________________ strategies

e. Adequate ______________ to excite dynamic modes

f. Adequate ______________ to get steady state motion

Objective 7:

Understand the precision tracking test technique.

Used to uncover ___________________. Aircraft dynamics must be ______________________; ________________________ is not an objective. The task consists of an ____________________ on a maneuvering target then 20 - 30 seconds of ___________________. All pipper excursions must be corrected _____________________. A ___________________ is used since a _____________________ may mask deficiencies. ___________________ should also not be used since it may mask deficiencies.

Objective 8:

Understand the air-to-air tracking test techniques.

- Wind-up turns
  Increasing __________________ (about ___________________)
- Constant α test
  Used for _____________________________

Objective 9:

Understand the air-to-ground tracking test techniques.

Disadvantages

- Target at ____________________

- Range not constant

Shallow dives

- _________________ track

- Avoid fixation

- Can change targets